# Studies of Aberrant Cerebral Lipid Metabolism in Scrapie-Affected Mice

Timothy Dudley Mark Perring

Doctor of Philosophy

The University of Edinburgh

1996

# Abstract

*Post mortem* histopathological examination of brain tissue is currently the only definitive means of identifying transmissible spongiform encephalopathy disease status. The inability to accurately diagnose TSE status *ante mortem*, and more importantly preclinically, serves as a serious impediment to the provision of proper patient/family counselling and care, and in the future should treatment become available, to the alleviation of neurological damage and suffering.

The studies described herein evaluate the application of magnetic resonance spectroscopy to the clinical diagnosis of scrapie in mice. Statistically significant changes were observed in cerebral levels of *N*-acetyl aspartate, glutamic acid and inositol in diseased animals. The relevance of these changes with respect to scrapie clinicopathological features are discussed. It is noted that these abnormalities are non-specific to scrapie and thus MRS finds application to ancillary diagnosis but not definitive diagnosis of TSE status.

The *in vivo* and *in vitro* application of proton MRS to the detection of intracerebral lipid disturbances is discussed with reference to spontaneous lipoma in a control mouse. This lipid accumulation, which comprised a high proportion of triglyceride, was fully characterized by *in vitro* proton MRS techniques.

The cerebral lipid profiles of eight murine-scrapie models were investigated by high performance thin layer chromatography. Concentrations of cholesterol, phospholipids and glycolipids in control and scrapie-affected animals were unchanged in all models studied. Cholesteryl ester levels were elevated in those models which exhibited marked neurological damage and prolonged incubation periods.

The biotransformational process resulting in the production of $PrP^{sc}$ is believed to occur on the neuronal cell membrane in discrete microdomains called caveolae. Lipids associated with GPI-anchored proteins were characterized in $PrP^{+/+}$, $PrP^{+/0}$ and $PrP^{0/0}$ mice. No significant changes in lipid composition were observed, implying that cellular PrP depletion does not have a detrimental effect on the structural integrity of caveolae. Similar studies were performed in control and scrapie mice. These showed highly significant changes in cholesteryl esters and cerebroside I. It is speculated that the altered structural composition of caveolae lipids may cause perturbations in the cell membrane sufficient to inhibit GPI-anchor cleavage of $PrP^{sc}$ by phosphatidyl inositol-specific phospholipase C.

## Dedication

This thesis is dedicated to the memory of my father.

Dudley Perring (1940 - 1993).

"Our species is the only creative species, and it has only one creative instrument, the individual mind and spirit of a man. Nothing was ever created by two men. There are no good collaborations, whether in music, in art, in poetry, in mathematics, in philosophy. Once the miracle of creation has taken place, the group can build and extend it, but the group never invents anything. The preciousness lies in the lonely mind of a man".

*East of Eden.*

John Steinbeck (1902-1968).

## Course Attendance

(i) Organic research seminars. Department of Chemistry, University of Edinburgh (3 years attendance);

(ii) Basic course in radiation protection in laboratory work in science and medicine. Dr. J.D. Simpson, Radiation Protection Service, University of Edinburgh (1991, 8 lectures);

(iii) Mass spectrometry in action. Professor J. Monaghan and Dr. J. Scrivens, I.C.I. Ltd. (1992, 6 lectures);

(iv) Medicinal chemistry. Professor R. Baker and colleagues, Merck, Sharp and Dohme (1992-1994);

(v) I.C.I. Pharmaceuticals presentation on Zoladex. Dr. B.J.A. Furr and colleagues, I.C.I. Ltd. (1992, 6 lectures);

(vi) Recent Advances in the synthesis and activity of agrochemicals. Drs. I Boddy and P.J. Dudfield, Schering Agrochemicals Ltd. (1992, 6 lectures);

(vii) NMR and its application to molecules of biological importance. Drs. I.H. Sadler and J.A. Parkinson, Department of Chemistry, University of Edinburgh (1993, 6 lectures);

(viii) Chemical development in the pharmaceutical industry. Dr. J.P. Clayton and colleagues, Smithkline Beecham Pharmaceuticals Ltd. (1993, 5 lectures);

(ix) Fluorine for the organic chemist. Professor R. Chambers, University of Durham (1994, 2 lectures);

(x) B.B.S.R.C. Biology of Spongiform Encephalopathies Meeting. University of Reading (April 1992-April 1994);

(xi) 1992 Pfizer International Symposium. The spongiform encephalopathies - current status and implications for other neurodegenerative disorders;

(xii) Poster Presentation - "Detection of aberrant cerebral cholesteryl ester accumulation in a mouse model of scrapie". The Biochemical Society Meeting No. 648. The Queens University, Belfast. Sept. 14-17, 1993.

## List of Abbreviations

| | |
|---|---|
| **AMPA** | α-amino-3-hydroxy-5-methyl-isoxazole |
| **BCA** | bicinchoninic acid |
| **BSA** | bovine serum albumin |
| **c** | complex |
| **CARD** | cardiolipin |
| **CB** | cerebroside |
| **CE** | cholesteryl esters |
| **CER** | ceramide |
| **CHOL** | cholesterol |
| **CI-MS** | chemical ionization mass spectrometry |
| **CJD** | Creutzfeldt-Jacob disease |
| **COSY** | correlated spectroscopy |
| **CNS** | central nervous system |
| **1D** | one-dimensional |
| **2D** | two-dimensional |
| **δ** | chemical shift (ppm) |
| **d** | doublet |
| **dd** | doublet of doublets |
| **EAA** | excitatory amino acid |
| **EDTA** | ethylene diaminetetraacetic acid |
| **FA** | fatty acid |
| **FID** | free induction decay |
| **FTIR** | Fourier transform infrared spectroscopy |
| **GAC** | galactose |
| **GSS** | Gerstmann-Sträussler Scheinker syndrome |
| **HPTLC** | high-performance thin layer chromatography |
| **Hz** | Hertz |
| **i.c.** | intracerebral |

| | |
|---|---|
| **mCi** | milliCurie |
| **ME7/VM** | VM mice affected with the ME7 strain of scrapie |
| **MES** | 2-[*N*-morpholino]ethanesulfonic acid |
| **ml** | millilitre |
| **mM** | millimolar |
| **MRI** | magnetic resonance imaging |
| **MRS** | magnetic resonance spectroscopy |
| **MS-MS** | tandem mass spectrometry |
| **mV** | millivolt |
| ***m/z*** | mass-to-charge ratio |
| **NAA** | *N*-acetyl aspartate |
| **NADH** | β-nicotinamide adenine dinucleotide |
| **NMDA** | *N*-methyl-*D*-aspartate |
| **NMR** | nuclear magnetic resonance spectroscopy |
| **OA** | oleyl alcohol |
| **PC** | phosphatidyl choline |
| **PE** | phosphatidyl ethanolamine |
| **p.i.** | post injection |
| **PI** | phosphatidyl inositol |
| **PIPLC** | phosphatidyl inositol-specific phospholipase C |
| **PLA** | plasmalogen |
| **ppm** | parts per million |
| **PrP** | protease-resistant protein |
| **$PrP^c$** | protease-resistant protein, scrapie isoform |
| **$PrP^{sc}$** | protease-resistant protein, cellular isoform |
| **PS** | phosphatidyl serine |
| **q** | quartet |
| **qu** | quintet |

| | |
|---|---|
| **s** | singlet |
| **SAF** | scrapie-associated fibrils |
| **SINC** | scrapie incubation |
| **SPH** | sphingomyelin |
| **SULF** | sulfatide |
| **t** | triplet |
| **TAG** | triacylglycerol (triglyceride) |
| **TLC** | thin layer chromatography |
| **TRIS** | tris[hydroxymethyl]aminomethane |
| **TSE** | transmissible spongiform encephalopathy |
| **TSP** | 3-trimethylsilyl-2,2',3,3'-tetradeuteropropionic acid |
| **vol.** | volume |

## Acknowledgements

No amount of words can express the deepest appreciation and love I have for my mother.

I gratefully acknowledge the support and advice of my supervisors Dr. James Hope and Dr. Robert Baxter. The magnetic resonance spectroscopy studies saw fruition under the invaluable and patient assistance of Dr. John Parkinson.

In addition to my supervisors I am deeply appreciative to the following people for their support and friendship: Miriam Anderson, Dr. Moira Bruce, Paula Dickinson, Dr. Christine Farquhar, Dr. Mandy Firoozan, Dr. Jim Foster, Dr. Hugh Fraser, Dr. Jan Fraser, Dr. Wilfred Goldmann, Dr. Stephen Horgan, Dr. Robert Somerville and Dr. Alan Williams.

Isolation of GPI-anchored protein sucrose gradient float fractions was performed by Miss Angela Chong (Neuropathogenesis Unit), to whom I am extremely grateful. *In vivo* $^{1}H$ NMR spectra of a spontaneous lipoma in a control mouse were kindly supplied by Miss Yuen-Li Chung of the Robert Steiner Magnetic Resonance Unit, Hammersmith Hospital, London. Chemical ionization mass spectrometry of purified cholesteryl esters was kindly performed by Mr. Richard Jennings and Dr. Hilary Yates of I.C.I. Ltd. Chemical ionisation mass spectrometry of fatty acid methyl esters of triglyceride was performed by Mr. Alan Taylor, Chemistry Department, University of Edinburgh. I also extend my thanks to Dr. Moira Bruce and Dr. Hugh Fraser for their permission to reproduce murine-scrapie model neuropathological lesion profiles and for helpful discussion.

The research described herein was generously supported by the Biotechnology and Biological Sciences Research Council (B.B.S.R.C.).

## Table of Contents

# CHAPTER ONE

# INTRODUCTION

## 1. 1 Scrapie and its relationship to bovine spongiform encephalopathy.

Scrapie is a transmissible neurological disorder of sheep and goats (Gordon, 1946; Pattison *et al.*, 1959) the prevalence of which has been recognized in U.K. flocks for over 250 years (Parry, 1983). It belongs to a family of related diseases known as transmissible spongiform encephalopathies which share distinct histopathological features including neuronal vacuolation, astrogliosis, and the formation of amyloid plaques (Fraser, 1979; Lampert *et al.*, 1972; Masters and Beyreuther, 1988). The potential for cross-species transmission of scrapie has been known for a number of years, as demonstrated by experimental inoculation studies in laboratory rodents (Dickinson and Fraser, 1977). In the mid 1980s the cross-species transmission of scrapie was further highlighted by the emergence of a novel progressive spongiform encephalopathy in cattle (Wells *et al.*, 1987). This disease which closely resembles scrapie on both histological (Wells *et al.*, 1987) and biochemical (Hope *et al.*, 1988) criteria was named bovine spongiform encephalopathy (BSE).

Comprehensive epidemiological studies support the hypothesis of a food-borne infectious source to the disease as a result of the widespread geographical distribution of cases within the U.K. (Dickinson and Taylor, 1988). The cause of BSE has subsequently been attributed to the practice of feeding proprietary concentrates derived from scrapie-infected meat and bone meal to dairy cattle (Morgan, 1988). It is believed that changes in the rendering process in the late 1970s, notably the shift away from solvent extraction and application of live steam on defatted products, allowed increasing quantities of infectious material to pass into ruminant feedstuffs (Wilesmith, 1990). Contaminated ruminant-derived meat and bone meal has also been incriminated in the occurrence of BSE-like conditions in African species of ruminants maintained in English zoological collections (Fleetwood and Furley, 1990; Jeffrey and Wells, 1988; Kirkwood *et al.*, 1990).

## 1. 2 Human transmissible spongiform encephalopathies.

Human forms of the disease include kuru, Creutzfeldt-Jacob disease (CJD) and Gerstmann-Sträussler Scheinker syndrome (GSS). These diseases emphasize mans susceptibility to variants in the family of spongiform encephalopathies.

Kuru was discovered during the late 1950s in a remote tribal population in the mountainous Fore region of Papua New Guinea (Gadjusek and Zigas, 1957). Transmission of kuru within members of this tribe was attributed to ritualistic cannibalism. It is understood that during ceremonial funeral proceedings, infectious brain material was handled and often consumed by under-nourished members of the tribe, especially women and children. Its transmissible and infectious nature was confirmed by the experimental innoculation of kuru-infected brain material into chimpanzees and other primates (Gadjusek *et al.*, 1966). The prognosis for kuru is very poor; the disease typically affects young adults and is characterized by a progressive ataxia with a shivering type of tremor, latter emotional instability and death within a year of onset (Gadjusek and Zigas, 1959).

Creutzfeldt-Jacob disease is the commonest member of the human transmissible spongiform encephalopathy family, affecting approximately one person in a million *per annum* and has a random world-wide distribution (Brown, 1988). The disease typically has a prevalence for females between 50 and 75 years of age. Clinical signs are characterized by a gradual progressive mental deterioration, initially manifested as memory loss or errors in judgement. Mental deterioration and mood alterations evolve to a state of dementia and confusion. In some individuals visual deterioration leads to cortical blindness (often interspersed with hallucinations), and motor impairments progress to a complete lack of coordination coupled with involuntary movements such as myoclonus and shivering (Brown, 1988). There are no recorded cases of recovery, with most patients dying within six months of disease onset. Infection in humans can be transmitted iatrogenically by implantation of contaminated electrodes, injection of

growth hormone derived from contaminated pituitary glands, and transplantation of contaminated corneas or *dura mater* (Bernoulli *et al.*, 1977; Brown *et al.*, 1985; Duffy *et al.*, 1974; Will and Matthews, 1982).

Gerstmann-Sträussler Scheinker syndrome (GSS) is a relatively rare familial variant of Creutzfeldt-Jacob disease associated with a codon 102 leucine for proline substitution in the PrP protein (Doh-ura *et al.*, 1989; Kretzschmar *et al.*, 1991). The clinical course of the disease is usually protracted, extending for three or more years (Brown *et al.*, 1991).

## 1. 3 Cellular biosynthesis of PrP and its key role in scrapie pathogenesis.

The identity of the aetiological agent responsible for transmissible spongiform encephalopathy pathology remains unresolved. Filtration and replication studies indicate that the pathogen has virus-like properties (Johnson and Gibbs, 1974), however other findings have shown it to be remarkably resistant to a wide range of adverse conditions which normally damage conventional viral nucleic acid. Exposure of infectious tissue to dry heat (Brown *et al.*, 1990), formalin fixation (Stamp, 1962), ionizing radiation (Alper *et al.*, 1966) and ultraviolet-irradiation (Alper *et al.*, 1967), does not significantly diminish infectivity. Likewise, the absence of attenuation after DNase and RNases treatment has led to the suggestion that the aetiological agent may even lack a conventional nucleic acid genome (Alper *et al.*, 1967). The agent is however partially sensitive to protease digestion (Prusiner *et al.*, 1979). In view of these unique biophysical properties, Griffith speculated that the agent responsible for transmissible spongiform encephalopathies may consist solely of a novel self-replicating protein (Griffith, 1967).

Electron microscopy studies of subcellular fractions from scrapie-affected brain material led to the discovery of abnormal fibrillar aggregates. These aggregates, or scrapie-associated fibrils, co-purify with scrapie infectivity (Merz *et al.*, 1981) and are observed in a number of transmissible spongiform encephalopathies (Gadjusek and Zigas, 1959; Hope *et al.*, 1988; Merz *et al.*, 1983). Purification studies showed the fibrils to be composed predominantly, if not exclusively, of a protease-resistant protein, designated PrP (Bolton *et al.*, 1982). Following partial degradation studies and cDNA cloning (Chesebro *et al.*, 1985), PrP was shown to be the product of a single copy gene in host neurones (Oesch *et al.*, 1985). The scrapie and normal cellular isoforms of PrP exhibit different biochemical properties. Whereas the cellular isoform ($PrP^{c}$) is susceptible to membrane release by phosphatidyl inositol-specific phospholipase C (PIPLC) and protease digestion, the scrapie isoform ($PrP^{sc}$) is not (Caughey and Raymond,

1991). The properties of the two isoforms also differ in aqueous detergents wherein $PrP^{sc}$ displays marked hydrophobicity and tendency to form amyloid aggregates whereas $PrP^{c}$ does not (Meyer *et al.*, 1986). Subsequent studies showed the scrapie isoform of PrP to have the same molecular weight and charge distribution as the normal host-encoded protein (Hope *et al.*, 1986). In the absence of altered PrP mRNA transcription/translation (Oesch *et a*l., 1985; Stahl and Prusiner, 1991), the difference in physicochemical properties between the two PrP isoforms is proposed to be the result of a post-translational modification event (Chesebro *et al.*, 1985; Hope *et al.*, 1986; Oesch *et al.*, 1985; Stahl and Prusiner, 1991).

The study of normal cellular and aberrant PrP metabolism has greatly benefited from the development of mouse neuroblastoma (MNB) cell lines which propagate scrapie infectivity (Race *et al.*, 1987). Cellular PrP biosynthesis is initiated by cleavage of the *N*-terminal signal sequence in the endoplasmic reticulum (Hope *et al.*, 1986; Hope *et al.*, 1988). A glycophosphatidyl inositol (GPI) anchor is attached following removal of a hydrophobic *C*-terminal domain and high mannose glycan chains are added to one or both of the two potential *N*-linked glycosylation sites (Stahl *et al.*, 1990). Pulse-chase metabolic labeling studies show that the mature $PrP^{c}$ species is transported to the cell surface within 60 minutes. Membrane-bound $PrP^{c}$ has a half-life of approximately 3 to 6 hours (Caughey *et al.*, 1989; Borchelt *et al.*, 1990; Caughey and Raymond, 1991) after which it is catabolized via conventional endocytic pathways (Caughey, 1991; Hare, 1990).

Pulse-chase metabolic labeling studies of $PrP^{sc}$ formation strongly suggest that the scrapie isoform is synthesized from $PrP^{c}$ (Borcheldt *et al.*, 1990; Caughey and Raymond, 1991). $PrP^{sc}$ is resistant to GPI-anchor cleavage from the cell membrane by phosphatidyl inositol-specific phospholipase C (Caughey *et al.*, 1990; Safar *et al.*, 1991) and its formation is inhibited in PIPLC-treated cells (Caughey and Raymond, 1991). These observations indicate that $PrP^{sc}$ is

produced from a precursor that resides on the cell surface, albeit transiently (Caughey, 1991). GPI-anchored proteins are directed to cholesterol- and glycolipid-rich membrane microdomains called caveolae (Simons and van Meer, 1988). The functional and structral integrity of caveolae is severely disrupted by the depletion of cholesterol (Anderson, 1992; Chang *et al.*, 1992; Rothberg *et al.*, 1992). The observation that cholesterol depletion of scrapie-affected mouse neuroblastoma cell cultures inhibits the formation of $PrP^{sc}$ lends further support to the importance of these discrete lipid microdomains as key biosynthetic sites in the formation of $PrP^{sc}$ (Taraboulos *et al.*, 1995). PrP and other cell membrane components are internalized in endosomes which upon fusing with Golgi-derived hydrolytic vesicles form endolysosomes and lysosomes. Protease-sensitive proteins are digested in these intracellular compartments and amino acid precursors are released (Hare, 1990). Although this mechanism accounts for the catabolism of $PrP^{c}$, $PrP^{sc}$ is only partially sensitive to hydrolysis. Protease-resistance must therefore be conferred prior to internalization within endolysosomes and lysosomes (Caughey and Raymond, 1991), thus again indirectly supporting the role of caveolae in $PrP^{sc}$ synthesis.

$PrP^{sc}$ is a metabolically stable molecule with a half-life in excess of 48 hours (Borchelt *et al.*, 1990; Caughey and Raymond, 1991). Despite numerous studies no chemical modifications in $PrP^{sc}$ structure have been found which distinguish it from $PrP^{c}$ (Hope *et al.*, 1986; Hope *et al.*, 1988; Meyer *et al.*, 1986; Oesch *et al.*, 1985; Stahl *et al.*, 1992; Stahl *et al.*, 1993). It has therefore been proposed that the contrasting properties exhibited by $PrP^{c}$ and $PrP^{sc}$ are the result of differences in tertiary protein structure. Fourier transform infrared spectroscopic (FTIR) studies of the two PrP isoforms provide evidence in support of this hypothesis (Baldwin *et al.*, 1994; Caughey *et al.*, 1991; Pan *et al.*, 1993; Safar *et al.*, 1993). $PrP^{c}$ contains a high proportion of α-helix (40%) but is devoid of β-sheet. Conversely, $PrP^{sc}$ has a high content of β-sheet (48%) which is further increased by limited proteolysis and *N*-terminal truncation. This latter process favours the formation of cross β-pleated sheet amyloid structures (Pan *et al.*, 1993). It

would therefore appear that the formation of $PrP^{sc}$ involves a biotransformational process by which a protein rich in α-helix structures to converted to one in which β-sheet predominates. Within the last couple of months elucidation of the tertiary structure of $PrP^{c}$ residues 121-231 has been provided by NMR methods (Riek *et al.*, 1996). This PrP polypeptide fragment is shown to contain three α-helices and a two stranded antiparallel β-sheet. Although these studies support earlier predictions for the high α-helix content of PrP (Pan *et al.*, 1993; Safar *et al.*, 1993), the detection of a short β-sheet structure between the amino acids sequences 128 to 131 and 161 to 164, is unprecedented. In view of the marked β-sheet content of $PrP^{sc}$, the authors propose that this novel β-sheet region in $PrP^{c}$ may act as a nidus or 'nucleation site' for $PrP^{sc}$ formation.

The intracellular accumulation of $PrP^{sc}$ is believed to be a major event governing neuronal cell death and the speed of disease progression. The mechanism by which $PrP^{sc}$ has its detrimental effect may be analogous to those processes by which accumulation of β/A4 amyloid protein in Alzheimer's disease (Hardy and Allsop, 1991) or the accumulation of gangliosides in lysosomal storage diseases (Watt, 1996) cause central nervous system damage. The observation that β-sheet-forming fragments of $PrP^{sc}$ possess neurotoxic properties provides an additional mechanism by which $PrP^{sc}$ may cause its pathological effect (Forloni *et al.*, 1993; Selvaggini *et al.*, 1993).

The production of transgenic mice which lack a functional PrP gene, and thus the neuronal cell-surface protein, has provided conclusive support for the central role of PrP in scrapie pathogenesis. Prior to these experiments, PrP was universally believed to serve an essential cellular function (Bendheim *et al.*, 1991; Hope and Baybutt, 1991) based on the observation that its gene is highly conserved in a broad range of animals (Robakis *et al.*, 1986; Sparkes *et al.*, 1986; Westaway and Prusiner, 1986). However in marked contrast to these assumptions, the absence of PrP does not confer a lethal trait, with PrP-null mice displaying similar behaviour and development to their wild-type counterparts (Büeler *et al.*, 1992).

However the two genotypes differ in their susceptibility to scrapie pathogenesis. Following scrapie inoculation, PrP-null mice remain healthy and free of disease symptoms for at least 2 years whereas PrP-homozygous controls all die within 6 months (Büeler *et al.*, 1993). In view of these findings it has been proposed that the production of transgenic animals lacking the PrP gene will be a logical progression towards the establishment of scrapie and bovine spongiform encephalopathy resistant domesticated animals. Whether such an objective, although theoretically possible, is an ethically and financially viable proposition remains a matter of debate.

## 1. 4 Bovine spongiform encephalopathy and the threat to human health.

The incidence of BSE (146,000 confirmed cases between 1986 and September 1995; Patterson and Dealler, 1995) has generated a substantial amount of media attention with the increasing public perception of potential human health risks associated with greater exposure to contaminated bovine products. It has generally been assumed that dietary exposure to scrapie-affected animal tissue constitutes little risk to human health, as human forms of progressive dementia occur with a similar frequency in countries in which scrapie is both endemic and absent (Taylor, 1989). In this regard it was commonly believed that human health was unlikely to be prejudiced by exposure to BSE infectivity (Department of Health, 1989). However with the development of the BSE epidemic, control measures were implemented in the U.K. to eliminate further spread of BSE to bovines and other domesticated species, as well as to minimize the amount of infectious material entering the human food chain. In this respect bovine spongiform encephalopathy and scrapie became notifiable diseases in June 1988 and January 1993 respectively. Also, from July 1988 the feeding of ruminant-derived protein to ruminants was prohibited and in November 1989 it became illegal to use specified bovine offals (brain, intestine, spinal cord, spleen, thymus and tonsils) for human consumption (Taylor, 1993).

Creutzfeldt-Jacob disease exists in three recognised forms with different frequencies of occurrence. The hereditary form is transmitted in an autosomal dominant manner and is associated with pathogenic mutations in the gene which encodes PrP (Collinge *et al.*, 1989; Collinge *et al.*, 1990; Prusiner, 1991). Acquired forms of the disease have been discussed above in relation to kuru and iatrogenic cases of transmission. The remaining 85% of CJD cases occur with a random distribution and unknown cause, these are classified as sporadic CJD. To reiterate the discussion above, this latter form of the disease has an incidence of approximately 1:1,000,000 per year, displays distinct clinical and neuropathological features (Budka *et al.*, 1995; Bell and Ironside, 1993) and has

an average age of onset at around 65 years. The clinical duration is between 2.5 and 6.5 months (Will *et al.*, 1996). As a consequence of the BSE epidemic in cattle, an epidemiological surveillance unit was formed in the U.K. for the purpose of monitoring and identifying any changes in the incidence of Creutzfeldt-Jacob disease within the British human population. Within the last couple of months evidence has been presented detailing the emergence of a new variant of Creutzfeldt-Jacob disease, apparently unique to the United Kingdom. (Will *et al.*, 1996). In an appraisal of 207 cases of CJD between May 1990 and April 1996, ten individuals were discovered to exhibit neuropathological features significantly different from previously described classical cases of sporadic CJD. In contrast to the disease characteristics displayed above, the affected individuals within this group (four male and six female) were much younger at disease onset, i.e. an average age of 29 years (range 18 to 41 years), and as opposed to the relatively short interval between the development of clinical signs and death outlined in the sporadic cases above, the mean clinical duration of this new variant of CJD was 12 months (range 7.7 to 22.5 months). Neuropathological examination of material from all ten individuals revealed spongiform change and PrP plaques consistent with CJD diagnosis (Bell and Ironside, 1993). However, the PrP plaques observed in the latter cases were found to possess features unusual to sporadic cases of CJD. As such these proteinaceous aggregates were noted to resemble kuru-type plaques in that they possessed dense eosinophilic centres and a pale periphery. Indeed the plaques were likened to similar features in scrapie-affected animals in that they exhibited a peripheral zone of florid spongiform change (Fraser, 1979a), a property unreported in sporadic CJD plaques (Will *et al.*, 1996). The authors concluded that the observation of this new variant of CJD was "a cause for great concern" and proposed food-borne exposure to BSE as the most plausible cause of disease.

The human PrP protein contains a common polymorphism at amino acid position 129, where methionine or, less commonly, valine may be present. PrP genotypes occur in the U.K. with frequencies of 37% methionine$^{129}$ homozygotes, 51%

methionine$^{129}$-valine$^{129}$ heterozygotes and 12% valine$^{129}$ homozygotes (Collinge, 1991). Interestingly iatrogenic and sporadic forms of CJD predominantly cause disease in specific PrP genotypes. Individuals with a valine$^{129}$ homozygote PrP genotype are significantly more susceptible to iatrogenic CJD following infection with CJD-contaminated growth hormone (Collinge *et al.*, 1991), whereas sporadic cases of CJD occur with a high frequency in both homozygote PrP genotypes but with a low incidence in heterozygotes (Palmer *et al.*, 1991). In marked contrast to the iatrogenic CJD predispostion described above 'new variant' CJD occurs in methionine$^{129}$ homozygotes (Will *et al.*, 1996). This preliminary although strikingly consistent result tentatively identifies a subgroup of the population at particular risk from the BSE infectious agent.

The production of transgenic mice expressing the human form of PrP (HuPrP) has provided an experimental model in which human susceptibility to transmissible spongiform encephalopathy agents can be assessed (Telling *et al.*, 1994). When mice expressing both murine (MoPrP) and human (valine$^{129}$ transgene) forms of PrP are inoculated with brain homogenate from CJD patients, neurological disease occurs approximately 200 days latter, with the production of human $PrP^{CJD}$ (Telling *et al.*, 1994). If the same mice are challenged with the BSE infectious agent they develop disease after a protracted incubation period (> 200 days) and with the production of murine $PrP^{BSE}$ (Colling *et al.*, 1995). Mice homozygous for the human PrP transgene have not been observed to develop clinical signs of disease following BSE infection. This is perhaps not entirely unexpected in view of the reported absence of PrP valine$^{129}$ homozygotes in individuals affected with the new CJD variant (Will *et al.*, 1996). Although the above transgenic studies lead one to believe that mankind is resistant to BSE infection (Collinge *et al.*, 1995) it is noted that studies involving the human methionine$^{129}$ PrP transgene, for which BSE susceptibility is suspected, have not yet been performed. Only when these results are available will a considered appraisal of the potential threat of BSE to human health be possible.

## 1. 5 *Ante Mortem* Diagnosis of TSE Disease Status.

Diagnosis of transmissible spongiform encephalopathy status is confirmed by the histopathological examination of central nervous system tissue in which neuronal vacuolation, astrocytic gliosis and amyloid plaque formation are diagnostic hallmarks of disease. Pathology can also be confirmed by the biochemical detection of the disease-specific protein $PrP^{sc}$. Unfortunately the above techniques are restricted to the analysis of *post mortem* tissue. The inexistence of a definative *ante mortem* diagnostic test serves as a serious impediment to the positive identification of preclinically-affected animals. Availability of such a test would allow effective disease-eradication programs to be initiated and eliminate the possibility of human consumption of affected animals products.

*Ante mortem* diagnosis of scrapie in sheep and BSE in cattle relies heavily on the presentation of clinical signs consistent with neurological damage, coupled with the elimination of common differential diagnoses (Scott and Henshaw, 1994). Scrapie-affected animals classically present in a poor body condition with areas of self-inflicted fleece loss over the flanks and tailhead. Cutaneous stimulation of the skin over the dorsal sacral area produces manic lip-smaking and swaying of the hindquarters in approximately 85% of affected animals. Cerebral damage is indicated by an altered mental state with marked depression and a vacant appearance but hyperaesthesia to visual, auditory and tactile stimuli. Cerebellar damage is exemplified by postural and gait abnormalities, typically hind-limb ataxia, dysmetria (most commonly hypermetria) of the fore-limbs, and a wide-based stance. As the disease progresses affected animals spend significantly more time in sternal recumbancy. These behavioural and postural signs are also exhibited by BSE-affected cows (Hourrigan, 1990a).

Although tentatively performed, *ante mortem* diagnosis of transmissible spongiform encephalopathy status in clinically-affected animals can be attained with a certain degree of accuracy, however in the absence of neurological signs

the identification of preclinically-affected individuals is impossible. In view of the considerable incubation period before clinical signs are exhibited, preclinically-affected animals represent a significant pool of otherwise undetectable infectious material. This sinister feature of the spongiform encephalopathies has served to frustrate scrapie eradication programs in the U.S.A. (Hourrigan, 1990b), and has made a significant contribution to the transmission of infectious material in iatrogenic cases of Creutzfeldt-Jacob disease (Bernoulli *et al.*, 1977; Brown *et al.*, 1985; Duffy *et al.*, 1974; Will and Matthews, 1982).

Definitive diagnosis of TSE status can be performed by cerebral biopsy (Will *et al.*, 1996), however this procedure is physically as well as mentally traumatic and involves considerable surgical expertise. The biochemical analysis of blood may provide an acceptible, relatively non-invasive means of clinical diagnosis. CJD infectivity has been isolated in and transmitted by human blood buffy coat constituents (Manuelidis *et al.*, 1985) and immunoreactivity to protease-resistant protein has been detected in the same (Sidle, 1992). $PrP^{c}$ mRNA is expressed in lymphocytes where the gene product, $PrP^{c}$, is anchored to the cell surface by a GPI moiety (Cashman *et al.*, 1990). In view of the intimate association between $PrP^{sc}$ and scrapie infectivity (Bolton *et al.*, 1982), it seems highly probable that this haematogenous fraction contains significant titres of the infectious agent. Establishment of experimental scrapie by blood-borne inoculation is very effective, with a high proportion of infectivity being taken up by spleen and lymph nodes (Kimberlin and Walker, 1988). Oral transmission of the infectious agent is undoubtedly directed to the same target organs *via* the tonsils, Peyer's patches, gastro-intestinal lymphatics, portal vein transport and systemic circulation. Studies of disease transmission in peripherally-inoculated splenectomized (Fraser and Dickinson, 1970; Clarke and Haig, 1971, Dickinson and Fraser, 1972) and thymectomized (Fraser and Dickinson, 1978) animals suggest that B cells play a more important role in the establishment of infection than T cells. Splenectomy confers a lengthened incubation period whereas thymectomy has little to no effect. Further support for the role of lymphocytes in the establishment of

infection come from experiments of scrapie pathogenesis following experimental challenge with vaccinia virus (Marsh, 1981) or methanol extracted residue of bacille Calmette-Guerin (Kimberlin and Cunningham, 1978). In these studies mitogenic stimulation of the immune response facilitated infection by shortening the scrapie incubation period. It is interesting to note that activation of lymphocytes significantly increases the surface abundance of $PrP^c$ thereby increasing the availability of $PrP^c$ for biotransformation to the scrapie isoform. Although $PrP^{CJD}$ is present in blood at the clinical stage of disease (Sidle, 1992), it has not been established at what stage of the incubation period the abnormal isoform of PrP is first detectable. Further studies in experimentally defined murine-scrapie models will clarify the suitability of this immunological technique to the preclinical diagnosis of TSE status.

Brugere and colleagues recently described an electrochemical method by which elevated levels of a chemical were detected in the urine of scrapie-affected sheep. The authors proposed that a similar metabolite is found in urine from Alzheimer's disease patients. This substance is reduced at 850 mV and oxidized at 1200 mV and is relatively unstable to the analytical technique. The identity of this compound has not been elucidated, however the existance of an aromatic or heterocyclic substance, possibly a metabolite of the catecholamines and/or serotonin, has been speculated (Brugere *et al.*, 1991). Although the observation of this biochemical abnormality allows the detection of clinically-affected animals, it is not clear at what stage of the disease elevated levels of this metabolite become statistically significant. In addition, the test does not appear to be scrapie-specific as similar changes are detected in other neurological disorders (Alzheimer's disease). Further studies in this area are in progress and an appraisal of its application to the diagnosis of BSE-affected cattle is being performed.

The investigation of cerebral metabolism during scrapie pathogenesis by *in vivo* $^1H$ MRS permitted the detection of two prominent changes in scrapie-affected

mice (Bell *et al.*, 1991). The first of these was observed as a reduction in a proton resonance at 1.9 ppm in clinically-affected scrapie animals. This resonance was assigned to *N*-methyl protons in *N*-acetyl aspartate (NAA). Similar reductions in NAA intensity are observed in a number of cerebral disorders, including acquired immunodeficiency syndrome (AIDS) (Menon *et al.*, 1990a), herpes simplex encephalitis (Menon *et al.*, 1990b), cerebral demyelinating disorders (Arnold *et al.*, 1992; van der Knapp *et al.*, 1992) and Creutzfeldt-Jacob disease (Bruhn *et al.*, 1991). Although the function of *N*-acetyl aspartate is unknown, its primary location in neurons (Birken and Oldendorf, 1989) makes it an excellent marker of neuronal status within the brain (Small *et al.*, 1990). In this respect the reduction in *N*-acetyl aspartate in the above murine-scrapie model (ME7/VM) is believed to be indicative of extensive neuronal loss/damage exhibited at the terminal stage of disease (Fraser, 1969; Fraser, 1995). The second abnormality, which generated more interest, was observed as a broad multi-component resonance between 1.5 and 1.8 ppm. This signal was detected in scrapie-affected animals but not in age-, strain- and sex-matched controls. The observation of this metabolic abnormality preceeded the detection of $PrP^{sc}$, the onset of vacuolation, and clinical signs of disease (Bell *et al.*, 1991). As such these findings stressed the importance and potential application of this technique to the *ante mortem*, preclinical diagnosis of scrapie, and perhaps other members of the transmissible spongiform encephalopathies. *In vitro* MRS studies of cerebral perchloric acid extracts failed to detect the metabolite, it was therefore proposed that the multicomponent resonance was attributable to a non-aqueous compound, possibly lipid. Under the experimental acquisition parameters ($T_2$ relaxation time = 420 ms) it was reasoned that the signal was unlikely to have arisen from subcutaneous fat which resonates between 1.2 and 1.5 ppm and has a $T_2$ relaxation time value of 47 ± 5 ms. Rather, it was speculated that the signal was attributable to lipids which had a mobile component and were in an environment different from that normally expected, or from mobile membrane-related compounds.

Although there is a great deal of evidence to support claims of abnormal lipid profiles in Creutzfeldt-Jacob disease (Bass *et al.*, 1974; Tamai *et al.*, 1978), the same level of investigation has not been parallelled in murine-scrapie models. In fact, results in this area have been few and often contradictory. The lipid composition in membrane vesicles prepared from scrapie-affected hamster brain have been reported to show no difference to normal hamster brain (Dees *et al.*, 1985). Similarly, studies of total cerebral lipids in scrapie-affected mice found no changes in the content or composition of cholesterol and phospholipids (Guan *et al.*, 1996), a result mirrored by earlier findings (Heitzman and Skipworth, 1969; Kimberlin and Millson, 1967). In contrast, others have investigated phospholipids in brains of scrapie-affected mice and found the total phospholipid content decreased, but the composition of individual phospholipids and fatty acids constant (Tamai *et al.*, 1978). Whilst others have reported the intracerebral accumulation of neutral lipid in scrapie-affected mice by histochemical techniques (Mackenzie and Wilson, 1966). In view of the earlier discussion, it was speculated that this latter observation may provide a source for the *in vivo* MRS multicomponent resonance.

The primary objective of the research described herein was to confirm the scrapie-specificity of the novel *in vivo* magnetic resonance spectroscopy observation, reproduce the finding *in vitro*, and subsequently identify the metabolite(s) responsible for this pathological change. Studies of cerebral lipid abnormalities in relation to neuropathological changes and protease-resistant protein formation also form an integral part of the thesis

# CHAPTER TWO

# EXPERIMENTAL

## 2. 1 Tissue Excision, Storage and Decontamination.

*Animal Tissue.*

Cerebral tissue of murine origin was obtained from the Biotechnology and Biological Sciences Research Council (B.B.S.R.C.) & Medical Research Council (M.R.C.) Neuropathogenesis Unit, Edinburgh. This was predominantly derived from the inbred VM strain of mice (*Sinc* p7p7 genotype), infected with the ME7 (135A) strain of scrapie. The mice destined for disease transmission received an intracerebrally inoculation of a standard dose of the scrapie agent [ME7, 6.5 i.c. $ID_{50}$ units (negative log per 0.02 ml dose)] and were sacrificed in the terminal stage of the disease (346 ± 3 days post inoculation) when severe symptoms of ataxia, myoclonus and emaciation were exhibited. Control mice of a similar strain, gender and age received an intracerebral inoculation of normal brain homogenate suspended in isotonic buffered saline (0.9% w/v, NaCl) and were sacrificed in an identical manner.

*Tissue Excision and Storage.*

Mice were sacrificed by cerebral dislocation and subsequent decapitation. The cranial cavity was exposed by the delicate removal of the upper part of the skull within the limits of the maxilla-frontal border rostrally, the parietal-occipital border caudally and the parietal-temporal border laterally. Brains were subsequently removed post-sectioning of the optic nerves.

Depending upon the purpose for which the tissue was required, brains were either drop-frozen or freeze-clamped in liquid nitrogen. The drop-freeze method was used exclusively for material destined for high performance thin layer chromatography lipid studies. The study of aqueous metabolites by nuclear magnetic resonance spectroscopy demanded tissue in which *post mortem* changes in metabolite levels were minimal. For this purpose, tissue was subjected to an instantaneous freeze-clamp procedure in liquid nitrogen following its rapid

excision. A small amount of tissue was required for cholesteryl ester hydrolase studies, these brains were neither freeze-clamped nor drop-frozen but were placed directly on ice

*Disinfection of Scrapie-Infected Tissue.*

Although evidence to suggest that the animal transmissible spongiform encephalopathies constitute a risk to humans is inconclusive, caution and containment were exercised at all times whenever handling tissue regardless of its origin, be it infectious or not. In addition to the more common precautions, i.e. plastic gloves and laboratory coat, all tissue was processed in a fume cupboard, with work spaces regularly swabbed with hypochlorite solution. All potentially infectious material, including hypochlorite swabs, towels, containers and test tubes were soaked in 2 M sodium hydroxide (Sigma Chemical Company Ltd., U.K.) for 24 hours (Taylor, 1991) with thorough dispersal of the contents ensured by periodic agitation.

## 2. 2 Acetone-Soluble Cerebral Metabolite Extraction Procedure.

*Materials.*

Acetone-$d_6$ (99.8 atom % D), deuterium oxide (99.9 atom % D) and 3-trimethylsilyl-2,2',3,3'-tetradeuteroproprionic acid were from the Aldrich Chemical Company Ltd., U.K.

*Procedure.*

Frozen brain tissue was weighed and placed in Eppendorf tubes with 0.6 ml of ice cold acetone-$d_6$, to which was added an aliquot of 100 mM 3-trimethylsilyl-2,2',3,3'-tetradeuteropropionic acid (TSP) in deuterium oxide (5 µl). The contents were dispersed by sonication (Soniprep 150, Millipore Scientific Equipment) on ice with 15 second high energy bursts. Sonication was interspersed by 30 second periods of abstinence in order to minimize heating the brain extract. The procedure was repeated until the brain tissue adopted a creamy consistency in the solvent. The Eppendorf tube was subsequently capped and centrifuged (15,000 rpm x 10 minutes, Microspin 12, Sorvall Instruments). Following centrifugation the supernatant was removed with a glass Pasteur pipette and transferred to another Eppendorf tube. This primary supernatant was subjected to a second centrifugation as previously described and the resulting secondary supernatant, a clear acetone suspension, placed directly in an NMR tube for analysis. The acetone-$d_6$ suspension was briefly stored between 0 to 4°C for a short period prior to proton NMR analysis. Low temperature storage (≤ -4°C) of the suspension was avoided as this proved to result in metabolite precipitation.

## 2. 3 Cerebral Lipid Extraction and Fractionation.

*Materials.*

Chloroform and methanol were obtained from Fisons Laboratory Reagents, U.K. and were of analar grade. Dry nitrogen gas was from the British Oxygen Company, U.K. DEAE Sephadex A-25 was obtained from Pharmacia Fine Chemicals, U.S.A. and sodium acetate was purchased from the Sigma Chemical Company Ltd., U.K.

*Procedures.*

*Lipid Extraction.*

The lipid extraction procedure was similar to that described by Folch *et al.* (1957) with minor modifications. All lipid extraction and storage solvents were purged with dry nitrogen prior to use. Frozen brains were weighed and homogenized with two volumes of ice cold chloroform/methanol (2:1, v/v) by sonication (Soniprep 150, Millipore Scientific Equipment) over ice. In a similar manner to the aqueous metabolite extraction procedure, adequate periods were included to prevent heating of the brain extract. An additional 18 volumes of solvent were added and sonication was repeated. The suspension was stored for two hours at 0°C followed by centrifugation (2300 rpm (900 g) x 15 minutes, Denley BR401 refrigerated centrifuge). The organic supernatant was removed with a glass Pasteur pipette and transferred to a glass container. The extraction procedure was repeated a further two times with an additional 40 volumes of solvent. Pooled supernatants were evaporated to dryness under a stream of dry nitrogen and subsequently stored at -20°C.

*Fractionation of Crude Lipid Extract into Neutral and Acidic Species.*

The crude lipid extract was suspended in methanol/chloroform/water (60:30:8, by vol., 5 ml) [solvent A]. DEAE Sephadex A-25 columns of 1 ml bed volume were prepared for lipid fractionation as previously described (Ledeen *et al.*, 1973).

Briefly, columns were washed with methanol/chloroform/0.8 M sodium acetate (60:30:8, by vol., 15 ml) [solvent B] followed by equilibration with solvent A (25 ml). A proportion of the crude lipid suspension (2 ml of a 5 ml suspension) was applied to the column and neutral lipids eluted with solvent A (10 ml). Acidic lipids were subsequently eluted with solvent B (10 ml) and collected in a separate container. The individual fractions were evaporated to dryness with dry nitrogen and stored as described above.

The acidic fraction required additional processing to remove sodium acetate (a component of solvent B detrimental to high performance thin layer chromatography lipid separation and analysis). Consequently, this fraction was suspended in chloroform/methanol (2:1, v/v, 3 ml) and distilled water (0.6 ml). The contents were vortexed thoroughly for 15 seconds (Whirlimixer WM/250/F/P, Fisons Scientific Equipment) and left to partition on ice. The upper aqueous phase was removed and discarded. Chloroform/methanol/water (3:48:47, by vol., 1.4 ml) was added to the organic phase and the procedure repeated. The resulting lower organic phase was evaporated to dryness with dry nitrogen and stored in a similar manner to the neutral lipid fraction.

## 2. 4 NMR Spectroscopy Analysis of Cerebral Metabolites.

Proton spectra were accumulated on a Varian VXR600S NMR spectrometer operating at a spectrometer frequency of 599.945 MHz with a Sun 4/110 host computer running VNMR (version 4.1) under SunOS 4.1.1. All homonuclear $^{1}H$ data sets were acquired using a dedicated proton probehead. Specific acquisition parameters relating to individual experiments are given below.

### 2. 4. 1 Assignment of Acetone-Soluble Metabolites at 600 MHz.

*Materials.*

Acetic acid, *N*-acetyl aspartate, *L*-alanine, *L*-asparagine, γ-aminobutyric acid, *L*-glutamic acid, *L*-glutamine, glycerophosphorylcholine, *L*-glycine, inositol, lactate, phosphorylcholine, phosphocreatine, taurine and *L*-threonine were from the Sigma Chemical Company Ltd., U.K. Acetone-$d_6$ (99.8 atom % D) was from the Aldrich Chemical Company Ltd., U.K.

*Acquisition Parameters.*

Control murine brain material was extracted with acetone-$d_6$ as described in Section 2. 2. One-dimensional spectra were acquired over a 6 kHz sweep width into 36K complex data points with an acquisition time of 3 seconds using a 2 second recycle delay. The residual water signal was suppressed by weak irradiation centered at the water frequency during the pulse delay.

Two-dimensional COSY 45 data sets were acquired over a sweep width of 6 kHz in both dimensions with an acquisition time of 171 milliseconds and a pulse delay of 4.8 seconds. 16 transients were accumulated for each of 256 FIDs into 2K complex data points in both dimensions. Data was apodized in both dimensions using a pseudo-echo type weighting function prior to Fourier transformation. Spectra were referenced to the *N*-acetyl aspartate methyl singlet at 2.02 ppm (Fan *et al.*, 1986).

Spectral assignment of acetone-soluble cerebral metabolites was normally made directly on tissue extracts using a combination of one-dimensional, *J*-resolved and two-dimensional COSY 45 NMR experiments. These were correlated with spectra of authentic compounds where possible. The identity of peaks chosen for quantification were verified by 'spiking' the cerebral extract with authentic compounds. The results thus obtained were compared with literature values if available.

### 2. 4. 2 Comparative Analysis of Acetone-Soluble Metabolites at 360 MHz.

Levels of aqueous metabolites were compared in six terminally-ill ME7-affected VM mice and an equal number of age- and sex-matched controls. Proton NMR spectra were recorded on a Brüker WH-360 MHz spectrometer at a spectrometer frequency of 360.135 MHz. One-dimensional spectra were acquired over a sweep width of 4 kHz into 32K complex data points with an acquisition time of 4 seconds and a recycle delay of 2 seconds. The residual water signal was suppressed by weak homogated decoupling centered at the water frequency during the pulse delay. A total of 64 acquisitions were found to be adequate for quantitative measurements. Spectra were referenced internally to the 3-trimethylsilyl-2,2',3,3'-tetradeuteropropionic acid (TSP) singlet at 0.00 ppm.

### 2. 4. 3 NMR Spectroscopy Analysis of Cerebral Lipids.

*Materials.*

Fully deuterated methanol (99.9 atom % D) and chloroform (99.9 atom % D) were from the Aldrich Chemical Company Ltd., U.K. Disodium hydrogen phosphate, sodium deoxycholate and ethylene diaminetetraacetic acid (EDTA) were purchased from the Sigma Chemical Company Ltd. Other chemicals were from the sources previously stated. Lipid standards including: cardiolipin, cholesterol, cholesteryl oleate, diglyceride, galactocerebrosides I and II, oleyl alcohol, phosphatidyl choline, phosphatidyl ethanolamine, phosphatidyl inositol, phosphatidyl serine, sphingomyelin, sulfatides I and II and triglyceride, were

obtained from the Sigma Chemical Company Ltd., U.K. and wherever possible were from a cerebral source.

*Acquisition Parameters.*

Extensive $^{1}H$, $^{13}C$ and $^{31}P$ NMR analysis was performed on the more prominent lipid species extracted from murine brains. Initially the investigations were centered on the assignment of lipid resonances and the identification of diagnostic lipid signals which would allow quantification of individual lipid species. Spectral assignment of cerebral lipids was normally made directly on tissue extracts using a combination of one-dimensional $^{1}H$, *J*-resolved, two-dimensional COSY 45, one-dimensional $^{13}C$, $^{13}C$-DEPT and HMQC NMR experiments. These were correlated with spectra of authentic compounds where possible. The identity of peaks chosen for quantification were verified by 'spiking' the cerebral extract with authentic compounds. The results thus obtained were compared with literature values if available.

Lipid fractions destined for $^{1}H$ and $^{13}C$ NMR spectroscopy experiments were dissolved in 0.65 ml of deuterated chloroform/deuterated methanol (2:1, v/v) and placed in NMR tubes of 5 mm internal diameter.

Phospholipid species purposed for $^{31}P$ NMR spectroscopy analysis required additional processing in order to optimize the resolution of individual lipid resonances. In this procedure the lipid fractions were washed with aqueous EDTA to remove endogenous cations and dispersed as micelles in a solution of deoxycholate (Capuani *et al.*, 1992). Briefly, the lipid fractions were suspended in chloroform/methanol (2:1, v/v, 3 ml) and washed with an equal volume of aqueous 100 mM EDTA, pH 7. The aqueous layer was discarded and the organic phase evaporated to dryness under dry nitrogen. Sodium deoxycholate was added to the lipid in a 3:1 (w/w) ratio with an aliquot of 100 mM aqueous disodium hydrogen phosphate (20 µl) for reference purposes, and deuterium oxide (0.65 ml). Lipid dispersion was achieved by sonication in a bath sonicator

(Sonicor, Sonicor Instrument Corporation, U.S.A.) and the pH adjusted to 11.4 with sodium hydroxide solution (0.5 M).

*$^{1}H$ NMR Spectroscopy Analysis of Cerebral Lipids.*

One-dimensional spectra were acquired over a 7 kHz sweep width into 41K complex data points with an acquisition time of 3 seconds using a 2 second recycle delay. The probe temperature was maintained at 25°C. *J*-resolved data sets were accumulated over a 5.48 kHz sweep width into 8K data points with a recycle delay of 2 seconds. 16 scans were acquired for each of 64 FIDs over an F1 sweep width of 30 Hz. Data was zero filled in F2 to 16K data points prior to Fourier transformation.

Two-dimensional COSY data sets were acquired using a COSY 45 scheme in absolute value mode. 16 transients were accumulated for each of 512 FIDs into 2K complex data points over a sweep width of 4.7 kHz in both dimensions. Data was apodized in both dimensions using a pseudo-echo type weighting function prior to Fourier transformation. Two-dimensional HMQC data was accumulated in a phase sensitive mode using a States method of phase cycling on a dual (inverse) probehead. 16 scans were acquired for each of 256 complex FIDs over a 4.7 kHz sweep width into 4K complex data points and an F1 sweep width of 33 kHz. A recycle delay of 2 seconds preceded a Bird null period to allow for elimination of $^{12}C$ attached proton signals. $^{13}C$ nucleus decoupling was achieved during the acquisition time by 'WALTZ' decoupling. Two dimensional data were acquired in an interleaved manner without spinning the sample. Data were processed on a remote Sun 4/330GX data station using VNMR software (version 4.1) operating under SunOs 4.1.1. Spectra were referenced internally to the methanol quintet at 3.30 ppm.

*$^{13}C$ NMR Spectroscopy Analysis of Cerebral Lipids.*

Due to the low sensitivity of this method, three brain lipid equivalents were used in the analysis without prior fractionation. $^{13}C$ spectra were accumulated at a spectrometer frequency of 150.869 MHz on a broadband probehead over a sweep width of 34 kHz with an acquisition time of 0.7 seconds and a recycle delay of 0.5 seconds using continuous proton 'WALTZ' decoupling. $^{13}C$ DEPT spectra were acquired concurrently using a recycle delay of 2 seconds and proton decoupling during the acquisition time only. Spectra were referenced internally to the methanol singlet at 49.0 ppm.

*$^{31}P$ NMR Spectroscopy Analysis of Cerebral Lipids.*

$^{31}P$ spectra were accumulated at 242.854 MHz over a 2.9 kHz sweep width into 9.3 K data points with an acquisition time of 1.6 seconds and a 2 second delay. The sample spin frequency was 15 Hz and probe temperature was maintained at 25°C. Spectra were referenced to the internal $PO_4^{3-}$ singlet at 3.509 ppm.

*In Vivo $^{1}H$ NMR Spectroscopy Analysis of Cerebral Metabolites.*

*In vivo* $^{1}H$ NMR analysis was performed at Queen Mary and Westfield College (University of London) by Drs. Jimmy Bell, Jane Cox and Stephen Williams. Spectra were obtained at 4.7 Tesla using an Oxford 30 cm horizontal bore magnetic controlled by a SISCO 200 spectrometer. Data were collected from an 8 mm diameter surface coli placed directly on the mouse head. Water suppression was achieved using the spin echo variant of the binomial pulse pulse sequence: 1331 TE/2 2662 TE/2-Acq with the excitation maximum centred for the *N*-acetyl aspartate methyl singlet at 2.02 ppm. Each spectrum acquired represented the sum of 1024 transients using an echo time of 420 milliseconds and a pulse repetition time of 1.8 seconds, giving an acquision time of approximately 30 minutes.

## 2. 5 HPTLC Analysis of Cerebral Lipids.

*Materials.*

High performance thin layer chromatography silica gel 60 plates (10 x 10 cm, silica gel thickness 200 μm, mean particle size 5 to 6 μm, mean pore diameter 60 Å) were purchased from B.D.H. Merck Ltd., U.K. Acetic acid, cupric acetate, diethyl ether, diisopropyl ether, formic acid and orthophosphoric acid were obtained from Fisons Laboratory Reagents, U.K. Lipid standards including: cardiolipin, cholesterol, cholesteryl oleate, diglyceride, galactocerebrosides I and II, oleyl alcohol, phosphatidyl choline, phosphatidyl ethanolamine, phosphatidyl inositol, phosphatidyl serine, sphingomyelin, sulfatides I and II and triglyceride, were obtained from the Sigma Chemical Company Ltd., U.K. and wherever possible were from a cerebral source.

*Procedure.*

The high performance thin layer chromatography methodology adopted was essentially that attributed to Macala *et al.* (1983). High performance thin layer chromatography plates were eluted with chloroform/methanol/water (60:30:8, by vol.) prior to loading with lipid for the purpose of removing substances bound to the silica which otherwise interfered with the visualization of lipid bands upon charring of the plate. Following 'clearing', plates were activated by heating at 110°C for 20 minutes and cooled in a vacuum desiccator. Authentic lipids obtained from the Sigma Chemical Company Ltd. were assessed for h.p.t.l.c. purity and subsequently used to produce calibration curves from which the unknown cerebral lipid quantities were calculated. A quantity of oleyl alcohol (2.5 μg) was applied to each lane for standardization purposes (Macala *et al.*, 1983).

Neutral and acidic lipid fractions were applied to separate h.p.t.l.c. plates in which lanes were positioned 1 cm above the bottom edge of the plate, were 5 mm in

width and separated by 5 mm divisions. Solvent systems were equilibrated one hour before use in glass t.l.c. tanks (Aldrich Chemical Company Ltd., U.K.) lined with filter paper. Neutral lipids were eluted with chloroform/methanol/acetic acid/formic acid/water (35:15:6:2:1, by vol.) until the solvent front was 5 cm above the origin. Acidic lipids were eluted in a similar manner until the solvent front was 5.5 cm above the origin. Following the separation of polar lipids, the plates were dried in a fume cupboard for 30 minutes followed by vacuum desiccation for at least eight hours, ensuring the complete removal of residual acetic acid. The non-polar lipid components were then separated by elution with hexane/diisopropyl ether/acetic acid (65:35:2, by vol.) allowing the solvent front to run to the top of the plate.

Following development and drying, plates were sprayed with a solution of 3% cupric acetate in 8% orthophosphoric acid until saturated and charred in an oven at 180°C for 15 minutes (Macala *et al.*, 1983). Cerebral lipids were identified by co-migration with authentic standards and subsequently quantified by laser scanning densitometry on a Molecular Dynamics Series 300 Computing Densitometer running the ImageQuant version 3.0 Fast Scan package. Minor adjustments were made to the calculations of lipid quantity to compensate for variations in experimental charring conditions by standardization to a known quantity of oleyl alcohol as described previously.

## 2. 6 Purification and Analysis of Specific Lipid Species.

*Materials.*

Aminopropyl silica SEP PAK columns were from Waters Chromatography Division (Millipore), U.K. Hexane was purchased from Fisons Laboratory Reagents Ltd., U.K. Other materials were from the sources previously stated.

*Procedure.*

A number of lipid abnormalities were detected by high performance thin layer chromatography in the cerebral extracts from scrapie-affected and control mouse brains. These lipids were characterized in greater detail by mass spectrometry and nuclear magnetic resonance spectroscopy. The lipid species were purified prior to analysis by bonded phase chromatography on aminopropyl silica SEP PAK columns. This greatly assisted the interpretation of analytical data, a factor most commendable in the clarification of nuclear magnetic resonance spectroscopy results.

***Cholesteryl esters.***

(High performance thin layer chromatography analysis of brain tissue from scrapie and control mice in the ME7/VM model revealed elevated levels of a non-polar, neutral lipid in diseased animals. This appeared to co-migrate with authentic cholesteryl oleate and is thus referred to as the 'cholesteryl ester' fraction).

*Purification by Bonded-Phase Column Chromatography.*

The 'cholesteryl ester' fraction was isolated by column chromatography on aminopropyl silica SEP PAK columns as described by Kaluzny *et al.* (1985). The procedure was as follows, bonded-phase columns were equilibrated with two quantities of hexane (2 x 4 ml) followed by the application of neutral lipid to the column in 200 µl of hexane. The fraction containing 'cholesteryl esters' was

eluted with 4 ml of hexane. The limited capacity of the columns (7 mg lipid/360 mg column) necessitated the use of several columns per brain extract to obtain a satisfactory yield of 'cholesteryl esters' in the absence of other lipid contaminants. An assessment of the degree of 'cholesteryl ester' isolation was afforded by the analysis of the pooled fractions by h.p.t.l.c. and confirmation that the fraction of interest co-migrated with cholesteryl oleate from an authentic source.

*Analysis by Chemical Ionization Mass Spectrometry (CI-MS).*

Mass spectrometry was performed on a Fisons VG Analytical ZAB-T instrument with BEBE geometry incorporating an array detector (Rollins *et al.*, 1990). Spectra were obtained in the positive chemical ionization (CI) mode using ammonia as the carrier gas, with a probe program of 30-620°C at 50°C per minute. For tandem mass spectrometry (MS-MS) the column energy was 4 kV, the array detector was adjusted for a mass range of 1.22:1, attenuation was 80%, and argon-$H_2O$ was used as the collision matrix.

***Triglycerides.***

*Purification by Bonded-Phase Column Chromatography.*

Following the elution of cholesteryl esters with 4 ml of hexane, the fraction containing the suspected triglyceride abnormality was eluted from the SEP PAK column with 5% ethyl acetate in hexane (4 ml). The degree of 'triglyceride' isolation was assessed by high performance thin layer chromatography in a similar manner to that described for cholesteryl esters.

*Analysis by $^1H$ NMR Spectroscopy.*

The cerebral 'triglyceride' fraction was dissolved in 0.65 ml of deuterated chloroform/deuterated methanol (2:1, v/v) and placed in an NMR tube of 5 mm internal diameter. The experimental acquisition parameters for proton NMR analysis were as described in Section 2. 4. 3 with spectra referenced to the methanol quintet at 3.30 ppm.

*Analysis by Chemical Ionization Mass Spectrometry.*

*(i) Production of Fatty Acid Methyl Esters.*

*Materials.*

Concentrated sulphuric acid and toluene were obtained from Fisons Laboratory Reagents, U.K. Sodium sulphate was from the Sigma Chemical Company Ltd., U.K. Methanol, from Fisons, was dried over calcium hydride, from the Aldrich Chemical Company Ltd., U.K.

*Procedure.*

The fatty acid constituents of the triglyceride fraction underwent analysis by chemical ionization mass spectrometry following derivative formation to fatty acid methyl esters. Fatty acid methyl esters were prepared following the method of Hitchcock and Hammond (1980). The transmethylation reagent was prepared by the cautious addition of concentrated sulphuric acid (5 ml) to anhydrous methanol (100 ml) with stirring. To this mixture was added dry toluene (50 ml). Triglyceride (5 mg), from the cerebral source, was placed in a 10 ml round bottom flask with the transmethylation reagent (5 ml) and an antibumping granule. The contents were refluxed for 60 minutes in a water bath. The cooled solution was transferred to a separating funnel, to which was added distilled water (3 ml) and diethyl ether (3 ml). The contents were shaken thoroughly to ensure adequate recovery of the fatty acid methyl esters in the organic phase. The lower aqueous phase was removed and discarded. The organic phase was dried over sodium sulphate (5 minutes), filtered, and evaporated under dry nitrogen to give a residue which was stored at -20°C prior to analysis.

*(ii) Chemical Ionization Mass Spectrometry of Fatty Acid Methyl Esters.*

Mass spectroscopy was performed on a Kratos MS50TC mass spectrometer incorporating a magnetic sector analyzer. Spectra were obtained in the positive chemical ionization (CI) mode using methane as the carrier gas, an ion source

pressure of 1 Torr and a probe program of 30 to 350°C at 60°C per minute. Accurate mass spectroscopy was performed on the molecular ion with a *m/z* ratio of 294 and an atomic composition peak-match program run on the same.

## 2. 7 Neutral Cholesteryl Ester Hydrolase Studies in Scrapie-Affected Mice (ME7/VM Model).

The determination of neutral cholesteryl ester hydrolase activity in murine cerebral tissue was attempted following a number of different procedures. Unfortunately, the primary objective of the exercise, that being to examine whether scrapie and control extracts exhibited different levels of activity, was not successful. However, the chronological progression of experiments leading to the optimization of incubation conditions are described herein in order that future investigators may avoid the same problem areas encountered by the author.

### *Synthesis and Purification of Cholesteryl [9, 10-$^{3}$H(N)] oleate.*

*Materials.*

[9,10-$^{3}$H(*N*)] oleic acid and [1-$^{14}$C]oleic acid were purchased from Du Pont (U.K.) Ltd., New England Nuclear Products. Dicyclohexylcarbodiimide and dimethyl aminopyridine were from the Sigma Chemical Company Ltd., U.K. Dichloromethane, ethyl acetate, hydrochloric acid and sodium bicarbonate were obtained from Fisons Laboratory Reagents, U.K. Silica gel 60 was from Fluka Chemika, U.K. and liquid scintillation fluid (6927-57) was from Koch-Light Laboratories Ltd. Other materials were from the aforementioned sources.

*Procedure.*

Cholesteryl [9,10-$^{3}$H(*N*)] oleate was synthesized from cholesterol and [9,10-$^{3}$H(*N*)] oleic acid following the method attributed to Neises and Steglich (1978). [9,10-$^{3}$H(*N*)] oleic acid (50 µmol, 0.5 Ci) and unlabelled oleic acid (50 µmol, 14.06 mg) were placed in a 5 ml Quickfit round bottom flask with dry dichloromethane (1 ml). The reagents were continually mixed with a magnetic stirrer on ice (B212 hotplate/stirrer, Bibby Science Products Ltd., U.K.). To the fatty acid was added dimethylaminopyridine (20 µmol, 2.44 mg), cholesterol (200 µmol, 77.34 mg) and dicyclohexylcarbodiimide (100 µmol, 20.63 mg). The

reaction mixture was kept at 0°C for 5 minutes and then at room temperature (20°C) for 3 hours. Upon completion of the reaction the products were filtered to remove precipitated urea. The filtrate was evaporated to dryness with dry nitrogen and resuspended in dry dichloromethane (0.5 ml). The filtration procedure was then repeated. The resulting filtrate was washed twice with 0.5 M hydrochloric acid (2 x 20 ml) and finally with a saturated solution of sodium bicarbonate (20 ml). The lipid solution was dried over anhydrous sodium sulphate (5 minutes), evaporated to dryness under dry nitrogen and stored at -20°C.

Separation of radiolabelled cholesteryl oleate from the crude methylated lipid mixture was performed by column chromatography on silica gel 60. A 10 ml bed volume column was equilibrated with 1% ethyl acetate in hexane (100 ml). The lipid mixture was applied to the column in a small volume of eluant (0.50 ml) and non-polar lipids eluted with 1% ethyl acetate in hexane. Fractions were collected in 0.5 ml aliquots and examined for lipids co-migrating with authentic cholesteryl oleate by high performance thin layer chromatography. Cholesteryl oleate eluted in fractions 13 to 19 (volume 6.5 to 9.5 ml), whilst what was believed to be the *N*-acylurea derivative of oleic acid eluted in fractions 21 to 24 (volume 10.5 to 12 ml). The cholesteryl oleate fractions were pooled and evaporated to dryness under dry nitrogen. On the basis of weight (10.2 mg), the purified radiolabelled cholesteryl oleate represented a 16% yield. A 20 µl aliquot of a 5 ml suspension of this lipid was found to have an activity of $2.98 \times 10^5$ dpm ($3.36 \times 10^{-5}$ Ci), thus a specific activity of 2.15 mCi/mmol (LKB Rackbeta Liquid Scintillation Counter). The cholesteryl [9,10-$^3$H(*N*)] oleate was subsequently diluted with non-radiolabelled cholesteryl oleate to give a specific activity of 0.6 mCi/mmol.

Each incubation mixture contained 125 µg of cholesteryl oleate and an activity of $2.5 \times 10^5$ dpm. Those in which the activity of authentic cholesteryl ester hydrolase (EC. 3.1.1.13, bovine pancreas) was assessed contained twice this amount.

***Neutral Cholesteryl Ester Hydrolase Assay.***

*Materials.*

Bovine serum albumin (> 98%), cholesteryl esterase EC. 3.1.1.13 (source: bovine pancreas), 2-(*N*-morpholino)ethanesulfonic acid, sodium phosphate, sodium taurocholate, sucrose, tris[hydroxymethyl]aminomethane and Triton X-100 were obtained from the Sigma Chemical Company Ltd., U.K. A bicinchoninic acid (BCA) protein assay kit was from Pierce Ltd., U.K. Other materials were from the sources previously stated.

*Procedures.*

*(i) Method attributed to Eto and Suzuki (1973).*

Control brain material was homogenized in 9 volumes of ice-cold 0.32 M sucrose (approximately 3.6 ml) in a Dounce homogenizer with a tight-fitting pestle. The enzyme source was either this homogenate or the supernatant produced after centrifugation (2,300 rpm (900g) x 15 minutes, Denley BR401 refrigerated centrifuge).

A 10 µl aliquot of both suspensions was diluted 100 fold with 0.99 ml of ice-cold 0.32 M sucrose. Protein determination was performed on a 0.1 ml aliquot of the diluted suspension by reaction with bicinchoninic acid (BCA) (Smith *et al.*, 1985). Briefly, an aliquot of brain suspension was mixed with 2.0 ml of working reagent (sodium carbonate, sodium bicarbonate, BCA detection reagent, sodium tartrate in 0.2 M sodium hydroxide and 4% copper sulphate) and incubated at 37°C for 30 minutes. The tubes were cooled to room temperature and the absorbance measured at 562 nm against a 0.32 M sucrose/reagent blank. The protein concentration of the brain suspension was determined following comparison with a standard calibration curve prepared from known concentrations of bovine serum albumin. The protein concentration of the brain suspension was adjusted to approximately 10 mg/ml for the enzyme assay. This was achieved following lyophilization and resuspension in a suitable volume of

distilled water. An aliquot of this crude homogenate (0.2 ml) was used as the enzyme source, this containing approximately 2 mg of protein.

Cholesteryl [9,10-$^{3}$H(*N*)] oleate (125 µg, 250,000 dpm) in hexane was placed in a glass test tube with sodium taurocholate (4 µmol) in methanol. The contents were dried under dry nitrogen. To this was added sodium phosphate buffer (0.1 M, pH 7.0, 1 ml) and the reagents evenly dispersed by bath sonication (Sonicor, Sonicor Instruments Corporation, U.S.A.). The suspension was temperature equilibrated in a water-bath at 37°C with gentle shaking. To the reagents was added a 0.2 ml aliquot of the brain extract and the incubation continued for two hours.

All incubation mixtures were terminated with the addition of chloroform/methanol (2:1, v/v, 3.0 ml) and subsequently treated identically. Additional chloroform was added (2.0 ml) together with oleic acid (200 µg) in methanol and 7,500 dpm of [1-$^{14}$C] oleic acid. The two phases were vortexed thoroughly (15 sec), then left for 12 hours at 0 to 4°C to partition. The lower organic phase containing the lipid extract was removed and evaporated to dryness under dry nitrogen.

Separation of [9,10-$^{3}$H(*N*)] oleic acid (the hydrolysis product) from cholesteryl [9,10-$^{3}$H(*N*)] oleate was performed on bonded phase aminopropyl silica SEP PAK columns following the procedure attributed to Kaluzny *et al.* (1985). The lipid suspended in hexane (200 µl) was applied to equilibrated SEP PAK columns (see Section 2. 6). Radiolabelled cholesteryl oleate, together with the majority of neutral lipids, were eluted with 15% ethyl acetate in hexane (5 ml) and discarded. Radiolabelled oleic acid was eluted with 2% acetic acid in diethyl ether (5 ml). This fraction was retained, evaporated to dryness under dry nitrogen and suspended in 2 ml of liquid scintillation fluid.

Liquid scintillation counting was performed on a LKB Rackbeta Liquid Scintillation Counter. The oleic acid fraction obtained from the above isolation

procedure contained both $^{3}H$ and $^{14}C$ isotopes. Tritium contributed insignificantly to the $^{14}C$ energy spectrum above the [345 - 354] energy window, this allowing the percentage contribution of the $^{14}C$ radiolabelled compound to be determined. Following its correction to a 100% reading, the $^{3}H$ oleic acid count was calculated by subtraction from the overall total. Corrections for lipid recovery, background emissions and counting efficiency were made and the quantity of [9,10-$^{3}H(N)$] oleic acid in the lipid extract determined.

*(ii) Method attributed to Shah and Johnson (1980).*

Brains were homogenized in ice-cold 0.32 M sucrose as described previously. Cholesteryl [9,10-$^{3}H(N)$] oleate (125 µg, 250,000 dpm) in hexane was placed in a glass test tube with Triton X-100 (2%, 0.2 ml) in methanol and the solvents evaporated under dry nitrogen. To this was added sodium phosphate buffer (0.1 M, pH 6.5, 0.8 ml) and the reagents dispersed by bath sonication. The incubation reaction was initiated with the addition of the brain suspension (2 mg of protein, 0.2 ml) and continued for three hours at 37°C. Termination of the reaction and processing of the lipid products has been described previously.

*(iii) Method attributed to Eto and Suzuki (1973) with Authentic Cholesteryl Ester Hydrolase.*

The reagents contained cholesteryl [9,10-$^{3}H(N)$] oleate (250 µg, 500,000 dpm), a range of sodium taurocholate concentrations (1 to 10 µmol) and sodium phosphate buffer (0.1 M, pH 7.0, 1.0 ml) which were prepared in glass test tubes as described above.

To these reagents was added $10^{-2}$ units of neutral cholesteryl ester hydrolase (EC. 3.1.1.13) in a 10 µl aliquot of distilled water. (1 unit of cholesteryl ester hydrolase enzyme being the quantity of enzyme that will hydrolyze 1 µmol of cholesteryl oleate per minute at 37°C and pH 7.0). The incubation was continued

at 37°C for 25 minutes and terminated with chloroform/methanol (2:1, v/v, 3.0 ml).

*(iv) Modification of the Method attributed to West and Shand (1991) with Authentic Cholesteryl Ester Hydrolase.*

Cholesteryl [9,10-$^{3}$H(*N*)] oleate (250 µg, 500,000 dpm) in hexane and various concentrations of sodium taurocholate (1 to 10 µmol) in methanol were dried in a glass test tube under dry nitrogen. To these were added 50 mM MES/50 mM Tris buffer (pH 7.0, 0.8 ml) and either (a) no bovine serum albumin or (b) bovine serum albumin (1%, w/v, 10 mg). The reagents were thoroughly dispersed in a Dounce homogenizer with a tight-fitting pestle.

An aliquot of commercial cholesteryl ester hydrolase ($10^{-2}$ units, 0.2 ml) was added to the reagents and the incubation continued at 37°C for 25 minutes.

*(v) Modification of the Method attributed to West and Shand (1991) with Murine Brain Extract.*

The incubation reagents were prepared as described above, each tube containing cholesteryl [9,10-$^{3}$H(*N*)] oleate (125 µg, 250,000 dpm), 4 µmol sodium taurocholate, 50 mM MES/50 mM Tris (pH 7.0, 0.8 ml) and bovine serum albumin (1%, w/v, 10 mg) with the contents dispersed in a Dounce homogenizer.

Brains were homogenized in 9 volumes of ice-cold buffered sucrose solution (0.32 M, 50 mM MES/50 mM Tris, pH 7.0) with a Dounce homogenizer with tight-fitting pestle. Half of the homogenate was used as a crude enzyme source whilst the other half was centrifuged (2,300 rpm (900g) x 15 minutes, Denley BR401 refrigerated centrifuge) and the resulting supernatant used as the enzyme source. Brain suspension (2 mg of protein, 0.2 ml) was added to the reagents and the mixture incubated at 37°C for two hours.

*(vi) Determination of the Presence of a Cholesteryl Ester Hydrolase Inhibitor(s) in Brain Homogenate.*

The assay system was prepared as previously described containing: cholesteryl [9,10-$^{3}$H(*N*)] oleate (250 µg, 500,000 dpm), 4 µmol sodium taurocholate, 50 mM MES/50 mM Tris (pH 7.0, 0.8 ml), bovine serum albumin (1%, w/v, 10 mg) and either (a) 0.2 ml of 50 mM MES/50 mM Tris (pH 7.0) or (b) 0.2 ml of crude homogenate (2 mg of protein).

The incubation was initiated upon the addition of $10^{-2}$ units of authentic cholesteryl ester hydrolase and maintained at 37°C for 25 minutes. Termination of the reaction and subsequent processing of the products has been described above.

***Lactate Dehydrogenase Studies.***

A potential cholesteryl ester hydrolase abnormality in scrapie material was investigated in parallel with studies of lactate dehydrogenase activity for the purpose of comparison.

*Materials.*

A lactate dehydrogenase kit (Procedure No. 500) was purchased from the Sigma Chemical Company Ltd., U.K. Other materials were from the sources previously mentioned.

*Procedure.*

The lactate dehydrogenase kit comprised: pyruvate substrate (0.75 mM, 1 ml), 2,4-dinitrophenylhydrazine (20 mg/dL, 1 ml) in 1 M hydrochloric acid, NADH (β-nicotinamide adenine dinucleotide, reduced form, disodium, 1.28 µmol, 1 mg) and sodium hydroxide solution (0.40 M, 10 ml). Brain tissue was homogenized in 9 volumes of ice-cold sucrose solution (0.32 M, 50 mM MES/50 mM Tris, pH

7.0) and centrifuged (2,300 rpm (900 g) x 15 minutes, Denley BR401 refrigerated centrifuge). The supernatant was diluted with additional buffer to give a protein concentration of approximately 24 μg/ml.

The incubation protocol is described briefly. Pyruvate substrate (0.75 mM, 1 ml) was added to a pre-weighed NADH vial (1.28 μg, 1 mg), and the contents placed in a water-bath at 37°C for a few minutes. Brain suspension (30 μg protein/ml, 0.1 ml) was added to the reagents, and the incubation continued at 37°C for 30 minutes. The reactions were terminated by removal of the reagents from the water bath and addition of 2,4-dinitrophenyhydrazine solution (20 mg/dL, 1 ml). The contents were mixed and the colour allowed to develop (room temperature, 20 minutes). Following this period, sodium hydroxide solution (0.4 M, 10 ml) was added to the vials, these were capped and mixed thoroughly by inversion. After five minutes a sample of the solution was transferred to a cuvette and the absorbance read at 450 nm against a buffer/reagent blank. Lactate dehydrogenase activity in the brain suspension was calculated from a calibration curve of enzyme activity in Berger-Broida (B-B) units against the absorbance of the colour produced by 2,4-dinitrophenylhydrazine with various concentrations of pyruvate solution. (One B-B unit being defined as that amount of lactate dehydrogenase activity which will reduce $4.8 \times 10^{-4}$ μmol of pyruvate per minute at 25°C). The results are discussed in Section 3. 4.

## 2. 8 A Study of Lipids Associated with Sucrose Gradient GPI-anchored Protein Float Fractions.

Studies of membrane lipids were performed on isolates of GPI-anchored proteins in which protein-lipid complexes remain essentially intact (Bordier 1984; Safar, 1990). The lipid composition of these complexes was analyzed by high performance thin layer chromatography as described below.

### *Detection of lipids associated with GPI-anchored proteins.*

*Materials.*

Sucrose gradient fractions were obtained from the B.B.S.R.C. & M.R.C. Neuropathogenesis Unit, Edinburgh. Silica gel thin layer chromatography plates (dimensions 20 x 20 cm, glass support, particle size 5 - 17 μm, gel thickness 250 μm) were purchased from the Sigma Chemical Company Ltd., U.K. Other materials were from the sources previously stated.

*Procedure.*

Eight samples were presented for analysis containing different density fractions from a sucrose gradient separation of glycosylphosphatidyl inositol-anchored proteins from a control VM mouse brain. Each of these were examined for the presence of lipid by thin layer chromatography.

The aqueous sucrose fractions were extracted and washed using a procedure essentially identical to that employed for the removal of sodium acetate from acidic lipid fractions (Section 2. 3). Pellets were suspended in ice-cold chloroform/methanol (2:1, v/v, 2.0 ml) and distilled water (0.4 ml). The contents were vortexed thoroughly (15 seconds) followed by centrifugation (2,300 rpm (900g) x 15 minutes, Denley BR401 refrigerated centrifuge) at 4°C. The upper aqueous phase was removed and discarded. Chloroform/methanol/water (3:48:47, by vol., 0.9 ml) was added to the organic phase and the procedure

repeated. The resulting organic phase, containing the lipids of interest, was evaporated to dryness under nitrogen and stored at -20°C prior to analysis.

Samples were resuspended in chloroform/methanol (1:1, v/v, 20 µl) of which 10 µl was applied to a 20 x 20 cm thin layer chromatography plate. Plates were cleared prior to the application of lipid as described in Section 2. 5. Polar lipids were eluted with propanol/proprionic acid/chloroform/water (3:2:2:1, by vol.) and visualized by charring with 3% cupric acetate in 8% orthophosphoric acid.

***A comparison of lipids associated with GPI-anchored proteins from PrP-homozygote, -heterozygote and -null mice.***

*Materials.*

High performance thin layer chromatography silica gel 60 plates (10 x 10 cm, silica gel thickness 200 µm, mean particle size 5 to 6 µm, mean pore diameter 60 Å) were purchased from B.D.H. Merck Ltd., U.K. Other materials were from the sources previously stated.

*Procedure.*

Sucrose gradient float fractions were obtained from each of the following: two PrP-homozygous, two PrP-heterozygous and two PrP-null mice. Lipids in these samples were extracted with ice-cold chloroform/methanol (2:1, v/v, 2.0 ml) and distilled water (0.4 ml) as described previously. Lipids were fractionated over DEAE Sephadex A-25 and evaporated to dryness under nitrogen. It was noted that these extracts appeared to contain more lipid than the former fractions presented for analysis. Neutral lipids were dissolved in 200 µl of chloroform/methanol (1:1, v/v) of which 3 µl was applied to a high performance thin layer chromatography plate. Following the removal of sodium acetate, acidic lipids were suspended in 50 µl of chloroform/methanol (1:1, v/v) of which 3 µl was plated. 2.5 µg of oleyl alcohol was applied for standardization purposes. High performance thin layer chromatography plates were developed sequentially

in chloroform/methanol/acetic acid/formic acid/ water (35:15:6:2:1, by vol.) and hexane/diisopropyl ether/acetic acid (65:35:2, by vol.). Lipids were visualized by charring with 3% cupric acetate in 8% orthophosphoric acid and quantified by laser scanning densitometry.

***A comparison of lipids associated with GPI-anchored proteins in scrapie and control isolates and a scrapie-associated fibril fraction.***

*Procedure.*

Seven samples were presented for high performance thin layer chromatography analysis. These comprised sucrose gradient float fractions of PrP obtained from three ME7 scrapie-affected VM mice and three VM controls, and an SAF pellet purified from a clinically-ill ME7/VM mouse (Somerville *et al.*, 1989). All fractions were extracted with ice-cold chloroform/methanol/water as described above. Crude lipid was dissolved in chloroform/methanol (1:1, v/v, 20 µl) of which 5 µl was applied to high performance thin layer chromatography plates as described in Section 2. 5. Plates were developed for the visualization of non-polar, neutral lipids and phospholipids in hexane/diisopropyl ether/acetic acid (65:35:2, by vol.) and in propanol/proprionic acid/chloroform/water (3:2:2:1, by vol.) respectively. Following charring with 3% cupric acetate in 8% orthophosphoric acid, lipids were quantified by laser scanning densitometry with reference to authentic standards.

# CHAPTER THREE

# RESULTS AND DISCUSSION

## 3. 1 NMR Spectroscopy Studies of Acetone-Soluble Cerebral Metabolites.

Recent studies of cerebral metabolism in scrapie-affected mice (ME7/VM) by *in vivo* $^{1}H$ NMR spectroscopy revealed the presence of two abnormalities (Bell *et al.*, 1991). The first abnormality, a reduction in levels of *N*-acetyl aspartate in clinically-ill scrapie animals, was believed to be a reflection of the severe vacuolar degeneration and neuronal damage associated with this particular murine-scrapie model (Fraser and Dickinson, 1968). The second abnormality, which attracted the greater interest, was visualized as a multicomponent resonance with a broad chemical shift ($\delta$ = 1.5 to 1.8 ppm) which increased in intensity with scrapie pathogenesis. The realization that the observation of this signal preceded the *in vitro* detection of protease-resistant protein ($PrP^{sc}$) and histopathological damage by several weeks, and the fact that the signal was not present in cerebral *in vivo* NMR spectra of rodents with other neurological disorders (Bates *et al.*, 1989; Gadian *et al.*, 1986), emphasized the potential application of this technique to the non-invasive, preclinical diagnosis and study of scrapie disease progression.

The identity of the multicomponent resonance was not elucidated by the authors, however it was speculated that the aforementioned signal was the result of a change in the mobility of intracerebral lipid (Bell *et al.*, 1991). This hypothesis remained unsubstantiated.

The research presented herein describes our independent investigation of changes in levels of cerebral metabolites in scrapie and control mice by *in vitro* NMR spectroscopy.

### 3. 1. 1 Assignment of $^{1}$H NMR Spectrum of Acetone-Soluble Cerebral Metabolites.

Prior to the comparative analysis of metabolites, a combination of MRS experiments including one-dimensional, two-dimensional shift correlated and *J*-resolved NMR spectroscopy, together with reference to literature values (notably Fan *et al.*, 1986) and authentic metabolite 'spiking' experiments were applied to the assignment of acetone-soluble metabolite resonances. This was a necessary prerequisite for the identification of 'diagnostic signals' which were subsequently used for metabolite quantification.

The structures of the following compounds are illustrated in Figure 3. 1. 1. Extensive reference is made to these in the following description of proton assignments.

*Acetate (Ac)* [**1**]. Acetate produces a characteristic methyl proton singlet resonance at 1.90 ppm in the one-dimensional proton NMR spectrum (Figure 3. 1. 2). Extracts prepared from fresh brain do not contain appreciable levels of acetate. The presence of a relatively intense signal in this spectrum is thus considered an artefact, the result of tissue storage at -70°C for several months (Gadian, 1990). Comparison of the above spectrum with Figures 3. 1. 6a/b, obtained from freeze-clamped, directly processed tissue, illustrates the effect that storage has on cerebral acetate concentrations.

*Alanine (Ala)* [**2**]. Following comparison with literature values and multiplicities, the β-methyl protons in alanine were assigned at 1.49 ppm, these producing a doublet on coupling to the α-methine proton. Examination of the two-dimensional shift correlated spectrum revealed the β-methyl protons to be coupled to a poorly resolved complex resonance at 3.72 ppm, of which the α proton was one component. The β-methyl proton signal was used for characterization and quantitative purposes.

[1]

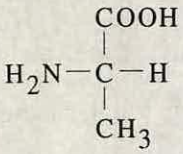

[2]

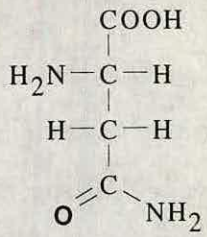

[3]

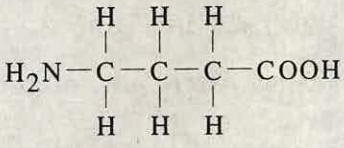

[4]

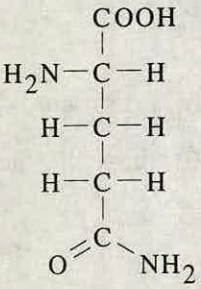

[5]

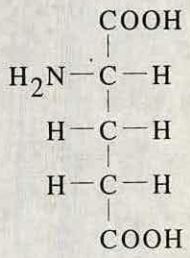

[6]

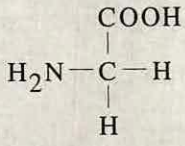

[7]

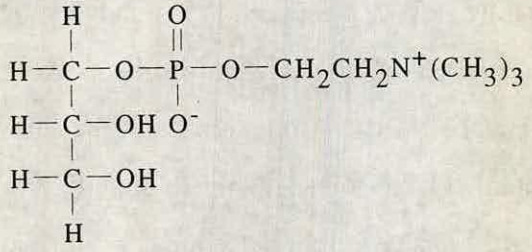

[8]

Figure 3. 1. 1a Chemical structures of acetone-soluble cerebral metabolites.

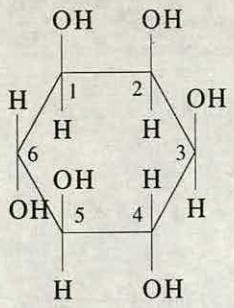

[9]

[10]

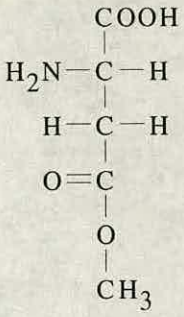

[11]

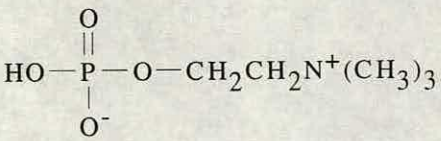

[12]

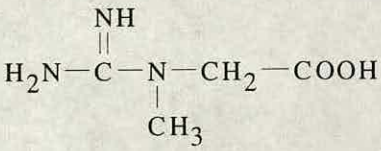

[13]

[14]

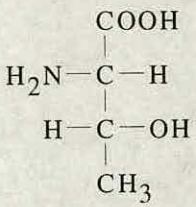

[15]

Figure 3. 1. 1b Chemical structures of acetone-soluble cerebral metabolites.

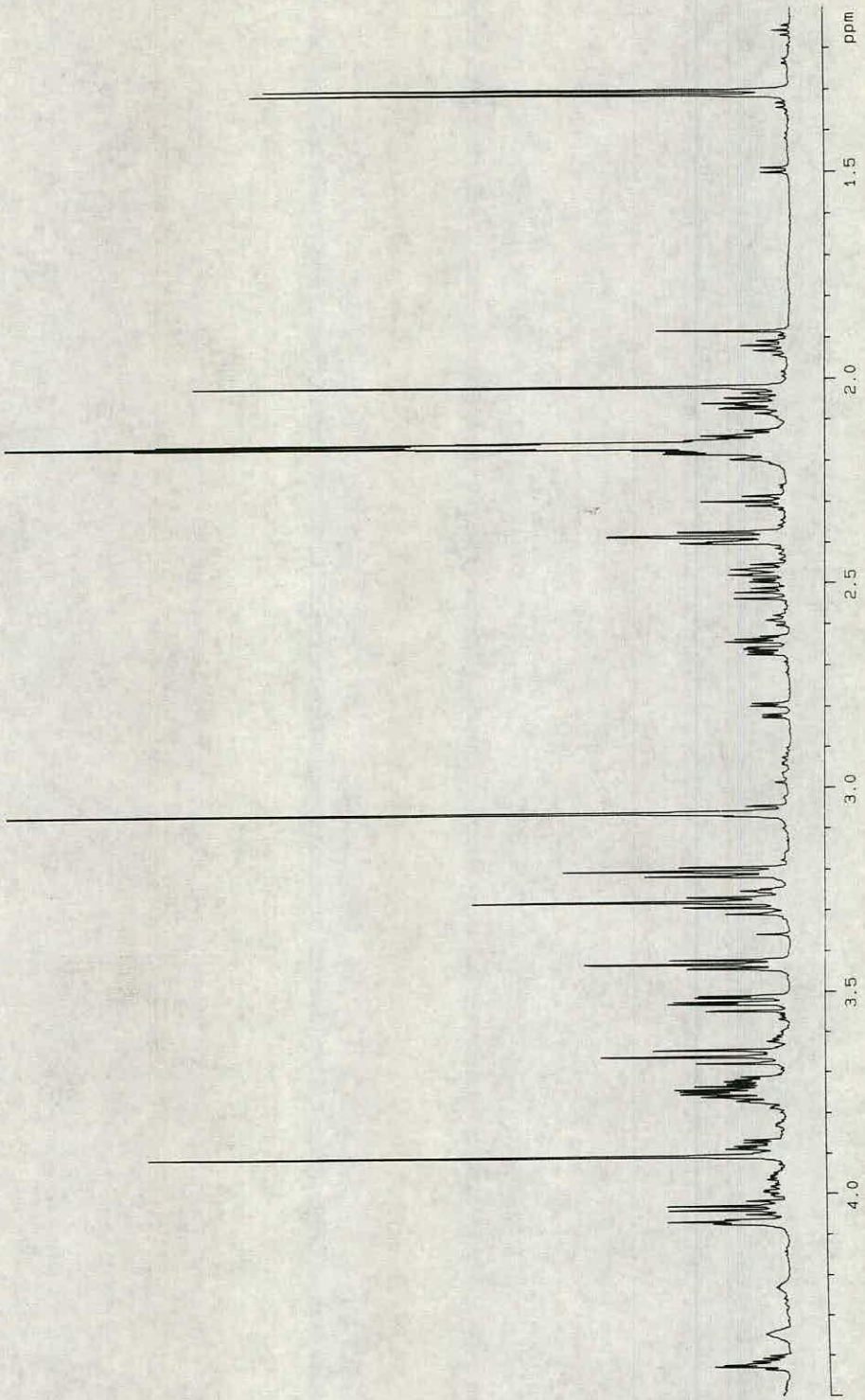


Figure 3. 1. 2a $^{1}$H NMR spectrum of acetone-soluble cerebral metabolites at 600 MHz.

Spectra where acquired as described in Experimental. Metabolite resonances were referenced to the *N*-acetyl aspartate methyl singlet at 2.02 ppm. See Section 3. 1. 1 for all metabolite abbreviations.

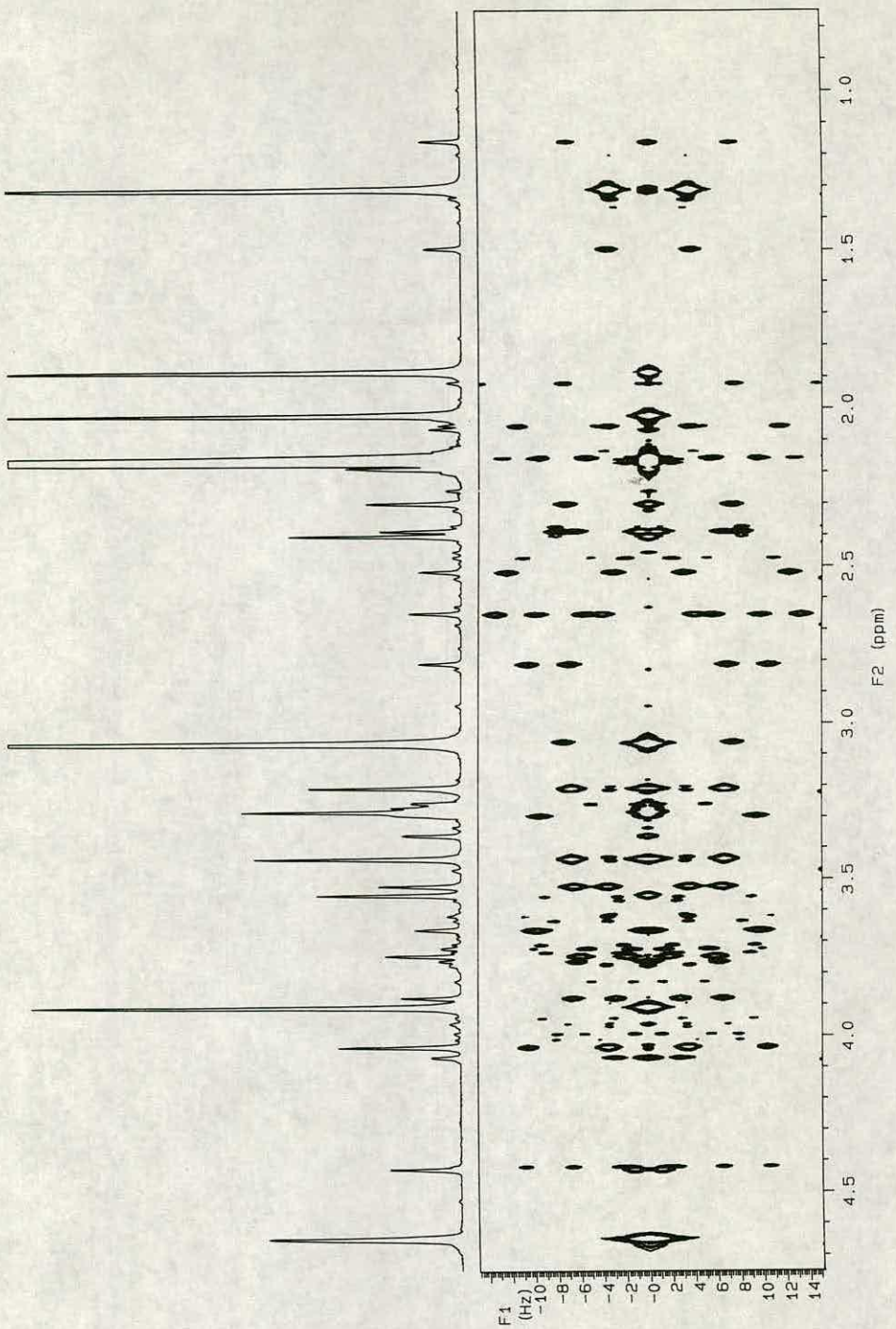


Figure 3. 1. 3 Two-dimensional *J*-resolved spectrum of acetone-soluble cerebral metabolites at 600 MHz.

Spectra where acquired as described in Experimental. Metabolite resonances were referenced to the *N*-acetyl aspartate methyl singlet at 2.02 ppm.

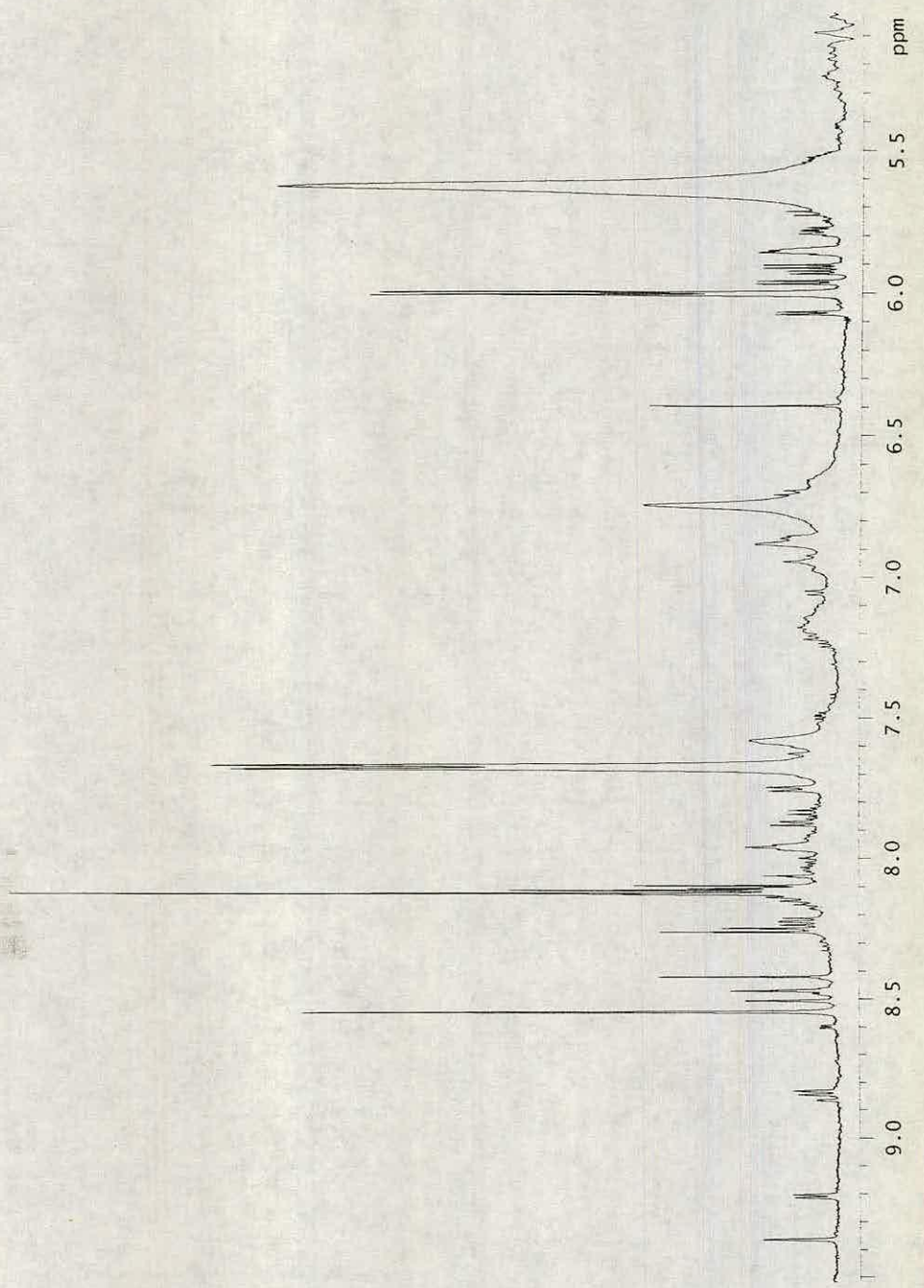


Figure 3. 1. 2b $^{1}$H NMR spectrum of acetone-soluble cerebral metabolites at 600 MHz.

Spectra where acquired as described in Experimental. Metabolite resonances were referenced to the *N*-acetyl aspartate methyl singlet at 2.02 ppm.

*Asparagine (Asp)* [**3**]. β-methylene protons in asparagine are diastereotopic giving rise to 'doublet of doublets' on coupling to the α-methine proton. In the following studies the methylene proton with a torsion angle of approximately 180° relative to the α proton was designated as $\beta^u$ and was assigned at 2.65 ppm with $^3J_{\alpha,\beta}{}^u$ of 9.4 Hz and $^2J_{\beta}{}^{u},{}_{\beta}{}^{d}$ of 17.5 Hz (Figure 3. 1. 3). The $\beta^d$ proton (with a torsion angle of approximately 60° relative to the α proton) was assigned at 2.80 ppm. This had the same geminal coupling as the $\beta^u$ proton resonance in addition to $^3J_{\alpha,\beta}{}^d$ of 3.6 Hz. Both protons were seen not only to produce cross-peaks with each other in the two-dimensional COSY 45 spectrum, but also with the α proton at 3.88 ppm (Figure 3. 1. 4). Inspection of the one-dimensional spectrum showed this signal to comprise a doublets of doublets with the *J*-resolved spectrum providing confirmatory coupling constants of $^3J_{\alpha,\beta}{}^u$ of 9.4 Hz and $^3J_{\alpha,\beta}{}^d$ of 3.6 Hz, in agreement with those previously found. The $\beta^d$ proton resonance at 2.80 ppm was sufficiently well resolved to be used for diagnostic and quantitative purposes.

*γ-aminobutyric acid (GABA)* [**4**]. GABA produces a characteristic quintet resonance from the β-methylene protons at 1.91 ppm. This was observed to produce cross-peaks with resonances at 2.30 and 3.05 ppm in the two-dimensional COSY 45 spectrum. These latter resonances were assigned to the α- and γ-methylene protons respectively, in agreement with literature values (Fan *et al.*, 1986). The γ-methylene proton was found to lie directly under the creatine methyl proton singlet at 3.06 ppm, however the α proton resonance at 2.30 ppm was well resolved and was consequently used for diagnostic purposes.

*Glutamine (Gln)* [**5**]. Glutamine resonances, although prominent, were not clearly distinguishable from other metabolite signals in the acetone-$d_6$ proton NMR spectra. On comparison with the perchloric acid extract proton spectra of Fan *et al.* (1986) and our own two-dimensional shift correlated experiments, it was noted that the β-methylene proton signal resonated under the residual acetone signal at 2.16 ppm. This signal was showed to couple to proton resonances at 2.46 and 3.76 ppm, corresponding to the γ-methylene and α-

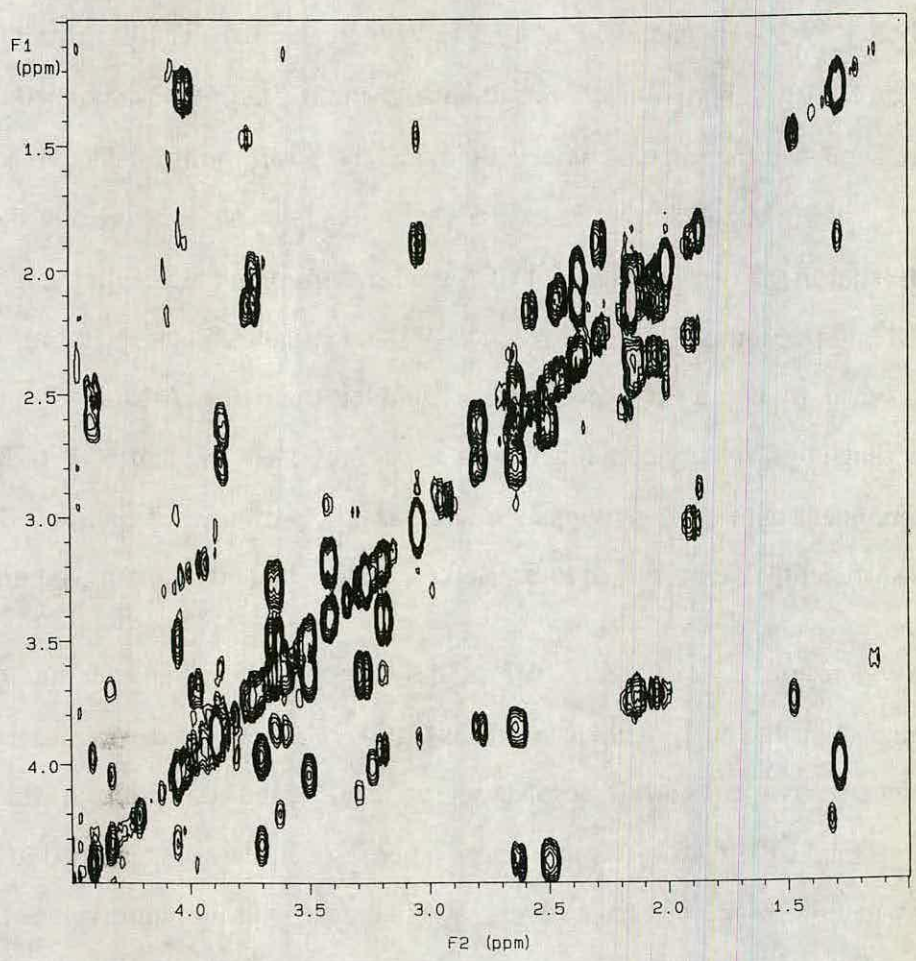


Figure 3. 1. 4 Homonuclear shift-correlated spectrum (COSY 45) of acetone-soluble cerebral metabolites at 600 MHz.

Spectra where acquired as described in Experimental. Metabolite resonances were referenced to the *N*-acetyl aspartate methyl singlet at 2.02 ppm.

methine protons respectively. Neither of these were suitable for quantitative purposes as they occurred in the proximity of resonances from *N*-acetyl aspartate ($\beta^u$-methylene proton, $\delta$ = 2.51 ppm, dd), alanine ($\alpha$-methine proton, $\delta$ = 3.72 ppm, q) and glutamate ($\alpha$-methine proton, $\delta$ = 3.75 ppm, t).

*Glutamate (Glu)* [**6**]. $\beta$-methylene protons in glutamate were observed as a complex signal at 2.06 ppm. These produced cross-peaks in the two-dimensional proton spectrum with signals at 2.39 and 3.75 ppm. These were assigned to the $\gamma$-methylene an $\alpha$-methine protons respectively. The latter $\alpha$ proton signal was obscured by resonances from alanine ($\alpha$-methine proton, $\delta$ = 3.72 ppm, q) and glutamate ($\alpha$-methine proton, $\delta$ = 3.75 ppm, t), however both $\beta$- and $\gamma$-methylene protons were suitable for diagnostic purposes, with the $\gamma$-methylene proton triplet being quantified in these studies.

*Glycine (Gly)* [**7**]. The magnetically equivalent methylene protons in glycine produce a distinctive singlet resonance at 3.55 ppm. This signal was distinguishable from the co-resonating inositol H1, H3 doublets of doublets at 3.52 ppm and was thus considered suitable for quantitative purposes.

*Glycerophosphorylcholine (GPC)* [**8**]. The terminal methyl proton singlet resonance was assigned at 3.28 ppm, this being the most prominent of the choline-associated signals. This resonance provided no connectivity information on the remaining choline head group/glycerol backbone protons which consequently were not assigned.

*Inositol (Ino)* [**9**]. Inositol proton resonances were assigned following inspection of literature values (Fan *et al.*, 1986; Dr. Jimmy Bell, personal communication), multiplicities and coupling constants, and comparing these to the test spectra. The H2 proton appeared to produce a triplet at 4.07 ppm in the one-dimensional $^1$H spectrum. Upon inspection of the *J*-resolved spectrum this was seen to comprise a doublet of doublets with identical $^3J_{1,2}$ and $^3J_{2,3}$ of 2.9 Hz in close agreement with the values found by Bell and colleagues (2.7 Hz; Dr. Jimmy Bell,

| Metabolite | Chemical shift /ppm | Multiplicity | Functional group |
|---|---|---|---|
| | | | |
| Acetate | 1.90 | s | $-CH_3$ |
| | | | |
| Alanine | 1.49* | d | $\beta$-$CH_3$ |
| | 3.72 | q | $\alpha$-CH |
| | | | |
| Asparagine | 2.65 | dd | $\beta$-$CH^u$ |
| | 2.80* | dd | $\beta$-$CH^d$ |
| | 3.88 | dd | $\alpha$-CH |
| | | | |
| $\gamma$-aminobutyrate | 1.91 | qu | $\beta$-$CH_2$ |
| | 2.30* | t | $\alpha$-CH |
| | 3.05 | t | $\gamma$-$CH_2$ |
| | | | |
| Glutamine | 2.16 | c | $\beta$-$CH_2$ |
| | 2.46 | c | $\gamma$-$CH_2$ |
| | 3.76 | t | $\alpha$-CH |
| | | | |
| Glutamate | 2.06 | c | $\beta$-$CH_2$ |
| | 2.39* | t | $\gamma$-$CH_2$ |
| | 3.75 | t | $\alpha$-CH |
| | | | |
| Glycine | 3.55* | s | $-CH_2$ |
| | | | |
| Glycerophosphoryl choline | 3.28* | s | $-N^+(CH_3)_3$ |
| | | | |
| Inositol | 3.29 | t | H5 |
| | 3.52* | dd | H1/H3 |
| | 3.66 | t | H4/H6 |
| | 4.07 | t(dd) | H2 |
| | | | |
| Lactate | 1.30* | d | $\beta$-$CH_3$ |
| | 4.07 | q | $\alpha$-CH |
| | | | |

Table 3. 1. 1 Assignment of aqueous cerebral metabolites in $^1$H NMR spectrum at 600 MHz.

Aqueous metabolites were extracted from murine brain with acetone-$d_6$. $^1$H NMR spectra were acquired on a Varian VXR600S NMR spectrometer operating at a spectrometer frequency of 599.945 MHz. Metabolites were referenced to the *N*-acetyl aspartate methyl singlet at 2.02 ppm (Fan *et al.*, 1988). For a full description of the procedure see Experimental.

* denotes $^1$H resonances used for metabolite quantification.

c, complex; d, doublet; dd, doublet of doublets; q, quartet; qu, quintet; t, triplet.

personal communication). The H2 proton couples to the magnetically equivalent H1 and H3 protons at 3.52 ppm producing doublets of doublets with identical $^3J_{2,3}$ and $^3J_{1,2}$ of 2.9 Hz in addition to another coupling constant of 10 Hz. This latter coupling constant was produced by coupling between the H1 and H6 protons on the one hand and the H3 and H4 protons on the other, (i.e. $^3J_{1,6}$ and $^3J_{3,4}$ = 10 Hz). This finding was also in agreement with those of Bell and colleagues (9.9 Hz; Dr. Jimmy Bell, personal communication). The two-dimensional COSY 45 showed the signal at 3.52 ppm to be coupled to a resonance at 3.66 ppm, this corresponding to the equivalent H4 and H6 protons. Lastly, the H5 proton was assigned at 3.29 ppm from the cross-peak produced in the COSY 45 spectrum upon its coupling to the equivalent H4 and H6 protons. Although inspection of the one-dimensional proton spectrum showed this latter signal to be partially obscured by the terminal methyl singlet resonance from glycerophosphorylcholine, the *J*-resolved spectrum revealed that the H5 resonance had identical $^3J_{4,5}$ and $^3J_{5,6}$ of 9.5 Hz. In conclusion, the H1 and H3 protons were used for quantitative and diagnostic purposes.

*Lactate (Lac)* [**10**]. Resonances from lactate were prominent and readily identifiable. The β-methyl protons produced a doublet at 1.30 ppm on coupling to the α-methine proton which consequently was assigned from the two-dimensional COSY 45 spectrum at 4.03 ppm. The β-methyl proton signal was used for diagnostic and quantitative purposes.

*N-acetyl aspartate (NAA)* [**11**]. NAA is recognized as a prominent compound in $^1$H NMR spectroscopic studies of brain (Birken and Oldendorf, 1989). The methyl proton singlet was readily assigned at 2.02 ppm and although it lies in the close proximity to a complex signal from glutamate β-methylene protons, was distinct enough to be used for diagnostic and quantitative purposes. The methyl proton singlet provided no connectivity information to assist in the assignment of the remaining α-methine and β-methylene protons. These were tentatively identified following comparison with published results (Fan *et al.*, 1986). The α-

| Metabolite | Chemical shift /ppm | Multiplicity | Functional group |
|---|---|---|---|
| | | | |
| *N*-acetyl aspartate | 2.02* | s | $-CH_3$ |
| | 2.51 | dd | $\beta$-$CH^u$ |
| | 2.65 | dd | $\beta$-$CH^d$ |
| | 4.42 | dd | $\alpha$-CH |
| | | | |
| Phosphorylcholine | 3.27* | s | $-N^+(CH_3)_3$ |
| | | | |
| Total Creatine | 3.06 | s | $-CH_3$ |
| | 3.90* | s | $-CH_2$ |
| | | | |
| Taurine | 3.20* | t | $H_2N$-C**H**$_2$- |
| | 3.43 | t | -C**H**$_2$-$SO_3H$ |
| | | | |
| Threonine | 1.34 | d | $\gamma$-$CH_3$ |
| | | | |

Table 3. 1. 1 *continued.* Assignment of aqueous cerebral metabolites in $^1$H NMR spectrum at 600 MHz.

Aqueous metabolites were extracted from murine brain with acetone-$d_6$. $^1$H NMR spectra were acquired on a Varian VXR600S NMR spectrometer operating at a spectrometer frequency of 599.945 MHz. Metabolites were referenced to the *N*-acetyl aspartate methyl singlet at 2.02 ppm (Fan *et al.*, 1988). For a full description of the procedure see Experimental.

* denotes $^1$H resonances used for metabolite quantification.

c, complex; d, doublet; dd, doublet of doublets; q, quartet; qu, quintet; t, triplet.

methine proton was assigned as a doublet of doublets at 4.42 ppm, in close agreement with the literature value of 4.38 ppm. This signal produced cross-peaks with the diastereotopic methylene protons at 2.51 and 2.65 ppm in the two-dimensional COSY 45 spectrum. Again, these values were in close agreement with those previously reported ($\beta^u$, $\delta$ = 2.48 ppm; $\beta^d$, $\delta$ = 2.67 ppm). Confirmation of the assignments was given upon inspection of the *J*-resolved spectrum with these signals comprising doublets of doublets with $^3J_{\alpha,\beta}{}^d$ and $^3J_{\alpha,\beta}{}^u$ of 4.4 and 9.0 Hz respectively in addition to a $^2J_{\beta}{}^u{}_{,\beta}{}^d$ of 15.3 Hz.

*Phosphorylcholine (PC)* [**12**]. The methyl proton resonance from phosphorylcholine was tentatively assigned at 3.27 ppm in the immediate proximity of the glycerophosphorylcholine singlet ($\delta$ = 3.28 ppm; Dr. Jimmy Bell, personal communication). However the presence of multiple signals over the 3.24 to 3.31 ppm region made discrete quantification of these resonances difficult.

*Total creatine (Cr)* [**13**]. Proton resonances from phosphocreatine and creatine were very prominent in the aqueous brain extract. The methyl proton singlet from 'total creatine' was assigned at 3.06 ppm and the methylene proton singlet at 3.90 ppm. The resonance at 3.90 ppm was used for quantitative purposes; the $\gamma$-methylene protons from GABA being found to contribute to the signal at 3.06 ppm.

*Taurine (Tau)* [**14**]. Two sets of taurine triplets, with equal vicinal coupling constants and of similar intensity, were assigned at 3.20 and 3.43 ppm corresponding to the $H_2N$-C$\underline{H}_2$- and -C$\underline{H}_2$-$SO_3H$ methylene protons respectively. Although the two triplet resonances appeared to be well distinguished from other metabolites, closer inspection of the two-dimensional COSY 45 and *J*-resolved spectra revealed that both signals were superimposed on top of doublet resonances from minor metabolites. These latter signals comprised two sets of doublets in the immediate proximity of each other, making their assignment difficult. The contribution of the aforementioned minor metabolites to the

intensity of the taurine triplets was considered minimal. Consequently, the triplet at 3.20 ppm was used for quantitative purposes.

*Threonine (Thr)* [**15**]. Threonine resonances were not particularly prominent in the acetone-$d_6$ $^1$H NMR spectrum. However, the γ-methyl proton doublet was assigned at 1.34 ppm in close agreement with the value previously reported (δ = 1.32 ppm, Fan *et al.*, 1986). The low concentration of this amino acid in the extract did not facilitate the identification or assignment of the α and β protons.

*Summary.*

The use of acetone-$d_6$ for the rapid preparation of aqueous extracts applicable to direct $^1$H NMR spectroscopy analysis merits attention. In its favour, the procedure for metabolite extraction is rapid, reproducible and relatively inexpensive. The proton spectra thus obtained are comparable in metabolite extraction to PCA extract spectra (see $^1$H NMR spectra in Bell *et al.*, 1991) and afford a marked improvement in spectral resolution. The requirement for perchlorate neutralization and pH adjustment is not necessary, obviating the possibility of metabolite oxidation or hydrolysis.

A total of 15 prominent metabolites were fully assigned in the proton spectra, of which 12 'diagnostic peaks' were chosen for metabolite quantification (Table 3. 1. 1). Although glutamine resonances were obscured by signals from other metabolites in the acetone-$d_6$ spectra, removal of the solvent by evaporation and subsequent resuspension in 0.65 ml of $D_2O$ may allow the visualization of the β-methylene proton signal at 2.06 ppm, thus permitting its quantification.

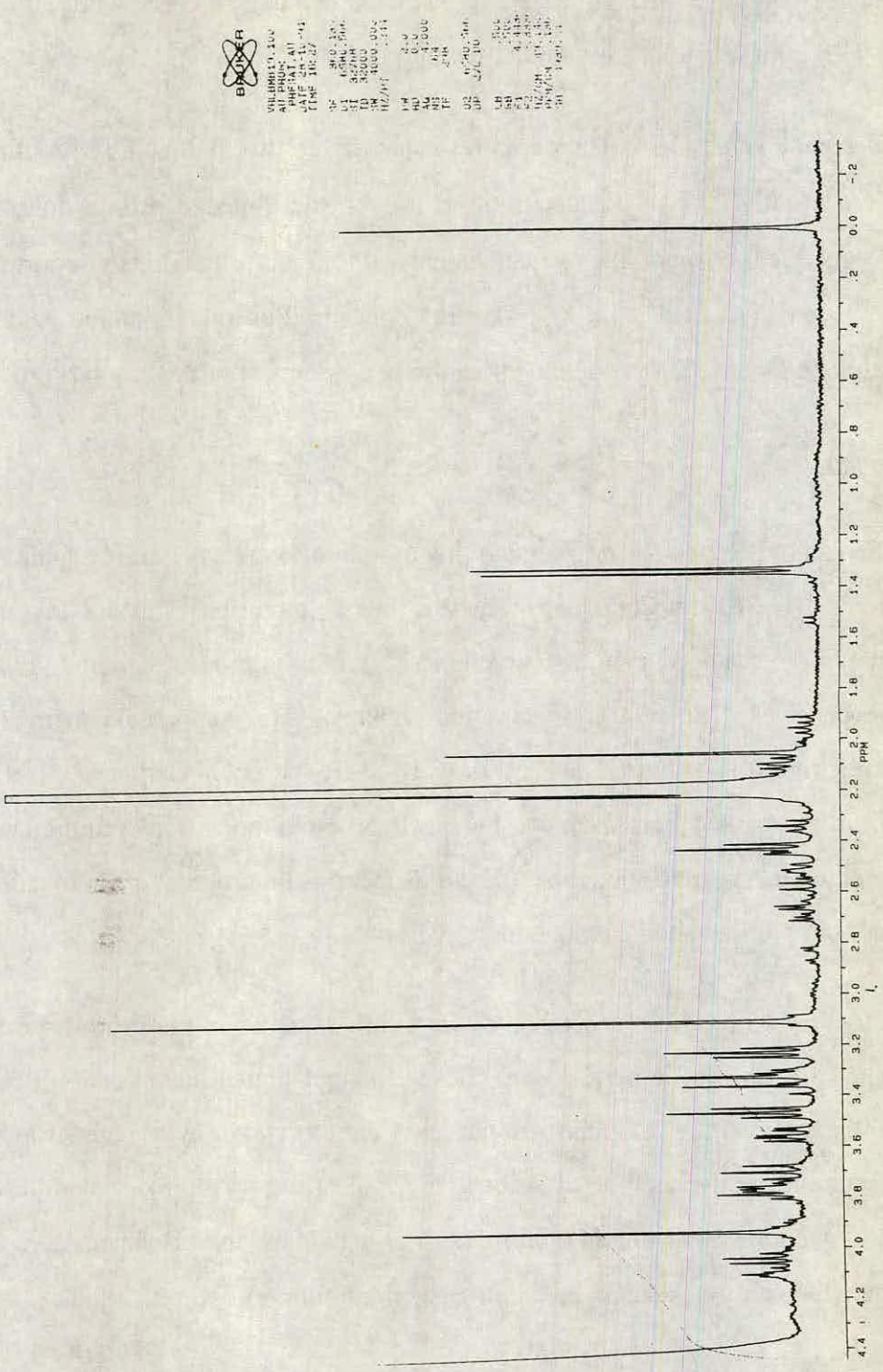


Figure 3. 1. 5a $^{1}$H NMR spectra of acetone-soluble cerebral metabolites in a control mouse at 360 MHz.

Spectra where acquired as described in Experimental. Metabolite resonances were referenced to the *N*-acetyl aspartate methyl singlet at 2.02 ppm.

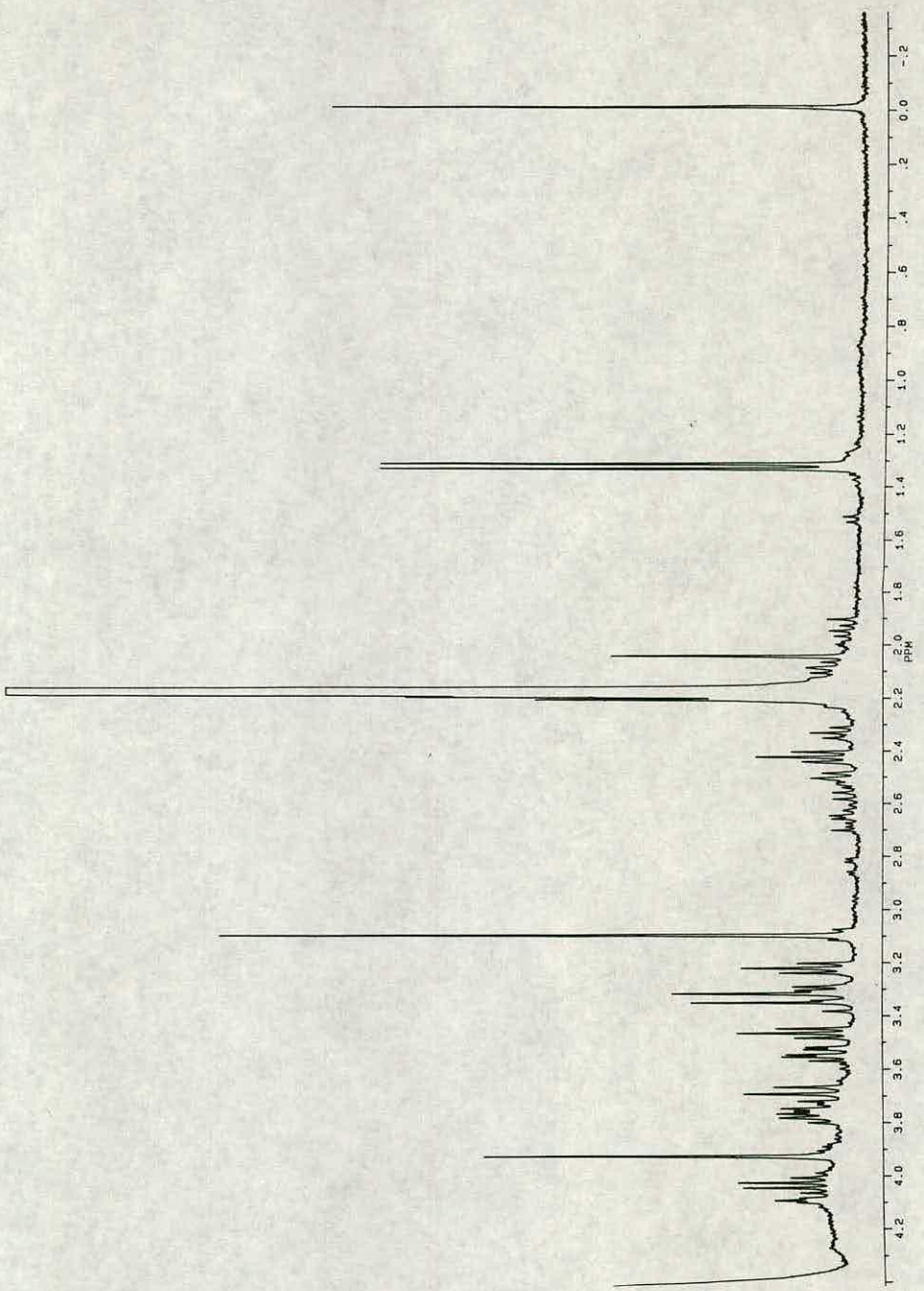


Figure 3. 1. 5b $^{1}$H NMR spectra of acetone-soluble cerebral metabolites in a scrapie-affected mouse at 360 MHz.

Spectra where acquired as described in Experimental. Metabolite resonances were referenced to the *N*-acetyl aspartate methyl singlet at 2.02 ppm. With comparison to control (facing page) note the reduction in the N-acetyl aspartate methyl singlet at 2.02 ppm. This observation is believed to be indicative of the severe neuronal degeneration exhibited in this murine-scrapie model.

### 3. 1. 2 Quantitative Comparison of Metabolites in Control and Scrapie Mice.

Acetone-$d_6$ extracts were prepared from the brains of six clinically-ill ME7-affected VM mice (360 days p.i) and an equal number of age- and sex-matched controls. Proton NMR spectra were acquired at 360.135 MHz as described previously (Section 2. 4. 2). Figures 3. 1. 5a/b illustrate representative one-dimensional proton spectra from control and scrapie-affected mice respectively.

For the purpose of metabolite comparison, diagnostic signals were quantitatively referenced to (a) the chemical shift reference compound, 3-trimethylsilyl-2,2',3,3'-tetradeuteropropionic acid (TSP) and (b) endogenous total creatine. When referenced to TSP, metabolites levels showed large differences between scrapie and control animals. The majority of these changes reflected the disease-related reduction in wet brain weight between scrapie and control tissue. The suitability of TSP as an internal reference (although used by Bell *et al.*, 1991) was questioned following the finding that the proprionic acid derivative has an affinity for protein (Dr. Jimmy Bell, personal communication). The availability of an alternative quantitative standard was presented by total creatine. A review of the literature would suggest that the concentration of total creatine remains constant under a variety of abnormal metabolic conditions (Gadian, 1990) and disease states (Gill *et al.*, 1990; Larsson *et al.*, 1991), including this model of murine-scrapie (Bell *et al.*, 1991). In conclusion *in vitro* metabolite levels were quantitatively referenced to endogenous creatine and levels compared. The results are recorded in Table 3. 1. 2.

*Results.*

A highly significant change was found in the ratio of *N*-acetyl aspartate/creatine in terminally-ill scrapie-affected animals relative to controls (control = 125.6 ± 11.8, scrapie 96.4 ± 4.1; $P < 0.001$) in close agreement with the percentage reduction reported by Bell and colleagues (1991) in their independent *in vitro* MRS studies

| Metabolite | Control | Scrapie |
|---|---|---|
| Alanine | 14.3 ± 2.2 | 15.7 ± 3.2 |
| Asparagine | 29.4 ± 4.6 | 27.4 ± 3.3 |
| γ-aminobutyrate | 53.3 ± 8.7 | 50.2 ± 3.4 |
| Glutamate* | 117.6 ± 8.2 | 103.3 ± 10.9 |
| Glycine | 16.0 ± 2.3 | 14.9 ± 3.5 |
| Glycerophosphorylcholine | 69.7 ± 4.7 | 73.4 ± 9.4 |
| Inositol* | 63.0 ± 4.7 | 78.7 ± 4.9 |
| Lactate | 236.9 ± 31.0 | 290.3 ± 61.8 |
| *N*-acetyl aspartate* | 125.6 ± 11.8 | 96.4 ± 4.1 |
| Phosphorylcholine | 27.1 ± 4.5 | 20.7 ± 5.6 |
| Taurine | 122.3 ± 13.0 | 113.6 ± 6.4 |

Table 3. 1. 2 $^{1}$H NMR spectroscopy analysis of aqueous cerebral metabolites in control and scrapie-affected (ME7/VM) mice.

Aqueous metabolites were extracted from murine brain with acetone-$d_6$. A total of six control and six scrapie animals were analyzed. $^{1}$H NMR spectra were acquired on a Brüker WH-360 MHz NMR spectrometer operating at a spectrometer frequency of 360.135 MHz. Metabolites were referenced to the *N*-acetyl aspartate methyl singlet at 2.02 ppm. Metabolite values are given relative to total creatine concentration as mean ± sem (multiplied by an arbitary factor of 150). For a full description of the procedure see Experimental.

* denotes metabolites which show statistically significant differences between control and scrapie groups.

(acetone-$d_6$ extract = 23% reduction; perchlorate extract = 28% reduction). In addition to this, scrapie-affected mice exhibited elevated ratios of inositol/creatine (control = 63.0 ± 4.7, scrapie = 78.7 ± 4.9; 25% elevation; $P < 0.001$) and reduced ratios of glutamate/creatine (control = 117.6 ± 8.2, scrapie 103.2 ± 10.9; 12% reduction; $P < 0.05$). Concentrations of other metabolites relative to total creatine remained unchanged.

The presence of an elevated multicomponent resonance ($\delta$ = 1.5 to 1.8 ppm) was not detected in the *in vitro* $^1$H NMR spectra of scrapie brain, this latter finding providing circumstantial support for the hypothesis that the signal was attributed to a change in a non-aqueous metabolite, possibly intracerebral lipid. This line of investigation is explored more fully in Section 3. 2. 4.

*Inferences.*

***N-Acetyl aspartate.*** A reduction in the ratio of *N*-acetyl aspartate to creatine, as determined by *in vivo* $^1$H NMR spectroscopy, has been recorded in a wide range of cerebral disorders including: acquired immune deficiency syndrome (Menon *et al.*, 1990a), herpes simplex encephalitis (Menon *et al.*, 1990b), cerebral demyelinating disorders (Arnold *et al.*, 1992; Larsson *et al.*, 1991) and the transmissible spongiform encephalopathies; Creutzfeldt-Jacob disease (Bruhn *et al.*, 1991) and scrapie (Bell *et al.*, 1991). The function of NAA is presently unclear, however it is known to be primarily located in neurons (Birken and Oldendorf, 1989; Koller *et al.*, 1984) and thus presents itself as a marker of neuronal status within the brain (Small *et al.*, 1990).

Bruhn *et al.* (1991) recently applied *in vivo* $^1$H MRS to the study of a patient in the late clinical stage of CJD. The proton spectra showed significant changes in NAA concentrations relative to creatine in both white and grey matter regions consistent with and indicative of neuronal loss. Frontal lobe biopsy, performed two days after MRS data acquisition, revealed spongiform change with a slight loss of neurons and gliosis. The authors speculated that *in vivo* MRS could find

application to the early diagnosis of CJD. This suggestion must be viewed with a degree of caution in the light of three major findings:

(i) The non-specific nature of an NAA reduction may equally be attributed to a host of different diseases (of which the examples in the paragraph above are but a few), in which neurological damage is a characteristic feature. Magnetic resonance imaging (MRI) in addition to MRS has been proposed as a means of clarifing early diagnosis by the visualization of brain atrophy, however the identification of CJD patients with apparently 'MRI-normal' brains indicates that this is not always a valid assumption to make (Bruhn *et al.*, 1991; Uchino *et al.*, 1991).

(ii) A considerable period of time may elapse between initial infection and signs of neurological damage, be they detected by histological techniques or otherwise. Our understanding of the limitations of monitoring changes in cerebral NAA concentrations for the diagnosis of neurodegeneration come from extensive studies in murine-scrapie models in which histopathological changes are consistent and well characterized. Although it is invalid to make the assumption that a causal relationship exists between neuronal degeneration and vacuolation (Gibson and Liberski, 1987; Scott and Fraser, 1984), it would appear that in the ME7/VM murine-scrapie model a good correlation exists between the degree of vacuolation and extent of degenerative nerve fibre damage both spatially and temporally (Fraser, 1969; Fraser, *et al.*, 1995). The total lesion score in this model thus gives a relatively accurate prediction of the extent of neuronal loss. Bell and colleagues (1991) investigated metabolic changes in the ME7/VM model by *in vivo* and *in vitro* proton MRS as described previously. No detectable differences were observed in NAA/Cr levels at the two initial time points of study (52 days p.i. and 108 days p.i.). In histopathological agreement, vacuolar damage (and thus presumably neuronal loss) is not seen before 140 days p.i. (Fraser and Dickinson, 1968). However, after 140 days vacuolar damage increases in severity and at 192 days p.i. (the third time point in the MRS study) appreciable

vacuolation is present in the hypothalamus and septal nuclei of the paraterminal body. Interestingly, Bell and colleagues found no significant depression in the NAA/Cr ratio at this time. It is possible that such limited, regionally-specific changes in NAA levels remain undetected as a result of volume averaging effects (van der Knaap *et al.*, 1992). This emphasizes an important point, that for those contemplating early TSE diagnosis on the basis of neuronal damage, the volume and locality of spectral analysis are very important factors. Consideration of this matter highlights an additional problem as sporadic (and for that matter iatrogenic) cases of CJD do not display the well defined neuropathological profiles of experimental murine-scrapie models with the same degree of consistency.

It was only in the late clinical stage of the disease (346 days p.i.), when mice showed signs of ataxia and other locomotory deficits, that significant changes in cerebral NAA concentrations were observed. Clearly the application of this technique to the early diagnosis of scrapie on the basis of changes in NAA is thus untenable. The point at which the NAA reduction became a significant feature of diseased animals was not precisely determined, as studies on mice between 192 and 325 days p.i. were not performed.

(iii) Some mouse models of scrapie display histopathological features in which severe spongiform damage occurs in the absence of appreciable neuronal destruction (Scott and Fraser, 1984). Clearly, should some populations of human CJD brains display similar characteristics, the diagnosis of spongiform damage based upon the *in vivo* MRS detection of NAA abnormalities would not be possible.

***Inositol.*** In addition to the NAA abnormality, Bruhn and colleagues found white matter regions of the CJD brain to exhibit elevated levels of inositol, notably in the parietal cortex. Although our studies of cerebral metabolites did not offer the same degree of spatial precision as those of the aforementioned authors, we too are able to report a highly significant elevation in levels of inositol in scrapie-

affected mouse brain at the clinical stage of the disease. A similar finding was not observed by Bell and colleagues (1991) although it is worth noting that with their *in vivo* MRS experimental acquisition parameters optimized for NAA measurement, changes in inositol signals may have been overlooked. The significance of the inositol elevation is presently unclear. Whether other murine-scrapie models exhibit a similar abnormality is not known, nor is the specificity of this change to the TSE disease class. However the similarity between the *in vivo* CJD and *in vitro* scrapie studies highlights the potential for further development in this area.

***Glutamate.*** Glutamate is widely and fairly uniformly distributed throughout the central nervous system where it has important excitatory effects on specific cell populations. The modest although significant reduction in glutamate concentrations may reflect a more dramatic change in localized regions of scrapie-affected brains. In view of the important neurotransmitter effect of glutamate, a reduction in its intracerebral concentration may have a marked effect on neuronal excitability. Although the following inferences are not deduced from the NMR results, it is interesting to speculate on the role of glutamate in relation to cation-gated channels and scrapie pathogenesis.

Glutamate has its excitatory effect *via* three major subtypes of receptor (NMDA, AMPA and kainate) where ligand interaction causes opening of cation selective channels and a rapid depolarization response (Watkins and Evans, 1981). NMDA receptors differ from those opened by AMPA and kainate in that they have a larger conductance and higher permeability to calcium ions relative to other cations. It is these and other special pharmacological properties which make the NMDA-channel of particular importance in long-term potentiation and excitotoxicity, two features which have particular relevance to the spongiform encephalopathies.

Long-term potentiation describes a long lasting enhancement of synaptic transmission which follows a short burst of presynaptic stimulation (Anwyl, 1989;

Collingridge and Bliss, 1987). It has received most extensive study in the hippocampus where its function is believed to be of importance in learning and memory. In this regard it is of significance to note that the ME7/VM model exhibits complete destruction of the pyramidal layer of hippocampal neurons (Scott and Fraser, 1984). Whether NMDA-receptor specific neuronal populations are particularly vulnerable to TSE aetiological agents is unknown, however such a finding would explain the high incidence of amnesia-like symptoms associated with CJD, the human form of the disease (Brown, 1988).

The relationship between selective cell death and vacuolar change may be explained by another property of NMDA receptors - that of excitotoxicity. Recent experimental evidence strongly indicates that glutamate and related EAAs are neurotoxic, even in low concentrations (Choi, 1988). It is now known that these cytotoxic actions are mediated through NMDA receptors, for they are blocked by NMDA antagonists such as ketamine and phencyclidine (Rang and Dale, 1991), and that calcium entry is a necessary step (Olney, 1990). The similarity between the cytotoxic effect - endoneuronal oedema followed by global loss of axons (Hugen *et al.*, 1987), is remarkably similar to vacuolar damage seen in the TSEs.

Within the last couple of years it has become clear that the neuronal cell surface sialoglycoprotein $PrP^c$ may have functional relevance to the retention of memory (Büeler *et al.*, 1992), to cation channel responsiveness to endogenous ligands (Kristensson *et al.*, 1993) and to the generation of a cytotoxic effect in response to challenge with the neurotoxic PrP fragment, PrP106-126 (Brown *et al.*, 1994; Forloni *et al.*, 1993). In view of these findings and the prior discussion, the question must ultimately be asked - does $PrP^c$ have a modulatory effect on cation channels and in particular the NMDA receptor?

Firstly, the speculative finding that $PrP^{0/0}$ mice have "superior spatial memory" (Büeler *et al.*, 1992) may indicate that in the absence of $PrP^c$, hippocampal

neurons have long term potentials of greater duration. Does the normal cellular protein therefore 'dampen-down' glutamate-induced excitations?

Secondly, scrapie infection has been shown to cause dysfunction of both intracellular calcium release and calcium channel opening, albeit in neuroblastoma cell lines and in response to the application of bradykinin (Kristensson *et al.*, 1993). It is noted that neither of the cell cultures in question (mouse neuroblastoma $N_2A$ and hamster brain HaB cells) exhibited voltage-dependent or glutamate-responsive calcium channels, and thus represented cell populations in which glutamate receptors were not expressed. Interestingly, scrapie infection conferred the aforesaid cell lines unresponsive to bradykinin application thus preventing an elevation in intracellular calcium concentration. It matters little that the response exhibited by the bradykinin receptor was opposite to the excitotoxic effect expected of the NMDA receptor; the significant finding of the study being that scrapie infection has a marked effect on receptor-mediated cation channel permeability. If scrapie status reduces bradykinin-receptor responsiveness in these cultured cell lines what is to say that it cannot have the opposite effect on the NMDA-receptor by increasing its responsiveness to glutamate; or for that matter on a whole host of other neurotransmitter receptors in as yet undiscovered ways?

Thirdly, the presence of $PrP^c$ appears to be a necessary prerequisite for the neurotoxic effects of PrP106-126 on a specific population of cortical cells *in vitro*, whilst having growth factor-like properties on cells which lack PrP (Brown *et al.*, 1994). How might these paradoxical differences be explained? This 21 amino acid peptide shares some common features with $PrP^{sc}$ in that it undergoes *in vitro* polymerization into fibrils, is protease resistant and forms a β-sheet structure (Selvaggini *et al.*, 1993). In view that scrapie infection can modify cation channel function (as discussed above), is it not possible that the effects displayed by PrP106-126 are the result of it interacting with $PrP^c$ to alter ion flux in neuronal cell populations with different cation channel repertoires? It is known

that $PrP^{sc}$ possesses qualities which stimulate the growth of astrocytes (DeArmond *et al.*, 1992) and that reactive astrocytic gliosis is often a prominent feature in the disease (Dormont *et al.* 1981; Mackenzie, 1983). Thus on the one hand 'neurotoxic' $PrP^{sc}$ may stimulate calcium channels which influence mitotic activity in cell types such as glia, and on the other hand cause dysfunction of calcium channels in neurons leading to their subsequent degeneration. It is not unreasonable to assume that differences in PrP alleles (and hence PrP tertiary structure) as well as scrapie strain variants may modify the effect that PrP has on these ion channels, thus partly explaining the wide range of histopathological features seen in different strains of mice infected with different scrapie isolates (Bruce *et al.*, 1991; Fraser and Dickinson, 1968; Kim *et al.*, 1990a; Kim *et al.*, 1990b).

*Summary.*

The analysis of aqueous metabolites by *in vitro* $^{1}H$ magnetic resonance spectroscopy identified abnormalities in cerebral concentrations of *N*-acetyl aspartate, inositol and glutamate in ME7-affected VM mice at the late clinical stage of the disease. The reduction in levels of *N*-acetyl asparate are believed to be indicative of neuronal damage (Small *et al.*, 1990), a feature consistent with this murine-scrapie model (Fraser, 1969). Similarly, reduced levels of glutamate may reflect degenerative changes in regions of the brain in which the acidic amino acid has an important function, for example the hippocampus (Scott and Fraser, 1984). The significance of the inositol elevation is presently unclear, although the observation of a similar abnormality in parietal white matter regions of a CJD patient by *in vivo* $^{1}H$ MRS (Bruhn *et al.*, 1991) strongly merits further investigation.

## 3. 2 Nuclear Magnetic Resonance Studies of Cerebral Lipids.

*Post mortem* histopathological examination of brain tissue is currently the only definitive means of identifying individuals previously affected with a transmissible spongiform encephalopathy (Kimberlin, 1991; Wells *et al.*, 1992). The inability to accurately diagnose TSE status *ante mortem*, and more importantly preclinically, is a serious impediment to the provision of proper patient/family counseling and care, and in the future should treatment become available, to the alleviation of neurological damage and suffering. The observation of a metabolic disturbance in the brains of scrapie-affected mice by *in vivo* magnetic resonance spectroscopy therefore created a great deal of interest, especially in the light that this abnormality was detected before appreciable $PrP^{sc}$ deposition and neurological damage (Bell *et al.*, 1991). Although the component responsible was not characterized, it was speculated that its broad proton resonance ($\delta$ = 1.5 to 1.8 ppm) was attributed to 'mobile lipid'. The objective of the analysis described herein was therefore to confirm the specificity of the 'multicomponent resonance' to scrapie-affected mice and provide its identification.

Recent studies of cerebral lipids by *in vitro* proton NMR spectroscopy have received relatively thorough investigation (Choi *et al.*, 1993; Gunstone, 1992). This information, in addition to our own NMR experiments, allowed the complete assignment of proton resonances in neutral and acidic lipid fractions. Having thus assigned the proton spectra, diagnostic resonances were identified for prominent lipid species and a comparison was made of scrapie and control cerebral lipid extracts.

The information provided by the assignment of proton resonances was directly applied to the assignment of $^{13}C$ lipid resonances in a cerebral extract following comparison with a $^{13}C$-$^{1}H$ two-dimensional shift correlated spectra. The application of a combination of these techniques to the study of lipids *in vitro* is discussed.

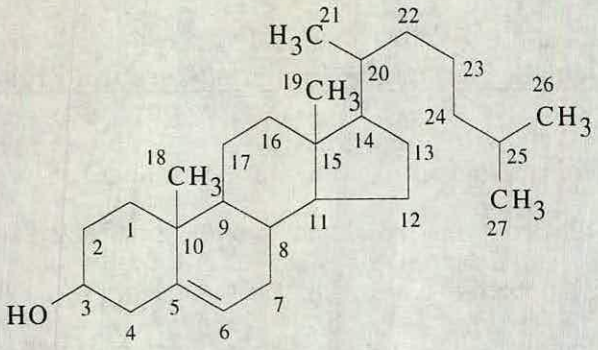

**[16]**

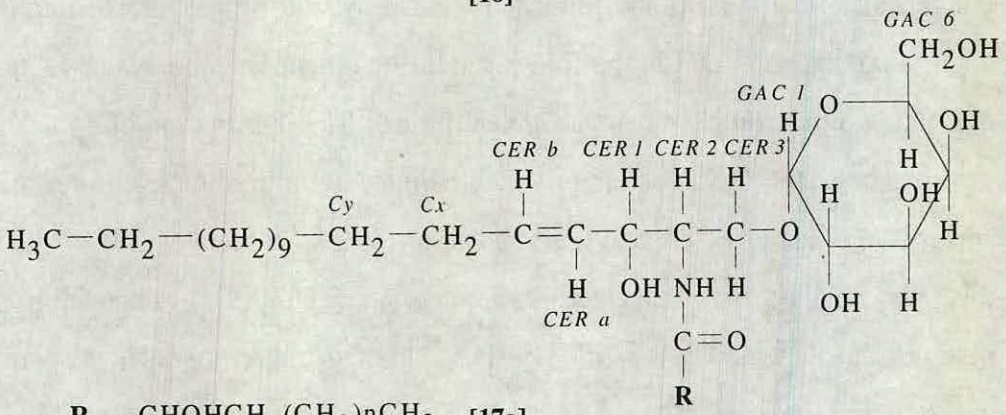

**R** = $CHOHCH_2(CH_2)nCH_3$ **[17a]**

$CH_2CH_2(CH_2)nCH_3$ **[17b]**

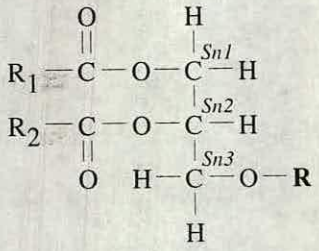

**R** = $PO_3CH_2CH_2NH_2$ **[18]**

$PO_3CH_2CH_2N^+(CH_3)_3$ **[19]**

$PO_3CH_2CHNH_2COOH$ **[22]**

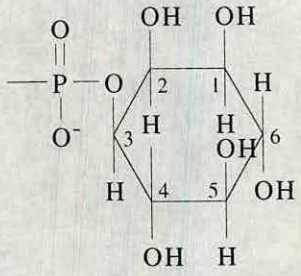

**[23]**

Figure 3. 2. 1a Chemical structures of cerebral lipids.

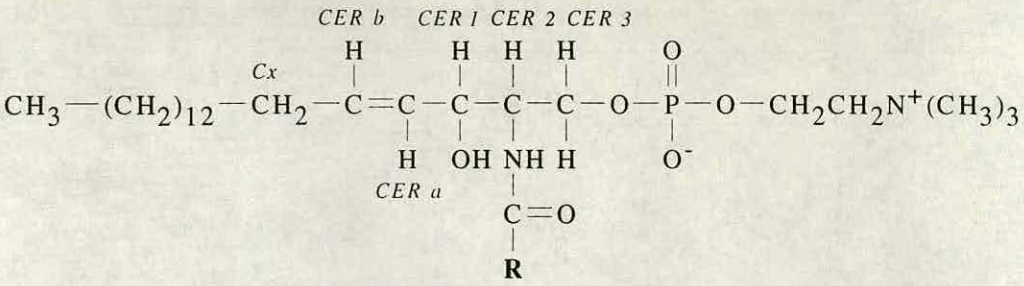


**[20]**

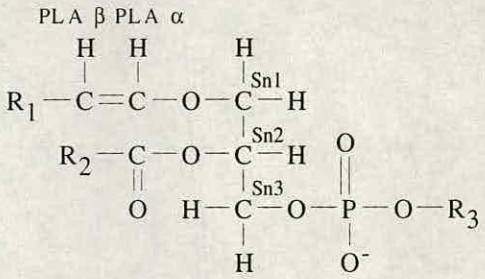


**[21]**

| | |
|---|---|
| $CH_3(CH_2)_4(CH{=}CHCH_2)_2(CH_2)_6COOH$ | (n-6) linoleic acid |
| $CH_3(CH_2)_4(CH{=}CHCH_2)_4(CH_2)_2COOH$ | (n-6) arachidonic acid |
| $CH_3CH_2(CH{=}CHCH_2)_6(CH_2)COOH$ | (n-3) docosahexaenoic acid |

**[24]**

Figure 3. 2. 1b Chemical structures of cerebral lipids.

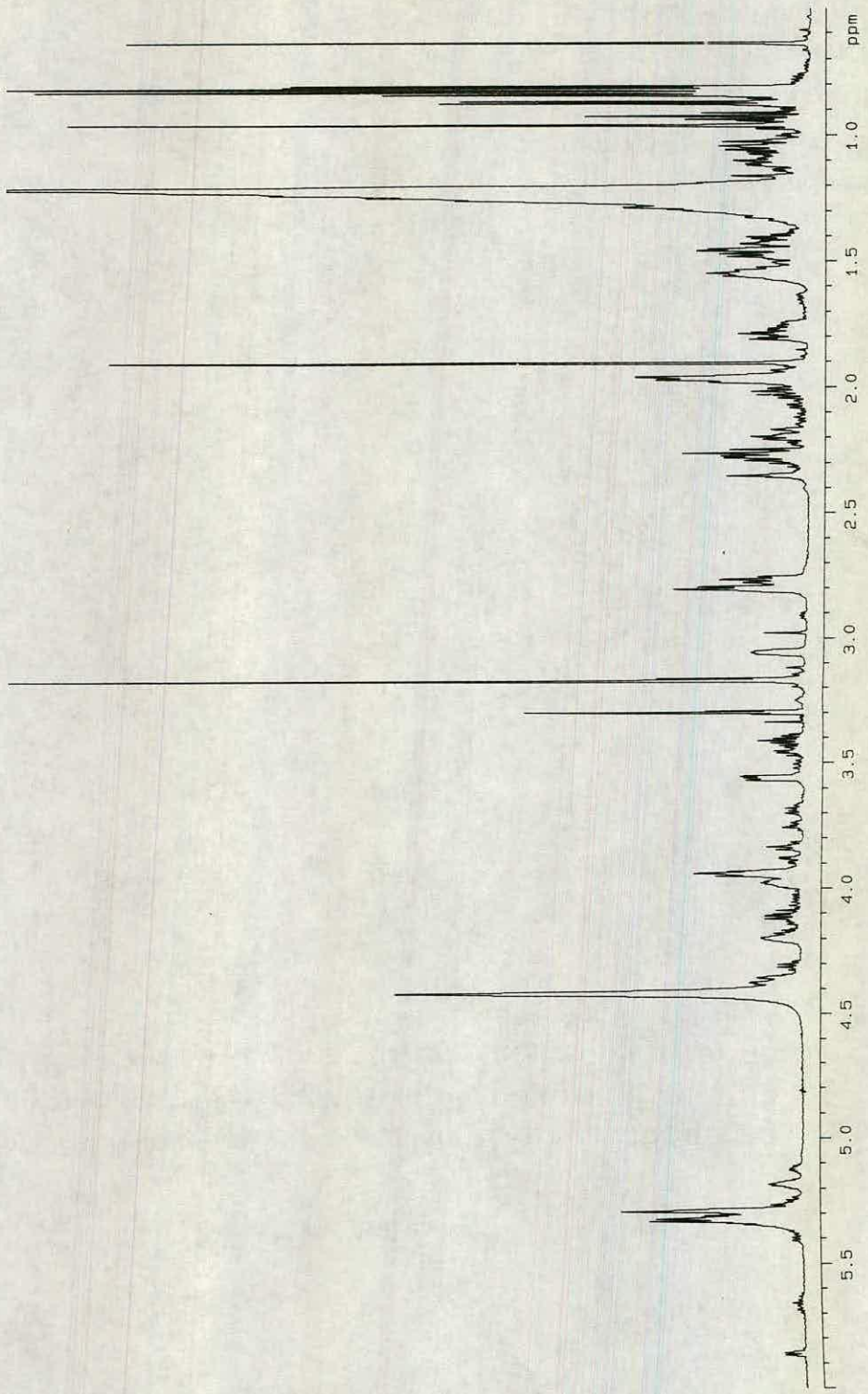


Figure 3. 2. 2 $^{1}$H NMR spectrum of neutral cerebral lipids at 600 MHz.

Spectra where acquired as described in Experimental. Lipid resonances were referenced to the methanol quintet centred at 3.3 ppm.

### 3. 2. 1 Assignment of $^{1}$H NMR Spectra.

The assignment of lipid resonances and improvement in spectral resolution was assisted by the prior fractionation of the crude lipid extract into neutral and acidic lipid species by column chromatography over DEAE Sephadex A-25. The components present in these fractions were putatively identified by high performance thin layer chromatography, allowing the assignment of proton resonances with reference to lipid structure, literature values (Choi *et al.*, 1993; Gunstone, 1992) and a variety of NMR experiments (described below). Structures and nomenclature for the cerebral lipids are illustrated in Figure 3. 2. 1 and relate to the assignment of resonances in the three following sections.

#### *Neutral Lipids.*

Six prominent components were identified in the neutral lipid fraction by high performance thin layer chromatography. These were cholesterol, galacto-cerebrosides I and II, ethanolamine phospholipids, choline phospholipids and sphingomyelin. Upon concentration of the fraction, a number of less abundant lipids were detected, these being cholesteryl esters, triglycerides and diglycerides. Whilst the former components were present in concentrations sufficiently high enough to allow spectral detection, the latter were not. The following discussion therefore relates to the assignment of the prominent lipid components.

*Cholesterol* [**16**].

Cholesterol is the most abundant lipid in the neutral lipid fraction, giving rise to high intensity proton and carbon resonances in the NMR spectra of cerebral lipids. With reference to literature values for $^{13}$C resonances and a $^{13}$C DEPT spectrum of the crude lipid extract (Figure 3. 2. 12), 24 out of 27 of the cholesterol carbon signals were positively assigned. Proton resonances were subsequently assigned with reference to the HMQC spectrum (Figure 3. 2. 13). The C18 carbon resonance at 12.245 ppm produced a cross-peak at 0.64 ppm in

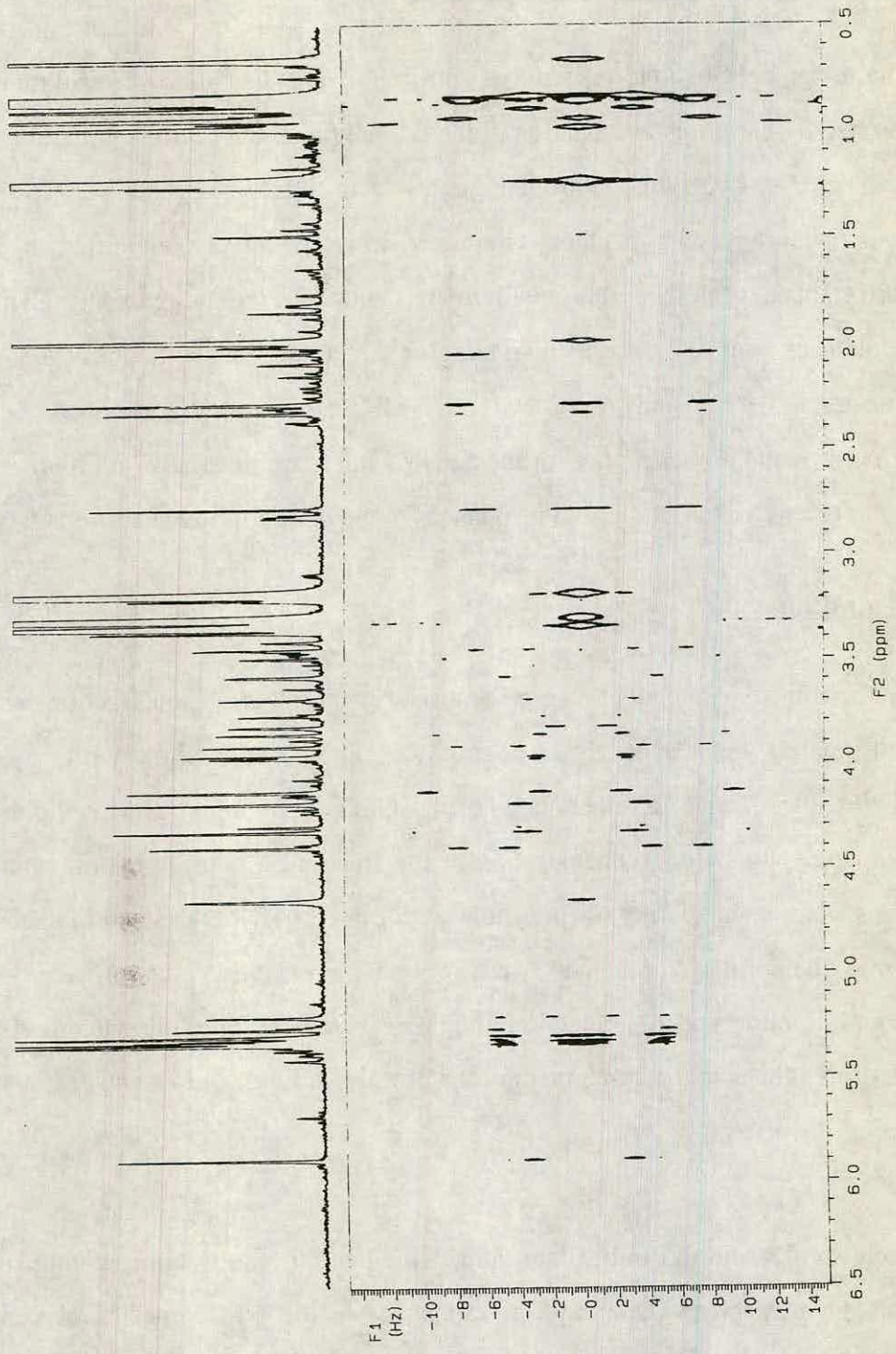


Figure 3. 2. 3 Two-dimensional *J*-resolved spectrum of cerebral lipids at 600 MHz.

Spectra where acquired as described in Experimental. Lipid resonances were referenced to the methanol quintet centred at 3.3 ppm.

the proton spectrum. This C18 methyl proton singlet was well distinguished from other resonances in the proton spectrum (Figure 3. 2. 2) and was subsequently used for diagnostic purposes. The C19 methyl proton singlet was assigned in a similar manner at a chemical shift of 0.97 ppm. The C21, C26 and C27 methyl protons are each coupled to one proton and thus give rise to doublet resonances. Signals for the C26 and C27 protons were seen to overlap at 0.82 ppm, both possessing identical $^{3}J$ coupling constants of 6.8 Hz (Figure 3. 2. 3). These resonances were not well distinguished, occurring at a similar chemical shift to ω1-methyl proton resonances from terminally saturated fatty acids. The C21 methyl doublet was observed at 0.88 ppm with an identical coupling constant to the C26 and C27 methyl proton resonances.

The majority of cholesterol signals occur over the 1.0 to 2.2 ppm range, often overlapping with other lipid resonances and thus making them inappropriate for diagnostic or quantitative purposes. In contrast, the cholesterol C3 proton adjacent to the hydroxy group was observed as a complex signal at 3.41 ppm. The olefinic C6 proton also resonates at an appreciably different chemical shift, but was not distinguishable in the one-dimensional spectrum due to overlapping resonances from other compounds, however its existence was detected in the *J*-resolved spectrum at 5.29 ppm. Confirmation of this assignment was given by the HMQC spectrum which showed a carbon-proton cross-peak at [121.99, 5.29] ppm.

*Galactocerebrosides* **[17a, 17b]**.

The complex structure of the galactocerebrosides (hereafter referred to as cerebroside) necessitated assignment of the spectra of authentic standards prior to their assignment in the cerebral lipid extract. Cerebroside I differs from its cerebroside II counterpart in possessing an α-hydroxy fatty acid. Examination of the two-dimensional COSY 45 spectrum of cerebroside I revealed a cross-peak between the α- (or C2 methine proton) and C3 methylene protons in the fatty acid (Figure 3. 2. 10). Consequently the methine proton was assigned to the

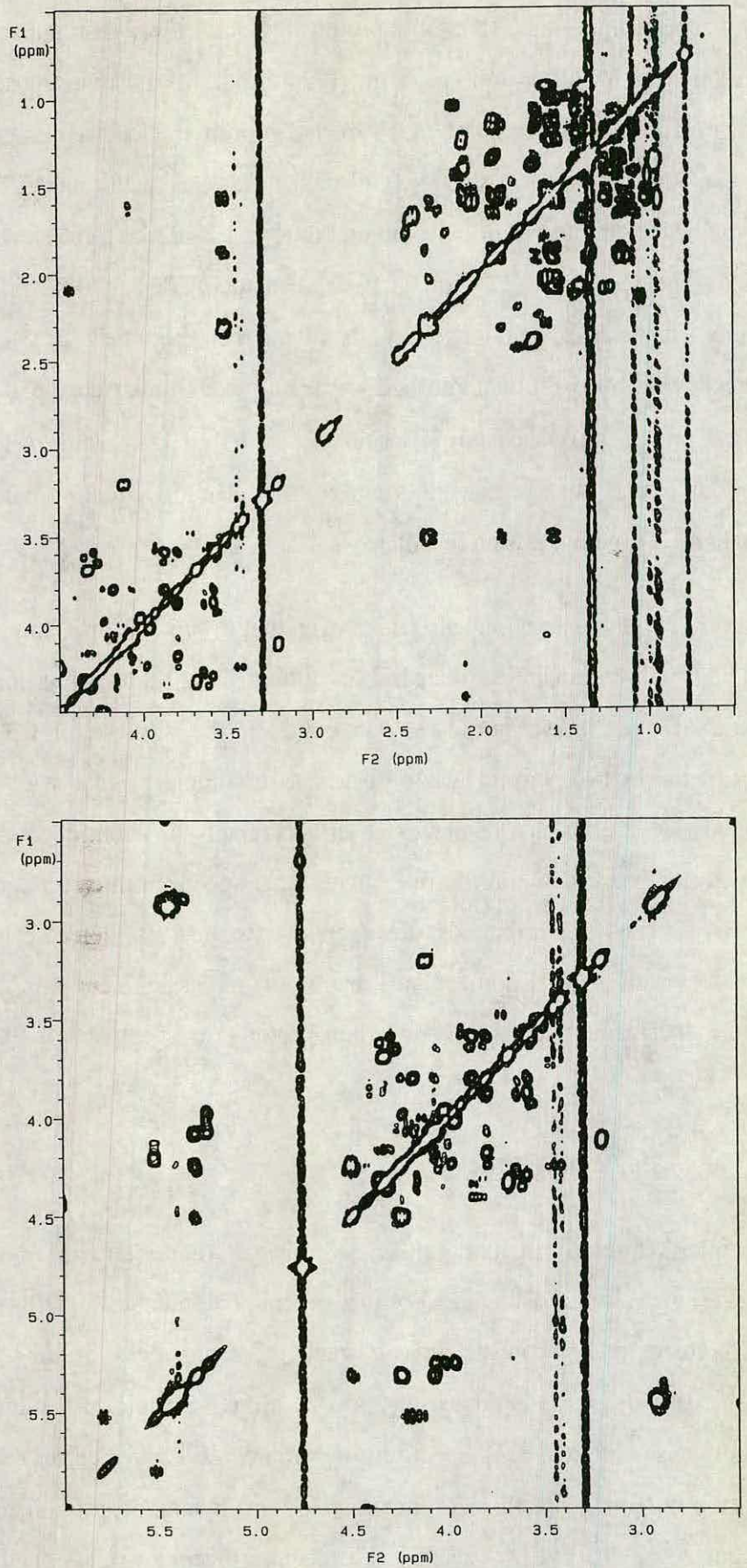


Figure 3. 2. 4 Homonuclear shift-correlated spectrum (COSY 45) of cerebral lipids at 600 MHz.

Spectra where acquired as described in Experimental. Lipid resonances were referenced to the methanol quintet centred at 3.3 ppm.

signal at 3.95 ppm and the methylene protons at 1.49 and 1.70 ppm. The C3 protons couple into the methylene envelope at 1.22 ppm. In contrast, cerebroside II does not possess an α-hydroxy fatty acid and does not exhibit a cross-peak in the same position (Figure 3. 2. 10). In this case the coupling of the C2 methylene protons to the C3 methylene protons produces a cross-peak at [2.12, 1.55] ppm. Neither of these signals were suitable for diagnostic purposes as they occurred at similar chemical shifts to C3 and C2 methylene proton resonances in other fatty acids.

Olefinic proton resonances in the sphingosine (ceramide) moiety occurred at 5.40 and 5.65 ppm (Figure 3. 2. 5). The 5.40 ppm signal was seen as a doublet of doublets with a $^3J_{b,1}$ of 7.5 Hz and a $^3J_{b,a}$ of 15.7 Hz and was assigned as CER *a*. The complex resonance at 5.65 ppm was consequently assigned as CER *b*. Additional support for these assignments was given by the two dimensional COSY 45 spectrum in which it was seen that the CER *b* resonance coupled to a signal at 1.97 ppm which was in turn coupled to an unresolved signal in the methylene envelope region at 1.30 ppm (Figure 3. 2. 8). It follows that the resonances at 1.97 and 1.30 ppm corresponded to methylene groups C*x* and C*y* respectively (Figure 3. 2. 5). These assignments were identical for both cerebrosides.

The COSY 45 spectrum of both cerebrosides also showed coupling between CER *a* and a proton resonance at 4.05 ppm (Figure 3. 2. 8). This signal was assigned as CER 1. Examination of the COSY 45 spectrum showed this proton to be coupled to a resonance at 3.95 ppm, which was assigned as CER 2. The one dimensional spectra of cerebrosides I and II showed marked differences over the 3.5 to 4.2 ppm range (Figures 3. 2. 6). In addition to cerebroside I possessing a C2 proton resonance from the α-hydroxy fatty acid at 3.95 ppm, doublets of doublets were observed at 3.69 ppm and 4.03 ppm which were not present in the proton spectrum of cerebroside II.

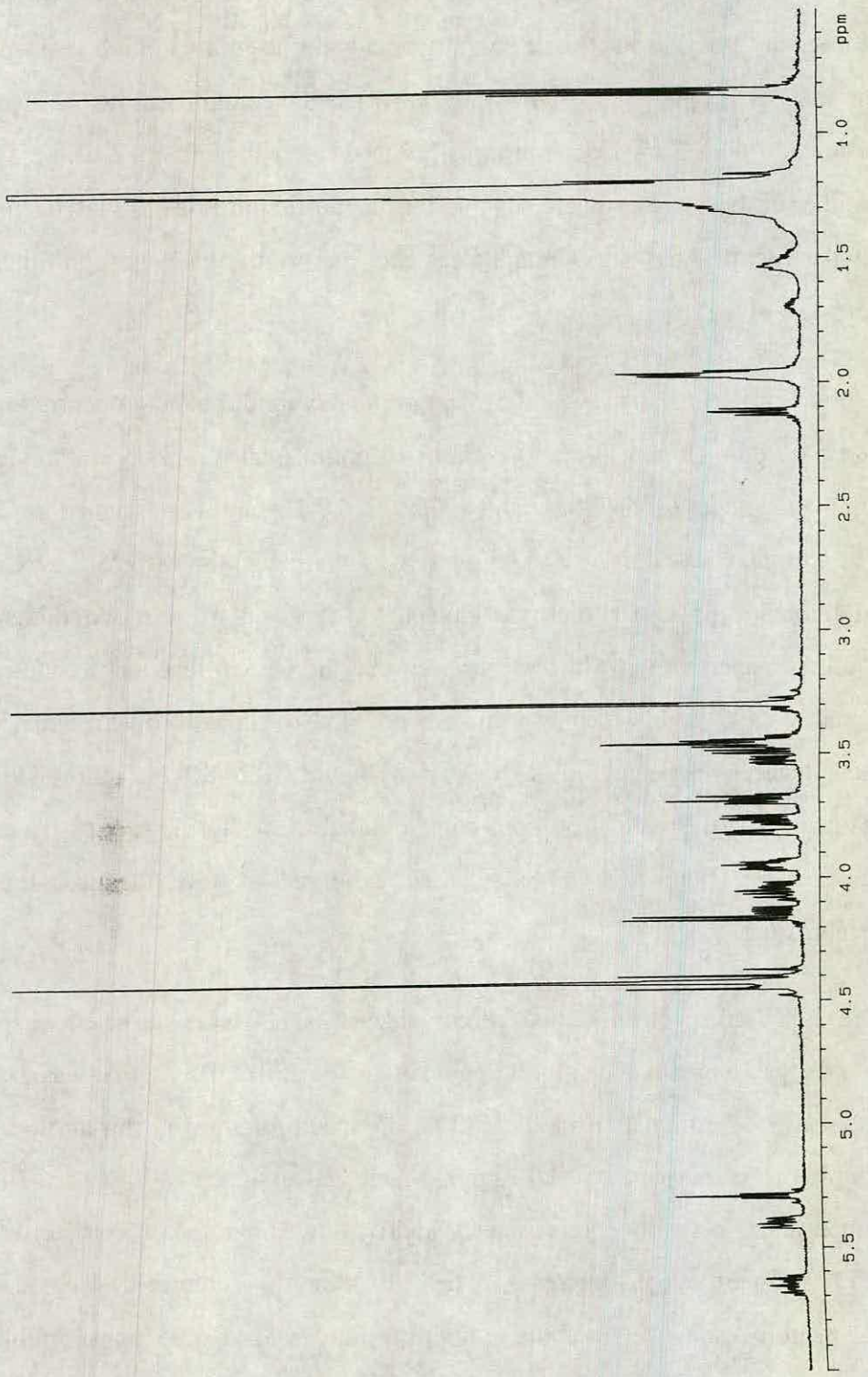


Figure 3. 2. 5 $^{1}$H NMR spectrum of a mixture of authentic galactocerebrosides (cerebrosides I and II) at 600 MHz.

Spectra where acquired as described in Experimental. Lipid resonances were referenced to the methanol quintet centred at 3.3 ppm.

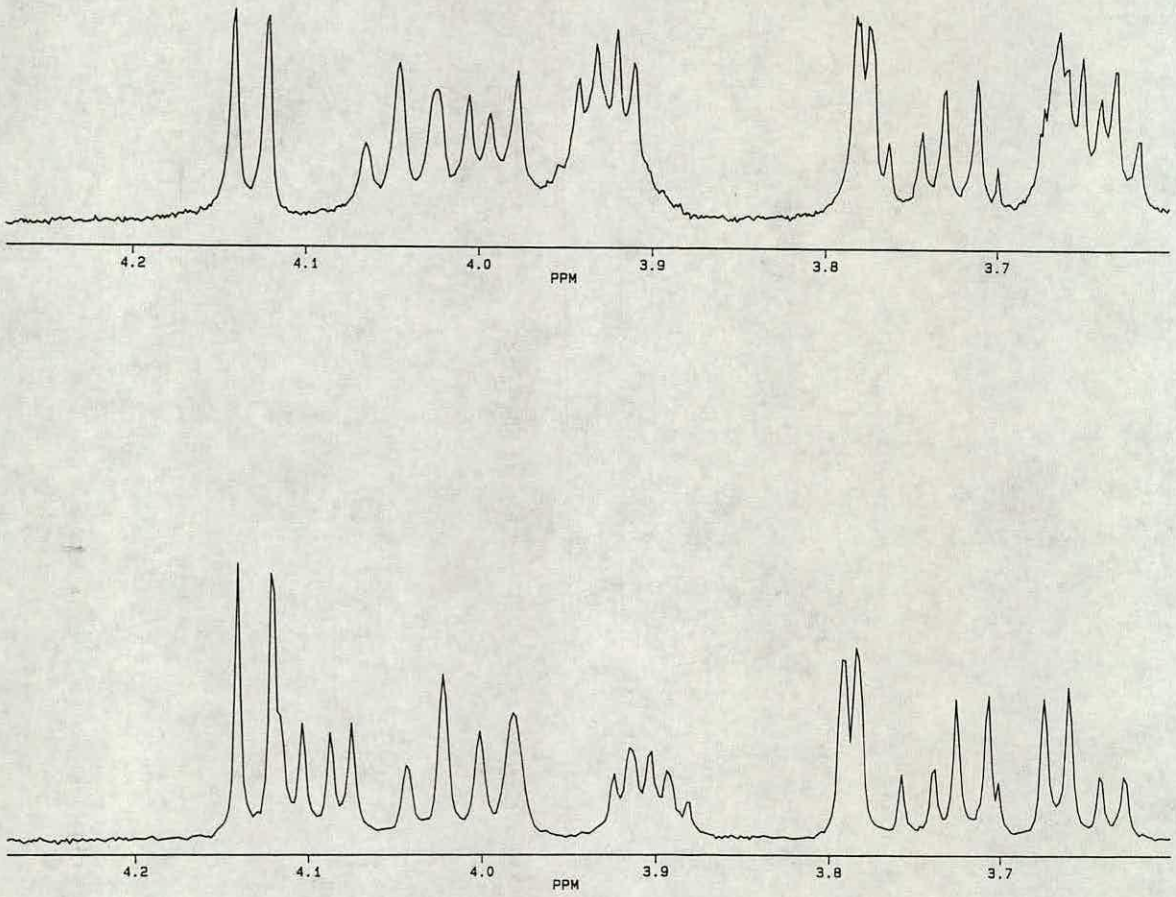


Figure 3. 2. 6 $^{1}H$ NMR spectrum of authentic galactocerebroside I (top figure) and galactocerebroside II (bottom figure) at 360 MHz.

Spectra where acquired as described in Experimental. Lipid resonances were referenced to the methanol quintet centred at 3.3 ppm.

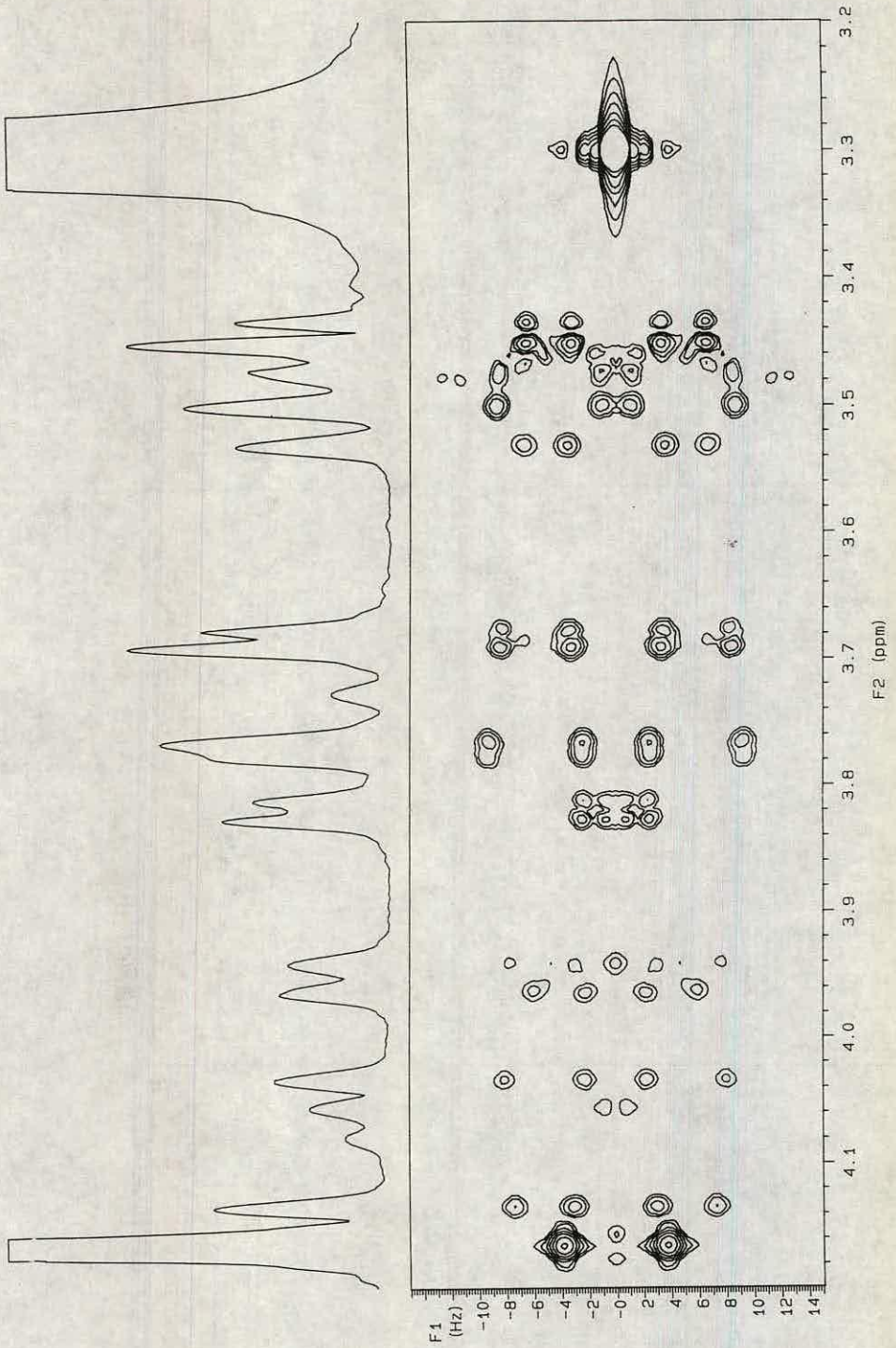


Figure 3. 2. 7 Two-dimensional *J*-resolved spectrum of a mixture of authentic galacto-cerebrosides (cerebrosides I and II) at 600 MHz.

Spectra where acquired as described in Experimental. Lipid resonances were referenced to the methanol quintet centred at 3.3 ppm.

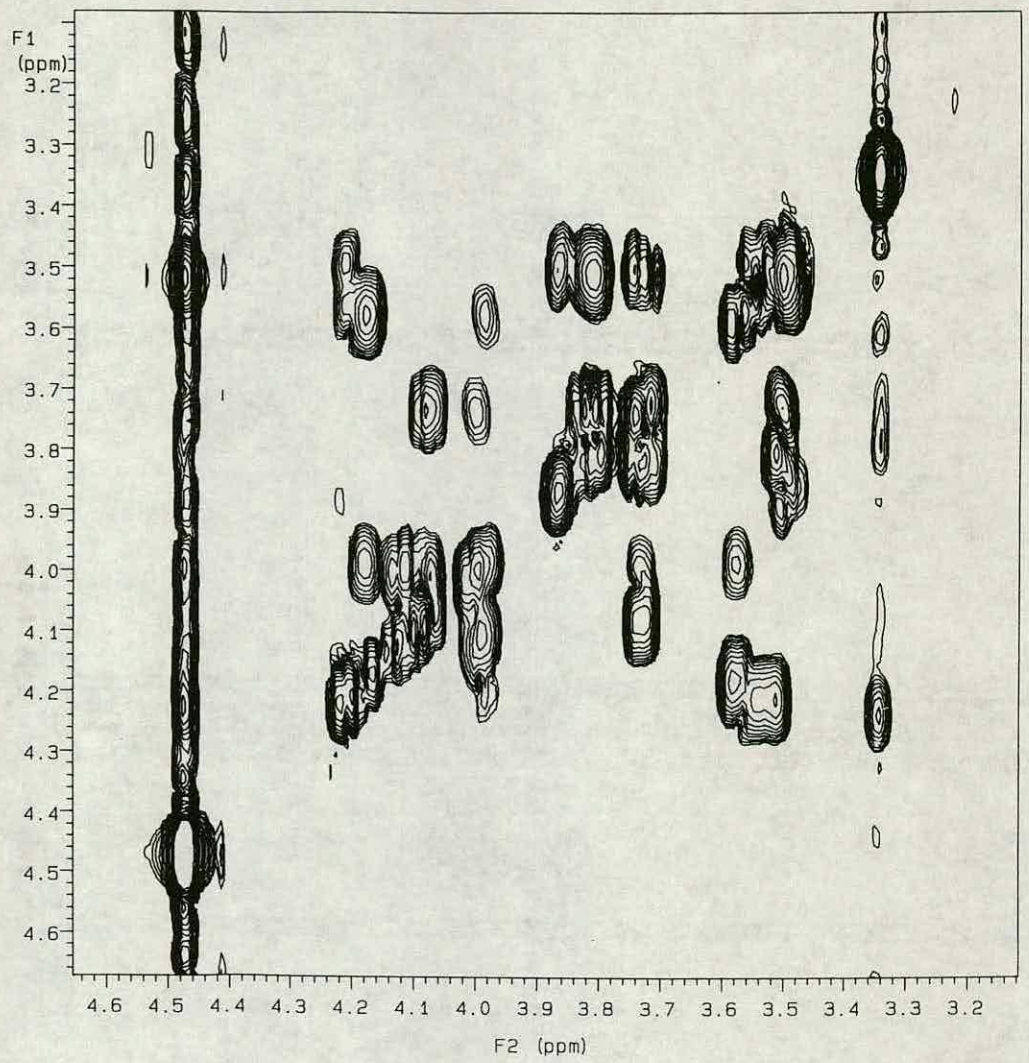


Figure 3. 2. 8 Homonuclear shift-correlated spectrum (COSY 45) of a mixture of authentic galactocerebrosides (cerebrosides I and II) at 600 MHz.

Spectra where acquired as described in Experimental. Lipid resonances were referenced to the methanol quintet centred at 3.3 ppm.

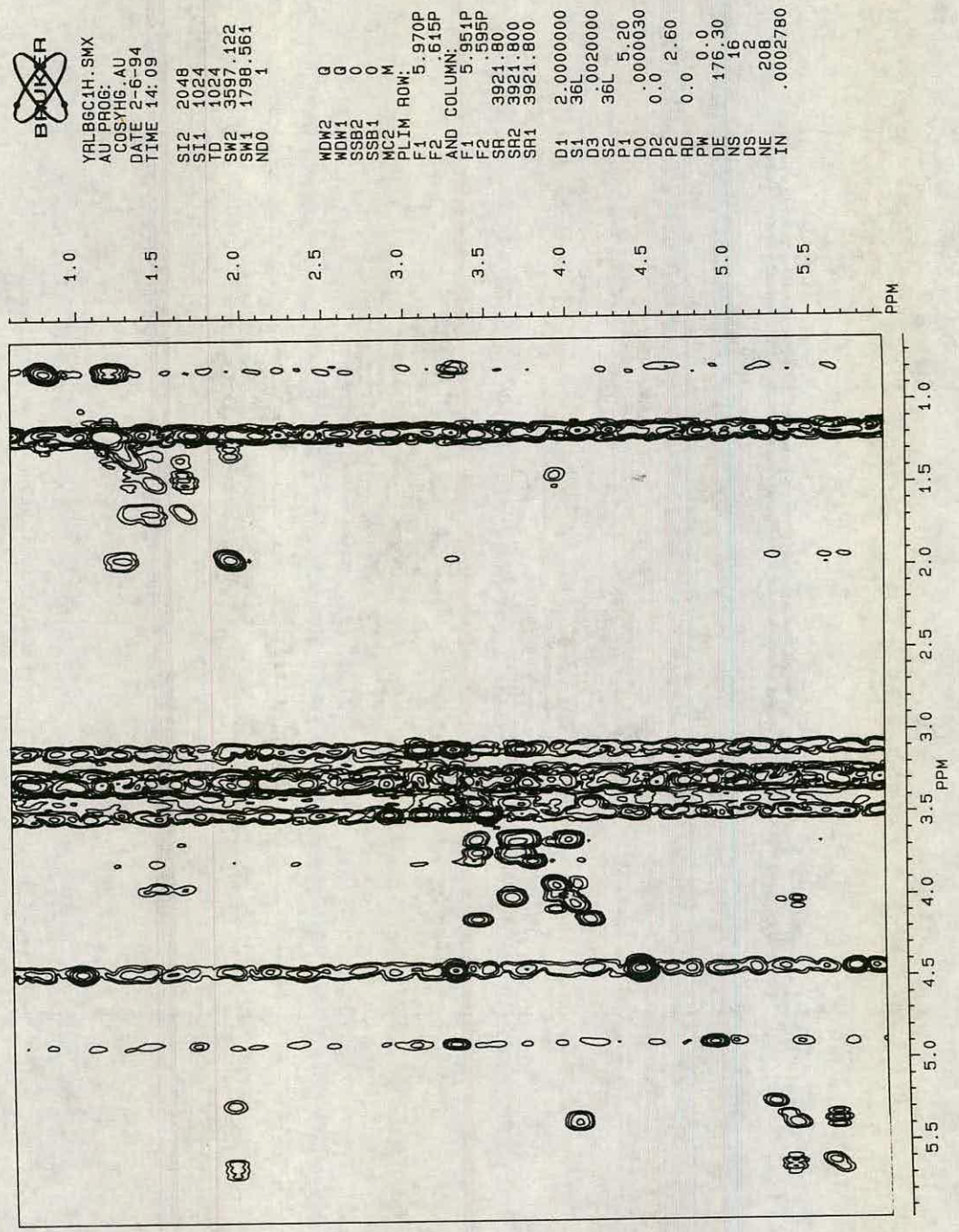


Figure 3. 2. 9 Homonuclear shift-correlated spectrum (COSY 45) of galactocerebroside I at 600 MHz.

Spectra where acquired as described in Experimental. Lipid resonances were referenced to the methanol quintet centred at 3.3 ppm.

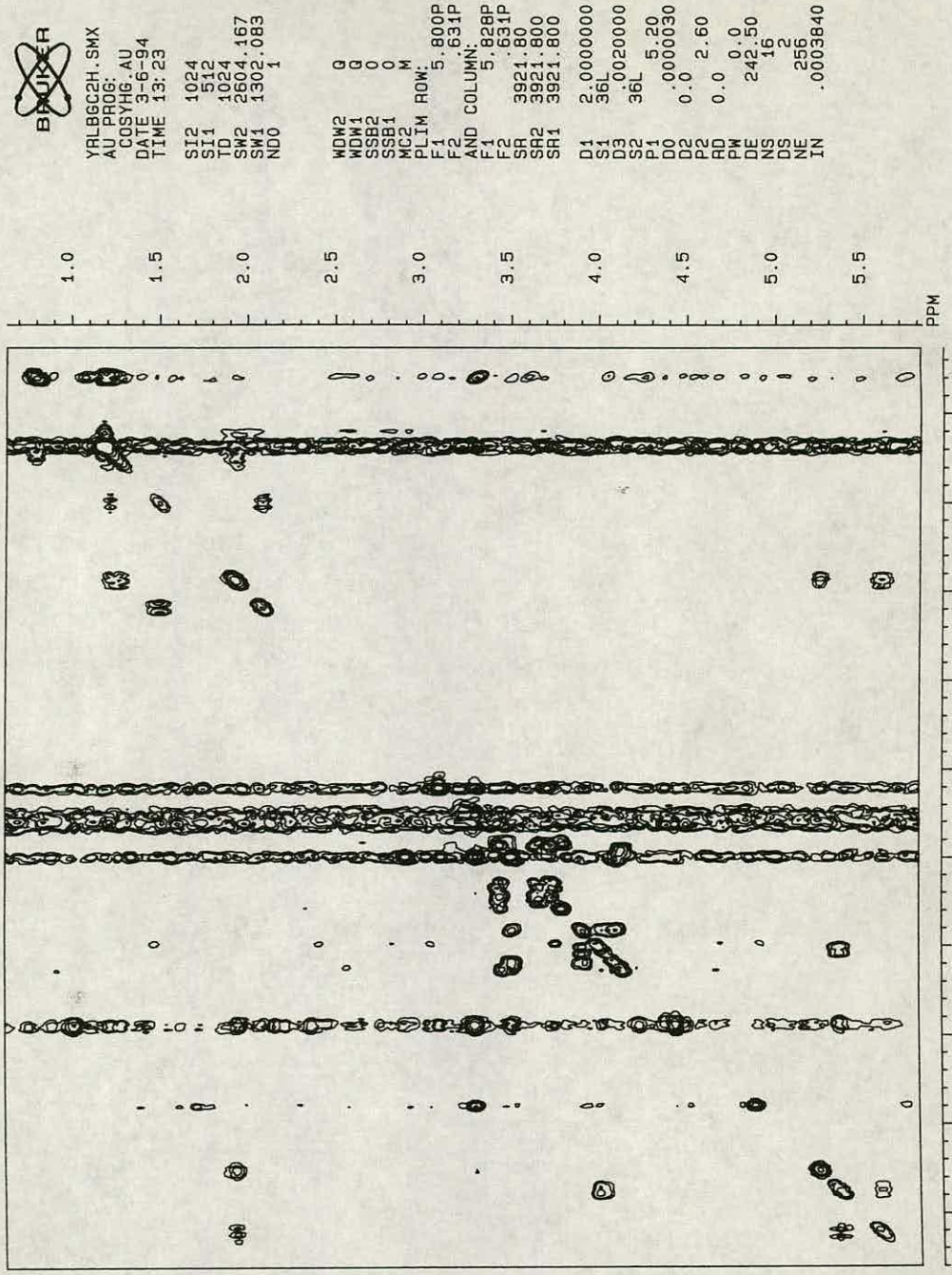


Figure 3. 2. 10 Homonuclear shift-correlated spectrum (COSY 45) of galactocerebroside II at 600 MHz.

Spectra where acquired as described in Experimental. Lipid resonances were referenced to the methanol quintet centred at 3.3 ppm.

Similarly, two signals at 3.54 and 4.14 ppm were observed in the proton spectrum of cerebroside II which were not present in the spectrum of cerebroside I. These two sets of resonances were found to couple to each other and to the CER 2 methine proton at 3.95 ppm, which in turn coupled to the CER 1 proton at 4.05 ppm and were consequently assigned to CER 3 diastereotopic methylene protons. In cerebroside I, with CER 3 protons resonating at 3.69 (CER $3^{u}$) and 4.03 ppm (CER $3^{d}$), the coupling constants of the former signal were not clearly identified as they occurred at a similar chemical shift to the galactose GAC $6^{u}$ resonance. The other signal at 4.03 ppm was seen to exhibit a $^{3}J_{2,3}{}^{u}$ of 4.5 Hz in addition to a $^{2}J_{3}{}^{u},_{3}{}^{d}$ of 10.4 Hz (Figure 3. 2. 7). Similar analysis was performed on the CER 3 proton resonances in the cerebroside II spectrum. Both of these signals gave rise to doublets of doublets and were clearly seen in the *J*-resolved spectrum. The signal at 3.54 ppm exhibited a $^{3}J_{2,3}{}^{d}$ of 3.3 Hz in addition to $^{2}J_{3}{}^{u},_{3}{}^{d}$ of 10.4 Hz, and the signal at 4.14 ppm showed a $^{3}J_{2,3}{}^{u}$ of 4.6 Hz and identical $^{2}J_{3}{}^{u},_{3}{}^{d}$ of 10.4 Hz. Proton NMR spectroscopy studies of rat cerebral lipids by Choi *et al.* (1993), reported the assignment of CER 3 methylene proton resonances at 3.7 and 4.1 ppm. We believe these to correspond to a cerebroside I CER $3^{d}$ methylene proton [3.69 ppm] and a cerebroside II CER $3^{u}$ methylene proton [4.14 ppm] in our proton spectra.

Both cerebrosides possess a galactose moiety, the GAC 1 position of which is covalently linked to the CER 3 position by an ether group. The C1 position proton of galactose (GAC 1) is coupled to a single proton at GAC 2 and thus produces a characteristic doublet which was observed at 4.18 ppm (Figure 3. 2. 5). The remaining galactose proton resonances were assigned following examination of the two dimensional COSY 45 and *J*-resolved spectra. GAC 1 couples to GAC 2 with a $^{3}J_{1,2}$ of 7.8 Hz. It would appear that GAC 2, GAC 3 and GAC 5 all contribute to the multitude of signals in the 3.44 to 3.55 ppm region, however examination of the *J*-resolved spectrum showed that GAC 2 resonates at 3.50 ppm and is coupled to GAC 3 with a $^{3}J_{2,3}$ of 10 Hz in addition to a $^{3}J_{1,2}$ of 7.8 Hz. It was predicted that the resonance arising from coupling

between GAC 3 and GAC 2/GAC 4 would be a doublet of doublets with a $^3J_{2,3}$ of 10 Hz and a $^3J_{3,4}$ between 3 and 4 Hz. Such a resonance was observed at 3.44 ppm with $^3J_{3,4}$ of 3.6 Hz, allowing the assignment of GAC 4 at 3.83 ppm. The GAC 5 proton couples to two GAC 6 protons in addition to a GAC 4 proton. Understandably this gives rise to a complex signal which was observed at 3.48 ppm. Coupling between GAC 5 and GAC $6^u$/GAC $6^d$ is illustrated in the COSY 45 spectrum of galactocerebroside II (Figure 3. 2. 10). This shows cross-peaks between GAC 5 and resonances at 3.70, 3.78 and 3.83 ppm, with the latter resonance previously assigned to GAC 4. It is noted that vicinal coupling between two protons with a torsion angle of 60° gives rise to a coupling constant in the region of 2 to 5 Hz, conversely vicinal coupling with a torsion angle of 180°, 9 to 12 Hz (Abraham *et al.*, 1988). Although the torsion angles and $^3J$ coupling constant vary, protons at theoretical values of 60° and 180° were designated $H^d$ and $H^u$ respectively. The resonances at 3.78 and 3.70 ppm showed identical $^2J$ of 11.8 Hz in addition to $^3J$ of 7 Hz and 5.3 Hz. These were consequently assigned to the GAC $6^u$ and GAC $6^d$ protons respectively. Inspection of the one dimensional proton NMR spectrum showed GAC $6^u$ to be the only resonance suitable for diagnostic and quantitative purposes, with other galactose signals overlapping with resonances from unrelated compounds.

*Ethanolamine phospholipids* [**18**].

Proton chemical shifts have previously been published for phosphatidyl ethanolamine in deuterated methanol by Birdsall *et al.* (1972). A complex resonance was observed at 3.06 ppm in the one-dimensional proton spectrum at a similar chemical shift to the literature value for the ethanolamine head group C2 methylene protons. This signal produced a cross-peak in the HMQC spectrum with a carbon resonance at 41.280 ppm (Figure 3. 2. 13) which was shown to arise from a $CH_2$ group in the $^{13}C$ DEPT spectrum (Figure 3. 2. 14). The broad nature of the proton resonance is believed to be attributed to the presence of a mixture of ethanolamine components, principally phosphatidyl ethanolamine and

phosphatidal ethanolamine (plasmalogen). In support of this, two marginally overlapping components were identified in the *J*-resolved spectrum at 3.09 ppm with similar coupling constants (Figure 3. 2. 3). The C1 head group methylene protons were subsequently identified in the COSY 45 spectrum from the cross-peak at [3.09, 3.98] ppm (Figure 3. 2. 4).

Values have also been reported for the glycerol part of the phospholipid (Birdsall *et al.*, 1972). The methine protons at the glycerol C2 position produce a complex multiplet of triplets upon coupling to the methylene protons at positions 1 and 3 of the glycerol backbone. A signal for both of these was seen at 5.27 ppm in close agreement with the literature value of 5.20 ppm. Examination of the two-dimensional COSY 45 spectrum showed cross-peaks between this glycerol C2 position proton and three other resonances at 3.95, 4.12 and 4.37 ppm (Figure 3. 2. 4). The magnetically equivalent methylene protons at the glycerol C3 position produce a doublet when coupled to the glycerol C2 proton and upon examination of the *J*-resolved spectrum these were assigned at a chemical shift of 3.95 ppm. Glycerol C1 methylene protons on the other hand are diastereotopic, with $^{2}J$ coupling in addition to $^{3}J$ coupling with the glycerol C2 methine proton. The signal at 4.12 ppm was seen to arise from coupling between the glycerol C1$^{u}$ proton and the glycerol C2 proton, with $^{3}J$ coupling of 9 Hz and $^{2}J$ coupling of 12 Hz. Conversely, the signal at 4.37 ppm was assigned to the glycerol C1$^{d}$ proton coupled to the glycerol C2 proton with a $^{3}J$ coupling of 3.2 Hz in addition to a $^{2}J$ coupling of 12 Hz. A description of the 'u' and 'd' nomenclature and their relation to torsion angles has been given previously.

*Choline phospholipids* [**19**, **20**].

Cerebral tissue normally contains three abundant choline phospholipids, i.e. phosphatidyl choline, phosphatidal choline (plasmalogen) and sphingomyelin. Methylene protons in the C1 and C2 positions of the choline head group were assigned at 4.20 and 3.56 ppm respectively in a similar manner to those of the ethanolamine phospholipids using a combination of literature values and the

COSY 45 spectrum. In addition to the C1 and C2 methylene protons, resonances from terminal $-N^{+}(CH_3)_3$ methyl protons were assigned at 3.17 and 3.18 ppm for sphingomyelin and phosphatidal/phosphatidyl choline respectively (Figure 3. 2. 2). These values are in close agreement with those previously reported by Choi *et al.* (1993). Glycerol backbone protons from phosphatidyl choline produced similar resonances to those of phosphatidyl ethanolamine and were assigned in an identical manner.

*Plasmalogens (ether phospholipids)* [**21**].

Plasmalogens are phospholipids containing an α, β unsaturated ether at the glycerol C1 position. Both phosphatidyl ethanolamine and phosphatidyl choline have their respective plasmalogens. The presence of an ether group alters the chemical environment of the glycerol backbone methylene protons resulting in a change in chemical shift values. This change is experienced least by the glycerol C3 methylene protons due to their greater distance from the ether group. These proton resonances were tentatively assigned at 3.95 ppm overlapping the corresponding diacyl glycerol phospholipid C3 resonances (Figure 3. 2. 2). The glycerol C2 methine proton (PLA 2) was assigned from the two-dimensional COSY 45 spectrum on the basis of a cross-peak between the glycerol C3 methylene protons at 3.95 ppm and a proton resonance at 5.12. The CH group nature of this latter resonance was confirmed following inspection of the HMQC and $^{13}C$ DEPT spectra (Figures 3. 2. 13 and 3. 2. 14 respectively). The COSY 45 spectrum revealed two additional couplings between the glycerol C2 position and protons with chemical shifts at 3.84 and 3.89 ppm. The *J*-resolved spectrum showed these resonances to be doublets of doublets with coupling constants very similar to those of the corresponding diacyl glycerol phospholipid $C1^{u}$ and $C1^{d}$ protons. These were consequently assigned at chemical shifts of 3.84 and 3.89 ppm respectively. In addition to the glycerol backbone proton resonances, olefinic protons from the ether linkage gave distinct, well resolved signals. The PLA α olefinic proton produced a doublet at 5.87 ppm on coupling with PLA β.

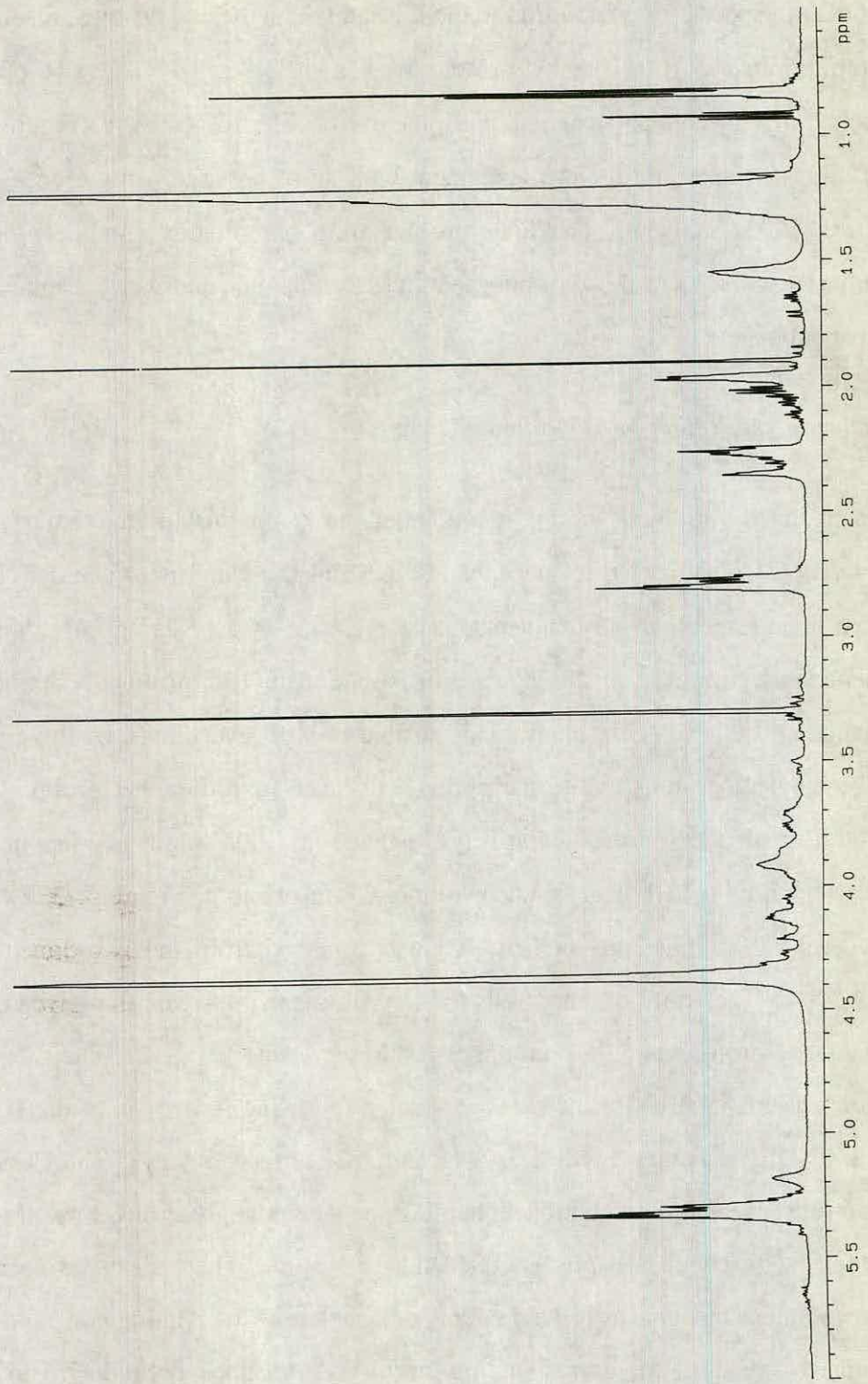


Figure 3. 2. 11 $^{1}$H NMR spectrum of acidic cerebral lipids at 600 MHz.

Spectra where acquired as described in Experimental. Lipid resonances were referenced to the methanol quintet centred at 3.3 ppm.

The vicinal coupling constant of 6.2 Hz confirmed the *cis* confirmation of the α, β olefinic protons (Figure 3. 2. 3). PLA β was assigned from the [PLA α, PLA β] cross-peak at [5.85, 4.31] ppm in the COSY 45 spectrum.

***Acidic Lipids.***

High performance thin layer chromatography analysis of the acidic fraction revealed the presence of four lipid constituents: cardiolipin, 3'-sulphate-galactocerebrosides (sulfatides I and II), serine phospholipids and inositol phospholipids. $^{1}$H NMR spectroscopy analysis demonstrated that the fractionation process was successful with the absence of cholesterol, ethanolamine phospholipid and choline phospholipid diagnostic resonances at 0.64, 3.05 and 3.56 ppm respectively.

*Sulfatides.*

Resonances from the ceramide moiety of 3'-sulphate-galactocerebrosides were detected at 5.40 and 5.65 ppm corresponding to the CER *a* and CER *b* olefinic protons, of which the latter was used for diagnostic purposes (Figure 3. 2. 11). Resonances from the galactose ring were not easily distinguished in the proton spectra due to a combination of low sulfatide concentration and spectral overlap with resonances from acidic phospholipids.

*Phosphatidyl serine and phosphatidyl inositol* [**22**, **23**].

The glycerol C2 methine proton resonance from phosphatidyl serine and phosphatidyl inositol were observed as a broad peak at 5.18 ppm, and at a similar chemical shift to the glycerol C2 methine proton of phosphatidyl ethanolamine and phosphatidyl choline in the neutral lipid fraction. The absence of PLA α and PLA 2 methine proton resonances at 5.87 and 5.12 ppm respectively argued against the presence of acidic plasmalogens in this fraction (Figure 3. 2. 11). A combination of low abundance and high degree of spectral overlap with 3'-

sulphate-galactocerebroside signals made phosphatidyl serine and phosphatidyl inositol difficult to differentiate and quantify in the proton spectra. The application of $^{31}P$ NMR spectroscopy to the quantification of phospholipids is discussed in Section 3. 2. 3.

*Fatty acid structures* [**24**].

Comparison of neutral and acidic lipid proton spectra over the 0.6 to 2.4 ppm chemical shift region allowed the putative identification of fatty acid resonances. The assignments were performed on the proton NMR spectrum of the acidic lipid fraction in which diagnostic fatty acyl resonances were more distingishable as a result of the absence of cholesterol signals. Terminal or ω1-methyl protons were assigned as triplet resonances at 0.82 and 0.93 ppm. The former signal arises from terminally saturated fatty acids, i.e. totally saturated or n-9 or n-6 family whereas the presence of an unsaturated bond in the close proximity of the ω1-methyl group, as observed in n-3 fatty acids, causes a change in the chemical shift of the ω1-methyl protons to 0.93 ppm. These assignments were in close agreement with those of Gunstone in which studies of various fatty acid methyl esters are described (Gunstone, 1992). The ratio of these two signals (both of which are distinguishable in the neutral and acidic spectra), gives a measure of the relative proportions of terminally saturated to n-3 fatty acids in the lipid extract. ω2-methylene proton resonances were assigned from the COSY 45 at 1.22 (terminally saturated) and 2.03 ppm (n-3) (Figure 3. 2. 4). The signal at 1.22 ppm was indistinguishable from the broad multicomponent resonance which comprised the 'methylene envelope'. In contrast, ω2-methylene protons in n-3 fatty acids were seen at 2.03 ppm, producing a cross-peak with olefinic protons at 5.35 ppm in the two-dimensional COSY 45 spectrum.

Choi and colleagues assigned diagnostic resonances for arachidonic ($C_{20:4}$) and docosahexaenoic ($C_{22:6}$) acids in the proton NMR spectra of rat cerebral lipid extracts (Choi *et al.*, 1993). We determined to assess whether these polyunsaturated lipid species could be identified in the proton spectra of our

murine lipid extract. Olefinic proton resonances were observed as a broad multicomponent signal in the one dimensional proton spectrum at 5.35 ppm. These triplets with vicinal coupling constants of 3.2 Hz, as seen in the *J*-resolved spectrum, were consistent with *cis* fatty acids (Figure 3. 2. 3). The same signal produced cross-peaks with resonances at 2.78, 2.35, 2.12, 2.03 and 1.97 ppm in the two-dimensional COSY 45 spectrum. Taking each of these in turn:

(i) The signal at 2.78 ppm coupled only to olefinic protons and was therefore deduced to arise from a methylene group between two vicinyl groups. Analysis of fatty acid species present in cholesteryl esters from a murine cerebral source by chemical ionization mass spectrometry (CI-MS), revealed arachidonic and docosaehexaenoic acids as the only polyunsaturated fatty acids present (Section 3. 3. 1), with linoleic acid ($C_{18:2}$) also in appreciable quantities. We therefore concluded that the broad resonance at 2.78 ppm was attributable to [-CH=CH-C<u>H</u>$_2$-CH=CH-] structures in these three fatty acids.

(ii) The signal at 2.35 ppm has been implicated to be diagnostic for C3 methylene protons in docosahexaenoic acid (Choi *et al.*, 1993). This resonance was seen to couple to a component in a broad resonance at 2.27 ppm in the lipid extract COSY 45 spectrum (Figure 3. 2. 4), which had been previously assigned to C2 methylene protons. Thus, coupling between the resonances at 5.35, 2.35 and 2.27 ppm allowed the elucidation of the structure [-CH=CH-$CH_2$-$CH_2$-$COO^-$] which is consistent with that of docosahexaenoic acid. Although another candidate for this combination of resonances does exist, that being docosapentaenoic acid ($C_{22:5}$), a molecular ion for this fatty acid was not seen in the CI-MS spectra (Section 3. 3. 1). In conclusion the signal at 2.35 ppm was believed diagnostic for the presence of docosahexaenoic acid in this murine lipid extract.

(iii) The signal at 2.12 ppm produced a cross-peak with a proton resonance at 1.65 ppm in the two dimensional COSY 45 spectrum, which in turn coupled to a signal at 2.27 ppm (previously assigned to C2 methylene protons). The

| Metabolite | Assignment | Chemical shift /ppm | Multiplicity | Functional group |
|---|---|---|---|---|
| | | | | |
| *Neutral lipids* | | | | |
| | | | | |
| Cholesterol | C18 | 0.64* | s | $CH_3$ |
| | C26/27 | 0.82 | d | $CH_3$ |
| | C21 | 0.88 | d | $CH_3$ |
| | C19 | 0.97 | s | $CH_3$ |
| | C14/17 | 1.0 - 1.5 | c | CH |
| | C24 | 1.0 - 1.15 | c | $CH_2$ |
| | C8 | 1.4 - 1.5 | c | CH |
| | C11 | 1.4 - 1.5 | c | $CH_2$ |
| | C1 | 1.8 | c | $CH_2$ |
| | C7/16 | 1.9 | c | $CH_2$ |
| | C4 | 2.2 | c | $CH_2$ |
| | | | | |
| Galactocerebrosides | CERa | 5.40 | dd | $-CH_2-CH=C\mathbf{H}-$ |
| | CERb | 5.65* | c | $-CH_2-C\mathbf{H}=CH-$ |
| | C*x* | 1.97 | c | $-C\mathbf{H}_2-CH=$ |
| | C*y* | 1.30 | c | $-CH_2$ |
| | CER1 | 4.05 | c | -C**H**OH- |
| | CER2 | 3.95 | c | -C**H**NH$CH_2$- |
| | GAC1 | 4.18 | d | -C**H**OH- |
| | GAC2 | 3.50 | dd | -C**H**OH- |
| | GAC3 | 3.44 | dd | -C**H**OH |
| | GAC4 | 3.83 | dd | -C**H**OH- |
| | GAC5 | 3.48 | c | -C**H**OH- |
| | GAC6$^u$ | 3.78 | dd | -C**H**$^u$OH |
| | GAC6$^d$ | 3.70 | dd | -C**H**$^d$OH |
| | | | | |
| Cerebroside I | C2 | 3.95 | dd | -C**H**OH- |
| | C3$^u$ | 1.49 | c | -CHOH-C**H**$^u$- |
| | C3$^d$ | 1.70 | c | -CHOH-C**H**$^d$- |
| | C4 | 1.22 | c | $-CH_2-C\mathbf{H}_2-$ |
| | CER3$^d$ | 3.69 | dd | -CHNHC**H**$^d$- |
| | CER3$^u$ | 4.03 | dd | -CHNHC**H**$^u$- |
| | | | | |

Table 3. 2. 1 Assignment of $^1$H NMR resonances in cerebral lipid extracts at 600 MHz.

Cerebral lipids were extracted from control murine tissue with chloroform/methanol (2:1, v/v). The crude lipid extract was fractionated into neutral and acidic lipid species over DEAE Sephadex-A25. $^1$H NMR spectra were acquired on a Varian VXR600S NMR spectrometer operating at a spectrometer frequency of 599.945 MHz. For a full description of the procedure see Experimental. Chemical structures are illustrated in Figure 3. 2. 1.

* denotes $^1$H resonances used for metabolite quantification.

c, complex; d, doublet; dd, doublet of doublets; q, quartet; qu, quintet; t, triplet.

combination of these resonances allowed the structure [-CH=CH-$CH_2$-$CH_2$-$CH_2$-$COO^-$] to be elucidated. This structure is consistent with the carboxyl terminus of arachidonic acid and eicosapentaenoic acid ($C_{20:5}$), however as a molecular ion for the latter was not present in the CI-MS spectra (Section 3. 3. 1) the proton resonances were assigned to structures in arachidonic acid. Of these, the signal with a chemical shift of 1.65 ppm was clearly seen in both the neutral and acidic spectra and was used for diagnostic purposes. It is clear therefore, that should the determination be so required, the intensities of the signals at 1.65 and 2.35 ppm would give a measure of the relative proportions of arachidonic and docosahexaenoic acids respectively.

(iv) The resonance at 2.03 ppm has previously been assigned to ω2-methylene protons next to an unsaturated group in n-3 fatty acids [-CH=CH-$C\underline{H}_2$-$CH_3$], of which docosahexaenoic acid is the primary component in this cerebral lipid extract.

(v) The large signal at 1.97 ppm was seen to couple to methylene envelope protons in addition to olefinic protons (Figure 3. 2. 4). This was therefore assigned to methylene protons between a vinyl group and the methylene envelope [-$(CH_2)_n$-$C\underline{H}_2$-CH=CH-$CH_2$-CH=CH-$C\underline{H}_2$-$(CH_2)_n$-].

And finally, C3 methylene protons in terminally saturated fatty acids were assigned at 1.55 ppm from the cross-peaks with C2 and C4 methylene envelope protons at 2.27 and 1.22 ppm respectively in the two-dimensional COSY 45 spectrum.

To summarize the above analysis, diagnostic resonances from the component fatty acids are as follows:

(i) $\delta = 0.82$ ppm, ω1-methyl protons from terminally saturated fatty acids;

(ii) $\delta = 0.93$ ppm, ω1-methyl protons from n-3 fatty acids;

(iii) $\delta = 1.65$ ppm, C3-methylene protons in arachidonic acid ($C_{20:4}$);

| Metabolite | Assignment | Chemical shift /ppm | Multiplicity | Functional group |
|---|---|---|---|---|
| | | | | |
| *Neutral lipids* | | | | |
| | | | | |
| Cerebroside II | C2 | 2.12 | t | -C**H**$_2$-CH$_2$- |
| | C3 | 1.55 | c | -CH$_2$-C**H**$_2$- |
| | CER3$^d$ | 3.54 | dd | -CHNHC**H**$^d$- |
| | CER3$^u$ | 4.14 | dd | -CHNHC**H**$^u$- |
| | | | | |
| Ethanolamine PL. | C1 | 3.98 | c | -C**H**$_2$CH$_2$NH$_2$ |
| | C2 | 3.06* | c | -CH$_2$C**H**$_2$NH$_2$ |
| | Sn1$^u$ | 4.12 | dd | -C**H**$^u$OCO- |
| | Sn1$^d$ | 4.37 | dd | -C**H**$^d$OCO- |
| | Sn2 | 5.27 | c | -C**H**OR- |
| | Sn3 | 3.95 | d | -C**H**$_2$OPO$_3$- |
| | | | | |
| Choline PL. | C1 | 4.20 | c | -C**H**$_2$CH$_2$N$^+$- |
| | C2 | 3.56 | c | -CH$_2$C**H**$_2$N$^+$- |
| | | 3.18* | s | -CH$_2$N$^+$(C**H**$_3$)$_3$ |
| | | | | |
| Sphingomyelin | | 3.17* | s | -CH$_2$N$^+$(C**H**$_3$)$_3$ |
| | | | | |
| Plasmalogen | PLAα | 5.87* | d | -O-C**H**=CH- |
| | PLAβ | 4.31 | q | -O-CH=C**H**- |
| | PLA1$^u$ | 3.84 | dd | -C**H**$^u$OCO- |
| | PLA1$^d$ | 3.89 | dd | -C**H**$^d$OCO- |
| | PLA2 | 5.12 | c | -C**H**OR- |
| | PLA3 | 3.95 | d | -C**H**$_2$OPO$_3$- |
| | | | | |
| *Acidic lipids* | | | | |
| | | | | |
| Sulfatides | CERa | 5.40 | dd | -CO-CH=C**H**- |
| | CERb | 5.65* | c | -CO-C**H**=CH- |
| | | | | |
| Serine PL. | Sn2 | 5.18 | c | -C**H**OR- |
| | | | | |
| Inositol PL. | Sn2 | 5.18 | c | -C**H**OR- |
| | | | | |

Table 3. 2. 1 *continued.* Assignment of $^1$H NMR resonances in cerebral lipid extracts at 600 MHz.

Cerebral lipids were extracted from control murine tissue with chloroform/methanol (2:1, v/v). The crude lipid extract was fractionated into neutral and acidic lipid species over DEAE Sephadex-A25. $^1$H NMR spectra were acquired on a Varian VXR600S NMR spectrometer operating at a spectrometer frequency of 599.945 MHz. For a full description of the procedure see Experimental. Chemical structures are illustrated in Figure 3. 2. 1.

* denotes $^1$H resonances used for metabolite quantification.

c, complex; d, doublet; dd, doublet of doublets; q, quartet; qu, quintet; t, triplet.

(iv) $\delta = 2.27$ ppm, C2-methylene protons in all fatty acids;

(v) $\delta = 2.35$ ppm, C3-methylene protons in docosahexaenoic acid ($C_{22:6}$);

(vi) $\delta = 2.79$ ppm, [-CH=CH-C$\underline{H_2}$-CH=CH-] methylene protons in poly-unsaturated fatty acids.

A comparison of the above integrals provides rapid information on the composition of fatty acids present in the cerebral lipid extract, i.e. saturated, mono-unsaturated, di-unsaturated and poly-unsaturated (arachidonic and docosahexaenoic acids), without the necessity for alternative analytical procedures. An example of the application of this analysis to the elucidation of triglyceride fatty acid composition is discussed below.

*Summary.*

Proton resonances from cholesterol, total ethanolamine phospholipids and total choline phospholipids were particularly prominent in the one-dimensional proton NMR spectra. High performance thin layer chromatography values for the percentage composition of these three lipid classes are 22.5, 21.8 and 23.5% respectively, indicating that they comprise over 67% of total cerebral lipids (Section 3. 3. 2). Cholesterol was readily characterized from its C18 methyl singlet signal at 0.64 ppm. Although cholesterol resonances were particularly prominent, it was reasoned that cholesteryl ester signals would make an insignificant contribution to the intensity of these resonances in normal brain tissue (less than 0.4%). Any change in cholesteryl esters would therefore be undetectable by NMR spectroscopy. Total ethanolamine phospholipids were quantified from the ethanolamine C2 methylene complex proton signal at 3.56 ppm. The contribution that plasmalogens or sphingosine derivatives made to this signal was not determined. Total choline phospholipids were quantified from their choline C2 methylene complex proton signal at 3.06 ppm. More detailed examination was given by comparison of the terminal methyl proton singlets at 3.17 and 3.18 ppm corresponding to sphingomyelin and phosphatidyl choline, the latter probably also containing phosphatidal choline. The contribution made by

| Assignment | Chemical shift /ppm | Multiplicity | Functional group |
|---|---|---|---|
| | | | |
| *Acidic lipids* | | | |
| | | | |
| Fatty acids | | | |
| | | | |
| ω1 (n-6, n-9) | 0.84 | t | $-CH_2CH_2C\mathbf{H}_3$ |
| ω1 (n-3) | 0.93 | t | $-CH=CHCH_2C\mathbf{H}_3$ |
| ω2 (sat.) | 1.22 | c | $-CH_2C\mathbf{H}_2CH_3$ |
| ω2 (n-3) | 2.03 | c | $-CH=CHC\mathbf{H}_2CH_3$ |
| ω3 (n-3) | 5.35 | c | $-CH=C\mathbf{H}CH_2CH_3$ |
| | | | |
| methylene envelope | 1.22 | c | $-(CH_2)_n-$ |
| | | | |
| olefinic groups | 5.35 | c | -CH=CH- |
| | | | |
| PUFA | 2.78 | c | $-CH=CH(C\mathbf{H}_2CH=CH)_n-CH_2-$ |
| PUFA | 1.97 | c | $-(CH_2)_nC\mathbf{H}_2CH=CH-$ |
| $C_{18:2}$ | 2.72* | t | $-CH=CHC\mathbf{H}_2CH=CH-$ |
| | | | |
| $C_{20:4}$ - C3 | 1.65* | q | $-CH=CHCH_2C\mathbf{H}_2CH_2COO^-$ |
| $C_{20:4}$ - C4 | 2.12 | t | $-CH=CHC\mathbf{H}_2CH_2CH_2COO^-$ |
| $C_{22:6}$ - C3 | 2.35* | c | $-CH=CHC\mathbf{H}_2CH_2COO^-$ |
| | | | |
| sat. - C2 | 2.27* | c | $-CH_2CH_2CH_2C\mathbf{H}_2COO^-$ |
| sat. - C3 | 1.55 | c | $-CH_2CH_2C\mathbf{H}_2CH_2COO^-$ |
| sat. - C4 | 1.22 | c | $-CH_2C\mathbf{H}_2CH_2CH_2COO^-$ |
| | | | |

Table 3. 2. 1 *continued.* Assignment of $^1$H NMR resonances in cerebral lipid extracts at 600 MHz.

Cerebral lipids were extracted from control murine tissue with chloroform/methanol (2:1, v/v). The crude lipid extract was fractionated into neutral and acidic lipid species over DEAE Sephadex-A25. $^1$H NMR spectra were acquired on a Varian VXR600S NMR spectrometer operating at a spectrometer frequency of 599.945 MHz. For a full description of the procedure see Experimental. Chemical structures are illustrated in Figure 3. 2. 1.

* denotes $^1$H resonances used for metabolite quantification.

c, complex; d, doublet; dd, doublet of doublets; q, quartet; qu, quintet; t, triplet.

plasmalogen to total choline phospholipids was not determined. Cerebrosides, comprising approximately 8% of total cerebral lipids (Section 3. 3. 2) were identified by their galactose GAC $6^d$ complex signal at 3.70 ppm in the neutral lipid proton spectrum. Choi *et al.* (1993) considered the galactose GAC 4 doublet of doublets at 3.84 ppm for this purpose, however this was found to overlap with plasmalogen glycerol $C1^u$ resonances in our proton spectra. The low concentration of this lipid did not facilitate its quantification. In addition, the inability to adequately distinguish cerebrosides I and II in the one-dimensional spectrum did not allow their separate quantification.

On the basis of high performance thin layer chromatography results, acidic lipids comprise approximately 25% of the total cerebral extract (Section 3. 3. 1), cardiolipin, sulfatides, phosphatidyl serine and phosphatidyl inositol contributing 5.3, 5.6, 10.3 and 3.1% respectively. The relatively smaller lipid quantities did not facilitate adequate quantification. Acidic sulfatides were determined from their sphingosine CER *b* olefinic proton complex signal at 5.65 ppm, it being found that the GAC $6^d$ resonance overlapped with serine head group C2 methylene protons in phosphatidyl serine (Figure 3. 2. 11). Resonances from phosphatidyl serine and phosphatidyl inositol were not well enough resolved to be used for quantitative purposes. Fatty acyl signals were particularly well distinguished in the acidic fraction in the absence of resonances from cholesterol, ethanolamine phospholipids and choline phospholipids. This assisted the assignment of diagnostic signals in terminally saturated fatty acids, n-3 fatty acids, linoleate ($C_{18:2}$), arachidonate ($C_{20:4}$), docosahexaenoate ($C_{22:6}$) and total polyunsaturated fatty acids at 0.82, 0.93, 2.72, 1.65, 2.35 and 2.79 ppm respectively.

In conclusion, a total of seven lipid species were identified from their diagnostic resonances in the one-dimensional proton NMR spectrum. Some degree of fatty acyl group determination was also offered (Table 3. 2. 1).

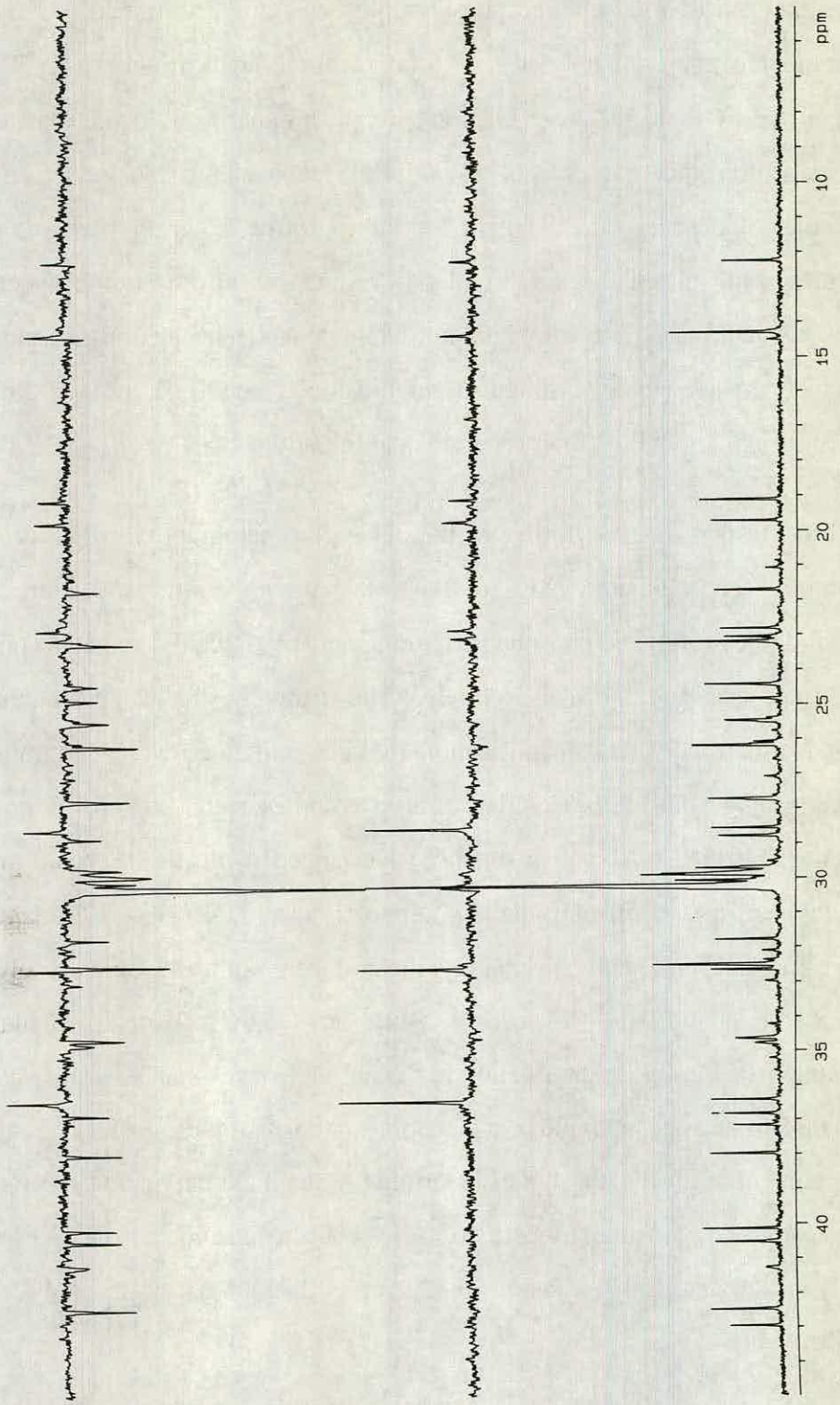


Figure 3. 2. 12 $^{13}C$ and $^{13}C$-DEPT NMR spectra of cerebral lipids at 150.869 MHz.

Spectra where acquired as described in Experimental. Lipid resonances were referenced to the methanol singlet at 51.0 ppm.

### 3. 2. 2 Assignment of $^{13}C$ NMR Spectra.

Although $^{13}C$ NMR spectroscopy does not lend itself to the quantitative analysis of metabolites, $^{13}C$ NMR studies on cerebral lipids were performed for the purpose of completeness. Due to the relative insensitivity of $^{13}C$ NMR spectroscopy, carbon resonances were assigned in a cumulative lipid extract obtained from three mouse brains without prior fractionation. The assignment of carbon signals was assisted by comparison with literature values (Gunstone, 1992), and by detailed examination of HMQC, one-dimensional $^{1}H$ and $^{13}C$-DEPT spectra.

***Neutral lipids.***

*Cholesterol.*

$^{13}C$ resonances for cholesterol are available in the literature (Johnson and Jenkowski, 1972). In addition, the high concentration of cholesterol in the lipid extract facilitated the assignment of resonances in the lipid extract spectra. The C18 carbon was tentatively assigned at 12.25 ppm (Figure 3. 2. 12) in close agreement with the literature value and was identified as arising from a CH or $CH_3$ group from the DEPT spectrum (Figure 3. 2. 12). Summary analysis of the HMQC spectrum showed this resonance to be coupled to protons at 0.64 ppm. The combination of this data confirmed the assignment of this resonance to the C18 cholesterol carbon. The C19 and C21 carbons were assigned from the HMQC spectrum by the carbon-proton cross-peaks at [19.73, 0.97] ppm and [19.12, 0.88] ppm (Figure 3. 2. 13). These proton resonances are known to arise from C19 methyl protons (0.97 ppm, singlet) and C21 methyl protons (0.88 ppm, doublet) as determined in the proton spectrum (Section 3. 2. 1). Consequently the C19 and C21 carbon resonances were assigned at 19.73 and 19.12 ppm respectively. Using a similar combination of literature values, DEPT and HMQC spectra, coupled with inspection of multiplicities in the proton spectrum, all of the cholesterol carbons were assigned in the one-dimensional carbon spectrum (three

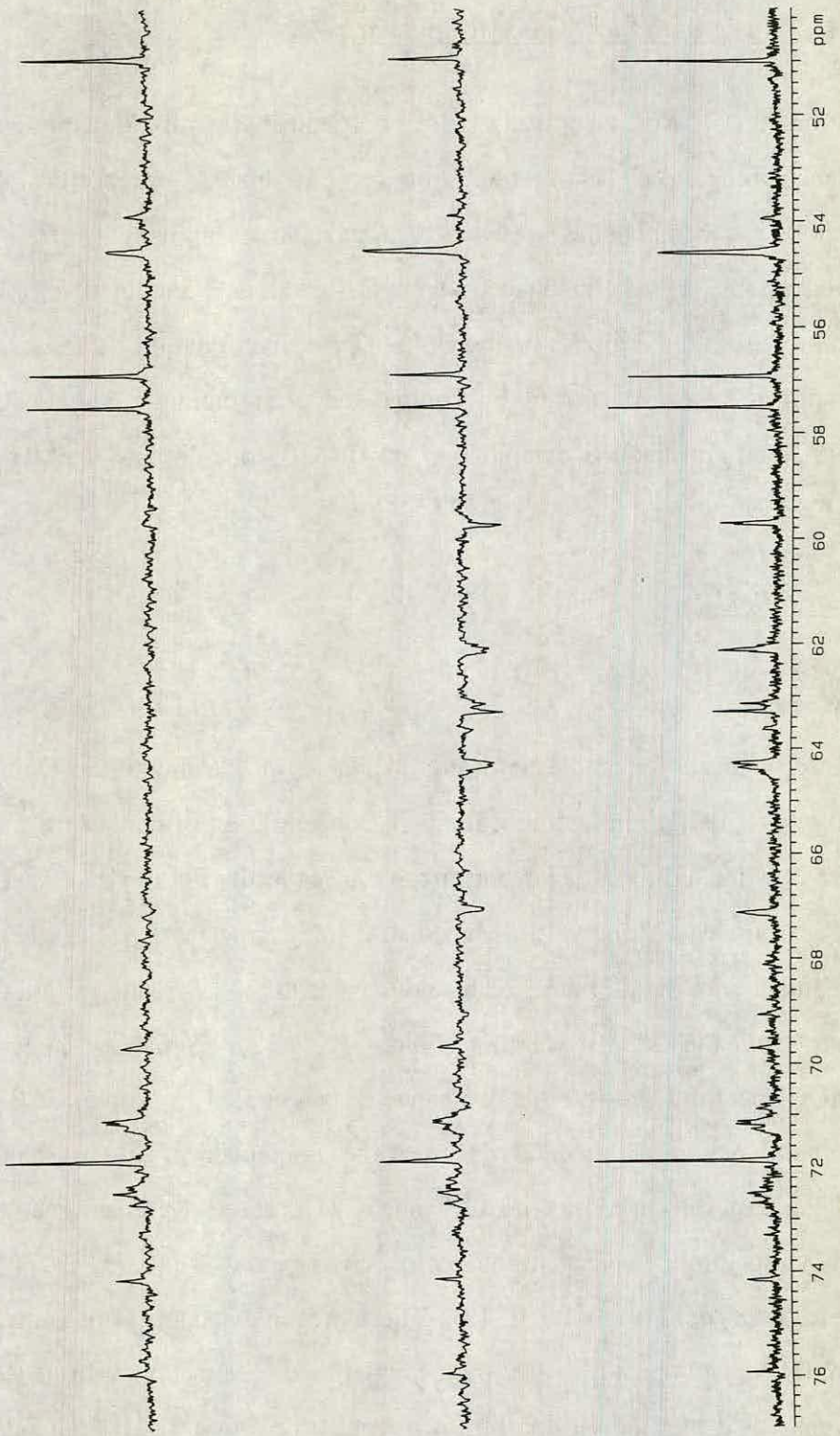


Figure 3. 2. 12 $^{13}C$ and $^{13}C$-DEPT NMR spectra of cerebral lipids at 150.869 MHz.

Spectra where acquired as described in Experimental. Lipid resonances were referenced to the methanol singlet at 51.0 ppm.

of these C2, C7 and C8, tentatively). The majority of carbon resonances are observed over the broad chemical shift range 12.25 to 57.51 ppm, these being assigned to methyl and methylene group carbons. Three exceptions are worth noting, these being the carbon atoms in positions C3, C5 and C6. The C3 hydroxy position carbon resonance was assigned at 71.89 ppm, (literature value 71.00 ppm) with the DEPT spectrum showing this signal to arise from a CH group and the HMQC spectrum showing coupling with a proton resonance at 3.41 ppm. The allylic carbon atoms at positions C5 and C6 resonate at appreciably higher chemical shifts. The literature values of 120.9 and 141.7 ppm for C6 and C5 corresponded closely to resonances at 121.99 and 141.57 ppm in the extract spectrum. Inspection of the DEPT spectrum allowed assignment of these signals to (CH or $CH_3$) and C groups respectively, (the C5 signal being absent in the DEPT spectrum). Final support for the assignments was given by the HMQC spectrum in which it was seen that the carbon resonance at 121.99 ppm coupled to a vinyl proton at 5.32 ppm. The combination of this data allowed the assignment of the resonances at 141.57 and 121.99 ppm to the C5 and C6 cholesterol carbons respectively.

*Galactocerebrosides.*

Galactocerebrosides, sulfatides and sphingomyelin possess a common sphingosine (ceramide) moiety and consequently these carbon resonances are shared between them. In the sphingosine moiety, the CER *b* proton produces a carbon-proton cross-peak in the HMQC spectrum at [134.73, 5.65] ppm allowing its assignment at 134.73 ppm in the carbon spectrum. The CER *a* carbon was less readily identified as this resonance appeared among a multitude of other olefinic signals in the 127.60 to 132.43 ppm region. Using the same system of analysis, (i.e. the HMQC spectrum and confirmation by the DEPT spectrum), CER 1, CER 2 and CER 3 were assigned to resonances at 54.58, 53.94 and 69.06 ppm. The later signal had carbon-proton cross-peaks at [69.06, 3.69] and [69.06, 4.05] ppm in the HMQC spectrum. With reference to the discussion on proton NMR spectral

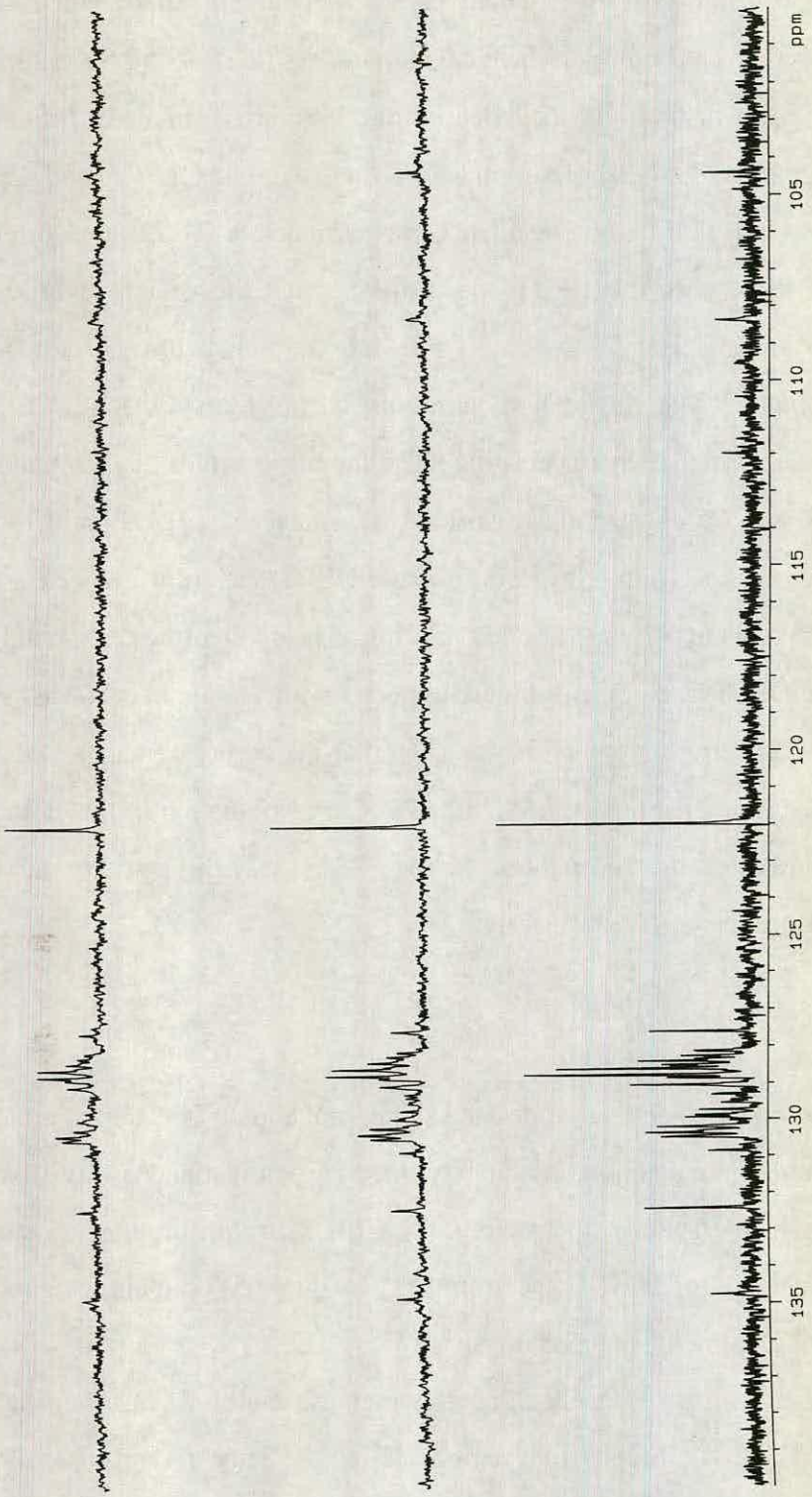


Figure 3. 2. 12 $^{13}C$ and $^{13}C$-DEPT NMR spectra of cerebral lipids at 150.869 MHz.

Spectra where acquired as described in Experimental. Lipid resonances were referenced to the methanol singlet at 51.0 ppm.

analysis of lipids, these proton signals were consistent for a ceramide moiety containing an α-hydroxy fatty acid, i.e. galactocerebroside I, (Section 3. 2. 1).

Focusing on the galactose group, GAC 1 was assigned on the basis of a carbon-proton cross-peak at [104.34, 4.18] ppm in the HMQC spectrum which was seen to arise from a $CH/CH_3$ group in the DEPT spectrum (Figures 3. 2. 13 and 3. 2. 12 respectively). The GAC 2 carbon was identified by the carbon-proton cross-peak at [71.89, 3.50] ppm, however this signal was not clearly seen in the carbon spectra as it lay under the cholesterol C3 resonance. GAC 3 was assigned in a similar manner from the carbon-proton cross-peak at [74.17, 3.44] ppm. GAC 4 and GAC 5 were also assigned from the carbon-proton cross-peaks at [69.71, 3.82] ppm and [75.93, 3.48] ppm respectively. GAC 6 was identified by the two carbon-proton cross-peaks produced with the diastereotopic protons $6^u$ and $6^d$ at [62.11, 3.96] ppm and [62.11, 3.75] ppm. The GAC 6 signal was not clearly seen in the carbon spectra, it being found to resonate at the same chemical shift as the phosphatidyl ethanolamine C1 head group signal.

*Ethanolamine phospholipids.*

Proton and carbon assignments have been performed on chloroform solutions of synthetic phosphatidyl ethanolamines and phosphatidyl cholines by Gunstone (1992). Using a combination of the data from these studies, proton and HMQC spectra and confirmatory DEPT analysis, the carbon resonances in phosphatidyl ethanolamine and phosphatidyl choline were assigned in the lipid extract spectra. The C1 methylene protons of the ethanolamine head group were observed as a broad resonance at 3.98 ppm, which produced a cross-peak in the HMQC spectrum at 62.11 ppm (Figures 3. 2. 13). The $CH_2$ nature of this signal was apparent from the DEPT spectrum. The C2 head group carbon was assigned at 41.280 ppm in the same way. Glycerol carbon resonances have been reported to fall in the chemical shift range 63.0 to 70.9 ppm (Gunstone, 1992). In the proton spectrum, the glycerol backbone protons were observed at 3.95, 4.12, 4.37 and 5.18 ppm corresponding to the C3, $C1^u$, $C1^d$ and C2 protons. Cross-peaks with

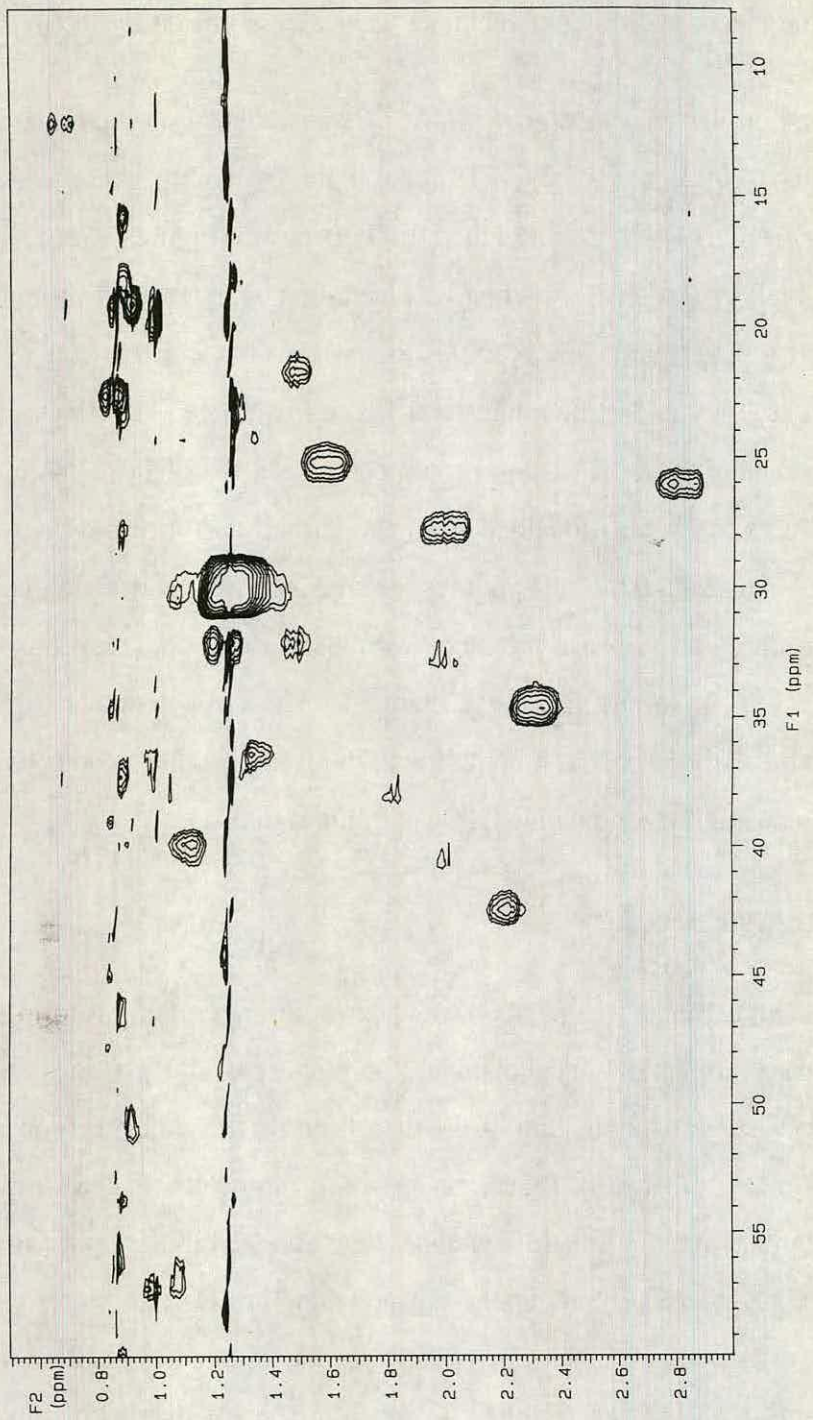


Figure 3. 2. 13 Two-dimensional HMQC spectrum of cerebral lipids at 150.869 MHz.

Spectra where acquired as described in Experimental. Lipid resonances were referenced to the methanol singlet at 51.0 ppm.

these resonances were observed in the HMQC spectrum at 64.26, 63.14, 63.14 and 71.17 ppm respectively (Figure 3. 2. 13) in close agreement with those previously reported (64.1, 63.0 and 70.9 ppm). Interestingly, a number of resonances were observed over this region in the one-dimensional carbon spectrum which coupled to the glycerol backbone protons in the HMQC spectrum. For example, two possible resonances for C1 glycerol backbone carbons were observed at 63.14 and 63.29 ppm, the later being at least twice as large as the former (Figure 3. 2. 12). Gunstone found glycerol C1 carbons in phosphatidyl ethanolamine and phosphatidyl choline to differ in chemical shift by 0.01 ppm. Therefore, the possibility exists that the resonance at 63.29 ppm arises from the combined C1 carbons of phosphatidyl ethanolamine and phosphatidyl choline and that the other resonance at 63.14 ppm arises from phosphatidyl serine and phosphatidyl inositol C1 glycerol carbons. On the basis of our h.p.t.l.c. results (Section 3. 3. 2) we observed the former two lipids to occur in appreciably greater quantities than the latter two. It is noted however, that without further purification of this crude lipid extract, positive assignment of these resonances cannot be made. A similar situation exists for the glycerol carbon atoms at positions 2 and 3. As previously mentioned in this section the glycerol C2 proton resonance couples to carbon signals at a chemical shift of 71.2 ppm. In reality three signals are present, at 71.12, 71.17 and 71.27 ppm, all of which are CH or $CH_3$ in character as evinced in the DEPT spectrum. Although glycerol C2 carbon resonances in phosphatidyl ethanolamine and phosphatidyl choline have been reported at 70.9 and 70.65 ppm (Gunstone, 1992), this did not assist their assignment in our lipid extract. The glycerol C2 carbon in phosphatidyl ethanolamine was however tentatively assigned at 71.17 ppm and that of phosphatidyl choline at 71.12 ppm. Some justification for these assignments is given by the observation that the former resonance is slightly more intense than the signal at 71.12 ppm and that phosphatidyl ethanolamine is present in the sample at a slightly higher concentration than phosphatidyl choline (Section 3. 2. 2). Multiple cross-peaks occur for the C3 glycerol carbon over the 64.26 to 66.49 ppm range in the HMQC spectrum, presumably reflecting the diverse

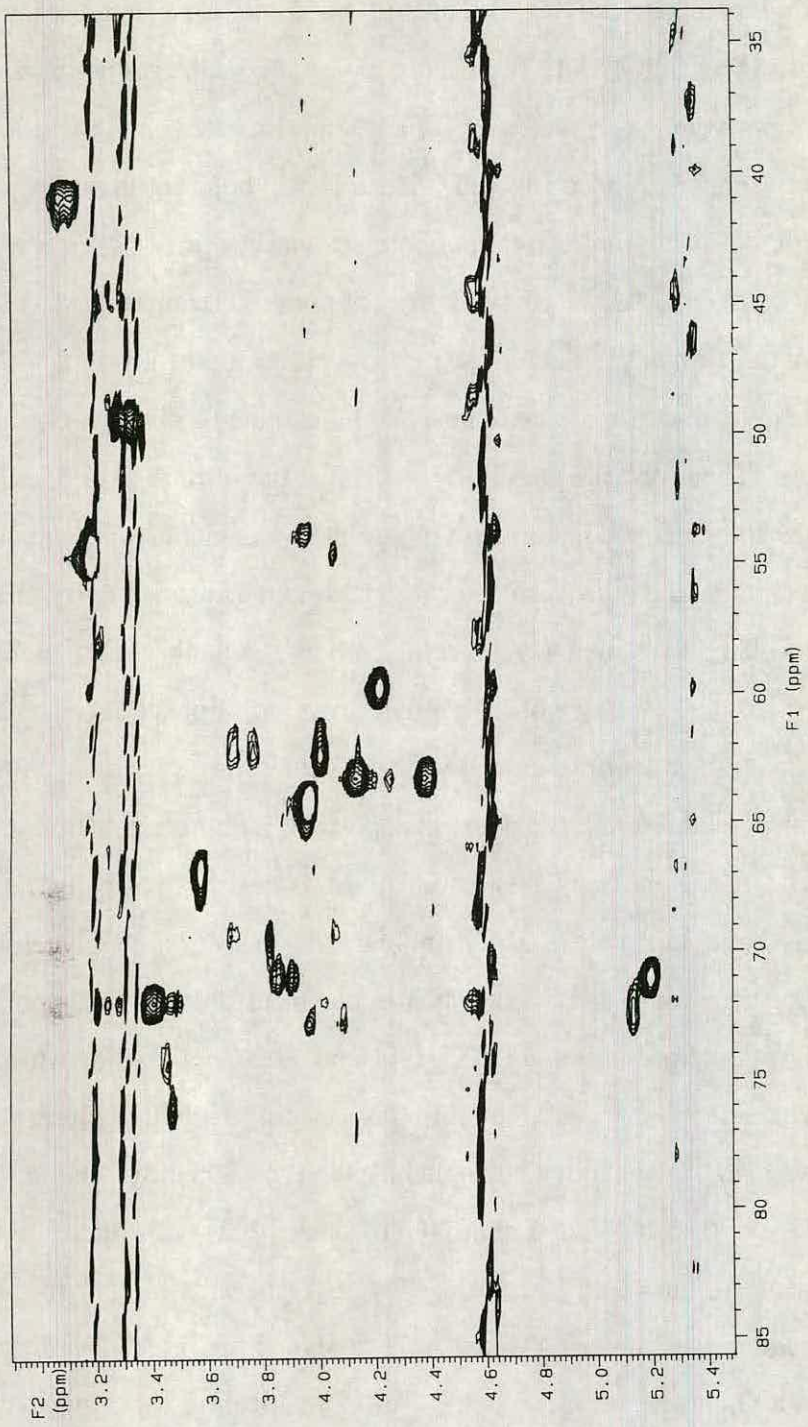


Figure 3. 2. 13 Two-dimensional HMQC spectrum of cerebral lipids at 150.869 MHz.

Spectra where acquired as described in Experimental. Lipid resonances were referenced to the methanol singlet at 51.0 ppm.

nature of phospholipids present in the extract. These signals could not be individually assigned, however all were $CH_2$ signals as determined from the DEPT spectrum.

*Choline phospholipids.*

The terminal methyl head group carbon resonance was assigned following examination of the HMQC spectrum. The large methyl proton signal at 3.18 ppm was seen to couple to a carbon signal at 54.58 ppm which was $CH/CH_3$ in character as determined from the DEPT spectrum. Closer examination of the HMQC spectrum showed the signal to be due to two carbon-proton couplings, at 3.17 and 4.05 ppm in addition to the phosphatidyl choline signal at 3.18 ppm (Figure 3. 2. 13). These former two signals were assigned to the terminal methyl head group protons in sphingomyelin and the sphingosine C1 position proton CER 1 as discussed earlier (Section 3. 2. 1). The C1 choline head group carbon was assigned directly from the HMQC spectrum following the visualization of a carbon-proton cross-peak at [59.70, 4.20] ppm. The C2 head group resonance was assigned at 67.13 ppm in a similar manner.

Sphingomyelin shares common choline and sphingosine moieties with phosphatidyl choline and galactocerebroside respectively. Carbon resonances for these two structural groups have been assigned previously. No differences were detected in the chemical shifts of carbon resonances in these two moieties in the three lipid species examined.

*Plasmalogens (ether phospholipids).*

As previously stated in the assignment of proton NMR lipid spectra (Section 3. 2. 1), plasmalogens possess an $\alpha$, $\beta$ unsaturated ether at the glycerol C1 position. The effect that this group has on carbon resonances at the glycerol C1 and C2 positions provides well distinguished signals. The glycerol C1 position methylene protons produce carbon-proton cross-peaks in the HMQC spectrum at [70.78,

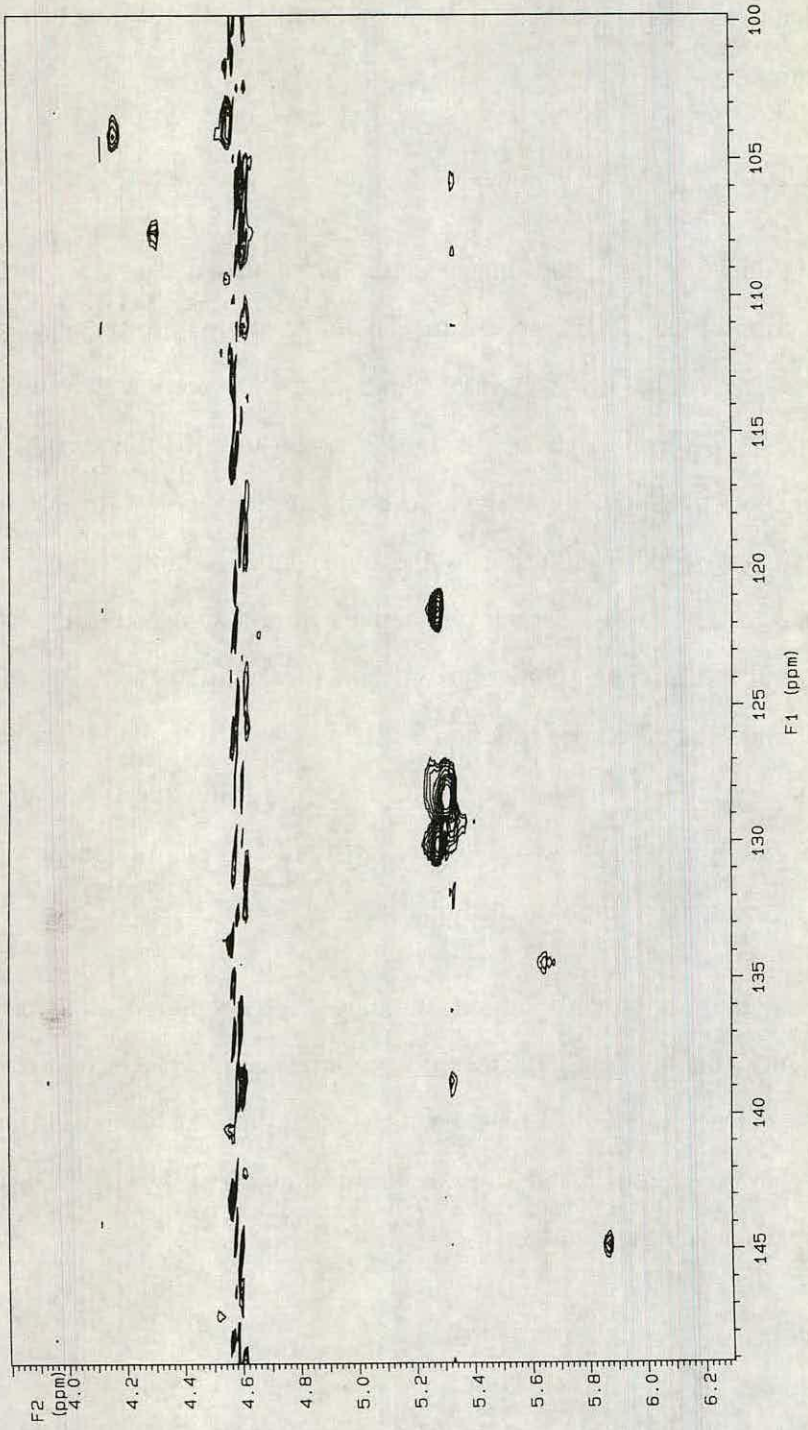


Figure 3. 2. 13 Two-dimensional HMQC spectrum of cerebral lipids at 150.869 MHz.

Spectra where acquired as described in Experimental. Lipid resonances were referenced to the methanol singlet at 51.0 ppm.

3.84] and [70.78, 3.89] ppm, reflecting coupling between the glycerol C1 carbon (defined as PLA 1) and the glycerol $C1^u$ and $C1^d$ diastereotopic protons respectively. Two carbon signals were observed at 70.779 and 70.88 ppm suggesting the presence of two species of plasmalogen, notably phosphatidal ethanolamine and phosphatidal choline. Analysis of the proton spectra of neutral and acidic lipids support this claim, with acidic plasmalogens unidentified in the acidic lipid fraction (Figure 3. 2. 11). The glycerol C2 carbon (defined as PLA 2) was identified in a similar manner from the HMQC spectrum by the presence of a carbon-proton cross-peak at [72.50, 5.12] ppm. A number of CH or $CH_3$ carbon resonances lie in close proximity to this signal with these coupling to proton resonances at 3.98 and 4.07 ppm Their assignment was not performed. The plasmalogen glycerol C3 carbon signal (defined as PLA 3) was found to virtually overlap the glycerol C3 carbon resonances from other phospholipids in the 64.26 to 64.49 ppm chemical shift region. Resonances from the PLA α and PLA β vinyl ether carbons were assigned at 145.34 and 108.38 ppm respectively from the carbon-proton cross-peaks at [145.34, 5.87] and [108.38, 4.31] ppm in the HMQC spectrum. The CH nature of these signals was confirmed by the DEPT spectrum.

***Acidic lipids.***

*Phosphatidyl serine, phosphatidyl inositol and sulfatides.*

The low concentration of the acidic phospholipids in the cerebral lipid extract, i.e. phosphatidyl serine and phosphatidyl inositol, made the assignment of head group resonances difficult. Distinguishable signals from the lipids were not discerned in the HMQC spectrum. It is assumed that glycerol backbone carbon resonances would appear in the same regions as those of the neutral phospholipids. Sulfatide carbon resonances were not distinguished from those of galactocerebrosides.

*Fatty acid structures.*

Carbon resonances in acylglycerols and fatty acid methyl esters have received considerable attention in the review by Gunstone (1992). In our studies, carbon resonances in fatty acid structures were assigned in the lipid extract with extensive reference to literature values and the NMR experiments outlined above.

ω1-methyl protons in terminally saturated fatty acids produce a cross-peak with a carbon resonance at 14.31 ppm in the HMQC spectrum, confirmation of the $CH_3$ character of this signal being given by the DEPT spectrum. Gunstone found corresponding ω1 carbon resonances from n-3 fatty acids to resonate approximately 0.12 ppm downfield (i.e. at a higher chemical shift) of the aforesaid signal, however the only resonance seen in this region was at 14.51 ppm, which proved to arise from a $CH_2$ group. Consequently the ω1 carbon from n-3 fatty acids was not assigned in our lipid extract carbon spectra. In a similar manner, the ω2 carbon in terminally saturated fatty acids was assigned at 23.21 ppm from the cross-peak in the HMQC spectrum with ω2-methylene protons. A $CH_2$ carbon was observed at 23.11 ppm which may have arisen from an n-6 fatty acid (Gunstone, 1992). ω3 carbons were assigned from the cross-peak with ω3-methylene protons in the HMQC spectrum over the 31.78 to 32.97 ppm region. The signal at 31.78 ppm was similar in intensity to the ω1 and ω2 carbon resonances previously assigned, supporting the tentative assignment of this signal to that of the ω3 carbon in terminally saturated fatty acids. It is noted however that without further purification to remove interfering cholesterol resonances, the positive assignment of these ω3 carbons remains unclear.

Methylene envelope protons were seen to produce a cross-peak with a large number of carbon resonances over the 29.52 to 30.25 ppm chemical shift region in the HMQC spectrum. Resolution of these signals to specific carbon atoms was not attempted.

Signals for allylic carbons at each end of a monoene or polyene system were seen at 27.74 ppm, these being assigned on the basis of the carbon-proton cross-peak at [27.74, 2.03] ppm in the HMQC spectrum. In a similar manner, resonances from the [-CH=CH-$\underline{C}H_2$-CH=CH-] group of methylene interrupted polyenes were assigned in the range 26.09 to 26.21 ppm (Figure 3. 2. 13). These comprised three signals which were all coupled to the broad proton resonance at 2.76 to 2.82 ppm. On the basis of our chemical ionization mass spectrometry results (Section 3. 3. 1), we believed the majority of these to be attributable to the poly-unsaturated fatty acids linoleic ($C_{18:2}$), arachidonic ($C_{20:4}$) and docosahexaenoic acid ($C_{22:6}$).

Resonances for olefinic carbon atoms were observed over the 127.60 to 132.43 ppm range, however without further purification to separate individual fatty acids and two-dimensional shift correlated $^{13}C$ COSY 45 experiments, the identity of these numerous signals remain largely unassigned.

Gunstone reported the assignment of C1 resonances from quaternary carbon atoms at 173.2 ppm (glycerol 1/3) and 172.8 ppm (glycerol 2) (Gunstone, 1992). Four signals were identified in our one-dimensional carbon spectrum, a large resonance at 174.49 ppm, a small resonance at 173.38 ppm and two signals of approximately equal intensity at 174.10 and 174.13 ppm. The former signal at 174.49 ppm was presumed to arise from the carboxylate carbons attached to the glycerol 1/3 positions since it was greater in intensity than the other signals. These other signals were not positively assigned. A similar difficulty in assigning signals to specific fatty acid carbon atoms was found with the C2 and C3 carbons, although the general chemical shift regions of these resonances were determined. A large proton-carbon cross-peak was observed for the C2 carbon at [$\underline{34.64}$, 2.26] ppm in the HMQC spectrum. Four distinct resonances existed in this region, at 35.22, 24.79, 34.64 and 34.21 ppm, all of which were $CH_2$ signals (Figure 3. 2. 12). These resonances were believed to include signals from the C2 acyl positions of phospholipids, galactocerebrosides and sulfatides present in the

| Metabolite | Assignment | Chemical shift /ppm | Functional group |
|---|---|---|---|
| | | | |
| *Neutral lipids* | | | |
| | | | |
| Cholesterol | C18 | 12.25 | $CH_3$ |
| | C21 | 19.12 | $CH_3$ |
| | C19 | 19.73 | $CH_3$ |
| | C11 | 21.72 | $CH_3$ |
| | C26 | 22.82 | $CH_3$ |
| | C27 | 23.06 | $CH_3$ |
| | C23 | 24.43 | $CH_2$ |
| | C15 | 24.85 | $CH_2$ |
| | C25 | 28.56 | CH |
| | C12 | 28.80 | $CH_2$ |
| | C20 | 36.44 | CH |
| | C22 | 36.84 | $CH_2$ |
| | C10 | 37.16 | C |
| | C1 | 37.99 | $CH_2$ |
| | C24 | 40.14 | $CH_2$ |
| | C16 | 40.53 | $CH_2$ |
| | C4 | 42.48 | $CH_2$ |
| | C13 | 42.98 | C |
| | C9 | 50.99 | CH |
| | C17 | 56.92 | CH |
| | C14 | 57.51 | CH |
| | C3 | 71.89 | CH |
| | C6 | 121.99 | C |
| | C5 | 141.57 | CH |
| | | | |
| Galactocerebrosides | CERa | 127.60 - 132.43 | -CH=CH- |
| | CERb | 134.77 | -CH=CH- |
| | CER1 | 54.58 | CH |
| | CER2 | 53.94 | CH |
| | CER3 | 69.06 | $CH_2$ |
| | GAC1 | 104.34 | CH |
| | GAC2 | 71.89 | CH |
| | GAC3 | 74.17 | CH |
| | GAC4 | 69.71 | CH |
| | GAC5 | 75.93 | CH |
| | GAC6 | 62.11 | $CH_2$ |
| | | | |

Table 3. 2. 2 Assignment of $^{13}C$ NMR resonances in cerebral lipid extracts at 600 MHz.

Lipids were extracted from three pooled murine brains. $^{13}C$ NMR spectra were acquired on a Varian VXR600S NMR spectrometer operating at a spectrometer frequency of 150.869 MHz. For a full description of the procedure see Experimental. Chemical structures are illustrated in Figure 3. 2. 1.

* denotes $^{13}C$ resonances used for metabolite quantification.

lipid extract. In a similar manner C3 carbons were assigned from the carbon-proton cross-peak in the HMQC spectrum at [25.48, 1.55] ppm. Three signals were present in this region lying very close to each other, however without further experiments on purified compounds they also remain unassigned.

*Summary.*

The low percentage abundance and consequent lack of sensitivity inherent in $^{13}C$ NMR makes this technique of limited value in the quantitative analysis of metabolites, however the information contained in the $^{13}C$ spectrum does provide an additional form of structural information on the lipid species present.

Cholesterol being the most prominent of the cerebral lipids in the murine extract, gave well distinguished signals in the carbon spectra. Twenty-four of the twenty-seven carbons were positively assigned, the remaining three tentatively.

Carbon sphingosine resonances in galactocerebrosides, sulfatides and sphingomyelin were fully assigned, however it was not possible to distinguish between the three lipid species on this basis. Similarly, galactose carbon signals were assigned for galactocerebrosides and sulfatides, but again these did not allow distinction between the two galactocerebrosides.

Carbon head group resonances in ethanolamine phospholipids were assigned in the carbon spectrum and were indistinguishable from phosphatidyl and phosphatidal compounds. The same was found for head group resonances in the choline-containing phospholipids: phosphatidyl choline, phosphatidal choline and sphingomyelin. However some differences were detected in the glycerol backbone carbons of these lipid species allowing their assignment from the two-dimensional HMQC spectrum and subsequently the one-dimensional $^{13}C$ spectrum.

The assignment of resonances in the acidic lipids phosphatidyl serine and phosphatidyl inositol was not assisted by their low concentration in the cerebral

| Metabolite | Assignment | Chemical shift /ppm | Functional group |
|---|---|---|---|
| | | | |
| *Neutral lipids* | | | |
| | | | |
| Ethanolamine PL. | C1 | 62.11 | -**C**$H_2$$CH_2$$NH_2$ |
| | C2 | 41.28 | -$CH_2$**C**$H_2$$NH_2$ |
| | Sn1 | 63.14 | -**C**$H_2$OCO$CH_2$- |
| | Sn2 | 71.17 | -**C**HOR-$CH_2$O- |
| | Sn3 | 64.26 | -CHO**C**$H_2$$OPO_3$- |
| | | | |
| Choline PL. | C1 | 59.70 | -**C**$H_2$$CH_2$$N^+$- |
| | C2 | 67.13 | -$CH_2$**C**$H_2$$N^+$- |
| | | 54.58 | -$CH_2$$N^+$**(C**$H_3$**)**$_3$ |
| | | | |
| Plasmalogen | PLAα | 145.34 | -O-**C**H=CH- |
| | PLAβ | 108.38 | -O-CH=**C**H- |
| | PLA1 | 70.78 | -**C**$H_2$O-CH= |
| | PLA2 | 72.50 | -**C**HOR-$CH_2$O- |
| | PLA3 | 64.26 - 64.49 | -CHO**C**$H_2$$OPO_3$- |
| | | | |
| *Acidic lipids* | | | |
| | | | |
| Fatty acids | | | |
| | | | |
| (sat., n-6, n-9) | w1 | 14.31 | -$CH_2$$CH_2$**C**$H_3$ |
| (sat., n-6, n-9) | w2 | 23.21 | -$CH_2$**C**$H_2$$CH_3$ |
| (sat., n-6, n-9) | w3 | 31.78 - 32.97 | -**C**$H_2$$CH_2$$CH_3$ |
| | | 29.52 - 30.25 | methyl envelope |
| | | 27.74 | =CH**C**$H_2$$(CH_2)_n$- |
| $C_{18:2}$, $C_{20:4}$, $C_{22:6}$ | | 26.09 - 26.21 | =CH**C**$H_2$CH= |
| | | 127.6 - 132.43 | -**C**H=**C**H- |
| | C1 | 173.38 - 174.49 | -$CH_2$$CH_2$**C**$OO^-$ |
| | C2 | 34.21 - 35.22 | -$CH_2$**C**$H_2$$COO^-$ |
| | C3 | 25.41 - 25.52 | -**C**$H_2$$CH_2$$COO^-$ |
| | | | |

Table 3. 2. 2 *continued.* Assignment of $^{13}C$ NMR resonances in cerebral lipid extracts at 600 MHz.

Lipids were extracted from three pooled murine brains. $^{13}C$ NMR spectra were acquired on a Varian VXR600S NMR spectrometer operating at a spectrometer frequency of 150.869 MHz. For a full description of the procedure see Experimental. Chemical structures are illustrated in Figure 3. 2. 1.

* denotes $^{13}C$ resonances used for metabolite quantification.

lipid extract. Carbon resonances in fatty acyl groups were not assigned in great detail as the result of the spectra containing multiple resonances from the broad and diverse fatty acid groups present. It was concluded that in order for more precise assignments to be made the lipid extract would require further fractionation to allow characterization of individual lipid species.

The $^{13}C$ NMR analysis of murine cerebral lipids in summarized in Table 3. 2. 2.

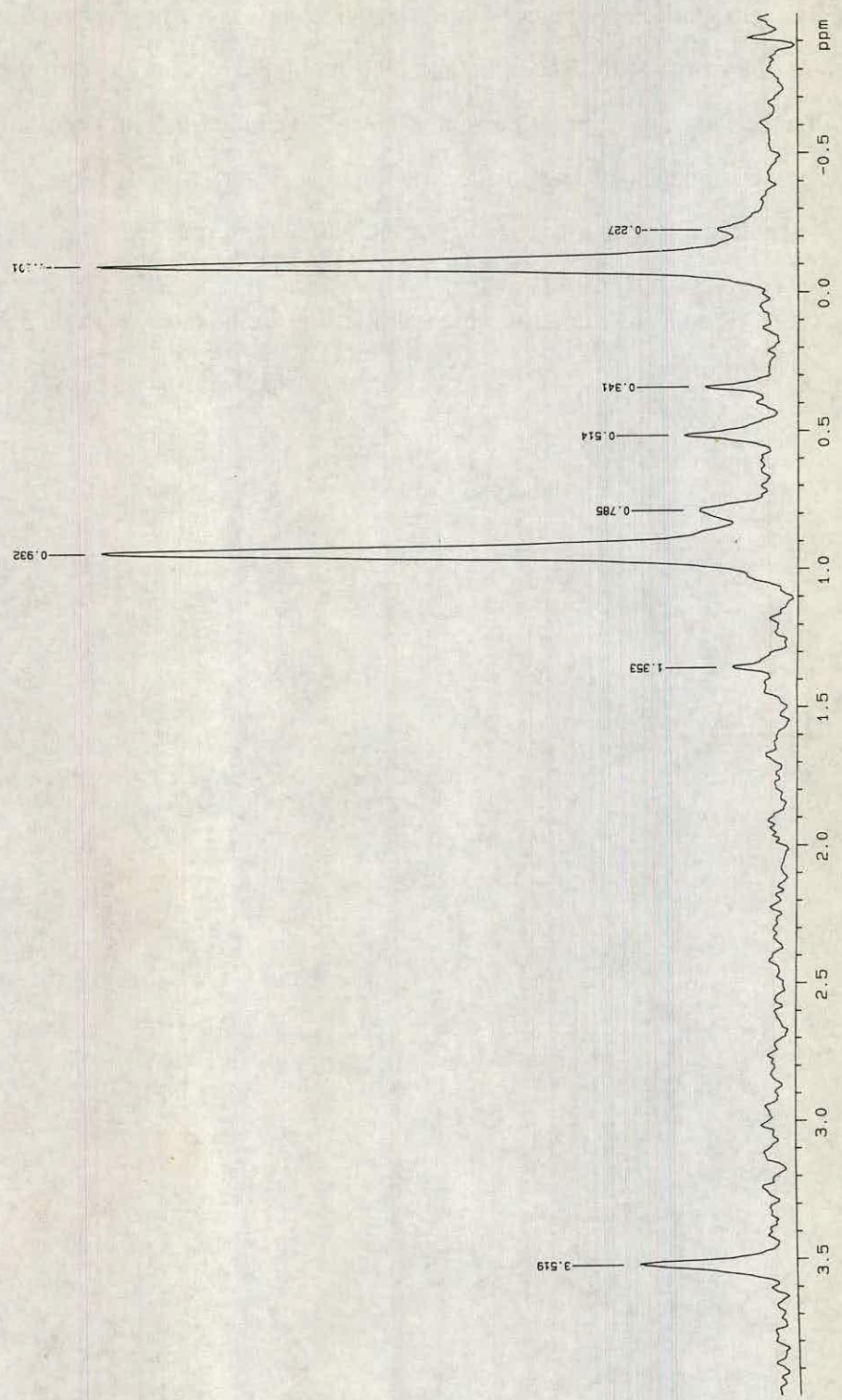


Figure 3. 2. 14 $^{31}P$ NMR spectrum of neutral cerebral lipids in aqueous deoxycholate at 242.854 MHz.

Spectra where acquired as described in Experimental. Lipid resonances were referenced to the $PO_4^{3-}$ singlet at 3.54 ppm.

### 3. 2. 3 Assignment of $^{31}P$ NMR Spectra.

Poor spectral resolution of phospholipid species in Bligh-Dyer organic phase extracts (chloroform/methanol, 2:1, v/v), has been an impediment to their quantitative and qualitative analysis by $^{31}P$ NMR spectroscopy. Recently, Capuani and colleagues described a technique in which phospholipids were processed to remove endogenous cations and dispersed as aqueous micelles in a deoxycholate/$D_2O$ mixture (Capuani *et al.*, 1992). These two processes, i.e., removal of metal cations, formation of aqueous micelles and subsequent adjustment of pH to 11.4, resulted in well resolved spectra for all the major phospholipid species thus allowing the aforesaid analysis to be performed. The authors assigned five cerebral phospholipid resonances in a rat extract by comparison with standard lipid samples.

The improvement in spectral resolution that this procedure appeared to offer over $^{1}H$ NMR analysis of phospholipids merited its application to the study of murine cerebral lipids in scrapie and control animals. In the studies described here, neutral and acidic lipid fractions were analyzed by $^{31}P$ NMR spectroscopy. Prior fractionation of the crude lipid extract allowed better discrimination of lipid species in the $^{31}P$ NMR spectrum. The results of the analysis are discussed below.

#### *Neutral Lipids.*

The $^{31}P$ NMR spectrum of the neutral lipid fraction contained prominent resonances at -0.10 and 0.93 ppm relative to the exogenous $PO_4^{3-}$ standard at 3.52 ppm (Figure 3. 2. 15). With reference to authentic $^{31}P$ NMR lipid spectra, and the results reported by Capunai *et al.* (1992), these two prominent lipid resonances were assigned to phosphatidyl choline and phosphatidyl ethanolamine respectively. In a similar manner a resonance at 0.51 ppm was assigned to sphingomyelin.

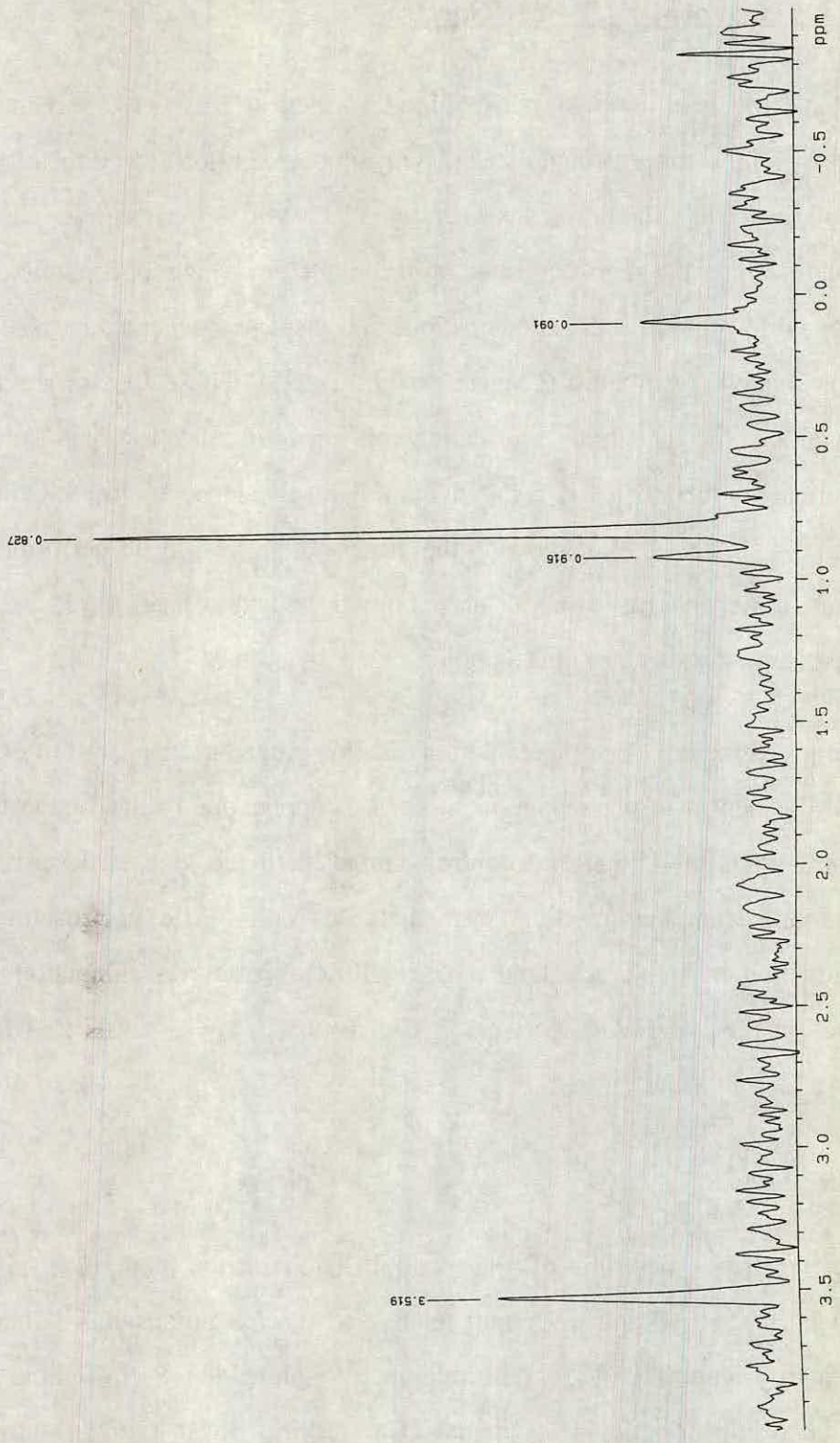


Figure 3. 2. 15 $^{31}P$ NMR spectrum of acidic cerebral lipids in aqueous deoxycholate at 242.854 MHz.

Spectra where acquired as described in Experimental. Lipid resonances were referenced to the $PO_4^{3-}$ singlet at 3.54 ppm.

Four additional resonances were seen in the neutral lipid fraction, at 0.23, 0.34, 0.79 and 1.35 ppm. These were not positively identified. It is possible that the signals at 0.34 and 1.35 ppm arise from phosphatidal choline and phosphatidal ethanolamine respectively, both occurring approximately 0.43 ppm downfield of their corresponding diacyl phospholipid resonances. The signal at 0.79 occurs at a similar chemical shift to that of phosphatidyl serine in the acidic fraction (Figure 3. 2. 15), and may represent a small proportion of this acidic lipid which was eluted in the neutral fraction.

***Acidic Lipids.***

Four resonances were detected in the $^{31}P$ NMR spectra of the acidic lipid fraction (Figure 3. 2. 15). All of these were assigned with reference to authentic standards. The signals at 0.09, 0.83, 0.92 and 4.70 ppm were seen to arise from phosphatidyl inositol, phosphatidyl serine, cardiolipin and phosphatidic acid respectively. Cardiolipin was observed to co-resonate with the signal arising from phosphatidyl ethanolamine, thus illustrating the necessity for lipid fractionation prior to quantitative analysis.

*General Summary - NMR Lipid Analysis.*

Application of proton and phosphorus NMR spectroscopy to the study of cerebral lipids offers a novel, non-destructive form of analysis from which structural information may be obtained on individual lipid species. In the studies described here, diagnostic resonances were assigned for a number of murine cerebral lipids allowing their comparative quantification. NMR spectroscopy was however not adopted for general lipid analysis, the primarily objection being the large amount of NMR time required for the detailed analysis of numerous brain samples and secondly because an alternative technique, high performance thin layer chromatography, offered a distinct advantage in that it afforded a relatively inexpensive form of lipid analysis with a high degree of sensitivity and lipid resolution. In addition it allowed the quantification of lipids in relatively low concentrations, notably galactocerebrosides I and II, sulfatides I and II, cholesteryl esters, triglyceride and diglyceride.

*In vitro* NMR spectroscopy did however find application to the comparative analysis of cerebral lipids in scrapie and control mice. This was primarily performed to investigate the hypothesis that the 'multicomponent resonance' detected by *in vivo* MRS in ME7-affected VM mice was attributed to lipid. It was proposed that having identified this component *in vitro* the improvement in spectral resolution would allow the nature and origin of the metabolite to be deduced. In view of this particular attention was given to the 1.5 to 1.8 ppm chemical shift region in the proton spectra, and secondly to relative peak intensities of diagnostic lipid resonances. A discussion of the findings is given is Section 3. 2. 4.

| Metabolite | Chemical shift /ppm | Control | Scrapie |
|---|---|---|---|
| | | | |
| *$^{1}$H NMR analysis* | | | |
| | | | |
| *Neutral lipids* | | | |
| | | | |
| Cholesterol | 0.64 | 90 ± 5 | 87 ± 3 |
| | | | |
| Ethanolamine PL. | 3.06 | 138 ± 15 | 143 ± 9 |
| | | | |
| Sphingomyelin | 3.17 | 43 ± 33 | 40 ± 3 |
| | | | |
| Phosphatidyl choline | 3.18 | 158 ± 10 | 164 ± 9 |
| | | | |
| Galactocerebrosides | 5.65 | 15 ± 2 | 16 ± 3 |
| | | | |
| Plasmalogen | 5.87 | 23 ± 2 | 21 ± 3 |
| | | | |
| *Acidic lipids* | | | |
| | | | |
| Total fatty acids | 2.27 | 120 ± 11 | 122 ± 9 |
| | | | |
| Linoleic ($C_{18:2}$) | 2.72 | 7 ± 1 | 6 ± 2 |
| | | | |
| Arachidonic ($C_{20:4}$) | 1.65 | 19 ± 2 | 20 ± 3 |
| | | | |
| Docosahexaenoic ($C_{22:6}$) | 2.35 | 45 ± 2 | 41 ± 4 |
| | | | |
| *$^{31}$P NMR analysis* | | | |
| | | | |
| Ptd. choline | -0.10 | 34 ± 1 | 33 ± 2 |
| | | | |
| Ptd. ethanolamine | 0.93 | 46 ± 4 | 43 ± 4 |
| | | | |
| Sphingomyelin | 0.34 | 11 ± 2 | 12 ± 2 |
| | | | |
| Ptd. inositol | 0.09 | 17 ± 2 | 17 ± 1 |
| | | | |
| Ptd. serine | 0.83 | 14 ± 1 | 14 ± 1 |
| | | | |

Table 3. 2. 3 *In vitro* NMR spectroscopy analysis of cerebral lipid extracts from control and scrapie mice at 600 Mhz.

For description of procedure see Experimental. Values are expressed as mean ± sem in units proportional to the intensity of 'diagnostic' $^{1}$H and $^{31}$P lipid resonances and subsequently standardized to wet brain weight. Five control and five scrapie animals were analyzed in each group.

Neither $^{1}$H nor $^{31}$P NMR analysis revealed statistically significant difference between the two groups.

### 3. 2. 4 Comparative Analysis of Cerebral Lipids in Scrapie-Affected and Control Mice by NMR Spectroscopy.

The detection of a scrapie-specific *in vivo* MRS multicomponent resonance and its potential application to the non-invasive, pre-clinical diagnosis of a transmissible spongiform encephalopathy disease state has received earlier discussion. The primary objective of the research described here was to reproduce these novel findings *in vitro* and subsequently identify the metabolite(s) responsible for this pathological change. The absence of the signal in aqueous perchlorate and acetone-$d_6$ cerebral extracts argued strongly against the compound having a hydrophilic nature. Attention was therefore focused on changes in hydrophobic compounds and most notably lipid. For the purpose of these studies, cerebral lipid extracts were prepared from a small number of terminally-ill scrapie mice (ME7/VM) and an equal number of age- and sex-matched controls. Following resuspension in the appropriate deuterated solvents (Section 2. 4. 3) the lipid fractions were analyzed by a combination of proton and phosphorus NMR spectroscopy. Representative one-dimensional spectra of scrapie and control cerebral lipids for the aforementioned techniques are displayed in Figures 3. 2. 16a/b and 3. 2. 17a/b respectively.

*Results.*

Upon initial examination of the *in vitro* proton spectra, the absence of an intense multicomponent resonance over the 1.5 to 1.8 ppm chemical shift region was immediately evident in scrapie as well as control lipid extracts. Although more detailed quantitative comparison of diseased and control lipid profiles was afforded by high performance thin layer chromatography (Section 3. 3), the above proton and phosphorus spectra provided complementary data to support past findings that no appreciable differences exist in the major cerebral lipids or their fatty acid components between scrapie and control mice (Dees *et al.*, 1985; Heitzman and Skipworth, 1969; Kimberlin and Millson, 1967) (Table 3. 2. 3).

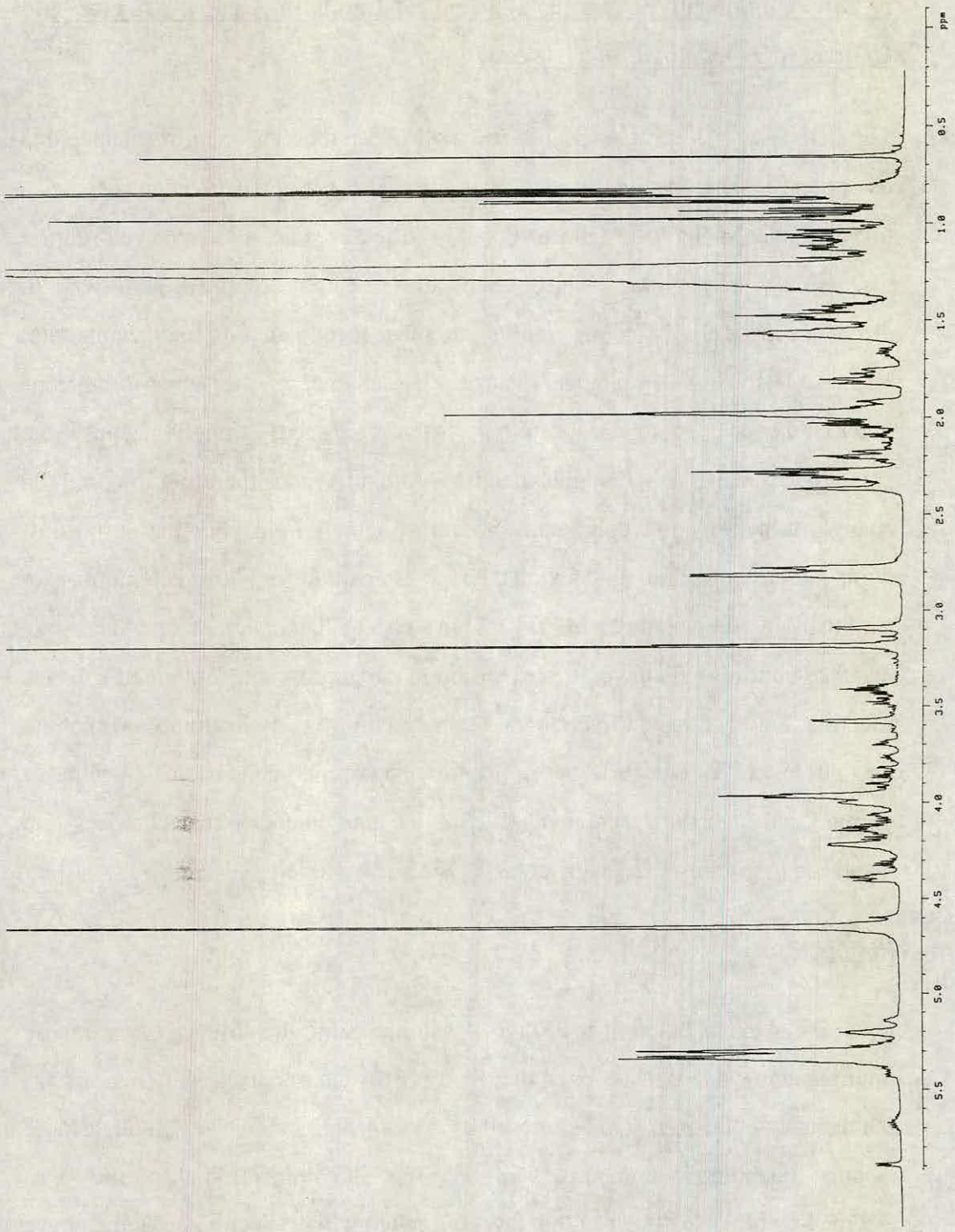


Figure 3. 2. 16a $^{1}$H NMR spectra of cerebral lipids from control mice at 600 MHz.

Spectra where acquired as described in Experimental. Lipid resonances were referenced to the methanol quintet centred at 3.3 ppm. In a comparison between control and scrapie-affected samples, no differences were detected in lipid composition relative to wet brain weight.

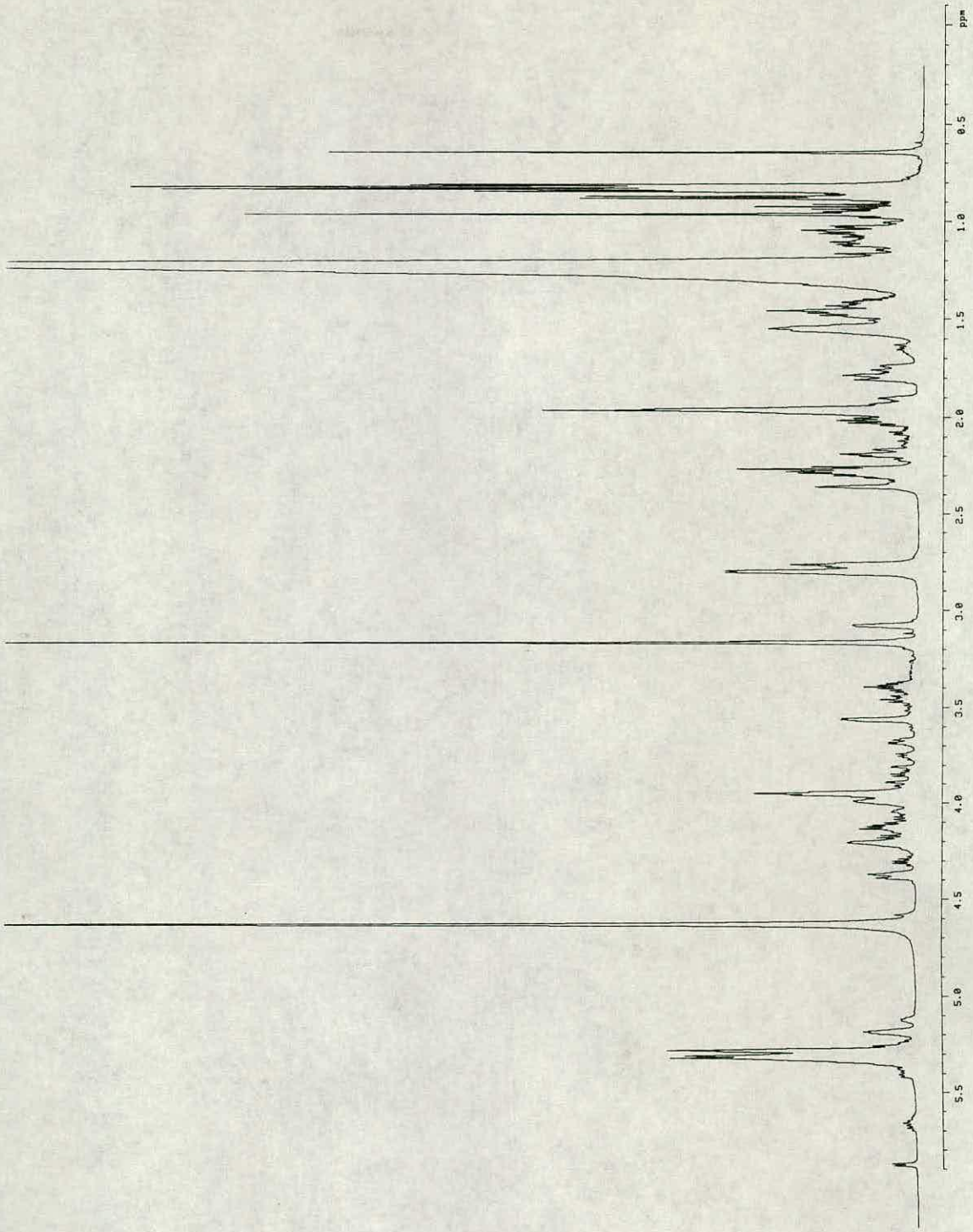


Figure 3. 2. 16b $^{1}$H NMR spectra of cerebral lipids from scrapie-affected mice at 600 MHz.

Spectra where acquired as described in Experimental. Lipid resonances were referenced to the methanol quintet centred at 3.3 ppm. In a comparison between control and scrapie-affected samples, no differences were detected in lipid composition relative to wet brain weight.

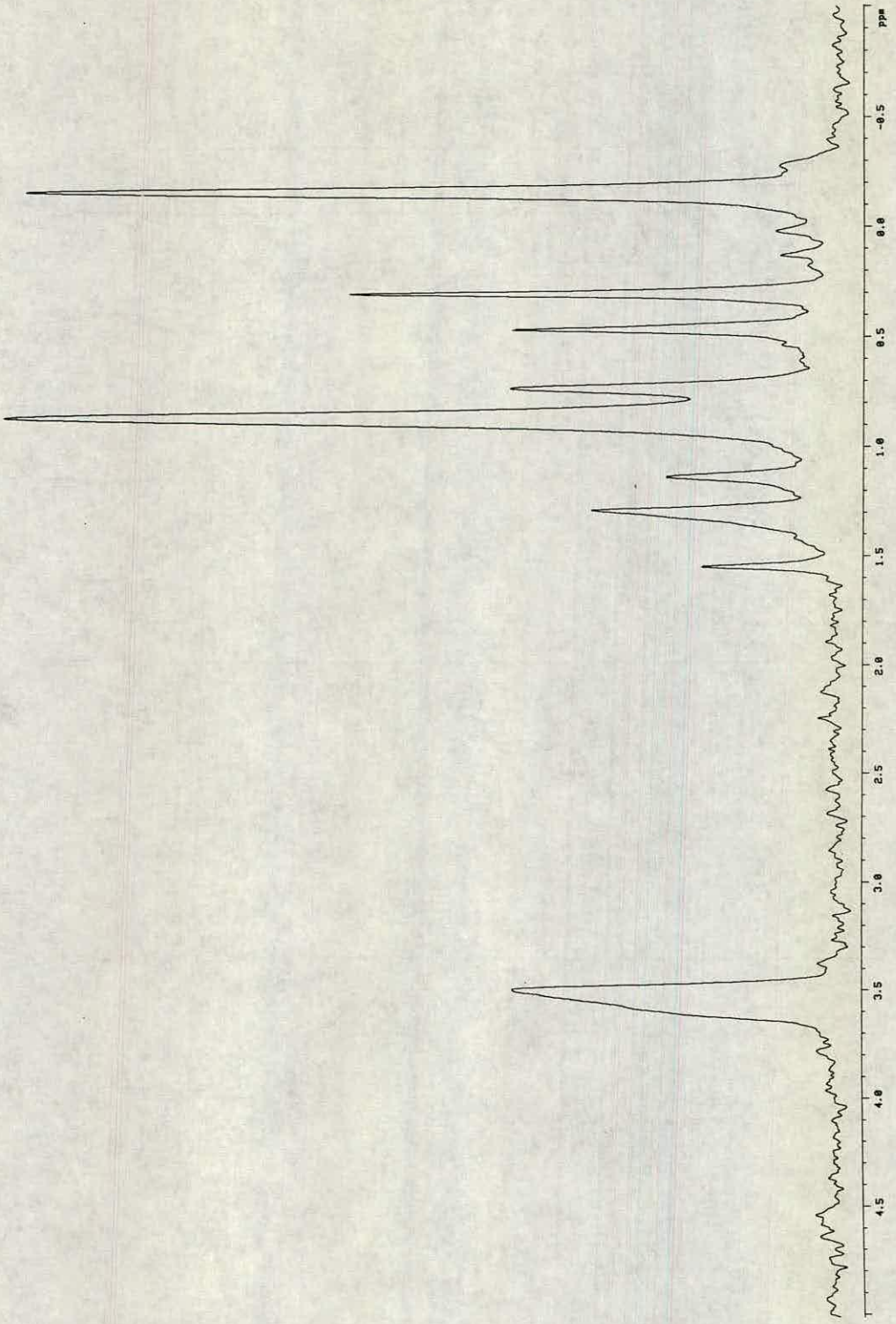


Figure 3. 2. 17a $^{31}P$ NMR spectra of cerebral lipids from control mice at 242.854 MHz.

Spectra where acquired as described in Experimental. Lipid resonances were referenced to $PO_4^{3-}$ singlet at 3.54 ppm. In a comparison between control and scrapie-affected samples, no differences were detected in lipid composition relative to wet brain weight.

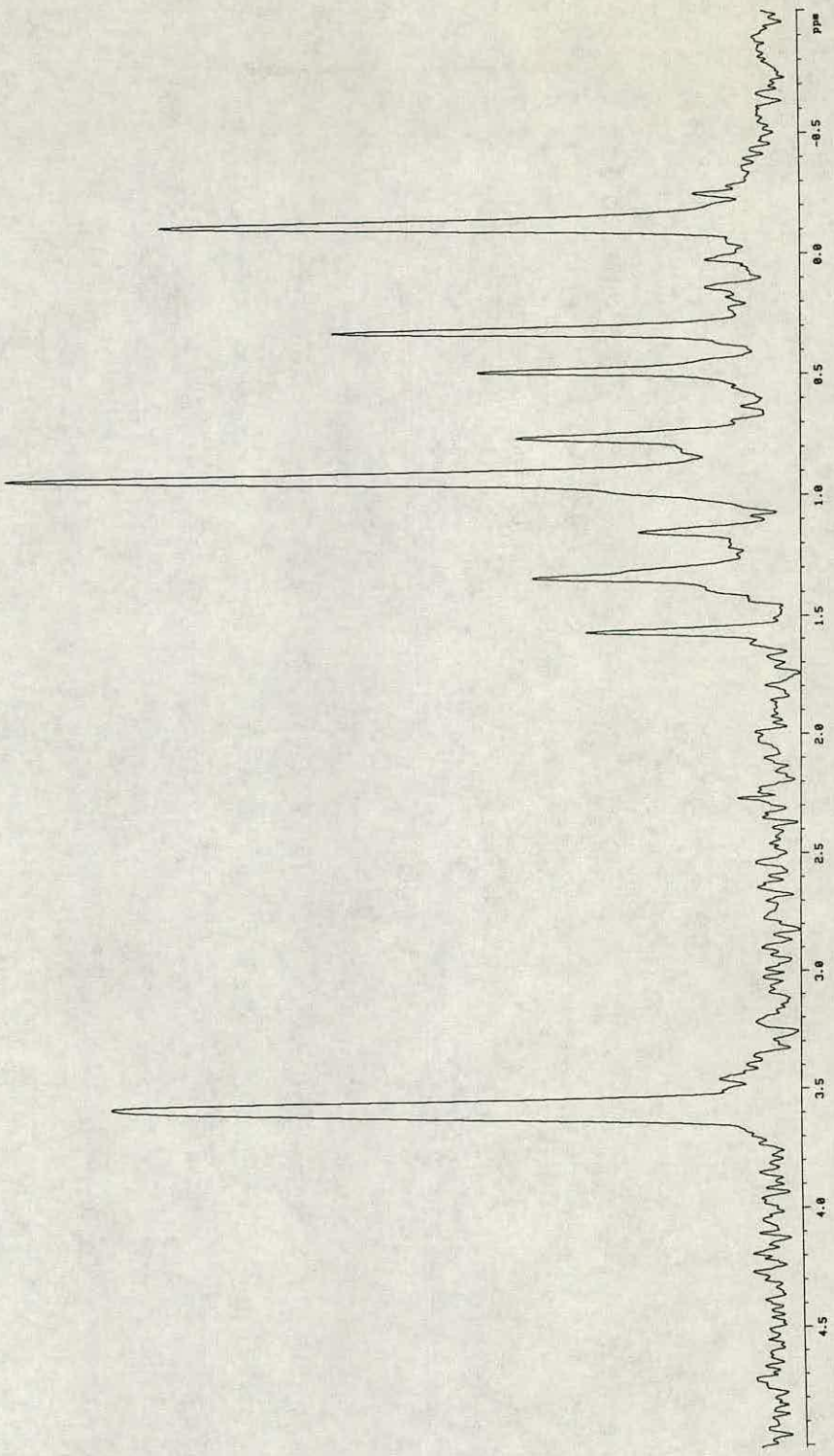


Figure 3. 2. 17b $^{31}P$ NMR spectra of cerebral lipids from scrapie-affected mice at 242.854 MHz.

Spectra where acquired as described in Experimental. Lipid resonances were referenced to $PO_4^{3-}$ singlet at 3.54 ppm. In a comparison between control and scrapie-affected samples, no differences were detected in lipid composition relative to wet brain weight.

*Inferences.*

In the absence of a quantitative lipid change, the multicomponent resonance was speculated to arise from lipid which had undergone a disease-related environmental disturbance. Under the experimental *in vivo* $^{1}$H MRS acquisition parameters incorporating a $T_2$ relaxation time of 420 milliseconds, lipid signals are markedly attenuated and thus not observed (Bell *et al.*, 1991). The visualization of lipid resonances under the aforesaid conditions would therefore indicate a change in lipid mobility or environment, with an associated increase in the time for the radiofrequency excitation of protons to decay. Bell and colleagues thus proposed that the multicomponent resonance "may arise from lipids which have a mobile component and are in an environment different from that normally expected, or from mobile membrane-related compounds" (Bell *et al.*, 1991). Although this was an interesting hypothesis, it was one for which the validity was difficult to evaluate.

The attribution of the multicomponent resonance to lipid was questioned following a review of the limited articles on the detection of intracerebral changes in lipid flux by *in vivo* $^{1}$H MRS (Davie *et al.*, 1993; Larsson *et al.*, 1991; Koopmans *et al.*, 1993). Demyelination and cholesteryl ester elevation are prominent events in white matter regions of patients suffering from multiple sclerosis (Ghosh and McLean Grogan, 1991; Maggio *et al.*, 1972). The former authors recorded the observation of resonances between 1.2 and 1.4 ppm in white matter regions which they speculated to be attributed to lipid disturbances. Comparison of these documented *in vivo* lipid signals with the scrapie-specific multicomponent resonance (1.5 to 1.8 ppm) highlighted a striking disparity in the frequency at which the two sets of signals were observed. Our *in vitro* $^{1}$H MRS lipid studies support the independent findings above in that methylene envelope proton resonances produce prominent signals over the 1.2 to 1.4 ppm region (Figure 3. 2. 2). In contrast the observation of the scrapie multicomponent peak

at an appreciably higher frequency to that expected for methylene envelope signals did not support its lipid origin.

A suitable non-invasive means of testing the association between the multicomponent resonance and changes in intracerebral lipid concentration or relaxation properties was not immediately forthcoming. However, during the process of analyzing cerebral lipids from three murine-scrapie models (ME7/VM, 87V/VM and 301V/VM) during their disease progression by h.p.t.l.c., a very marked abnormality was detected in levels of triglyceride in one control mouse. *In vitro* lipid analysis was performed as part of a collaborative study in which scrapie and control mice underwent routine *in vivo* $^{1}H$ MRS examination at Queen Mary and Westfield College, London. *In vivo* proton MRS spectra of the aforesaid abnormal mouse and a littermate control in which no h.p.t.l.c. lipid abnormality was detected are illustrated in Figure 3. 2. 18. The proton spectrum of the mouse with a lipid abnormality clearly exhibits an intense resonance between 1.15 and 1.40 ppm in agreement with the lipid signals previously described in multiple sclerosis plaques (Davie et al., 1993; Larsson *et al.*, 1991; Koopmans *et al.*, 1993). A similar signal was not observed in the normal mouse. This incidental finding provided evidence in disproof of the hypothesis that the 1.5 to 1.8 ppm multicomponent resonance was attributable to lipid, be it mobile or otherwise. The failure to detect a 'multicomponent peak' in either aqueous or non-aqueous solvents raised considerable uncertainty as to the origin of this abnormality. The importance and scrapie-specificity of the multicomponent peak was later discounted when repeated studies found the signal in control as well as scrapie mice in an apparently haphazard distribution and at all stages of disease progression (Progress Report AFRC Grant LRG 103/503 - April 1993). The validity of the original results were understandably viewed with a degree of caution and further studies in this area were suspended pending clarification of the original results by the Queen Mary and Westfield College group - a pursuit which has been unfruitful to date.

Figure 3. 2. 18a *In vivo* $^{1}$H NMR spectra of control murine brain at 200 MHz.

Spectra where acquired as described in Experimental. Metabolite resonances were referenced to the *N*-acetyl aspartate methyl singlet at 2.02 ppm.

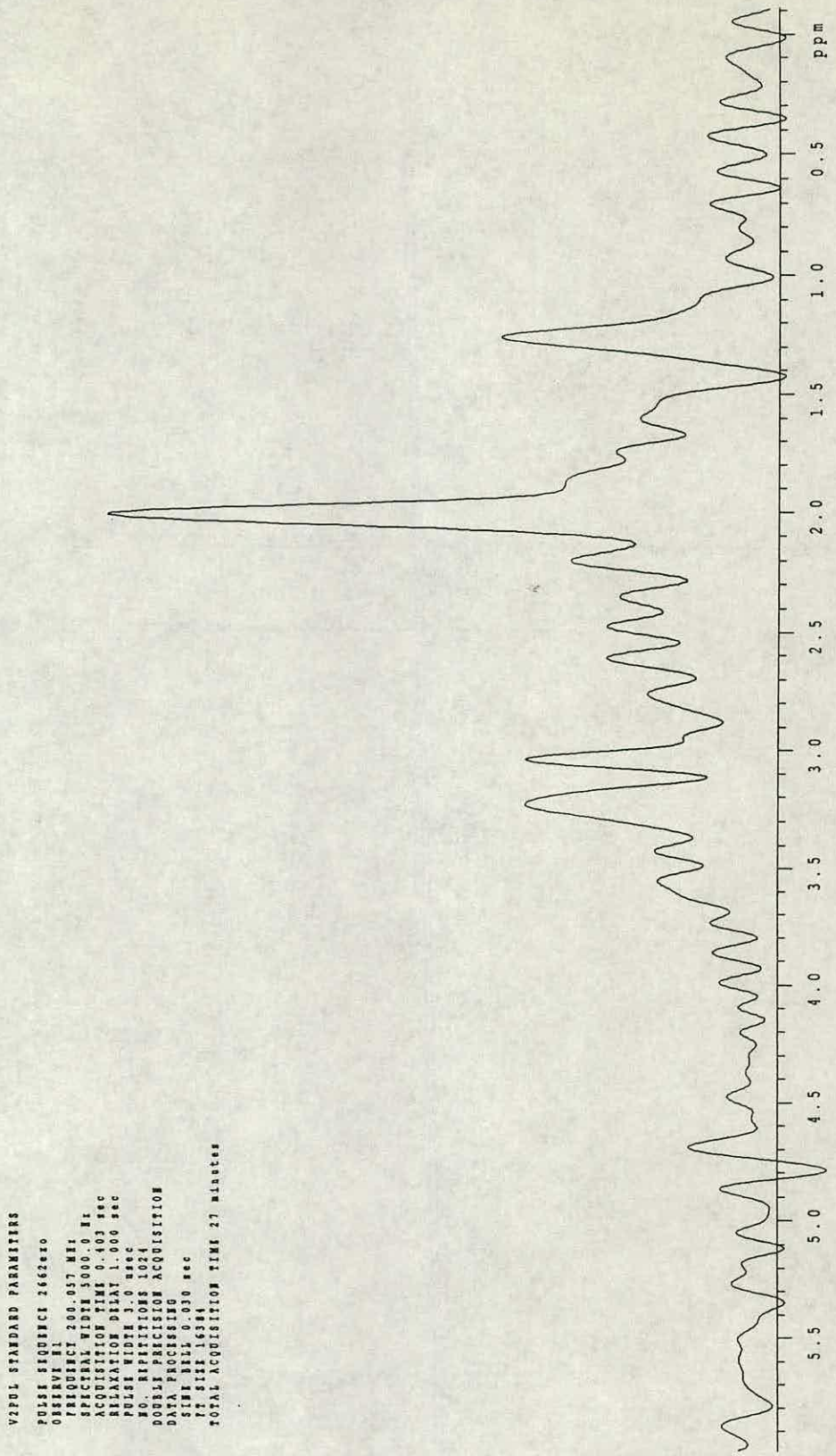


Figure 3. 2. 18b *In vivo* $^{1}$H NMR spectra of lipomateous abnormality in murine brain at 200 MHz.

Spectra where acquired as described in Experimental. Metabolite resonances were referenced to the *N*-acetyl aspartate methyl singlet at 2.02 ppm. With comparison to control (facing page), this spectra displays a broad signal between 1.15 and 1.4 ppm. This resonance was believed to be indicative of a marked intracerebral lipid abnormality.

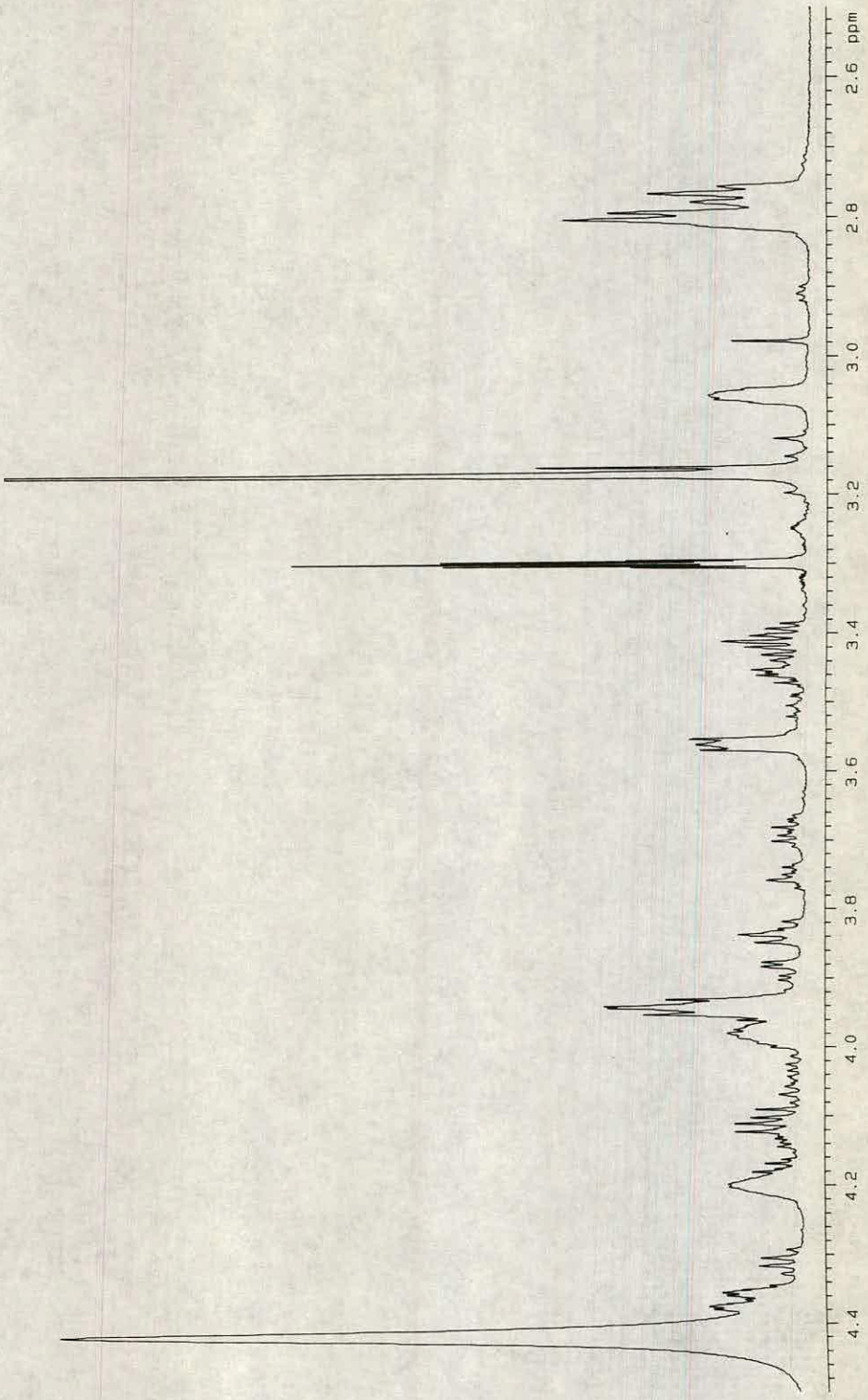


Figure 3. 2. 19a *In vitro* $^{1}$H NMR spectra of neutral cerebral lipids at 600 MHz. The same tissues were used as in Figure 3. 2. 18. Control sample.

Spectra where acquired as described in Experimental. Metabolite resonances were referenced to the *N*-acetyl aspartate methyl singlet at 2.02 ppm.

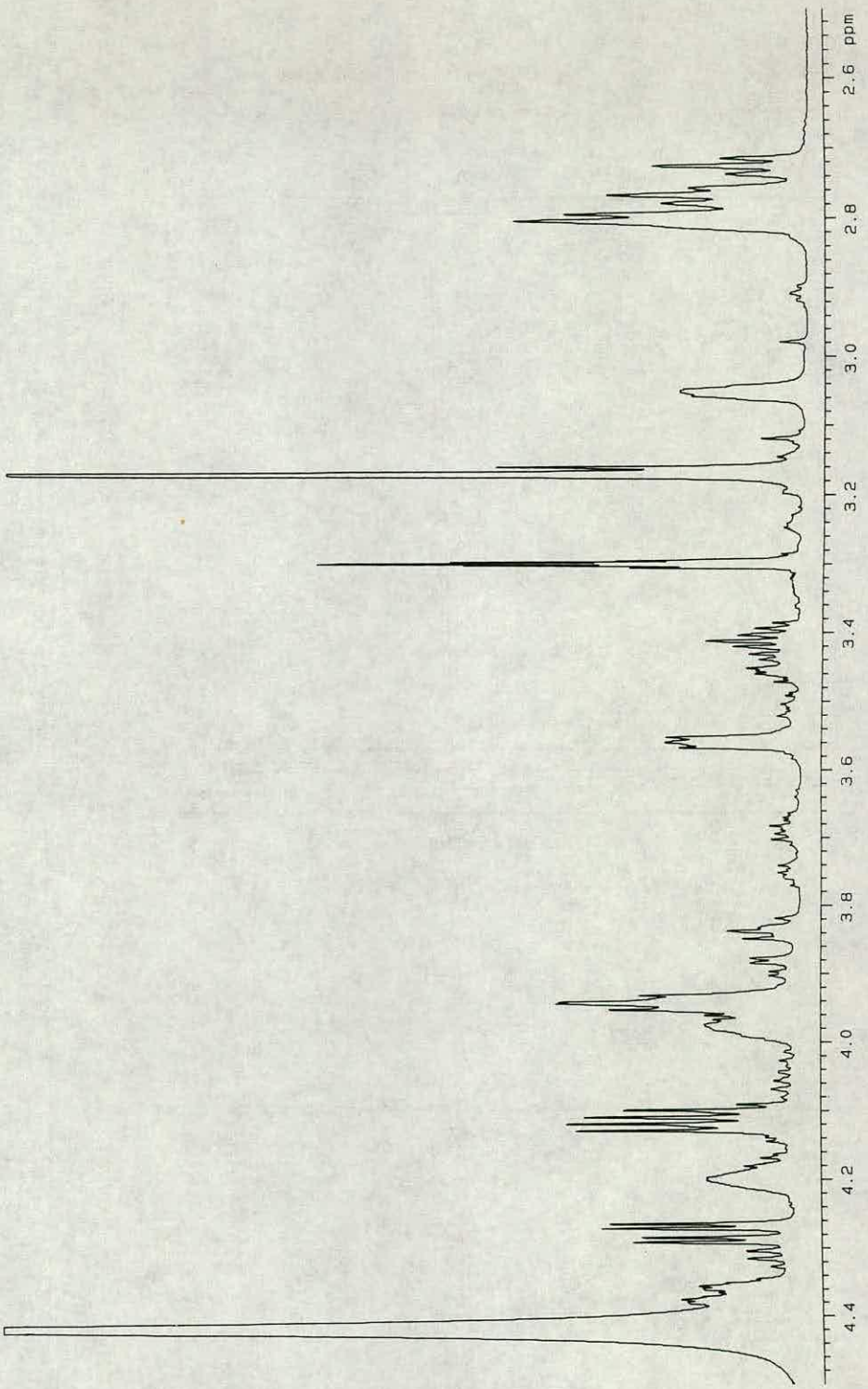


Figure 3. 2. 19b *In vitro* $^{1}$H NMR spectra of neutral cerebral lipids at 600 MHz. The same tissues were used as in Figure 3. 2. 18. Lipomateous abnormality sample.

Spectra where acquired as described in Experimental. Metabolite resonances were referenced to the *N*-acetyl aspartate methyl singlet at 2.02 ppm. With comparison to control (facing page), the presence of two sets of doublets of doublets at 4.08 and 4.25 ppm are in agreement with Sn1 and Sn3 methylene protons in the glycerol backbone of triglyceride. In addition, resonances at 2.69 ppm indicated appreciable levels of linoleic acid.

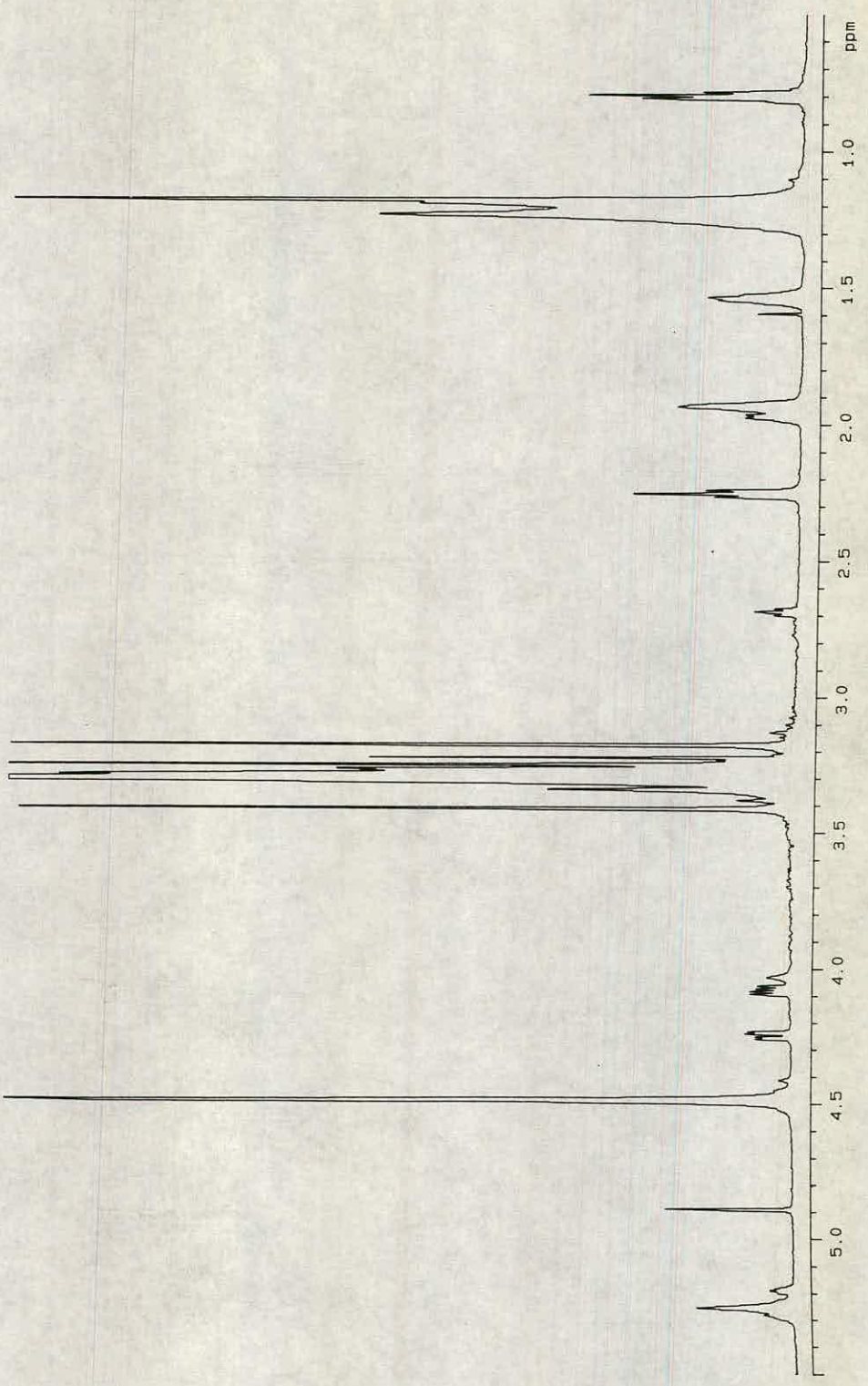


Figure 3. 2. 20 $^{1}$H NMR spectrum of isolated lipomateous abnormality at 600 MHz.

Spectra where acquired as described in Experimental. Metabolite resonances were referenced to the *N*-acetyl aspartate methyl singlet at 2.02 ppm. This spectrum confirms the identity and allows the elucidation of the fatty acid composition of the purified triglyceride.

### 3. 2. 5 Detection and Characterization of a Cerebral Lipid Abnormality by *in Vivo* and *in Vitro* $^{1}H$ and $^{31}P$ NMR Spectroscopy.

The detailed purification and subsequent characterization of the aforementioned triglyceride abnormality is described as an example of the application of *in vitro* $^{1}H$ and $^{31}P$ NMR spectroscopy to the characterization of a cerebral lipid change.

*Results.*

High performance thin layer chromatography analysis of murine cerebral lipids identified a control individual which exhibited a marked elevation in a non-polar, neutral lipid. This was seen to co-migrate with authentic triglyceride under conditions for non-polar lipid separation (hexane/diisopropyl ether/acetic acid, 65:35:2, by vol.). H.p.t.l.c. studies were performed as a sequel to *in vivo* $^{1}H$ MRS analysis, the latter providing circumstantial proof of the ability to non-invasively detect intracerebral lipid accumulations as broad resonances over the 1.15 to 1.40 ppm chemical shift region. Consideration of this finding and its implications for the 'scrapie-specific multicomponent peak - mobile lipid' hypothesis have received prior discussion.

Neutral and acidic cerebral lipid fractions from the 'abnormal' mouse and a littermate control in which no abnormality was observed, were evaporated to dryness under dry nitrogen and resuspended in fully deuterated chloroform/methanol (2:1, v/v) for *in vitro* $^{1}H$ MRS analysis and subsequently in aqueous deoxycholate solution for *in vitro* $^{31}P$ MRS analysis (Section 2. 4. 3). One-dimensional proton NMR spectroscopy of the neutral fraction revealed quantitative changes in the intensities of hitherto undetected cerebral lipid resonances. These were seen as two prominent sets of 'doublets of doublets' centered at 4.11 and 4.28 ppm and two sets of triplets at 2.73 and 5.23 ppm (Figure 3. 2. 19). The former two signals were believed to originate from Sn1 and Sn3 glycerol methylene protons in triglyceride in close agreement with those values reported by Choi and colleagues (1993). The triplet at 5.23 ppm was

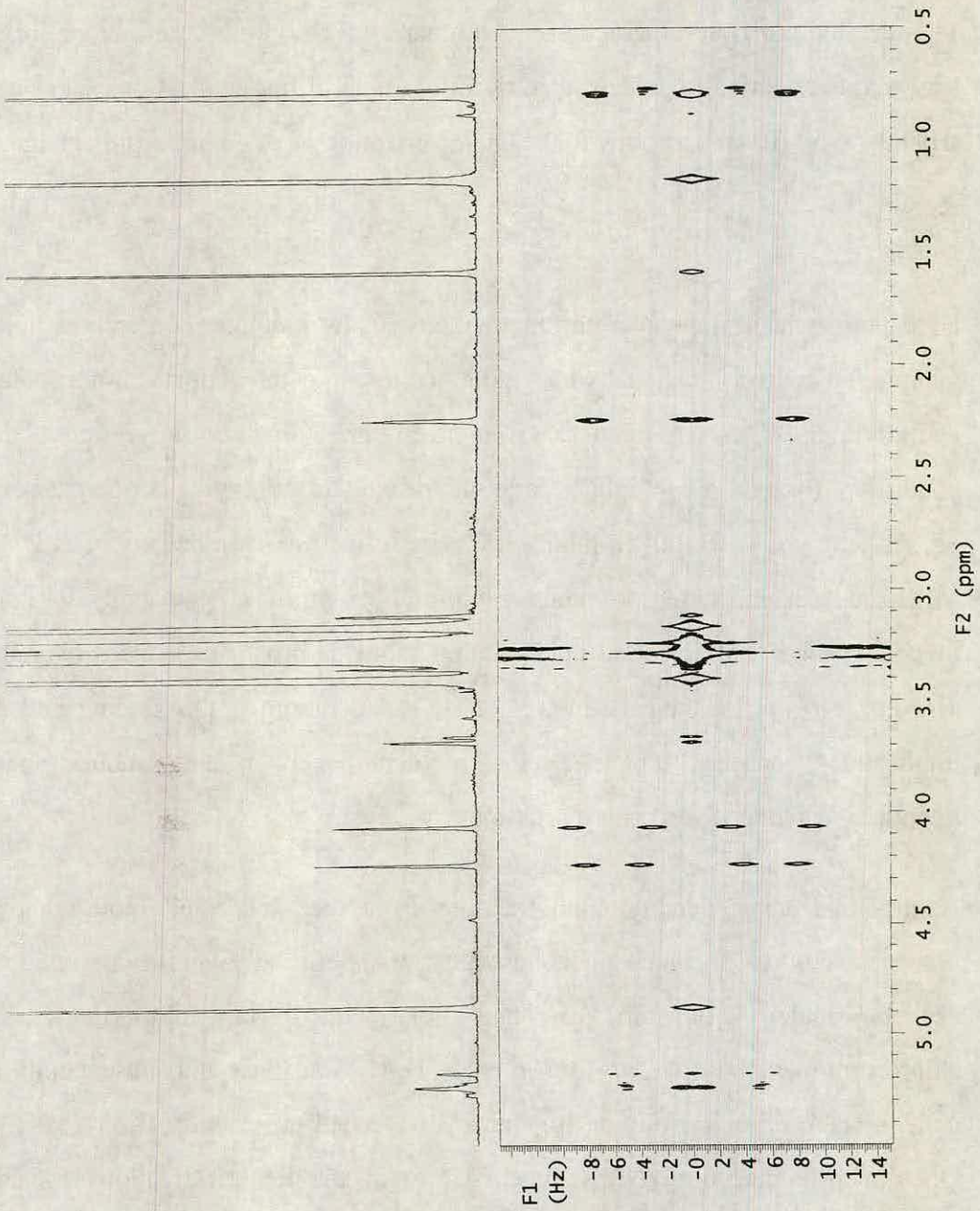


Figure 3. 2. 21 Two-dimensional *J*-resolved spectrum of isolated lipomateous abnormality at 600 MHz.

Spectra where acquired as described in Experimental. Metabolite resonances were referenced to the *N*-acetyl aspartate methyl singlet at 2.02 ppm. This spectrum confirms the identity and allows the elucidation of the fatty acid composition of the purified triglyceride.

assigned to the Sn2 methine proton between the Sn1 and Sn3 methylene protons and the triplet at 2.73 ppm was believed to be indicative of a high concentration of linoleic acid ($C_{18:2}$) in the neutral lipid fraction (Section 3. 2. 1). Whether this latter finding was associated with the triglyceride abnormality was not determined at this stage, however it was noted that the signal was not observed in the corresponding control lipid spectrum (Figure 3. 2. 2). In addition to these changes the intensity of methylene envelope proton resonances over 1.24 to 1.32 ppm were markedly elevated in the 'abnormal' extract. It was noted that similar changes in signal intensity (although less well resolved) were observed in this region in the *in vivo* $^{1}$H MRS spectrum (Figure 3. 2. 18). Levels of other lipids appeared unchanged relative to each other as determined from the intensities of their diagnostic proton resonances. Likewise, $^{31}$P NMR spectroscopy analysis revealed insignificant changes in phospholipids in agreement with the h.p.t.l.c. and $^{1}$H MRS results.

Extensive $^{1}$H MRS analysis of the lipid abnormality was performed following its purification over aminopropyl silica SEP PAK columns (Section 2. 6 - *Triglyceride*). On the basis of weight (8.3 g) this isolate represented 18% of total cerebral lipid and just over 2% of wet brain weight. Diagnostic proton resonances in the triglyceride glycerol backbone were assigned from the one dimensional and two-dimensional COSY 45 proton spectra (Figures 3. 2. 20 and 3. 2. 22 respectively). The signal at 5.20 ppm was assigned to the triglyceride glycerol Sn2 methine proton in close agreement with Sn2 methine protons in corresponding diacyl phospholipids (Section 3. 2. 1). This resonance was observed to couple to signals at 4.08 and 4.25 ppm in the COSY 45 spectrum, both of which were doublets of doublets with geminal coupling constants of 12.4 Hz in addition to vicinal coupling constants of 6.6 and 4.4 Hz respectively (Figure 3. 2. 21). Consequently these signals were assigned to the $Sn1^{u}/Sn3^{u}$ and $Sn1^{d}/Sn3^{d}$ protons respectively.

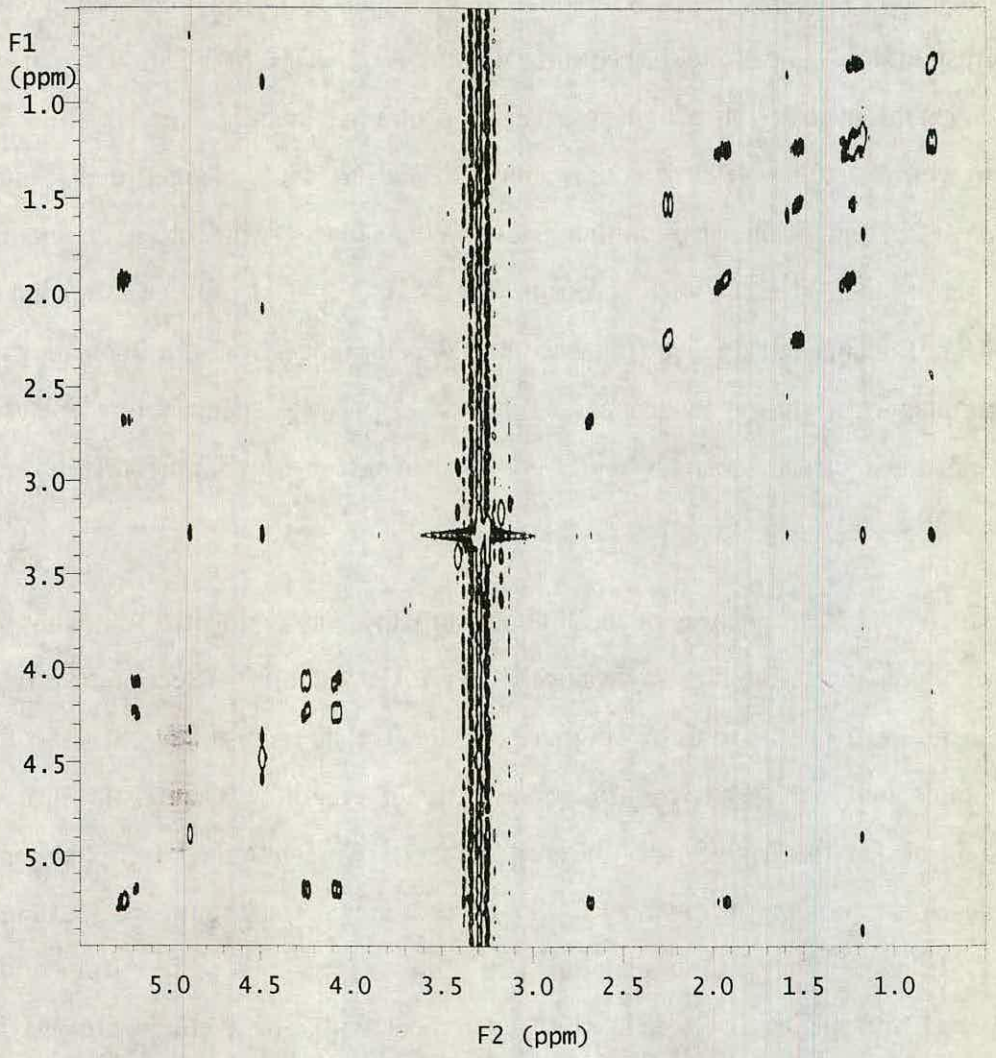


Figure 3. 2. 22 Homonuclear shift-correlated spectrum (COSY 45) of isolated lipomateous abnormality at 600 MHz.

Spectra where acquired as described in Experimental. Metabolite resonances were referenced to the *N*-acetyl aspartate methyl singlet at 2.02 ppm. This spectrum confirms the identity and allows the elucidation of the fatty acid composition of the purified triglyceride.

Proton NMR spectroscopy analysis provided additional information on triglyceride fatty acid composition. With reference to *in vitro* proton NMR spectroscopy studies of acidic lipids (Section 3. 2. 1.):

(i) the observation of an ω1-methyl proton resonance at 0.80 ppm confirmed the presence of terminally saturated fatty acids;

(ii) the absence of a signal at 0.92 ppm argued against the presence of n-3 fatty acids such as docosahexaenoic acid ($C_{22:6}$);

(iii) the absence of a signal at 1.65 ppm argued against the presence of arachidonic acid ($C_{20:4}$);

(iv) the absence of a broad signal at 2.79 ppm argued against the presence of poly-unsaturated fatty acids;

(v) the observation of a triplet resonance at 2.69 ppm suggested the presence of linoleic acid ($C_{18:2}$).

The total degree of unsaturation was afforded by the integral of the signal at 5.27 ppm and in the absence of resonances from poly-unsaturated fatty acids at 2.79 ppm the degree of mono-unsaturation was determined by subtracting the area of the peak at 2.69 ppm (di-unsaturated linoleic acid) from that at 5.27 ppm. The resonance at 2.25 ppm afforded a measure of total fatty acids present. Thus, following adjustment for proton contributions to signal intensities the relative proportions of saturated and unsaturated fatty acids were calculated.

Two-dimensional COSY 45 NMR spectroscopy of the above purified lipid extract, in addition to mass spectrometry analysis of fatty acid methyl ester derivatives (results not shown), provided support for the inference that linoleic acid was the most probable candidate for the prominent di-unsaturated fatty acid resonance at 2.69 ppm. The ratio of the vinyl peak at 5.27 ppm to the C2 fatty acid methylene resonance at 2.25 ppm indicated that linoleic acid was not the

| Chemical shift /ppm | Functional group | Proton intensity |
|---|---|---|
| | | |
| 0.80 | ω1-$CH_3$ (sat., n-6, n-9) | 104 |
| | | |
| 1.18 - 1.22 | methylene envelope | nd |
| | | |
| 1.54 | -$CH_2$C**H**$_2$$CH_2$$COO^-$ | nd |
| | | |
| 1.94 | -C**H**$_2$CH=CHC**H**$_2$- | 70 |
| | | |
| 1.97 | -$(CH_2)_n$C**H**$_2$CH=CH- | 31 |
| | | |
| 2.25 | -$CH_2$$CH_2$C**H**$_2$$COO^-$ | 71 |
| | | |
| 2.69 | -CH=CHC**H**$_2$CH=CH- | 14 |
| | | |
| 4.08 | $Sn1^u$/$Sn3^u$ | nd |
| | | |
| 4.25 | $Sn1^d$/$Sn3^d$ | nd |
| | | |
| 5.19 | Sn2 | nd |
| | | |
| 5.26 | -C**H**=C**H**- | 66 |
| | | |

Table 3. 2. 4 *In vitro* $^1$H NMR spectroscopy analysis of purified triglyceride from a suspected case of spontaneous lipoma at 600 MHz.

*In vivo* cerebral $^1$H NMR analysis of a control mouse revealed a broad resonance over 1.2 to 1.35 ppm. HPTLC analysis suggested the presence of high levels of triglyceride in the same. Cerebral lipids from this mouse were subsequently analyzed by *in vitro* $^1$H NMR spectroscopy. For description of procedure see Experimental. The intensity of the proton resonances tabulated above are expressed in arbitary units.

The presence of two sets of doublets of doublets at 4.08 and 4.25 in the $^1$H NMR spectrum strongly supported the HPTLC diagnosis of triglyceride.

nd, not determined.

With reference to proton contributions to the above peaks, the fatty acid composition of the isolated triglyceride was deduced:

Total fatty acids contribute 71 units (-$CH_2$C**H**$_2$COO-);
Total unsaturated fatty acids contribute 66 units (-$CH_2$-C**H**=C**H**-$CH_2$-);
Poly-unsaturated fatty acids - absent;
Linoleic acid ($C_{18:2}$) contributes 14 units (-CH=CH-C**H**$_2$-CH=CH-), and thus 28 units to total unsaturated fatty acids (-C**H**=C**H**-$CH_2$-C**H**=C**H**-);
By deduction mono-unsaturated fatty acids comprise (66 - 28) = 38 units;
By deduction saturated fatty acids comprise (71 - 14 - 38) = 19 units;

Therefore the ratio of saturated:mono-unsaturated:di-unsaturated = 19:38:14

only unsaturated fatty acid present with mono-unsaturated fatty acids also in appreciable quantities. On the basis of relative peak intensities (Figure 3. 2. 20), it was speculated that part of the broad resonance centered at 1.95 ppm was attributed to methylene protons on either side of the vinyl groups in linoleate [-$CH_2$-C$\underline{H_2}$-CH=CH-$CH_2$-CH=CH-C$\underline{H_2}$-$CH_2$-], and that the slightly more intense signal centered at 1.94 ppm was attributed to similar protons in mono-unsaturated fatty acids [-$CH_2$-C$\underline{H_2}$-CH=CH-C$\underline{H_2}$-$CH_2$-]. Thus comparison of the integrals of the signals at 1.97 and 1.94 ppm gave a measure of the relative proportions of di-unsaturated and mono-unsaturated fatty acids respectively. Finally in the absence of appreciable poly-unsaturated fatty acid signals, the proportion of saturated fatty acids was assessed by subtracting the contribution made by unsaturated fatty acid resonances to the total fatty acid signal at 2.25 ppm. This revealed that saturated components made a significant contribution to the proton spectrum of the triglyceride. A summary of the above findings is given in Table 3. 2. 4.

*Inferences.*

The origin of the triglyceride abnormality is speculative, however its visualization by *in vivo* proton MRS would suggest that the lipid accumulation occurred in an environment markedly different to that normally experienced by intracerebral lipid. It is considered that this property coupled with the relatively large proportion present (18% of total cerebral lipid) made its non-invasive detection possible.

An increase in lipid methylene envelope $^1$H MRS $T_2$ relaxation time behaviour has been noted in suspensions of cancer cells and excised tumours following the acquisition of metastatic competence, i.e. ability to generate secondary tumours (Mountford *et al.*, 1984). Chemical analysis of the above adenocarcinoma cell lines showed triglyceride to comprise a significant proportion of plasma membrane lipids (May *et al.*, 1986). In this respect it was interesting to note that the frequency incidence of the triglyceride abnormality (approximately 1%) was similar to that reported for spontaneous astrocytoma in VM mice (Fraser, 1986).

A hypothesized relationship between the occurrence of astrocytoma and an elevation in triglyceride was investigated by the examination of cerebral lipid profiles in twelve VM mice which had received an intracerebral inoculation with an aliquot of a cell suspension derived from a case of spontaneous astrocytoma (Fraser, 1980). Brains were divided sagittally, one half was examined histologically to confirm the presence of astrocytoma and the other half underwent solvent extraction and high performance thin layer chromatography analysis. Although histological examination confirmed that all brains exhibited astrocytomas, h.p.t.l.c. analysis failed to identify any lipid abnormalities (results not shown). It was therefore concluded that spontaneous astrocytoma was not a probable cause for this pathology-linked elevation in triglyceride.

An alternative explanation for the incidence of a large triglyceride deposition is offered by the occurrence of a relatively benign spontaneous intracerebral lipoma. Such tumour-like lesions have been reported to be the most commonly occurring neoplasms in the brains of laboratory mice (Morgan *et al.*, 1984) and in this particular strain ranking second only to the occurrence of spontaneous astrocytoma (Fraser, 1980). Lipomas, consisting of lobules of adipose tissue separated by fibrous bands and septa, are the result of dysraphic malformations during early embryogenesis (Greenfield, 1976). Embryonic cell lines have been reported to display properties of high resolution NMR relaxation behaviour (May *et al.*, 1986). It is thus presumed that morphogenic accumulations of adipose tissue could possess similar properties. As such this hypothesis provides the most plausible explanation for the origin of the lipid abnormality observed by *in vivo* $^{1}$H NMR spectroscopy.

### 3. 2. 6 A Summary of the MRS Analysis of Cerebral Metabolites in Scrapie-Affected and Control Mice.

***Acetone-Soluble Metabolites.***

The study of acetone-soluble metabolites in scrapie-affected and control mice revealed three statistically significant differences. A reduction in cerebral levels of *N*-acetyl aspartate in scrapie animals is believed to be indicative of neuronal loss/dysfunction, likewise a more modest reduction in levels of glutamate may mirror extensive damage to regions of the brain in which this excitatory amino acid serves an important function, e.g. in the hippocampus. Both inferences are consistent with the neuropathology exhibited by this murine-scrapie model (Fraser and Dickinson, 1968). An explanation for the observation of a prominent elevation in cerebral inositol concentration was not forthcoming, however the report of a similar finding in parietal white matter regions of a patient with CJD (determined by *in vivo* MRS) raises an important question as to the significance of this abnormality with regards to TSE disease status.

Although an aqueous extraction protocol was developed which afforded a high degree of spectral resolution and reproducibility, the presence of the 'scrapie-specific multicomponent peak' was not detected and attention was therefore focused on changes in non-aqueous metabolites - with special reference to lipids.

***Non-aqueous Metabolites.***

Extensive attention was given to the assignment of cerebral lipid resonances in *in vitro* $^{1}H$, $^{13}C$ and $^{31}P$ NMR spectra. Comparison of scrapie and control non-aqueous extracts by a combination of the aforementioned techniques failed to identify any significant changes in the concentrations of prominent cerebral lipids. In addition, the inability to detect a quantitative lipid change over the 1.5 to 1.8 ppm region served as a serious impediment to the elucidation of the nature and origin of the component(s) responsible for the *in vivo* signal. Although it was

speculated that the multicomponent signal was attributed to mobile lipid, it was noted that the frequency over which this broad resonance was detected was significantly downfield (i.e. at a higher chemical shift) of documented lipid disturbances detected by similar *in vivo* $^{1}$H MRS experiments (Davie *et al.*, 1993; Larsson *et al.*, 1991; Koopmans *et al.*, 1993). Additional support in disproof of the 'mobile lipid' hypothesis was afforded by the detection of what was speculated to be a spontaneous lipoma in a control VM mouse. This lipid abnormality was detected by *in vivo* $^{1}$H MRS and subsequently characterized following *in vitro* $^{1}$H MRS, high performance thin layer chromatography and mass spectrometry analysis.

The incidental occurrence of the above triglyceride abnormality presented a unique opportunity to assess the ability of *in vitro* NMR spectroscopy to characterized an intracerebral lipid change. However of considerable importance to these studies was the finding that this marked lipid disturbance could be detected non-invasive by *in vivo* proton MRS. As such this broad signal over the 1.15 to 1.40 ppm chemical shift region was entirely consistent with the position of resonances from methylene envelope protons as assigned in *in vitro* lipid spectra (Section 3. 2. 1). The attribution of the 'scrapie-specific' multicomponent resonance to lipid, be it mobile or otherwise, was consequently viewed with sceptism. The absence of an alternative hypothesis for the origin of the scrapie-specific signal coupled with our frustrating inability to detect the signal *in vitro* did not assist further studies. It was at this stage of perplexity that Bell and colleagues reported the presence of the multicomponent peak in control as well as scrapie animals with a random and haphazard distribution (Progress Report AFRC Grant LRG 103/503 - April 1993). Understandably the continuation of investigations in this area were suspended pending clarification of the original results.

Further lipid analysis was performed by high performance thin layer chromatography. This line of investigation is explored in Section 3. 3.

## 3. 3 High Performance Thin Layer Chromatography Analysis of Cerebral Lipids.

The study of cerebral lipid changes in the transmissible spongiform encephalopathies Creutzfeldt-Jacob disease and scrapie have received earlier discussion (Section 1). Although it would appear that various lipid abnormalities are present in CJD-affected brain tissue from human patients (Ando *et al.*, 1984; Bass *et al.*, 1974; Korey *et al.*, 1961), chimpanzees (Yu *et al.*, 1974) and guinea pigs (Yu and Manuelidis, 1978), similar findings are not observed in scrapie-affected hamsters (Dees *et al.*, 1985) or mice (Tamai *et al.*, 1978).

The ability to draw constructive conclusions from the aforementioned scrapie studies have been hampered by the singular number of hamster- and murine-scrapie models examined and by the relatively non-precise analytical techniques employed. In addition, contradictory reports of lipid abnormalities in the same scrapie models by other authors (Di Martino *et al.*, 1993; Mackenzie and Wilson, 1966) raise serious questions as to the consistency and validity of the earlier findings.

In view of these discrepancies and in the light of the speculated detection of a scrapie-specific lipid abnormality by *in vivo* NMR spectroscopy, the cerebral lipid composition of a number of murine-scrapie models were investigated in a quantitative and comparative manner. For this purpose high performance thin layer chromatography was employed in conjunction with the *in vitro* NMR spectroscopy experiments described previously. In our consideration h.p.t.l.c. offered distinct advantages over NMR spectroscopy in that lipid species were readily separated, observed and quantified. In addition the improved sensitivity of lipid detection associated with this technique permitted the observation of a minor lipid abnormality in scrapie-affected mice. A discussion of the findings is given below.

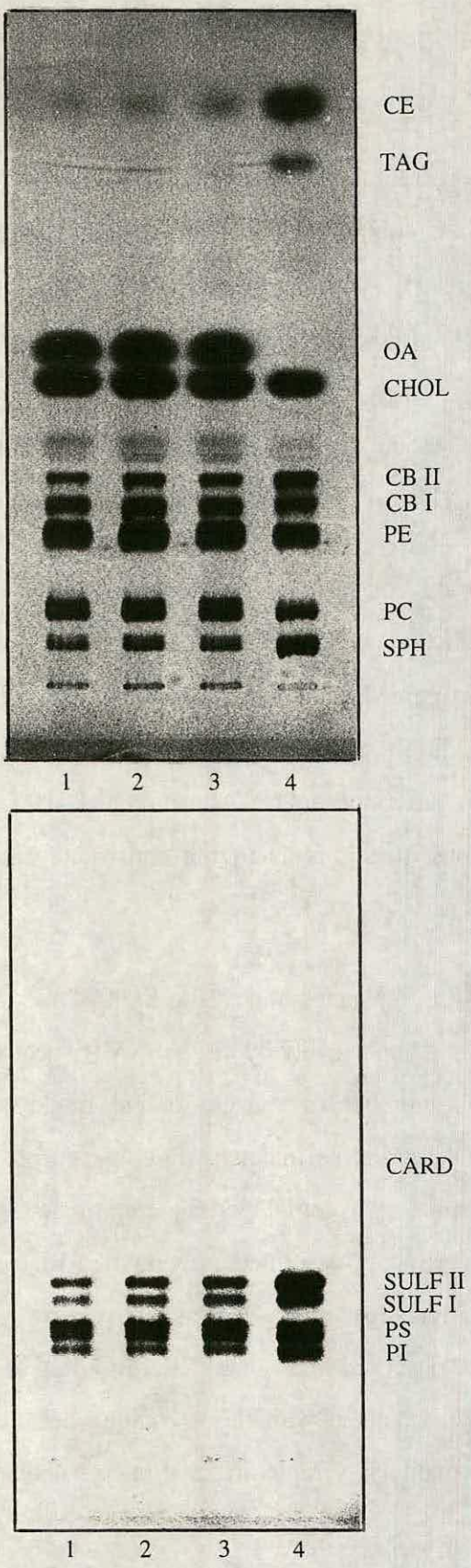


Figure 3. 3. 1 HPTLC analysis of neutral (top figure) and acidic (bottom figure) cerebral lipids.

Cerebral lipid fractions were analyzed as described in Experimental. Lanes 1 - 3 cerebral lipid extracts, lane 4 authentic lipids. CARD, cardiolipin; CB I, cerebroside I; CB II, cerebroside II; CE, cholesteryl ester; CHOL, cholesterol; DAG, diacylglycerol; FA, fatty acid; OA, oleyl alcohol (internal standard); PC, phosphatidyl choline; PE, phosphatidyl ethanolamine; PI, phosphatidyl inositol; PS, phosphatidyl serine; SPH, sphingomyelin; SULF I, sulfatide I; SULF II, sulfatide II; TAG, triacylglycerol.

## 3. 3. 1 Detection and Characterization of a Lipid Abnormality in Scrapie-Affected Mice.

*Results.*

High performance thin layer chromatography studies were performed on VM mice affected with the ME7 scrapie strain at the late clinical stage of the disease (346 ± 3 days p.i.). Cerebral lipids from these animals were compared with an equal number of age- and sex-matched controls. Lipid species were identified on the basis of polarity and acidity by their co-migration with authentic lipids on an h.p.t.l.c. silica plate (Macala *et al.*, 1985). The neutral lipid fraction contained: cholesteryl esters, triglycerides, diglycerides, cholesterol, galactocerebrosides I and II, ethanolamine phospholipids and choline phospholipids (including sphingomyelin) (Figure 3. 3. 1a), and the acidic lipid fraction: cardiolipin, sulfatides I and II, serine phospholipids and inositol phospholipids (Figure 3. 3. 1b). Quantification of cerebral lipids was performed following charring by laser scanning densitometry and with reference to standard lipid calibration curves (Macala *et al.*, 1985; Section 2. 5).

A comparison of scrapie and control animals showed that the majority of cerebral lipids remain essentially unchanged, indeed no statistical difference was detected in levels of the prominent neutral lipids: cholesterol, cerebrosides, ethanolamine phospholipids and choline phospholipids (including sphingomyelin), or in the prominent acidic lipids: cardiolipin, sulfatides, serine phospholipids and inositol phospholipids (Table 3. 3. 1). In contrast a highly significant elevation was detected in the concentration of a minor, non-polar, neutral lipid in scrapie-affected material which co-migrated with authentic cholesteryl oleate (Figure 3. 3. 2). As such, this lipid abnormality provided a candidate compound for the neutral fat accumulations observed in mice affected with scrapie by histological techniques (Mackenzie and Wilson, 1966) and which were speculated to arise from the breakdown of brain lipids (Kimberlin and Millson, 1967). In this regard, and consistent with the above combination of features, an elevation in cholesteryl

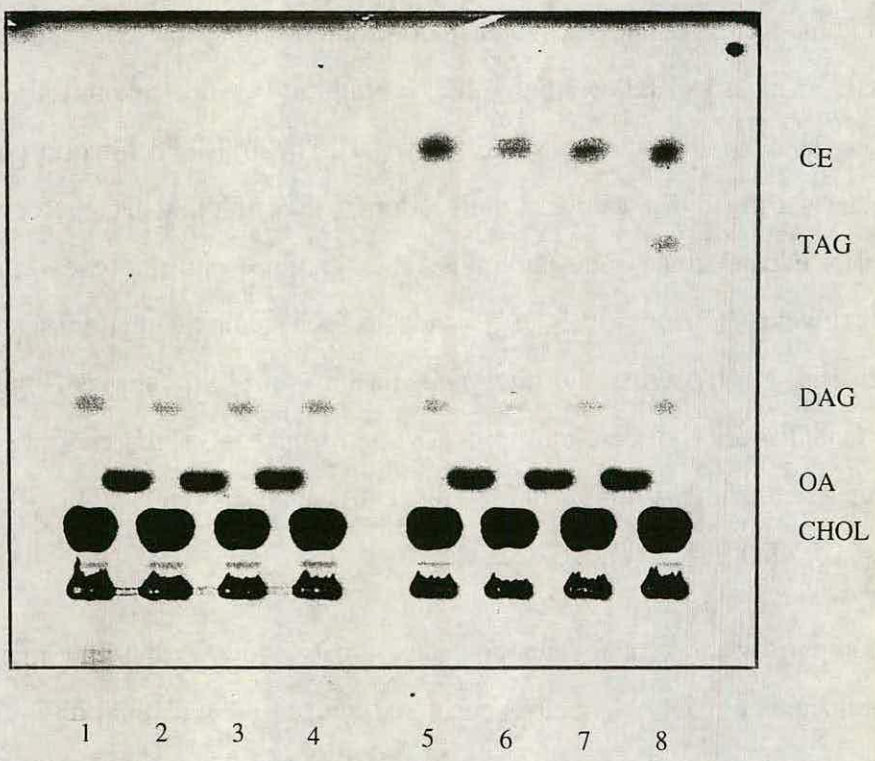


Figure 3. 3. 2 HPTLC demonstration of a non-polar, neutral lipid abnormality in scrapie-affected mice.

Cerebral lipid fractions were analyzed as described in Experimental. Lanes 1 - 4 control cerebral lipid extracts, lanes 5 - 8 scrapie cerebral lipid extracts. Lipid abbreviations are as previously listed. Note the elevated levels of cholesteryl esters.

esters was initially hypothesized to be the most probable source of the scrapie-specific multicomponent resonance detected by *in vivo* $^{1}H$ NMR spectroscopy (Bell *et al.*, 1991).

The nature of this lipid was confirmed to comprise cholesteryl esters following its isolation by bonded phase column chromatography on aminopropyl silica SEP PAK columns and subsequent characterization by chemical ionization mass spectrometry (Section 2. 6). Preliminary electron impact studies of the purified material revealed the presence of an ion fragment with a *m/z* ration of 369.1. A similar ionic species was identified in the electron impact mass spectrum of authentic cholesterol and was attributed to the 'cholesterol minus water' molecular ion. The possibility of this lipid abnormality being attributed to free cholesterol was considered negligible in view of the fact that the isolated lipid eluted more readily than cholesterol in a non-polar solvent system ($R_f$ purified lipid = 0.76, $R_f$ cholesterol = 0.12; hexane/diisopropyl ether/acetic acid (65:35:2, by vol.). As such these results provided circumstantial evidence to suggest that the elevated lipid was cholesterol-containing.

Subsequent studies were performed on pooled fractions isolated from three scrapie (ME7/VM) and three control (VM) mouse brains of similar age and gender. Chemical ionization mass spectrometry of the above samples revealed high mass ions with *m/z* ratios between approximately 600 and 740, these being particularly well distinguished in the scrapie fraction as a result of the elevated quantity of lipid present (Figures 3. 3. 3a/b). Tandem mass spectrometry (MS-MS) of the prominent ions at 614.6, 642.6 and 668.6 showed all to possess a daughter (or product) ion with a *m/z* ratio of 369, which was also present in the MS-MS spectrum of authentic cholesteryl oleate and consistent with the 'cholesterol minus water' structure described above. This information provided conclusive evidence that the molecular ions with *m/z* ratios between 614.6 and 714.6 were attributable to cholesteryl esters. In view of this finding the scrapie-

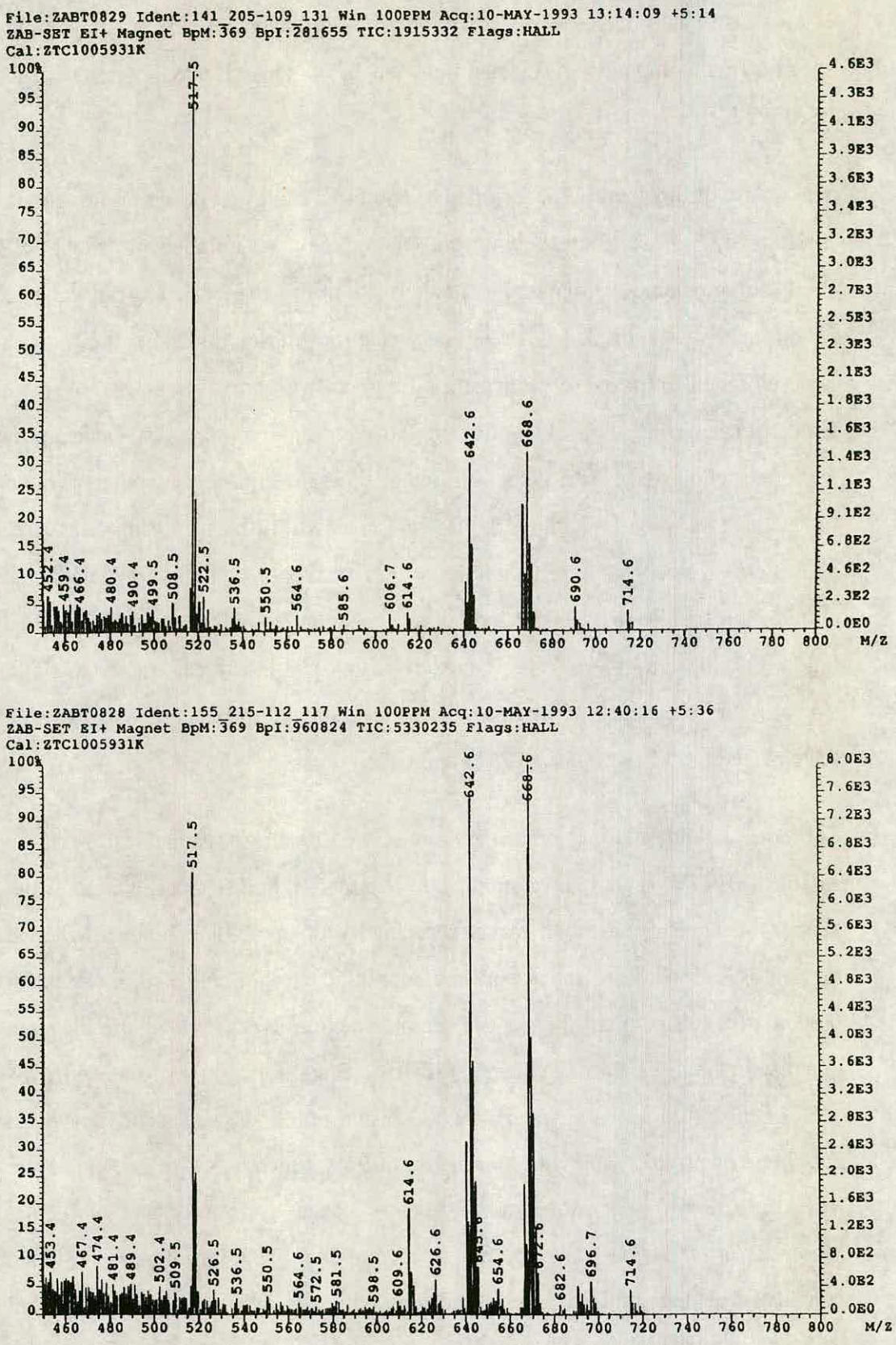


Figure 3. 3. 3 CI-MS of cholesteryl esters from control (top figure) and scrapie-affected (bottom figure) mice.

Cholesteryl esters were purified and analyzed by CI-MS as decribed in Experimental. Scrapie fractions contain appreciably more cholesteryl esters than controls. Significant changes were observed between the two fractions in cholesteryl myristate, cholesteryl oleate, cholesteryl linoleate, cholesteryl arachidonate and cholesteryl docosahexaenoate. Levels of cholesteryl palmitate, cholesteryl palmitoleate and cholesteryl stearate remained essentially unchanged.

specific cholesteryl ester abnormality was quantified by h.p.t.l.c. with reference to the staining properties exhibited by cholesteryl oleate (Table 3. 3. 1).

Having confirmed the nature of the lipid abnormality it was found that normal adult control VM mice contain low levels of cholesteryl esters in their brains (60 ± 5 μg cholesteryl ester/g wet brain weight), representing less than 0.1% of total brain lipids and approximately 0.33% of the concentration of cerebral cholesterol. In contrast, VM mice affected with the ME7 strain of scrapie exhibit elevated levels of cholesteryl esters (250 ± 40 μg cholesteryl ester/g wet brain weight) representing 0.33% total brain lipids and 1.6% of the concentration of cerebral cholesterol.

The molecular ions with *m/z* ratios of 614.6, 642.6 and 668.6 in the CI-MS spectra, were attributed to cholesteryl myristate ($C_{14:0}$), cholesteryl palmitate ($C_{16:0}$) and cholesteryl oleate ($C_{18:1}$) respectively. A number of less prominent ion species were also present, these corresponding to cholesteryl palmitoleate ($C_{16:1}$, *m/z* 640.6), cholesteryl linoleate ($C_{18:2}$, *m/z* 666.6), cholesteryl stearate ($C_{18:0}$, *m/z* 670.6), cholesteryl arachidonate ($C_{20:4}$, *m/z* 690.6), cholesteryl arachidate ($C_{20:1}$, *m/z* 696.1) and cholesteryl docosahexaenoate ($C_{22:6}$, *m/z* 714.6). The percentage contribution that these esters made to the cerebral lipid fraction was calculated as a proportion of the endogenous cholesteryl oleate peak (Table 3. 3. 2). The composition of prominent esters, notably cholesteryl stearate, oleate, palmitate and palmitoleate, appear relatively constant between samples. However a reduction in the proportion of cholesteryl linoleate was noted in the scrapie isolate with respect to control levels. The significance of this latter finding is unclear.

*Inferences.*

The cholesteryl ester abnormality was initially viewed with a degree of interest as it presented a potential candidate for the *in vivo* MRS observation (Bell *et al.*, 1991). This hypothesis, although attractive, was discounted on the basis of two

| | ME7/VM | 87V/VM | 301V/VM | VM |
|---|---|---|---|---|
| | | | | |
| *Neutral lipids* | | | | |
| | | | | |
| Cholesteryl esters | 0.25 ± 0.04 | 0.12 ± 0.02 | 0.06 ± 0.03 | 0.06 ± 0.01 |
| Cholesterol | 22.68 ± 1.69 | 21.72 ± 3.48 | 20.38 ± 1.16 | 21.22 ± 2.67 |
| Cerebroside I | 9.89 ± 0.39 | 9.59 ± 1.31 | 7.33 ± 0.70 | 8.56 ± 1.24 |
| Cerebroside II | 3.77 ± 0.19 | 3.49 ± 0.44 | 2.91 ± 0.44 | 3.51 ± 0.48 |
| Ethanolamine PL. | 22.43 ± 3.38 | 21.56 ± 2.52 | 26.63 ± 3.35 | 24.13 ± 0.88 |
| Choline PL. | 23.79 ± 0.50 | 20.25 ± 1.72 | 27.93 ± 6.88 | 21.00 ± 1.92 |
| Sphingomyelin | 2.23 ± 0.08 | 2.85 ± 0.31 | 2.99 ± 1.16 | 2.57 ± 0.23 |
| | | | | |
| *Acidic lipids* | | | | |
| | | | | |
| Cardiolipin | 4.62 ± 0.93 | 5.78 ± 1.16 | 4.07 ± 1.31 | 5.33 ± 1.48 |
| Sulfatide I | 3.18 ± 0.82 | 2.76 ± 0.55 | 1.39 ± 0.28 | 1.70 ± 0.63 |
| Sulfatide II | 4.19 ± 0.94 | 3.67 ± 0.80 | 2.28 ± 0.38 | 2.91 ± 1.03 |
| Serine PL. | 12.09 ± 3.48 | 12.33 ± 2.35 | 13.04 ± 1.76 | 10.78 ± 4.99 |
| Inositol PL. | 3.75 ± 1.12 | 3.88 ± 0.76 | 3.88 ± 0.67 | 3.01 ± 1.33 |
| | | | | |
| Wet brain weight /g | 336 ± 1 | 378 ± 17 | 406 ± 2 | 415 ± 36 |
| | | | | |
| Incubation period /days | 346 ± 3 | 290 ± 4 | 120 ± 7 | 350 |
| | | | | |

Table 3. 3. 1 HPTLC analysis of cerebral lipids in three murine-scrapie models with comparison to controls.

Cerebral lipids were extracted from between four and five mice per group. The above values are expressed as mean ± sem in μg lipid/g wet brain weight. Lipids were quantified with respect to calibration curves of authentic lipid standards as described in Experimental.

Levels of cholesteryl esters in ME7-affected VM mice are markedly elevated in the late-clinical stage of the disease. This change in cholesteryl esters is perhaps unsurprising when one considers that this murine-scrapie model exhibits highly significant neurological damage as indicated by depreciation in wet brain weight. Levels of other lipids remained essentially unchanged between control and scrapie animals.

facts. Firstly, the quantitative change in cholesteryl esters was very small, i.e. in the region of 190 μg lipid/g wet brain weight. In consideration of the relative insensitivity of the NMR technique, an abnormality of this magnitude would not be readily detected by *in vivo* proton NMR spectroscopy. Secondly, the chemical shift range over which methylene protons in cholesteryl esters resonate in a proton spectrum is considerably upfield (i.e. at a lower chemical shift) of that reported for the *in vivo* scrapie multicomponent signal. In conclusion, the above features did not support the case for a cholesteryl ester origin to the *in vivo* multicomponent MRS signal, indeed the latter observation argued strongly against the presence of lipid in the hypothesized 'mobile lipid' signal (Section 3. 2. 4).

Cholesteryl esters accumulate in a wide range of neurodegenerative disorders (Borri *et al.*, 1969; Maggio, *et al.*, 1972; Mezei, 1970; Norton *et al.*, 1966). In these, the central event culminating in the accumulation of neutral lipid involves damage to myelin. Myelin is a lipid-rich extension of the oligodendrocyte cell body arranged as a multilamella spiralling structure around an axon. As such, this structure functions to insulate the axon and facilitates saltatory conduction along the same (Landowne *et al.*, 1975). Demyelination typically takes one of two forms, either primary or secondary, depending on whether the pathological insult is to the myelin sheath or the neuronal cell body. Irrespective of the cause, the process of demyelination always presents the same features. The earliest recognizable histological change is swelling of the myelin sheath followed by the appearance of intracellular vacuoles. As the myelin sheath disintegrates, lipids are released in the extracellular space and are subsequently engulfed by phagocytic cells of the central nervous system - microglia and/or macrophages. Cholesterol released from the breakdown of myelin is converted into cholesteryl esters by combination with fatty acids released from phospholipids and stored as intracellular droplets (Ramsey, 1973). The accumulation of cholesteryl esters is likely to arise from an imbalance between the rate of lipid flux in myelin formation

| Cholesteryl ester fatty acid composition | Control | Scrapie |
|---|---|---|
| | | |
| $C_{14:0}$ | 2.7 | 5.9 |
| | | |
| $C_{16:0}$ | 25.8 | 29.4 |
| $C_{16:1}$ | 7.6 | 9.8 |
| | | |
| $C_{18:0}$ | 10.4 | 11.4 |
| $C_{18:1}$ | 27.1 | 31.3 |
| $C_{18:2}$ | 19.0 | 7.4 |
| | | |
| $C_{20:1}$ | 0.8 | 1.9 |
| $C_{20:4}$ | 3.6 | 1.6 |
| | | |
| $C_{22:6}$ | 3.0 | 1.3 |
| | | |

Table 3. 3. 2 A comparison of the fatty acid composition of cerebral cholesteryl esters from control and scrapie-affected (ME7/VM) mice.

Cholesteryl esters from pooled control and pooled scrapie tissue were purified over aminopropyl silica SEP PAK columns and analyzed by chemical ionization mass spectrometry (see Experimental). Values represent the percentage proportion that individual cholesteryl esters made to the total cerebral cholesteryl ester isolate.

Significant changes were observed between control and scrapie fractions in cholesteryl myristate, cholesteryl oleate, cholesteryl linoleate, cholesteryl arachidate, cholesteryl arachidonate and cholesteryl docosahexaenoate. Levels of cholesteryl palmitate, cholesteryl palmitoleate and cholesteryl stearate remained essentially unchanged.

and maintenance on the one hand, and degenerative changes resulting in demyelination on the other.

Animals affected with scrapie typically exhibit pathological changes consisting of neuronal vacuolation, loss of neurons and astrocytosis (Fraser, 1969). The histopathological features of brain lesions in the ME7/VM murine-scrapie model have been extensively documented (Fraser, 1969; Fraser & Dickinson, 1968). In this, lesions in the form of neuronal vacuolation are initially evident after an incubation period of approximately 21 weeks. The distribution and concentration of the lesions increases in grey matter regions, notably the thalamus (*masa intermedia* and central nuclei) and septal nucei of the paraterminal body until approximately 49 weeks when animals die. In view of the intimate association between axons and oligodendrocytes within the CNS, such neurodegenerative changes must be accompanied by some degree of Wallerian degeneration (secondary demyelination). The extent of the cholesteryl ester change (0.08% total lipids, control mice; 0.33% total lipids, scrapie mice) would suggest that demyelinating events are minimal. In support of this presumption, Fraser and Dickinson (1968) reported negligible vacuolation in white matter regions in this model. In addition, changes in levels of cholesterol, cerebrosides and phospholipids (the major components of myelin) are insignificant as determined by h.p.t.l.c. (Table 3. 3. 1).

Although the process of secondary demyelination provides the most logical explanation for the accumulation of cholesteryl esters, an alternative mechanism culminating in their production may exist. Evidence for this alternative hypothesis focuses on the fatty acid composition of cholesteryl esters in a number of aetiologically unrelated demyelinating disorders (Borri *et al.*, 1969; Gerstl *et al.*, 1966; Norton *et al.*, 1966; Suzuki *et al.*, 1969; Sweasey & Patterson, 1974). It would appear that regardless of the nature of the disease the fatty acid composition of the esters are remarkably similar (Eto & Suzuki, 1971; Ramsey, 1973), but levels of cholesteryl oleate are consistently elevated (Sweasey &

| Murine-scrapie model | Cholesteryl ester conc. | Wet brain weight | Areas with vacuolation score > 3.0 | Incubation period |
|---|---|---|---|---|
| | | | | |
| VM (control) | 60 ± 10 | 415 ± 36 | none | - |
| | | | | |
| ME7/VM | 250 ± 35 | 366 ± 1 | 4, 5, 7, 9 | 346 ± 3 |
| 87V/VM | 120 ± 20 | 378 ± 17 | (2.73 to 5) | 290 ± 4 |
| 301V/VM | 60 ± 30 | 406 ± 2 | (2.67 to 1) | 120 ± 7 |
| | | | | |
| | | | | |
| SV (control) | 40 ± 10 | 468 ± 4 | none | - |
| | | | | |
| ME7/SV | 50 ± 10 | 457 ± 10 | 7 | 178 ± 1 |
| 79A/SV | 140 ± 40 | 423 ± 28 | 1*, 3* | 153 ± 2 |
| 22A/SV | 40 ± 10 | 424 ± 2 | none | 441 ± 2 |
| | | | | |
| | | | | |
| C57BL (control) | 60 | 405 | none | - |
| 79A/C57BL | 340 | 291 | 3* | 161 ± 2 |
| 22L/C57BL | 60 | 367 | none | 170 ± 1 |
| | | | | |

Table 3. 3. 3 A comparison of cerebral cholesteryl ester concentrations in three murine-scrapie models and its relationship to neuropathological damage and disease incubation period.

Cholesteryl ester concentrations were determined in eight murine-scrapie models by HPTLC (see Experimental). Values are expressed as mean ± sem. Cholesteryl ester concentration is given as μg lipid/g wet brain weight. Wet brain weight is given in grammes. Incubation period is given in days.

The vacuolar degeneration scores are based on the Fraser and Dickinson (1968) system. The above grey matter areas are: 1, dorsal medulla; 4, hypothalamus; 5, medial thalamus; 7, septum; 9 medial cerebral cortex at the level of the septum. The above white matter areas are: 1* cerebellar white matter; 3* pyramidal tract.

Statistically significant changes in cholesteryl ester concentration were detected in the ME7/VM, 87V/VM, 79A/SV and 79A/C57BL murine-scrapie models with respect to their comparative controls.

Patterson, 1974). A comparison of the major cholesteryl esters present in cerebral tissue from a 90 day old piglet (control), VM mice (control), ME7/VM mice, and the demyelinating disorders: multiple sclerosis, chronic sclerozing panencephalitis, border disease, delayed swayback, congenital tremors types AII and AIV, sudanophilic leucodystrophy and Tay-Sachs disease clearly indicates that although concentrations of cholesteryl oleate are markedly elevated in the demyelinating diseases (Sweasey and Patterson, 1974), the same is not true in ME7-affected VM mice, despite the presence of a 300% elevation of cholesteryl esters. Indeed the percentage proportion of cholesteryl oleate appears similar in control VM mice, ME7/VM mice and the 90 day old piglet.

The previous discussion of demyelination and cholesteryl ester accumulation focuses on the role of microglia and/or macrophages as the 'lipid-scavenging' cells of the central nervous system. These cells operate in the presence of inflammatory mediators to phagocytose components of oligodendrocytes (Zajicek *et al.*, 1992). However, in the absence of an inflammatory response as seen during transmissible spongiform encephalopathy pathogenesis (Bolton & Bendheim, 1988), does the same mechanism operate? Growing evidence is accumulating that astrocytes assume the function of microglia in attempting to repair neuronal damage in the absence of inflammation (Diedrich *et al.*, 1991). As such these cells produce high levels of apolipoprotein E, presumably in an attempt to retain myelin breakdown products, i.e. lipids, at the site of injury (Mahley, 1988). Assuming that astrocytes also perform the function of microglia/macrophages in the phagocytosis and processing of cholesterol to cholesteryl esters, is it not possible that subtle changes in intracellular metabolic pathways may produce cholesteryl esters in different proportions to those normally produced by microglia/macrophages in Wallerian degeneration? In support of this hypothesis is the finding that in the scrapie fraction the proportion of cholesteryl oleate is unchanged and that of cholesteryl linoleate ($C_{18:2}$) is markedly reduced relative to control levels. Detectable changes were also present in the proportions of minor cholesteryl esters, notably: cholesteryl

myristate ($_{C14:0}$), cholesteryl arachidate ($C_{20:1}$), cholesteryl arachidonate ($C_{20:4}$) and cholesteryl docosahexaenoate ($C_{22:6}$) (Table 3. 3. 2). To our knowledge the investigation of intracellular lipid accumulations in astrocytes during scrapie pathogenesis has not been performed but presents an area for future research.

The relationship between the accumulation of cholesteryl esters and demyelination was investigated by measuring the activity of the myelin-specific enzyme neutral cholesteryl ester hydrolase (EC. 3.1.1.13) in ME7/VM mice at the terminal stage of the disease. This was performed in conjunction with the determination of lactate dehydrogenase activity for comparative purposes (Section 3. 4).

In addition to the above, the relationship between changes in cholesteryl ester concentrations and neuropathological damage was assessed by the comparison of cerebral cholesteryl esters in a total of eight murine-scrapie models (each at the terminal stage of disease). Changes, if present, were correlated with site-specific vacuolation scores, the degree of wet brain weight reduction, and the scrapie incubation period (Bruce *et al.*, 1991; Fraser and Dickinson, 1968) (Section 3. 3. 2).

## 3. 3. 2 Cholesteryl Ester Concentrations and Neurological Lesions in Eight Murine Models of Scrapie.

*Results.*

The ME7, 87V and 301V scrapie strains were propagated in VM (*Sinc* p7p7 genotype) mice to investigate the relationship between neurological damage, changes in lipid composition (as assessed *in vitro*) and the *in vivo* MRS multicomponent resonance described by Bell *et al.* (1991) during the progression of the disease. The ME7/VM model was sampled at 40, 180, 300 and 346 days post injection (p.i.), the 87V/VM model at 47, 85, 200 and 288 days p.i., and the 301V/VM model at 25, 50, 75 and 106 days p.i.

None of the above murine-scrapie models displayed significant changes in cholesterol, phospholipids or glycolipids at any time during the disease (data not shown). Changes were however detected in concentrations of cholesteryl esters in the ME7/VM and 87V/VM models; these abnormalities occurring in the ME7/VM model at 300 and 346 days p.i. and in the 87V/VM model at 288 days p.i. A comparison of the cerebral lipid composition in these three murine-scrapie models at their respective terminal stages of disease is shown in Table 3. 3. 1.

Five other murine-scrapie models, exhibiting different degrees of neurological damage, were examined for elevated concentrations of cerebral cholesteryl esters. The ME7, 79A, 22A and 22C scrapie strains in SV and C57BL mice were chosen for comparison, as these produce extremes of vacuolar damage in well defined neuroanatomical regions (Bruce *et al.*, 1991). The results of the analysis of cholesteryl ester levels in eight murine-scrapie models relative to wet brain weight, degree of neurological damage, and disease incubation period, are displayed in Table 3. 3. 3. Significant elevations were detected in cholesteryl ester concentrations in the ME7/VM, 87V/VM, 79A/SV and 79A/C57BL models in the late clinical stage of the disease, in contrast significant changes were not observed in the 301V/VM, ME7/SV, 22A/SV and 22C/C57BL models.

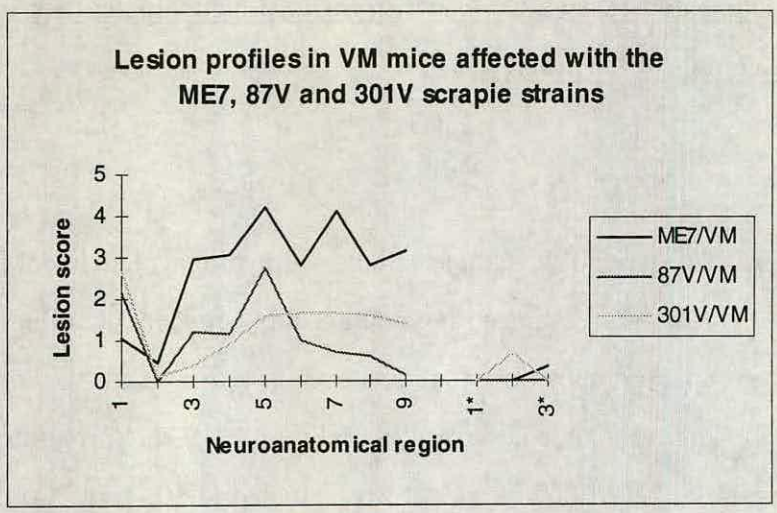


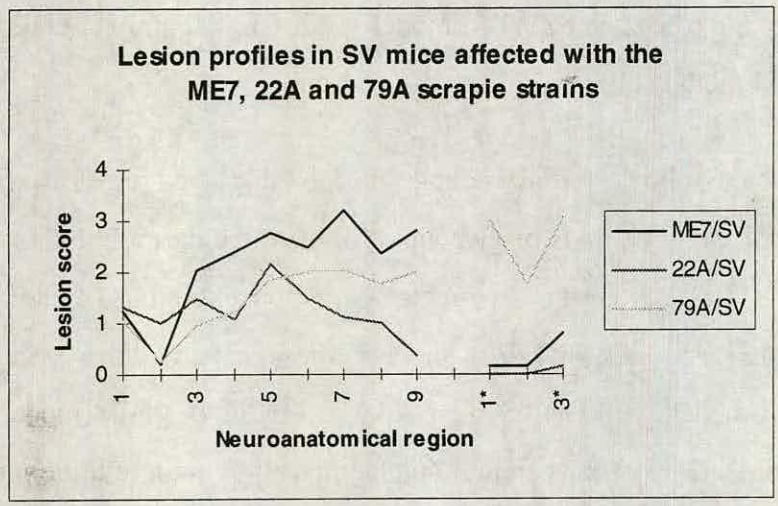


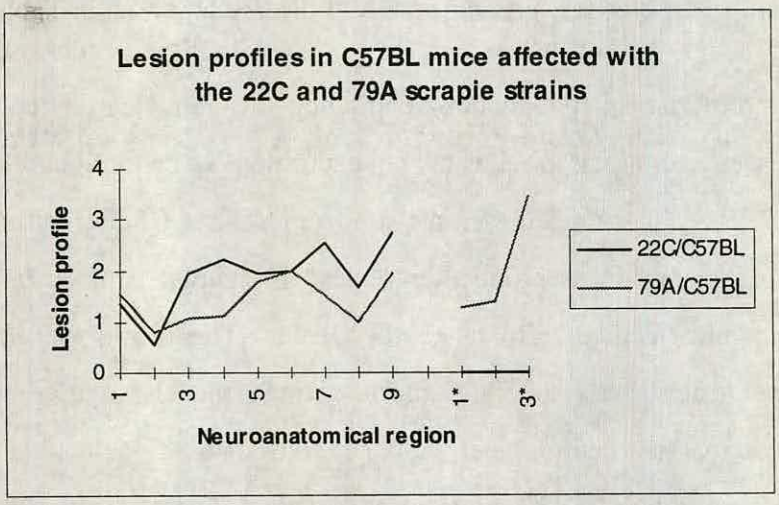


Figure 3. 3. 4 Lesion profiles in eight murine-scrapie models.

The vacuolar degeneration scores (lesion profiles) are based on the Fraser and Dickinson (1968) system. The grey matter areas are: 1, dorsal medulla; 2, cerebellar cortex; 3, superior colliculus; 4, hypothalamus; 5, medial thalamus; 6, hippocampus; 7, septum; 8, medial cerebral cortex at the level of the thalamus; 9, medial cerebral cortex at the level of the septum. The white matter areas are: 1*, cerebellar white matter; 2*, white matter of the mesencephalic tegmentum; 3*, pyramidal tract.

Figures reproduced with permission.

*Inferences.*

The absence of appreciable changes in prominent cerebral lipids in mice terminally-affected with scrapie is consistent with past results (Dees *et al.*, 1985; Guan *et al.*, 1996; Kimberlin and Millson, 1967). However, the detection of changes in cerebral cholesteryl esters, although reported in human patients with CJD (Ando *et al.*, 1984; Tamai *et al.*, 1978), has not been described in murine-scrapie models.

In the following discussion extensive reference is made to murine-scrapie model 'lesion scores' in specific brain regions (Bruce *et al.*, 1991; Fraser and Dickinson, 1968). In order to clarify the reader's understanding of the lesion score concept, a brief summary of the various scores is given in relation to the extent of vacuolar damage. A lesion score of: (1.0) - indicates "a few vacuoles, widely and unevenly scattered", (2.0) - indicates "a few vacuoles evenly scattered", (3.0) - indicates "moderate numbers of vacuoles, evenly scattered", (4.0) - indicates "many vacuoles with some confluence", and (5.0) - indicates "dense vacuolation with most of the field confluent" (Fraser and Dickinson, 1968).

The ME7/VM model, in which the initial cholesteryl ester elevation was identified, exhibits lesion scores > 3.0 in the hypothalamus, medial thalamus (4.21), septum (4.10) and medial cerebral cortex at the level of the septum, at the terminal stage of the disease (346 days p.i.) (Figure 3. 3. 4). As such, this degree of neurological damage is consistent with the proposed relationship between neurodegenerative changes and an elevation in cerebral cholesteryl esters. The same model sampled at 300 days p.i. also shows significant changes in cholesteryl esters (180 ± 60 µg/g wet brain weight). Although neurological damage at this time is not as extensive as later on in the disease, lesion scores of 2.10 and 2.40 are present in the hypothalamus and septum respectively. It is proposed that the prolonged progression of spongiform damage in the ME7/VM model (Fraser and Dickinson, 1968) contributes to the accumulation of cholesteryl esters in appreciable quantities, which in other models with a more rapid incubation

period, may not have sufficient time to occur. This concept is expanded below in the discussion relating to neurodegenerative damage in grey matter regions, secondary demyelination and elevated levels of cholesteryl esters.

The 87V scrapie strain in VM mice also displays a significant elevation in cerebral cholesteryl ester concentrations at the terminal stage of the disease (180 ± 20 µg/g wet brain weight; 288 days p.i). The finding that the ME7/VM and 87V/VM models show reductions in wet brain weight of the magnitude 12% and 9% respectively undoubtedly reflects the severe degenerative changes which occur in the brains of these animals. In view of these findings, it is perhaps unsurprising that cerebral cholesteryl esters are elevated.

The 301V/VM murine-scrapie model does not exhibit marked neuropathological changes; lesion scores are < 2.0 in all brain regions except the dorsal medulla (2.7). Significant changes are not detected in concentrations of cerebral cholesteryl esters, nor in *post mortem* wet brain weight. Thus, in this model at least, limited neurological damage coupled with the short incubation period (110 ± 2 days p.i.) does not favour an accumulation of cholesteryl esters.

Comparison of the above three murine-scrapie models reveals a clear relationship between the degree of neuronal vacuolation, the disease-related reduction in wet brain weight and the scrapie incubation period. In those murine-scrapie models in which the development of brain lesions occurs over a prolonged period of time, the accumulation of cerebral cholesteryl esters is more readily detected. In the classical experiments investigating secondary demyelination (Wallerian degeneration) as a result of nerve crush or section in the peripheral nervous system, elevated levels of cholesteryl esters reach statistical significance at about the eighth day post section (Johnson *et al.*, 1949). During the next 24 days as myelin degeneration releases increasing quantities of cholesterol, the cholesteryl ester concentration rises dramatically (Mezei, 1970). One can envisage that a similar process exists in the above murine-scrapie models, but with a few additional provisos. The histopathological studies of Fraser and Dickinson

(1968) report that the primary insult in these murine-scrapie models is to the neuronal cell body. In examples of unrelated diseases of the CNS (e.g. rabies) the interval between nerve cell necrosis, axonal degeneration and demyelination typically approaches 10 to 21 days (Watt, 1996). Thus in relation to the above murine-scrapie models, a period of approximately five to seven weeks may lapse between neuronal death and the detection of appreciably elevated levels of cholesteryl esters. In this respect, the relatively long incubation periods in the ME7/VM and 87V/VM murine-scrapie models coupled with the progression of vacuolar damage over approximately 45 to 50% of the incubation period (i.e. 25 weeks, ME7/VM; 21 weeks, 87V/VM) is believed to favour the accumulation of cholesteryl esters, making their detection possible.

Comparison of the ME7/VM and ME7/SV models illustrates the effect that the *Sinc* gene product has on both neuropathology and cholesteryl ester changes in mice which are otherwise genetically identical (Bruce *et al.*, 1991). In the former, cholesteryl ester levels reach 250 ± 35 μg/g wet brain weight at 346 ± 3 days p.i. and a 11.7% reduction in *post mortem* brain weight is recorded. In contrast, the ME7/SV model does not display significant changes in cholesteryl esters or *post mortem* brain weight, and does not exhibit as striking neuropathological features as the ME7/VM model (Figure 3. 3. 4), it also has a much shorter incubation period (178 ± 1 days).

Significant changes in cerebral cholesteryl esters are also found in SV and C57BL mice affected with the 79A scrapie strain. Both models display limited damage to grey matter regions with vacuolation scores barely reaching a value of 2.0 in two (SV) and three (C57BL) areas (Figure 3. 3. 4). In contrast, damage to white matter regions in both models is highly significant with lesions scores > 3.0 in the cerebellar white matter and pyramidal tract in the 79A/SV model, and a lesion score > 3.5 in the pyramidal tract in the 79A/C57BL model. Although a lesion score of > 3.5 is only found in the pyramidal tract of the 79A/C57BL model, neurological damage must be extensive as construed from the highly significant

reduction in wet brain weight at the terminal stage of the disease (C57BL, 405 g; 79A/C57BL, 291 g). This change is mirrored by a cholesteryl ester elevation in scrapie brain in excess of 500% of control levels (C57BL, 60 μg/g wet brain weight; 79A/C57BL, 340 μg/g wet brain weight). Thus, although these two models have fairly similar lesion profiles in grey matter regions, and for that matter similar incubation periods, they differ in the degree of vacuolar damage to white matter regions and in the severity of brain atrophy as determined by terminal wet brain weight. In this respect the changes in cerebral cholesteryl ester levels in these two models would appear entirely consistent with demyelinating events.

The 87V/VM and 22C/C57BL models display similar neuropathological features as illustrated by the lesion score studies (Bruce *et al.*, 1991). In the same, lesions scores < 3.0 are present in all grey matter regions and negligible vacuolation is present in white matter areas. In addition both models exhibit similar reductions in *post mortem* wet brain weight (87V/VM, 8.8%; 22C/C57BL, 9.3%), but in the former cholesteryl ester levels are significantly raised, whereas in the latter they are not. The explanation for this disparity between cholesteryl ester levels presumably lies in the difference between incubation periods in the two diseases (87V/VM, 290 ± 4 days p.i.; 22C/C57BL, 170 ± 1 days p.i.). It is proposed that in the latter model, changes in grey matter pathology occur at such a speed that insufficient time is available for cholesteryl ester levels to reach significant levels before death ensues. It is noted that in the 79A/SV and 79A/C57BL models, which display slightly shorter incubation periods than the 22C/C57BL model (153 ± 2 days p.i. and 161 ± 2 days p.i. respectively), the primary insult is to white matter, thus the interval between neuronal cell death and subsequent degeneration of myelin is not present and cholesteryl ester concentrations rise in close parallel with demyelinating events.

Vacuolar damage in the 22A/SV is largely restricted to grey matter regions with lesions scores below 2.0 in all areas except the medial thalamus (2.1). Changes in

cholesteryl ester concentrations are insignificant, although a 9.5% reduction in wet brain weight is recorded at the terminal stage of the disease (441 ± 2 days p.i). In view of the relatively limited vacuolar damage in this model, the absence of an elevation in cerebral cholesteryl esters is not unexpected. In addition the reduction in brain weight in these 441 day old mice may partly be attributed to normal aging processes (Greenfield, 1976).

*Summary.*

The above analysis suggests that the scrapie-related cerebral cholesteryl ester elevation is directly related to the degree of neurological damage, more specifically in white matter regions. In those murine-scrapie models in which significant damage is present in grey matter regions, e.g. ME7/VM and 87V/VM, and in which the disease incubation period is particularly prolonged, cholesteryl ester levels are similarly raised. The process culminating in the elevation of cholesteryl esters in the latter murine-scrapie models is believed to involve nerve cell necrosis, axonal degeneration, and subsequent secondary demyelination. In this respect, the importance of a lengthy incubation period to the accumulation of cholesteryl esters is evident. In those models in which the interval between neuronal degeneration and secondary demyelination exceeds the incubation period of the disease (22C/C57BL), cholesteryl ester levels are not significantly altered.

Although the presence of demyelination in the 79A/SV and 79A/C57BL murine-scrapie models is supported by histological studies (Bruce *et al.*, 1991), evidence for extensive axonal degeneration/demyelination is not found in the ME7/VM model (Fraser, 1969). Thus, in order to clarify the proposed relationship between neuronal damage and secondary demyelination in the latter model, the activity of myelin-specific neutral cholesteryl ester hydrolase was assayed in scrapie and control mice at the terminal stage of the disease. A discussion of the findings is given in Section 3. 4.

### 3. 4. 1 Neutral Cholesteryl Ester Hydrolase Studies in Mouse Brain.

Myelin was believed to be a relatively inert membrane as a result of its metabolic stability and apparent absence of enzymes. More recently this concept has received extensive revision with the discovery of a whole host of myelin-associated enzymes (Ledeen, 1984). It would appear that the myelin sheath undergoes a dynamic cycle of degradation and remodeling, in which many of the breakdown products are re-utilized for membrane biosynthesis. Although a number of enzymes have been found to be associated with myelin, only two of these are myelin-specific, namely neutral cholesteryl ester hydrolase (Eto and Suzuki, 1973; Johnson and Shah, 1978) and 2',3'-cyclic nucleotide 3'-phosphohydrolase (Kurihara and Tsukada, 1967).

The activity of cholesteryl ester hydrolase is closely associated with myelinating events. In diseases in which demyelination is a prominent feature, a strong negative correlation exists between the activity of this enzyme and the accumulation of cholesteryl esters (Ghosh and McLean Grogan, 1991; Johnson and Shah, 1978; Mezei, 1970; Shah and Johnson, 1980). Conversely, during the recovery or active myelination stage of experimental allergic encephalomyelitis (Grosh and McLean Grogan, 1991), or for that matter during active myelination in the foetal nervous system (Ghosh and McLean Grogan, 1990), the opposite is seen. It would therefore appear that any insult to the myelin sheath causes a significant reduction in cholesteryl ester hydrolase activity. In view of the intimate association between neutral cholesteryl ester hydrolase and myelin, the relationship between a cholesteryl ester elevation and demyelinating events was investigated in the ME7/VM murine-scrapie model.

*Results.*

In the first set of experiments using the procedure attributed to Eto and Suzuki (1973), cholesteryl ester hydrolase activity was not detected in either the crude brain homogenate or the 900 g supernatant in either scrapie or control brains

relative to the sucrose blanks (results not shown). Similar results were obtained using the experimental approach described by Shah and Johnson (1980). The former of these two procedures was repeated using authentic cholesteryl ester hydrolase, again no activity was recorded (results not shown).

The activity of authentic cholesteryl ester hydrolase was measured employing the method described by West and Shand (1991). This procedure differed from the above in containing a 50mM Tris-50mM MES buffer (pH 7.0) system, (i) with or (ii) without the addition of bovine serum albumin (1%, w/v). The activity of the hydrolase enzyme was investigated with taurocholate concentrations ranging from 0 to 10 mM. All assays were performed in duplicate. In the absence of BSA, $10^{-2}$ units of authentic cholesteryl ester hydrolase activity reached a maximum value of 0.37 nmol/minute (taurocholate 10 mM), whereas at the same taurocholate concentration and with BSA, $10^{-2}$ units of authentic cholesteryl ester hydrolase activity reached a value of 2.33 nmol/minute; a 530% increase in activity. As such this analysis illustrates the importance of bovine serum albumin in the incubation mixture.

The above procedure (West and Shand, 1991) was repeated with crude homogenate and 900 g supernatant from control VM brain. Taurocholate was included at 4 mM in agreement with the optimum concentration reported by Eto and Suzuki (1973). Neither the crude homogenate nor the 900 g supernatant showed appreciable cholesteryl ester hydrolase activity relative to sucrose blanks (results not shown).

The presence of a hydrolase inhibitor was investigated by the addition of crude brain homogenate to authentic cholesteryl ester hydrolase in the West and Shand assay system described above. The results of the analysis reveal that a factor(s) in crude mouse brain homogenate markedly inhibits authentic cholesteryl ester hydrolase. Prior heat treatment of the brain homogenate (95°C x 5 minutes) abolishes about 4% of the effect of the inhibitor. The inhibitor was not identified.

*Inferences.*

The initial two procedures (Eto and Suzuki, 1973; Shah and Johnson, 1980) gave poor activity in both crude brain homogenate and the 900 g supernatant. The reason for this was not clear, although West and Shand also had difficulty obtaining satisfactory results with the same assay systems (personal communication). Following the adoption of the latter author's procedure (West and Shand, 1990), satisfactory activity was achieved with authentic cholesteryl ester hydrolase, albeit at less than optimum levels. It was noted that the inclusion of bovine serum albumin at a concentration of 1% (w/v) markedly assisted the dispersion of cholesteryl oleate in the taurocholate detergent. This may partly explain the improved activity of cholesteryl ester hydrolase in the latter incubation mixtures as a result of improved enzyme-substrate presentation.

Although the greatest enzyme activity was achieved with 10 μmol of taurocholate in these studies, Eto and Suzuki found optimum enzyme activity in crude brain homogenate with 4 mM of detergent (Eto and Suzuki, 1973). The latter taurocholate concentration was therefore adopted in our studies using brain homogenate as the crude enzyme source.

When crude brain homogenate and 900 g supernatant were assessed for cholesteryl ester hydrolase activity in the above assay system, none was detected. It was therefore proposed that an inhibitor of cholesteryl ester hydrolase was present in brain homogenate. Indeed evidence in support of this hypothesis was found when authentic cholesteryl ester hydrolase incubation mixtures were 'spiked' with a small quantity of brain homogenate. Pretreatment of the brain homogenate by heating at 95°C for five minutes had little effect on the activity of the mouse brain cholesteryl ester hydrolase inhibitor. This is markedly different to a heat-labile rat liver cytosolic cholesteryl ester hydrolase inhibitor described previously (Shand and West, 1992). Inhibition was not believed to be an artefact due to dilution of the radiolabelled cholesteryl oleate with endogenous brain cholesteryl esters (the latter constituting approximately 0.16% of total cholesteryl

esters present in the reaction mixture). However it is possible that the presence of cellular debris had a detrimental effect on the presentation of cholesteryl oleate to the hydrolase enzyme. Fractionation and characterization of the mouse brain cholesteryl ester hydrolase inhibitor was not attempted.

Although an elevation in cholesteryl esters may be explained by myelin destruction, it may equally be the result of diminished cholesteryl ester hydrolase activity without an associated change in cholesteryl ester hydrolase concentration. In this respect the presence of a cholesteryl ester hydrolase inhibitor in mouse brain was viewed with some interest. Studies were subsequently performed in collaboration with Dr. David West and Mr. John Shand (Hannah Research Institute, Ayr, Scotland) to investigate whether clinically-ill scrapie brain (ME7/VM) contained more inhibitor than age- and sex-matched controls. A total of five scrapie and five control brains were examined, however no difference was detected in inhibitor concentrations between the two groups (Dr. David West, personal communication).

Unfortunately growing restrictions on the availability of research time at this stage of the study necessitated further studies of cholesteryl ester hydrolase to be discontinued. Thus, although the preceding experiments served as a limited exercise in experimental enzymology, the purpose for which they were performed was not realized. As such a relationship between the cholesteryl ester elevation and secondary demyelination in the ME7/VM murine-scrapie model was not confirmed - nor was it disproven.

## 3. 4. 2 Lactate Dehydrogenase Studies in the ME7/VM Murine-Scrapie Model.

*Results.*

The activity of lactate dehydrogenase was assessed in parallel with studies of neutral cholesteryl ester hydrolase for comparative purposes. A 900 g supernatant was used in order to exclude the major proportion of cellular debris, and had a protein concentration of approximately 6 mg/ml. This was diluted by a factor of 250-fold to give aliquots from which enzymatic activity was assessed, with protein concentrations of approximately 24 μg/ml. A calibration curve of lactate dehydrogenase activity was produced with various quantities of pyruvate substrate (Sigma Procedure 500) and the absorbance measured at 450 nm. The coefficient of linear regression for this calibration curve was -0.997, allowing the formulation of the calibration equation:

absorbance = $0.905 - (5.0 \times 10^{-3})$.activity (BB units)

from which lactate dehydrogenase activity in brain homogenate was calculated.

*Inferences.*

Studies of lactate dehydrogenase in brain and spinal cord regions from a human CJD-affected patient revealed reduced activity in diseased material (Friede and DeJong, 1964; Robinson, 1969). This biochemical change was confined to neurons and preceded neuronal degeneration (Friede and DeJong, 1964). In our studies the activity of lactate dehydrogenase was assessed in ME7-affected VM mice at the late clinical stage of the disease, when neuronal loss is most extensive (Fraser, J. *et al.*, 1995). Although the aforementioned experiments imply a pathological failure of oxidative enzyme supply to neurons in CJD, we questioned whether the same mechanism is present in scrapie-affected mouse brain.

The activity of lactate dehydrogenase in heat-treated (95°C x 10 minutes) brain supernatant was found to be negligible. Scrapie brain homogenate had a lactate dehydrogenase specific activity of 1.12 ± 0.08 μmol pyruvate hydrogenated/minute /mg protein, and control homogenate 1.03 ± 0.09 μmol pyruvate hydrogenated /minute/mg protein at 25°C. Student's t-test provided evidence for no statistical difference between the two groups. Thus, although brain atrophy as determined by reduction in wet brain weight is highly significant in scrapie-affected mice at the terminal stage of the disease, significant changes in lactate dehydrogenase are absent relative to total protein concentrations.

Interestingly this conclusion is supported by *in vitro* measurements of cerebral lactate concentration by $^{1}H$ magnetic resonance spectroscopy (Section 3. 1. 2). In these, lactate/creatine levels were 290.3 ± 61.8 intensity units in scrapie animals and 236.9 ± 31.0 intensity units in controls (Table 3. 1. 2). The means of these values were not statistically different. As such, the two sets of results illustrate the complementary and diagnostic application of MRS to biomedical studies.

## 3. 5 Studies of Lipids Associated with GPI-anchored Proteins in Control and Scrapie Isolates.

Over the past decade overwhelming evidence has accumulated for the central role of PrP in the pathogenesis of spongiform encephalopathies (reviews see Bendheim *et al.*, 1991; Hope and Baybutt, 1991; Prusiner, 1991). Susceptibility to this class of diseases appears critically dependent on the formation of a protease-resistant form of the normal cellular protein, $PrP^{sc}$ (Büeler *et al.*, 1993), which is derived from $PrP^{c}$ by an unknown post-translational process. Whilst this change confers distinct biochemical and biophysical properties to $PrP^{sc}$ (Meyer *et al.*, 1986; Prusiner *et al.*, 1983), it does not appear to involve chemical modifications to $PrP^{c}$ structure (Stahl *et al.*, 1993).

The normal cellular isoform is anchored to the extracellular surface of neurons and lymphocytes at its carboxyl-terminus by a glycosylphosphatidyl inositol (GPI) moiety (Cashman *et al.*, 1990; Stahl *et al.*, 1987). This intimate association between PrP and the lipid membrane is believed to be responsible for the highly hydrophobic nature of the protein (Safar *et al.*, 1990). Interestingly $PrP^{c}$ and $PrP^{sc}$ differ in their susceptibility to GPI anchor cleavage by phosphatidylinositol-specific phospholipase C (PIPLC), $PrP^{sc}$ being resistant to release (Caughey *et al.*, 1990; Stahl *et al.*, 1990). Safar and colleagues speculated that this abnormal property of the scrapie isoform may be the result of a structural change in the GPI anchor (Safar *et al.*, 1991), however this hypothesis was subsequently invalidated by mass spectrometry studies (Stahl *et al.*, 1992). An alternative hypothesis proposed a conformational difference between membrane/phospholipid-bound $PrP^{c}$ and $PrP^{sc}$ molecules (Safar *et al.*, 1991). Whilst support for significant changes in the tertiary structure of $PrP^{c}$ and $PrP^{sc}$ have been found (Pan *et al.*, 1993; Safar *et al.*, 1993), studies of membrane lipids associated with the two PrP isoforms have not received attention.

The studies described here were therefore undertaken to investigate the composition of membrane lipids associated with GPI-anchored proteins in murine

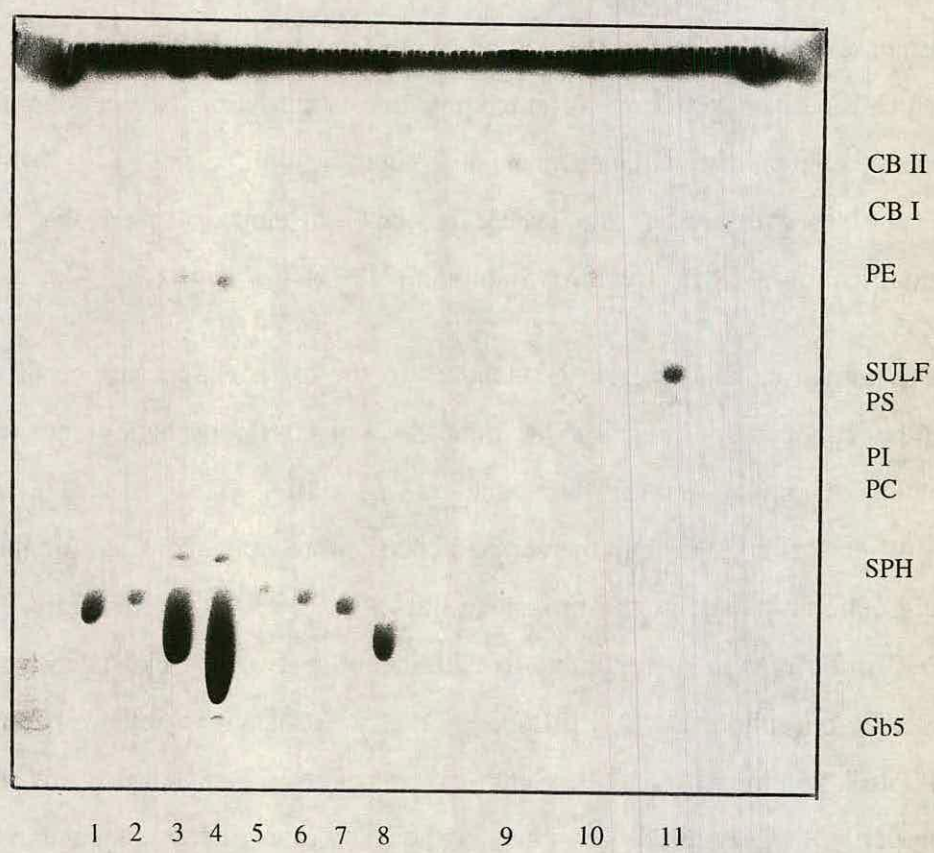


Figure 3. 5. 1 HPTLC analysis of lipids associated with cerebral GPI-anchored proteins.

Cerebral lipid fractions were analyzed as described in Experimental. Lanes 1, 2, 5 - 8 cerebral float fractions which did not contain protein as determined by SDS-PAGE and silver staining. Lanes 3 and 4 contained GPI-anchored proteins as determined by SDS-PAGE and silver staining. Lanes 9 - 11, authentic lipid standards. Gb5, Forssman antigen. Other lipid abbreviations are as previously listed. Note the presence of lipid asociated with the GPI-anchored protein fraction.

brains and provide a comparison of the same in control and scrapie-affected animals.

***Results.***

*Detection of lipids associated with GPI-anchored proteins.*

Isolation of GPI-anchored proteins was performed at the B.B.S.R.C. & M.R.C. Neuropathogenesis Unit following the procedure described by Safar *et al.*, 1990, but omitting phosphatidyl inositol-specific phospholipase C (PIPLC) digestion. GPI-anchored proteins were separated by sucrose gradient centrifugation and subsequently fractionated to give six 'float fractions'. These fractions were individually analyzed by sodium dodecyl sulphate-polyacrylamide gel electrophoresis (SDS-PAGE) and silver staining for the study of protein components and by high performance thin layer chromatography for the study of lipids.

Our investigations revealed that two of these fractions contained appreciable quantities of lipid (see lanes 3 and 4, Figure 3. 5. 1). Sphingomyelin, phosphatidyl choline, phosphatidyl ethanolamine and cerebroside I (α-hydroxy fatty acid) were identified in both fractions by co-migration with authentic standards. The presence of an extremely polar lipid band near the origin was speculated to arise from Forssman antigen (Gb5) on the basis of similarities between its elution coefficient and previous results (Brown and Rose, 1992). In addition to the above polar lipids, a prominent band was observed at the solvent front corresponding to non-polar lipid constituents; these were identified in subsequent studies. The absence of acidic lipids in these fractions was noted in marked contrast to the aforementioned neutral lipid components.

SDS-polyacrylamide gel electrophoresis and silver staining of the above fractions was performed by colleagues at the B.B.S.R.C. & M.R.C. Neuropathogenesis Unit. Protein constituents were detected in fractions 3 and 4, whilst negligible

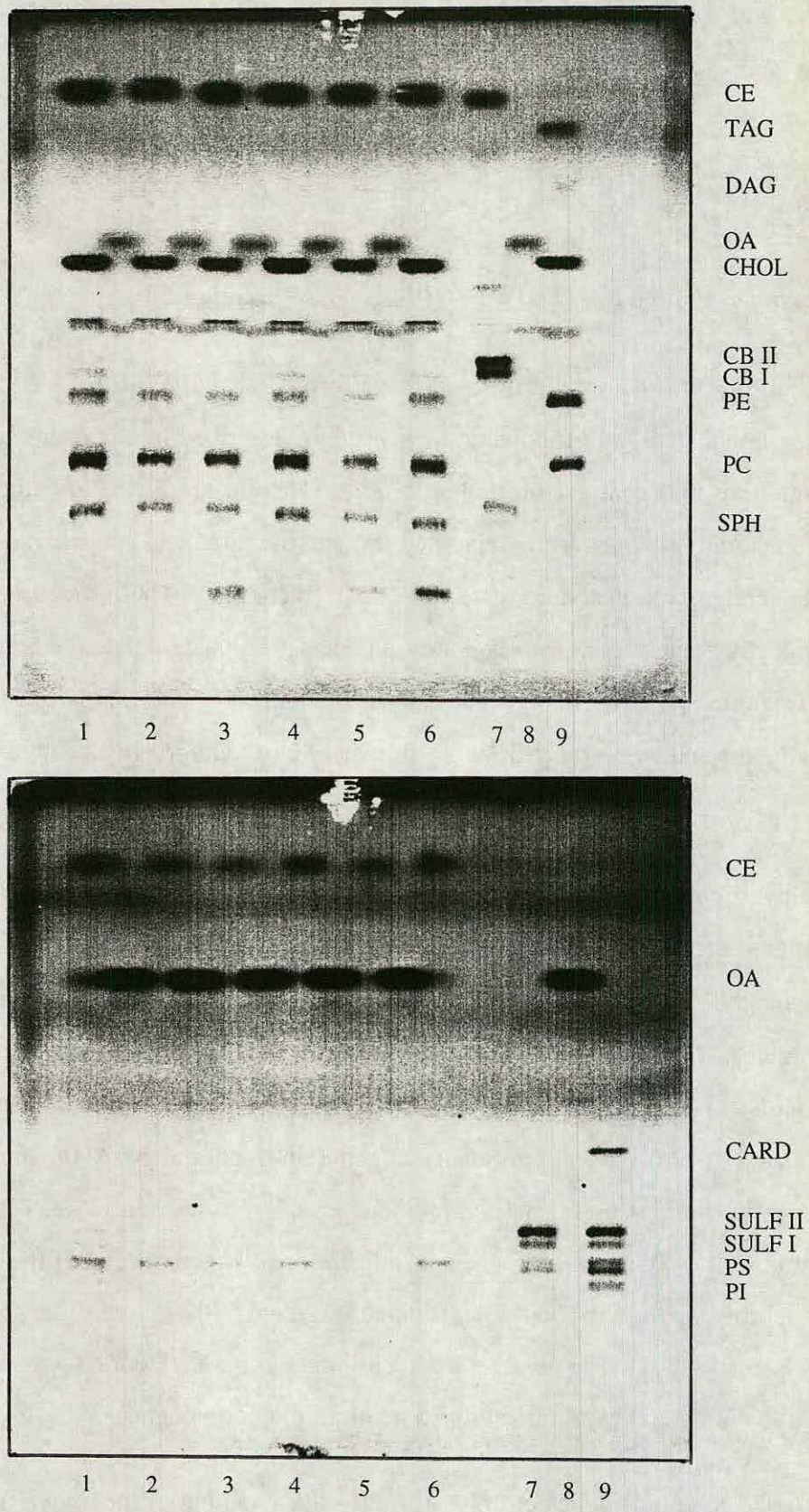


Figure 3. 5. 2 HPTLC analysis of neutral and acidic lipids (top and bottom figures respectively) associated with cerebral GPI-anchored proteins in $PrP^{+/+}$, $PrP^{+/0}$ and $PrP^{0/0}$ mice.

Cerebral lipid fractions were analyzed as described in Experimental. Lanes 1 and 2, $PrP^{+/+}$; lanes 3 and 4, $PrP^{+/0}$; and lanes 5 and 6 $PrP^{0/0}$, GPI-anchored protein float fractions. Lanes 7 - 9, authentic lipid standards. Lipid abbreviations are as previously listed.

amounts were detected in the other fractions (results not shown; Dr. James Hope, personal communication). The two protein-containing fractions exhibited banding at 33-35 kDa as well as at both higher and lower molecular weights. The 33-35 kDa protein band immunostained with the rabbit anti-mouse PrP antibody IB4, demonstrating the presence of $PrP^c$ in this otherwise heterogeneous GPI-anchored protein fraction.

*A comparison of lipids associated with GPI-anchored proteins from PrP-homozygote, -heterozygote and -null mice.*

Having demonstrated the presence of lipids associated with a diverse population of GPI-anchored proteins, it was questioned whether more specific information could be gathered on those lipids exclusively associated with PrP. For this purpose GPI-anchored proteins were isolated from selected genotypes of transgenic mice in which the PrP gene had been genetically ablated.

Analysis of the neutral lipid fractions provided information on the composition of non-polar lipids associated with GPI-anchored proteins in addition to the polar lipid profiles obtained above. The neutral fractions contained appreciable quantities of cholesterol, cholesteryl esters, sphingomyelin, phosphatidyl choline, phosphatidyl ethanolamine and cerebroside I (Figure 3. 5. 2). The acidic lipid fractions contained phosphatidyl inositol, phosphatidyl serine, sulfatides I and II, free fatty acids and minor quantities of cardiolipin (Figure 3. 5. 2). An additional band was observed on the acidic fraction h.p.t.l.c. plate near the solvent front which we speculated to arise from cholesteryl esters which for unknown reasons failed to elute in the neutral fraction. This may have been the result of overloading the ion exchange chromatography material with excess cholesteryl esters in the crude lipid extract or signify the detection of an as yet unidentified cerebral lipid species. In view of the high concentration of cholesteryl esters present in the neutral lipid fractions the first hypothesis was favoured.

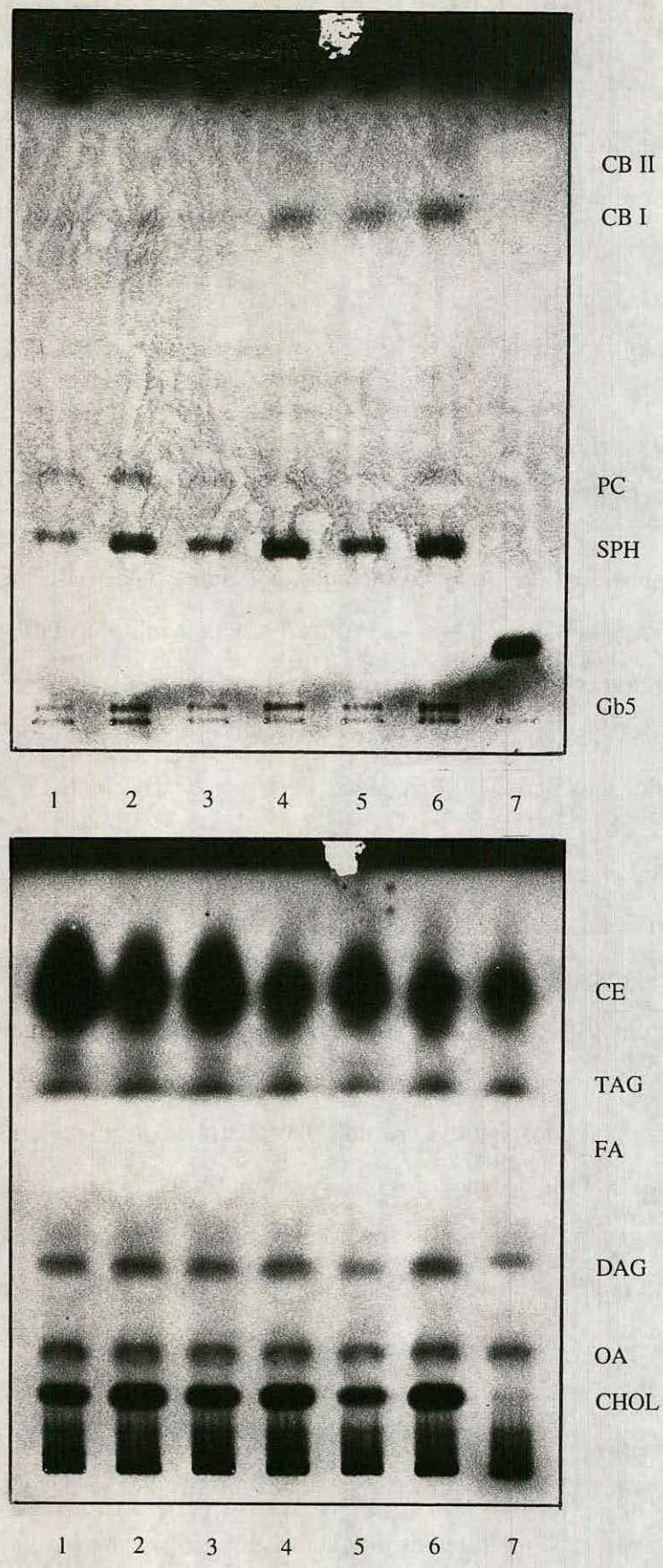


Figure 3. 5. 3 HPTLC analysis of polar and non-polar lipids (top and bottom figures respectively) associated with cerebral GPI-anchored proteins in control and scrapie-affected mice.

Cerebral lipid fractions were analyzed as described in Experimental. Lanes 1 - 3, $PrP^{c}$; lanes 4 - 6, $PrP^{sc}$, GPI-anchored protein float fractions; lane 7, SAF. Lipid abbreviations are as previously listed. Note in the top plate the presence of elevated levels of cerebroside I in scrapie isolates. Also note the reduction in cholesteryl ester levels in scrapie isolates in the bottom plate. Interestingly the SAF sample displayed a similar non-polar lipid profile to the $PrP^{sc}$ isolates but contained negligible cholesterol.

Comparison of neutral and acidic lipids associated with GPI-anchored protein from PrP-homozygote ($^{+/+}$), -heterozygote ($^{+/0}$) and -null ($^{0/0}$) mice revealed insignificant differences between the three groups. The results of the quantitative analysis are displayed in Table 3. 5. 1. Interestingly the concentration of cholesteryl esters is highly enriched in the above GPI-anchored protein fractions comprising in the order of 12% of total neutral lipids and representing an approximate 250-fold increase in the cholesteryl ester/cholesterol ratio relative to similar determinations in crude brain lipids. The significance of this finding and the apparent absence of differences between the three PrP genotypes is discussed below.

*A comparison of lipids associated with GPI-anchored proteins in scrapie and control isolates and a scrapie-associated fibril fraction.*

Although the detection of discrete lipid changes associated with PrP was not realized, the potential to examine the composition of total lipids located within caveolae microdomains in both control and scrapie-disease states was recognized as a feasible objective. For this purpose, lipid studies were performed on GPI-anchored protein fractions from scrapie-affected and control mice as well as an isolate of scrapie-associated fibrils.

The non-polar lipid profiles in the three fractions were essentially very similar with some noteworthy exceptions. All fractions contained cholesteryl esters, triglyceride, diglyceride and fatty alcohol, however whilst cholesterol was present in appreciable quantities in the two 'float fractions' it was almost completely absent in the SAF isolate (Figure 3. 5. 3). In agreement with the results above, cholesteryl esters were present in markedly elevated concentrations in all fractions, representing a highly significant enrichment in this non-polar, neutral lipid relative to cerebral levels of cholesterol. In addition, a statistically significant difference in cholesteryl esters was present between scrapie and control float fractions (cholesteryl esters (μg) per float fraction: 30 ± 7, control; 14 ± 2, scrapie; $P < 0.001$), with a similar reduction in cholesteryl esters being

| Lipid | $PrP^{+/+}$ GPI-anchored protein fraction | $PrP^{+/0}$ GPI-anchored protein fraction | $PrP^{0/0}$ GPI-anchored protein fraction |
|---|---|---|---|
| | | | |
| Cholesteryl esters | 41.4 ± 0.1 | 41.5 ± 1.5 | 40 ± 0 |
| Cholesterol | 82.8 ± 11.0 | 80.8 ± 11.3 | 62 ± 10.4 |
| Cerebroside I | 4.6 ± 0.4 | 4.1 | 3.4 ± 0.7 |
| Phosphatidyl ethanolamine | 44.3 ± 9.0 | 31.0 ± 2.4 | 28.4 ± 11.2 |
| Phosphatidyl choline | 156.7 ± 43.7 | 131.5 ± 21.3 | 103.7 ± 31.9 |
| Sphingomyelin | 40.8 ± 14.5 | 39.8 ± 17.4 | 31.5 ± 9.4 |
| | | | |
| Cardiolipin | 8.9 ± 2.9 | 3.3 ± 0.3 | 2.7 ± 1.2 |
| Sulfatide I | 4.9 ± 1.7 | 2.8 ± 0.7 | 2.9 ± 1.0 |
| Sulfatide II | 4.4 ± 1.8 | 2.4 ± 0.2 | 2.1 ± 0.4 |
| Phosphatidyl serine | 17.7 ± 4.2 | 10.4 ± 0.6 | 5.8 ± 3.4 |
| Phosphatidyl inositol | 6.3 ± 1.9 | 3.2 ± 0.2 | 1.9 ± 0.7 |
| | | | |
| Lipid | $PrP^{c}$ GPI-anchored protein fraction | $PrP^{sc}$ GPI-anchored protein fraction | SAF |
| | | | |
| Cholesteryl esters | 30 ± 7 | 14 ± 2 | 12 |
| Triglyceride | 9 ± 1 | 9 ± 1 | 7 |
| Diglyceride | 46 ± 6 | 46 ± 17 | 43 |
| Fatty alcohol | 3 ± 1 | 3 ± 1 | 3 |
| Cholesterol | 8 ± 3 | 10± 4 | nd |
| | | | |

Table 3. 5. 1 Lipids associated with GPI-anchored protein fractions from control and scrapie affected mice.

Values are expressed as mean ± sem in µg lipid/½ brain equivalent. Each value in the $PrP^{+/+}$ to $PrP^{0/0}$ series represents the mean of two samples per group. The values in the $PrP^{c}$ and $PrP^{sc}$ series represent the mean of three samples per group.

observed in the SAF isolate. The results of the quantitative analysis are displayed in Table 3. 5. 1.

Analysis of the polar lipid components revealed the presence of sphingomyelin, phosphatidyl choline and cerebroside I in addition to what was speculated to be Forssman antigen (Gb5) (with an elution coefficient ($R_f$) value of 0.025). There was an almost complete absence of polar lipids in the SAF sample apart from a translucent band which migrated with an $R_f$ value of 0.84 and a charred band with an $R_f$ value of 0.10. Neither of these were identified but were speculated to be SAF isolation procedure artefacts on the basis that no authentic cerebral lipids migrate at these positions. A highly significant difference was observed in levels of cerebroside I between scrapie and control GPI-anchored protein fractions, with the former containing appreciable quantities whilst the latter did not (Figure 3. 5. 3). Unfortunately lipid quantification was not performed on this h.p.t.l.c. plate and thus absolute values for this lipid changes are not available.

The absence of phosphatidyl ethanolamine in both scrapie and control samples and the almost complete absence of cerebroside I in the control sample is markedly different to the lipid profiles obtained in the studies described above. The reason for this difference is not believed to be simply the result of lipid fraction dilution (compare Figures 3. 5. 1 and 3. 5. 3), and must therefore represent subtle changes in the composition of the GPI-anchored protein isolates obtained from the B.B.S.R.C. & M.R.C. Neuropathogenesis Unit. It was noted that the total amount of lipid supplied in the above samples was significantly less than that provided in the initial studies (Tables 3. 5. 1). Whether this reflects a slight modification of the GPI-anchored protein isolation procedure in the latter studies is not known.

Regardless of questions raised concerning discrepancies between the above isolation protocols, the latter isolates, which were chronologically prepared under identical conditions, clearly demonstrate highly significant changes in the concentrations of two lipids closely associated with GPI-anchored proteins in

scrapie and control material, namely cholesteryl esters and cerebroside I. In view of the intimate relationship between lipid composition and the structural and functional properties of caveolae microdomains, it may be inferred that the above lipid abnormalities would produce a detrimental effect on caveolae function. The speculated significance of the above lipid disturbances in relation to cellular PrP metabolism is discussed below.

*Discussion.*

The central event underlying transmissible spongiform encephalopathy pathogenesis is believed to be the conversion of the cell surface protein PrP to a protease-resistant isoform (Caughey and Raymond, 1991; Czub *et al.* 1988; Prusiner, 1991). The mechanism by which this transformation process produces two distinct isoforms differing in physiochemical properties (Meyer *et al.*, 1986; Prusiner *et al.*, 1983) and tertiary structure (Pan *et al.*, 1993; Safar *et al.*, 1993) has not been elucidated. However within the last year cholesterol-rich membraneous microdomains have been implicated as key structures in which this transformational process occurs (Taraboulos *et al.*, 1995). As such, Taraboulos and colleagues showed that cholesterol-depletion of scrapie-affected neuroblastoma cell cultures slowed the degradation of $PrP^{c}$ and inhibited the formation of $PrP^{sc}$. Cholesterol depletion of Madin-Darby canine kidney (MDCK) cell lines is known to have a detrimental effect on the number and structural integrity of caveolae (Anderson *et al.*, 1992). Thus it is inferred that PrP by nature of its GPI moiety is directed to these membraneous microdomains, in both normal and scrapie-affected cells, where its metabolism is dependent on the structural and functional integrity of the same.

Our results demonstrate that PrP co-purifies with a diverse population of GPI-anchored proteins in a sucrose gradient float fraction. The finding that these proteins partition at an unusually low density in the sucrose gradient was taken as evidence in support of their intimate association with membrane lipids. The lipids associated with these GPI-anchored proteins were determined by high

performance thin layer chromatography. Similarities in lipid composition were observed in cholesterol, phosphatidyl ethanolamine, sphingomyelin and Forssman antigen (Gb5) between cerebral caveolae and MDCK cell lines described previously (Rose and Brown, 1992). However the report of high concentrations of cholesteryl esters in the former is unprecedented, raising intriguing questions as to the significance of this lipid in cerebral caveolae. It is possible that cholesteryl esters perform a role in the maintenance of caveolae structure and function akin to that attributed to cholesterol. Levels of cholesteryl esters associated with these GPI-anchored proteins amount to approximately 75% of all cerebral cholesteryl esters. Mechanisms must exist to regulate and maintain the high concentrations of cholesterol and cholesteryl esters present in caveolae. In this regard it is tempting to speculate that caveolae microdomains contain GPI-anchored proteins which perform functions of receptor-mediated cholesterol endocytosis and cholesterol esterification (Section 4, Future Directions).

A comparison of lipids associated with GPI-anchored proteins in the three transgenic PrP genotypes $PrP^{+/+}$, $PrP^{+/0}$ and $PrP^{0/0}$ indicates that partial or complete absence of PrP does not have a significant effect on caveolae lipid composition. It is not possible to infer whether the absence of PrP has a detrimental effect on the function of these lipid microdomains, however the apparent absence of adverse conditions in PrP-null mice would suggest otherwise (Büeler *et al.*, 1992). The known association between caveolae and folate potocytosis (Anderson *et al.*, 1992; Chang *et al.*, 1992; Rothberg *et al.*, 1990) presents an opportunity for investigating the functional integrity of caveolae during scrapie pathogenesis, thus providing clarification in this area (Section 4, Future Directions).

Studies by Safar and colleagues have shown $PrP^{c}$, $PrP^{sc}$ and infectivity to be associated with the most hydrophobic components of synaptosomal and microsomal membranes (Safar *et al.*, 1990). This is perhaps unsurprising when one considers that $PrP^{c}$ is directed to caveolae microdomains in which

concentrations of cholesteryl esters are markedly elevated. Cholesteryl esters are the most non-polar lipid present in murine cerebral lipid extracts and may therefore make an important contribution to the hydrophobicity of the two PrP isoforms. Safar and colleagues speculated that conformation differences between membrane/phospholipid-bound $PrP^{c}$ and $PrP^{sc}$ molecules may contribute towards the resistance of $PrP^{sc}$ to phosphatidyl inositol-specific phospholipase C (PIPLC) cleavage (Safar *et al.*, 1991). In this respect we report significant changes in the lipid composition of GPI-anchored proteins in scrapie-affected mice. It is interesting to speculate that reduced concentrations of cholesteryl esters and increased levels of cerebroside I may produce localized changes in caveolae microenvironment sufficient to cause inhibition of PIPLC activity. Interestingly the inability of PIPLC to induce GPI-anchor cleavage applies to both $PrP^{c}$ and $PrP^{sc}$ in scrapie-affected hamster synaptosomal/microsomal membranes (Safar *et al.*, 1991). This would suggest that disrupted caveolae structure and/or function rather that a conformational change in PrP protein structure is responsible for resistance to PIPLC cleavage.

The cellular concentration of $PrP^{c}$ appears to be critically important to the rate at which scrapie disease progresses. This has been elegantly demonstrated in $PrP^{+/0}$ heterozygote mice, which although susceptible to scrapie, accumulate $PrP^{sc}$ and develop disease after a much longer incubation period than their wild-type counterparts (Büeler *et al.*, 1993). Transgenic studies suggest that the production of $PrP^{sc}$ involves the formation of an intermediate complex in which $PrP^{sc}$ and $PrP^{c}$ interact (Prusiner *et al.*, 1990; Scott *et al.*, 1993). This association must involve intimate contact between the two isoforms. In view that caveolae concentrate GPI-anchored proteins (Rothberg *et al.*, 1990), it seems highly probable that these plasmalemmal structures provide a microenvironment in which interaction between the two PrP isoforms is favoured and the post-translational modification of $PrP^{c}$ to $PrP^{sc}$ takes place. It follows that a reduction in cellular PrP concentration by genetic ablation of a PrP gene would reduce the frequency with which PrP molecules interact, thus slowing down the formation of

$PrP^{sc}$ and delaying the onset of clinical disease. A similar situation would presumably exist in cholesterol-depleted cells in which the ability of caveolae to concentrate GPI-anchored proteins is adversely compromised as a result of disruption to caveolae number, structure and function (Anderson *et al.*, 1992).

Amphotericin B, a polyene antibiotic used in the treatment of fungal diseases, has been shown to delay the onset of clinical signs in golden Syrian hamsters experimentally infected with the 263K strain of scrapie (Pocchiari *et al.*, 1987). In this model, amphotericin B treatment slows both the scrapie agent replication rate (Pocchiari *et al.*, 1989) and the formation of $PrP^{sc}$ (McKenzie *et al.*, 1994). Amphotericin B has a high affinity for membrane sterols causing lethal permeability changes in susceptible cells by the formation of transmembrane ion channels (Bolard, 1986). In view of the adverse effect that cholesterol depletion has on $PrP^{sc}$ formation (Taraboulos *et al.*, 1995), we propose that amphotericin B has its anti-scrapie effect by causing a disruption in the structural and functional integrity of caveolae. In consideration of the discussion above, such action would be expected to reduce PrP oligomeric interactions and inhibit the mechanism by which $PrP^{sc}$ is formed (Hope *et al.*, 1988). Interestingly, initiating amphotericin B treatment two weeks prior to scrapie inoculation prolongs the incubation period of the disease by a much greater extent than administration of the therapeutic agent one week after infection (Pocchiari *et al.*, 1989). This observation has been suggested to be attributable to modification of a hypothetical receptor molecule (Pocchiari *et al.*, 1989), however in view of the above discussion, we believe that this phenomenon can be explained by cell membrane dissolution of caveolae and reduced availability of $PrP^{c}$ for prion transformation. The PrP conformational change produces protein-lipid complexes of greater stability as demonstrated by the inability of PIPLC to cleave $PrP^{sc}$ from the lipid bilayer (Safar *et al.*, 1991), it is therefore proposed that the reduced effect of amphotericin B one week after infection is the result of greater stability or tighter binding of lipids to PrP molecules within caveolae microdomains. In this respect the observed changes in

caveolae cholesteryl esters and cerebroside I may have functional significance to the physiochemical properties of caveolae in the prion biotransformation process.

This section would not be complete without some consideration of the fact that amphotericin B does not have any therapeutic value in the alleviation of 139A or 139H scrapie in hamsters, 263K scrapie in mice (Xi *et al.*, 1992), hamster-adapted DY transmissible mink encephalopathy (Bessen and Marsh, 1992), or clinical cases of human Creutzfeldt-Jacob disease (Masullo *et al.*, 1992). Assuming that the therapeutic effect of amphotericin B is directly related to its disruptive effect on caveolae structure and function, the inability to ameliorate TSE pathogenesis in the above models may be the result of subtle changes in caveolae structure, reduced concentrations of cholesterol or increased concentrations of PrP within the same, or increased affinity between PrP-lipid complexes making their destabilization less possible. In view that different strains of the scrapie agent exhibit different pathological profiles and areas of $PrP^{sc}$ accumulation (Bruce *et al.*, 1991; Fraser and Dickinson, 1968), it has been proposed that amphotericin B has its therapeutic effect on hamsters affected with the 263K scrapie strain by selectively targeting those cell types in which $PrP^{sc}$ propagation occurs (McKenzie *et al.*, 1994). An explanation for the mechanism by which such selective action may occur was not given.

Although disruption of caveolae structural and functional integrity presents a particularly attractive mechanism for the therapeutic effect of amphotericin B, we cannot discount the possibility that amphotericin B has a direct inhibitory influence on $PrP^{sc}$ transformation as a result of non-selective protein binding. Although less elegant than the above hypothesis, this mode of action may account for the disease-specific effect of amphotericin B in 263K-hamsters. As such, it is proposed that amphotericin B exerts its effect by competitively inhibiting the interaction between cellular $PrP^{c}$ and 263K prions, thus slowing the molecular transformation process by which $PrP^{sc}$ is formed. Whether this involves direct binding of amphotericin B to $PrP^{c}$ or destabilization of the $PrP^{c}$-$PrP^{sc}$ oligomeric

complex is not known. However in the models for which amphotericin B treatment is not therapeutic, it is speculated that $PrP^{c}$ has greater affinity for infectious prions than it does for amphotericin B. Amphotericin B may also bind the scrapie infectious agent (assumed to be $PrP^{sc}$), thus presenting a subtle variation by which interaction between the two isoforms may be sterically hindered. However, in view of the finding that treatment with amphotericin B prior to scrapie infection has a greater therapeutic effect than when given afterwards (Pocchiari *et al.*, 1989), interaction between amphotericin B and $PrP^{c}$ may be of greater inhibitory significance than that between amphotericin B and $PrP^{sc}$.

Areas for further investigation are outlined in Section 4 - Future Directions.

# CHAPTER FOUR

# FUTURE DIRECTIONS

## 4. Future Directions.

The application of NMR spectroscopy to the non-invasive study of cellular metabolism during scrapie pathogenesis presents a novel approach to the investigation of disease-related disturbances. Unfortunately the full potential of MRS was not realized during these studies. An important area for future research could utilize $^{13}C$ isotopically-enriched compounds to study brain metabolism in normal and diseased animals. Whilst studies *in vivo* may be limited by the selective permeability of the blood-brain barrier, the availability of *in vitro* cell cultures, which propagate scrapie infection, presents an attractive and more readily manipulated alternative. If aberrant metabolism is observed in scrapie-affected tissue, the ability to determine this metabolite(s) intracerebrally could be developed into techniques which would allow the localization of neurodegenerative lesions to be determined *in vivo*. For example, if metabolism of an isotopically-enriched compound is diminished in diseased tissue, this compound may be expected to accumulate in those regions of the brain which experience the greatest neurological damage, albeit after a specific lag period. Regions of neurodegeneration could then be identified using a combination of *in vivo* MRS and MRI techniques, following irradiation of the brain at an excitation frequencies similar to that of the $^{13}C$ resonance in the exogenous compound. The observation of significantly elevated levels of inositol in scrapie-affected mice (ME7/VM) and parietal white matter regions in patients suffering from Creutzfeldt-Jacob disease (Bruhn *et al.*, 1991), suggests that cerebral inositol metabolism is adversely affected in TSE disease. Inositol may therefore present a suitable metabolite for application to the above studies. The above techniques could also provide a non-invasive means by which therapy aimed at alleviating such disorders may be assessed.

Studies of lipids associated with GPI-anchored proteins in $PrP^{+/+}$, $PrP^{+/0}$ and $PrP^{0/0}$ mice did not reveal striking differences between the three groups. Thus, in view of the intimate association between lipid composition and the structural and

functional integrity of caveolae (Chang *et al.*, 1992; Rothberg *et al.*, 1991), it was proposed that the absence of PrP does not produce a detrimental effect on caveolae homeostatic functions. The observation that PrP-null mice develop and behave in a similar manner to their wild-type counterparts (Büeler *et al.*, 1992) supports this inference. In view of the finding that caveolae serve an important role in the endocytosis of small molecules such as folate (Anderson *et al.*, 1992), the effect that PrP-ablation has on caveolae functional integrity may be assessed by the investigation of folate potocytosis in the above transgenic mouse models.

In contrast to the above studies, a comparison of control and scrapie-affected mice demonstrated marked abnormalities in the composition of lipids associated with GPI-anchored proteins. In view of the above discussion, it is speculated that the structural and functional integrity of caveolae is disrupted in scrapie-affected mice. Again, evidence in support or disproof of this hypothesis may be provided by studies of folate potocytosis. In view of the essential function of folic acid in cellular amino acid and DNA synthesis, the hypothesized disturbance of folate potocytosis in scrapie-affected neuronal cells may present an elaborate mechanism by which scrapie infection causes cell death.

# BIBLIOGRAPHY

Abraham, R.J., Fisher, J. & Loftus, P. (1988). In *Introduction to NMR spectroscopy*. John Wiley and Sons Ltd., Chichester. pp. 43-46.

Adams, C.M.W. & Davison, A.N. (1959). The occurrence of esterified cholesterol in the developing nervous system. *Journal of Neurochemistry*. **4**, pp. 282-289.

Alper, T., Cramp, W.A., Haig, D.A. & Clarke, M.C. (1967). Does the agent of scrapie replicate without nucleic acid? *Nature (London)*. **214**, pp. 764-766.

Alper, T., Haig, D.A. & Clarke, M.C. (1966). The exceptionally small size of the scrapie agent. *Biochemical and Biophysical Research Communications*. **22**, pp. 278-284.

Anderson, R.G.W., Kamen, B.A., Rothberg, K.G. & Lacey, S.W. (1992). Potocytosis: sequestration and transport of small molecules by caveolae. *Science*. **255**, pp. 410-411.

Ando, S., Toyoda, Y., Nagai, Y. & Ikuta, F. (1984). Alterations in brain gangliosides and other lipids of patients with Creutzfeldt-Jacob disease and subacute sclerosing panencephalitis (SSPE). *Japanese Journal of Experimental Medicine*. **54**(6), pp. 229-234.

Anwyl, R. (1989). Protein kinase C and long-term potentiation in the hippocampus. *Trends in Pharmacological Sciences*. **10**, pp. 236-239.

Arnold, D.L., Matthews, P.M., Francis, G.S., O'Connor, J. & Antel, J.P. (1992). Proton magnetic resonance spectroscopy imaging for metabolic characterization of demyelinating plaques. *Annals of Neurology*. **31**(3), pp. 235-241.

Baldwin, M.A., Pan, K.-M., Nguyen, J., Huang, Z., Groth, D., Serban, A., Gasset, M., Mehlhorn, I., Fletterick, R.J., Cohen, F.E. & Prusiner, S.B. (1994). Spectroscopic characterization of conformational differences between $PrP^{c}$ and $PrP^{sc}$: an α-helix to β-sheet transition. *Philosophical Transactions of the Royal Society, London*. B series. **343**, pp. 435-441.

Bass, N.H., Hess, H.H. & Pope, A. (1974). Altered cell membranes in Creutzfeldt-Jacob disease. *Archives in Neurology*. **31**, pp. 174-182.

Bates, T.E., Williams, S.C.R., Kauppinen, R.A. & Gadian, D.G. (1989). Observation of cerebral metabolites in an animal model of acute liver failure in vivo: a $^{1}H$ and $^{31}P$ nuclear magnetic resonance study. *Journal of Neurochemistry*. **53**, pp. 102-110.

Bell, J.D., Cox, I.J., Williams, S.C.R. Belton, P.S., McConnell, I. & Hope, J. (1991). *In vivo* detection of metabolic changes in a mouse model of scrapie using nuclear magnetic resonance spectroscopy. *Journal of General Virology*. **72**, pp. 2419-2423.

Bell, J.E. & Ironside, J.W. (1993). Neuropathology of spongiform encephalopathies in humans. *British Medical Bulletin*. **49**, pp. 738-777.

Bendheim, P.E., Kascsak, R.J., Cashman, N.R. & Bolton, D.C. (1991). Distribution and possible functions of the normal isoform of the scrapie agent protein. *Seminars in Virology*. **2**, pp. 197-201.

Bernoulli, C.C., Siegfried, J., Baumgartner, G., Regli, F., Rabinowicz, T., Gadjusek, D.C. & Gibbs, C.J., Jr. (1977). Danger of accidental person-to-person transmission of Creutzfeldt-Jacob disase by surgery. *Lancet*. **1**, pp. 478-479.

Bessen, R.A. & Marsh, R.F. (1992). Identification of two biologically distinct strains of transmissible mink encephalopathy in hamsters. *Journal of General Virology*. **73**, pp. 329-334.

Birdsall, N.J.M., Feeney, J., Lee, A.G., Levine, Y.K. & Metcalfe, J.C. (1972). Dipalmitoyl-lecithin: assignment of the $^{1}H$ and $^{13}C$ nuclear magnetic resonance spectra, and conformational studies. *Journal of the Chemical Society, Perkin II*. pp. 1441

Birken, D.L. & Oldendorf, W.H. (1989). *N*-acetyl-*L*-aspartic acid: a literature review of a compound prominent in $^{1}H$ NMR spectroscopic studies of brain. *Neuroscience & Biobehavioural Reviews*. **13**, pp. 23-31.

Bolard, J. (1986). How do the polyene macrolide antibiotics affect the cellular membrane properties? *Biochimica et Biophysica Acta*. **864**, pp. 257-304.

Bolton, D.C. & Bendheim, P.E. (1988). A modified host protein model of scrapie. In *Novel infectious agents and the central nervous system*. G. Bock and J. Marsh (Eds.). Ciba Foundation Symposium 135. Chichester, John Wiley. pp. 146-181.

Bolton, D.C., McKinley, M.P. & Prusiner, S.B. (1982). Identification of a protein that purifies with the major scrapie prion. *Science*. **218**, pp. 1309-1311.

Borchelt, D.R., Scott, M., Taraboulos, A., Stahl, N. & Prusiner, S.B. (1990). Scrapie and cellular prion proteins differ in the kinetics of synthesis and topology in cultured cells. *Journal of Cell Biology*. **110**, pp. 743-752.

Bordier, C. (1981). Phase separation of integral membrane proteins in Triton X-114 solution. *Journal of Biological Chemistry*. **256**(4), pp. 1604-1607.

Borri, P.F., Bertinelli, R.P., Toso, V., Taramelli, M., Paci, M. & Pacini, A. (1969). *Acta Neurologica*. **24**, pp. 593-602.

Brown, D.A. & Rose, J.K. (1992). Sorting of GPI-anchored proteins to glycolipid-enriched membrane subdomains during transport to the apical cell surface. *Cell*. **68**, pp. 533-544.

Brown, D.R., Herms, J. & Kretzschmar, H.A. (1994). Mouse cortical cells lacking cellular PrP survive in culture with a neurotoxic PrP fragment. *NeuroReport*. **5**, pp. 2057-2060.

Brown, P. (1988). The clinical neurology and epidemiology of Creutzfeldt-Jacob disease, with special reference to iatrogenic cases. In *Novel infectious agents and the central nervous system*. G. Bock and J. Marsh (Eds.). Ciba Foundation Symposium 135. Chichester, John Wiley. pp. 3-23.

Brown, P., Gadjusek, D.C., Gibbs, C.J. Jr. & Asher, D.M. (1986). Potential epidemic of Creutzfeldt-Jacob disease from human growth hormone therapy. *New England Journal of Medicine*. **313**, pp. 728-731.

Brown, P., Goldfarb, L.G. & Gadjusek, D.C. (1991). The neurobiology of spongifrom encephalopathy: infectious amyloidoses with a genetic twist. *Lancet*. **337**, pp. 1019-1022.

Brown, P., Liberski, P.P., Wolff, A. & Gadjusek, D.C. (1990). Resistance of scrapie infectivity to steam autoclaving after formaldehyde fixation and limited survival after ashing at 360°C: practical and theoretical implications. *Journal of Infectious Diseases*. **161**, pp. 467-472.

Bruce, M.E., McConnell, I., Fraser, H. & Dickinson, A.G. (1991). The disease characteristics of difference strains of scrapie in *Sinc* congenic mouse lines: implications for the nature of the agent and host control of pathogenesis. *Journal of General Virology*. **72**, pp. 595-603.

Brugere, H., Banissi, C., Brugere-Picoux, J., Chatelain, J. & Buvet, R. (1991). Recherche d'un temoin biochimique urinaire de l'infection du mouton par la tremblante. *Bulletin d'Academe Veterinaire de France*. **64**, pp. 139-145.

Bruhn, H., Frahm, J., Gyngell, M.L., Merboldt, K.D., Hanicke, W. & Sauter, R. (1988). Localized proton spectroscopy of tumours *in vivo*: patients with primary and secondary cerebral tumours. *Society of Magnetic Resonance in Medicine*. San Francisco meeting. Book of abstracts, p. 253.

Bruhn, H., Weber, T., Thorwirth, V. & Frahm, J. (1991). *In vivo* monitoring of neuronal loss in Creutzfeldt-Jacob disease by proton magnetic resonance spectroscopy. *Lancet*. **337**, pp. 1610-1611.

Budka, H., Aguzzi, A., Brown, P., et al., (1995). Neuropathological diagnostic criteria for Creutzfeldt-Jacob disease (CJD) and other human spongiform encephalopathies (prion diseases). *Brain Pathology*. **5**, pp. 459-466.

Büeler, H., Aguzzi, A., Sailer, A. Greiner, R.-A., Autenried, P., Aguet, A. & Weissmann, C. (1993). Mice devoid of PrP are resistant to scrapie. *Cell*. **73**, pp. 1339-1347.

Büeler, H., Fischer, M., Lang, Y., Bluethmann, H., Lipp, H.-P., DeArmond, S.J., Prusiner, S.B., Aguet, M. & Weissmann, C. (1992). Normal development and behaviour of mice lacking the neuronal cell-surface PrP protein. *Nature (London)*. **356**, pp. 577-582.

Capuani, G., Aureli, T., Miccheli, A., Di Cocco, M.E., Ramacci, M.T. & Delfini, M. (1992). Improved resolution of $^{31}P$ nuclear magnetic resonance spectra of phospholipids from brain. *Lipids*. **27**(5), pp. 389-391.

Cashman, N.R., Loertscher, R., Nalbantoglu, J., Shaw, I., Kascsak, R.J., Bolton, D.C. & Bendheim, P.E. (1990). Cellular isoform of the scrapie agent protein participates in lymphocyte activation. *Cell*. **61**, pp 185-192.

Caughey, B. (1991). Cellular metabolism of normal and scrapie-associated forms of PrP. *Seminars in Virology*. **2**, pp. 189-196.

Caughey, B., Dong, A., Bhat, K.S., Ernst, D., Hayes, S.F. & Caughey, W.S. (1991). Secondary structure analysis of the scrapie-associated protein PrP 27-30 in water by infrared spectroscopy. *Biochemistry*. **30**, pp. 7672-7680.

Caughey, B., Neary, K., Butler, R., Ernst, D., Perry, L.C., Cheseboro, B. & Race, R.E. (1990). Normal and scrapie-associated forms of prion protein differ in their sensitivities to phospholipase and proteases in intact neuroblastoma cells. *Journal of Virology*. **64**, pp. 1093-1101.

Caughey, B., Race, R.E., Ernst, D., Buchmeier, M.J. & Chesebro, B. (1989). Prion protein (PrP) biosynthesis in scrapie-infected and uninfected neuroblastoma cells. *Journal of Virology*. **63**, pp. 175-181.

Caughey, B. & Raymond, G.J. (1991). The scrapie-associated form of PrP is made from a cell surface precursor that is both protease- and phospholipase-sensitive. *Journal of Biological Chemistry*. **266**, pp. 18217-19223.

Chang, W.J., Rothberg, K.G., Karman, B.A. & Anderson, R.G. (1992). Lowering the cholesterol content of MA104 cells inhibits receptor-mediated transport of folate. *Journal of Cell Biology*. **118**, pp. 63-69.

Chesebro, B., Race, R., Wehrly, K., Nisho, J., Bloom, M., Lechner, D., Bergstrom, S., Robbins, K., Mayer, L., Keith, J.M., Garon, C. & Haase, A. (1985). Identification of a scrapie prion protein-specific mRNA in scrapie-infected and uninfected brain. *Nature*. **315**, pp. 331-333.

Choi, D.W. (1988). Calcium-mediated neurotoxicity: relationship to specific channel types and role in ischaemic damage. *Trends in Neurosciences*. **11**, pp. 465-469.

Choi, G.T.Y., Casu, M. & Gibbons, W.A. (1993). NMR lipid profiles of cells, tissues and body fluids: neutral, non-acidic and acidic phospholipid analysis of Bond Elut chromatographic fractions. *Biochemical Journal*. **290**, pp. 7171-721.

Clarke, M.C. & Haig, D.A. (1971). Multiplication of scrapie agent in mouse spleen. *Research in Veterinary Science*. **12**, pp. 195-197.

Collinge, J., Owen, F., Lofthouse, R., Shah, T., harding, A.E., Poulter, M., Boughey, A.M. & Crow, T.J. (1989). Diagnosis of Gerstmann-Sträusser Scheinker syndrome in familial dementia with prion protein gene analysis. *Lancet*. **ii**, pp. 15-17.

Collinge, J., Poulter, M., Leach, M., Crow, T.J., Rossor, M.N., Hardy, J., Mullan, M.J., Janota, I. & Lantos, P.L. (1990). Prion dementia without characteristic pathology. *Lancet*. **336**, pp. 7-9.

Collinge, J. (1991). Genetics and etiology of CJD. *Neuroscience Facts*. **2**(19), p. 3.

Collinge, J., Palmer, M.S. & Dryden, A.J. (1991). Genetic predisposition to iatrogenic Creutzfeldt-Jacob disease. *Lancet*. **337**, pp. 1441-1442.

Collinge, J., Palmer, M.S., Sidle, K.C.L., Hill, A.F., Gowland, I., Meads, J., Asante, E., Bradley, R., Doey, L.J. & Lantos, P.L. (1995). Unaltered susceptibility to BSE in transgenic mice expressing human prion protein. *Nature (London)*. **378**, pp. 779-783.

Collingridge, G.L. & Bliss, T.P. (1987). NMDA receptors - their role in long-term potentiation. *Trends in Neurosciences*. **10**, pp. 288-293.

Czub, M., Braig, H.R. & Diringer, H. (1988). Replication of the scrapie agent in hamsters infected intracerebrally confirms the pathogenesis of an amyloid-inducing virosis. *Journal of General Virology*. **69**, pp. 1753-1756.

Davie, C.A., Hawkins, C.P., Barker, G.J., Brennan, A., Tofts, P.S., Miller, D.H. & McDonald, W.I. (1993). Detection of myelin breakdown products by proton magnetic resonance spectroscopy. *Lancet*. **341**, pp. 630-631.

DeArmond, S.J., Kristensson, K. & Bowler, R.P. (1992). $PrP^{sc}$ causes nerve cell death and stimulates astrocyte proliferation: a paradox. In *Progress in Brain Research*. Chapter 37. A.C.H. Yu, L. Hertz, M.D. Norenberg, E. Sykova & S.G. Waxman (Eds.). Elsevier Science Publishers B.V. **94**, pp. 437-446.

Dees, C., German, T.L., Wade, W.F. & Marsh, R.F. (1985). Characterization of lipids in membrane vesicles from scrapie-infected hamster brain. *Journal of General Virology*. **66**, pp. 861-870.

Dickinson, A.G. & Fraser, H. (1972). Scrapie: effect of *Dh* gene on incubation period of extraneurally injected agent. *Heredity*. **29**, pp. 91-93.

Dickinson, A.G. & Fraser, H. (1977). Scrapie pathogenesis in inbred mice: an assessment of host control and response involving many strains of agent. In *Slow virus infections of the central nervous system*. V. ter Meulen and M. Katz (Eds.). New York, Springer-Verlag. pp. 3-14.

Dickinson, A.G. & Taylor, D.M. (1988). Options for the control of scrapie in sheep and its counterpart in cattle. Proceedings of the Third World Congress on Sheep and Cattle Breeding. Paris, June 19-23. Volume 1, pp. 553-564.

Diedrich, J.F., Minnigan, H., Carp, R.I., Whitaker, J.N., Race, R., Frey (II), W. & Haase, A.T. (1991). Neuropathological changes in scrapie and Alzheimer's disease are associated with increased expression of apolipoprotein E and cathepsin D in astrocytes. *Journal of Virology*. **65**(9), pp. 4759-4768.

Di Martino, A., Safar, J., Callegaro, L., Salem, N. & Gibbs, C.J. (1993). Ganglioside composition changes in spongiform encephalopathies: analyses of 263K scrapie-infected hamster brains. *Neurochemical Research*. **18**(8), pp. 907-913.

Doh-ura, K., Tateishi, J., Sasaki, H., Kitamoto, T. & Sakaki, Y. (1989). Proline to leucine change at position 102 of prion protein is the most common but not the sole mutation related to Gerstmann-Sträussler syndrome. *Biochemical and Biophysical Research Communication*. **163**, pp. 974-979.

Dormont, D., Delpech, A., Courcel, M.-N., Viret, J., Markovits, P. & Court, L. (1981). Hyperproduction de proteine glio-fibrillaire acide (GFA) au cours de l'évolution de la tremblante experimentale de la soruis. *C. R. Acad. Sci. (Paris)*. **293**, pp. 53-56.

Duffy, P., Wolf, J., Collins, G., et al. (1974). Possible person-to-person transmission of Creutzfeldt-Jacob disease. *New England Journal of Medicine* **290**, pp. 692-693.

Eto, Y. & Suzuki, K. (1971). Fatty acid composition of cholesteryl esters in brains of patients with Schilder's disease, $G_{M1}$-gangliosidosis and Tay-Sach's disease, and its possible relationship to the β-position fatty acids of lecithin. *Journal of Neurochemistry*. **18**, pp. 1007-1016.

Eto, Y. & Suzuki, K. (1973). Cholesterol ester metabolism in rat brain: a cholesterol ester hydrolase specifically localized in the myelin sheath. *Journal of Biological Chemistry*. **248**(6), pp. 1986-1991.

Fan, T.W.-M., Higashi, R.M., Lane, A.N. & Jardetzky, O. (1986). Combined use of $^{1}$H-NMR and GC-MS for metabolite monitoring and *in vivo* $^{1}$H-NMR assignments. *Biochimica et Biophysica Acta*. **882**, pp. 154-167.

Fleetwood, A.J. & Furley, C.W. (1990). Spongiform encephalopathy in an eland. *Veterinary Record*. **126**, p. 408.

Folch, J., Lees, M. & Sloane-Stanley, G.H. (1957). A simple method for the isolation and purification of total lipides from animal tissues. *Journal of Biological Chemistry*. **226**, pp. 497-509.

Forloni, G., Angeretti, N., Chiesa, R., Monzani, E., Salmona, M., Bugiani, O. & Tagliavini, F. (1993). Neurotoxicity of a prion protein fragment. *Nature (London)*. **362**, pp. 543-546.

Fraser, H. (1969). The occurence of nerve fibre degeneration in brains of mice inoculated with scrapie. *Research in Veterinary Science*. **10**(4), pp. 338-341.

Fraser, H. (1979a). The pathogenesis and pathology of scrapie. In *Aspects of slow and persistent virus infections*. D.A.J. Tyrell (Ed.). The Hague, Martinus Nijhoff. pp. 30-58.

Fraser, H. (1979b). Neuropathology of scrapie: the precision of the lesion and their significance. In *Slow transmissible diseases of the nervous system*. S.B. Prusiner and W.J. Hadlow (Eds.). New York, Academic Press. pp. 387-406.

Fraser, H. (1980). Spontaneous astrocytoma in mice and its transmission with viable cells. In *Animal Models of Neurological Disease*. F.C. Rose & P.O. Behan (Eds.). London, Pitman Medical. Chapter 31. p. 393-404.

Fraser, H. (1986). Brain tumours in mice, with particular reference to astrocytoma. *Food and Chemical Toxicology*. **24**(2), pp. 105-111.

Fraser, H. & Dickinson, A.G. (1968). The sequential development of the brain lesions of scrapie in three strains of mice. *Journal of Comparative Pathology*. **78**, pp. 301-311.

Fraser, H. & Dickinson, A.G. (1970). Pathogenesis of scrapie in the mouse: the role of the spleen. *Nature (London)*. **226**, pp. 462-463.

Fraser, H. & Dickinson, A.G. (1978). Studies of the lymphoreticular system in the pathogenesis of scrapie: the role of the spleen and thymus. *Journal of Comparative Pathology*. **88**, pp. 563-573.

Fraser, J., Jeffrey, M., Halliday, W., Fowler, N., Goodsir, C. & Brown, D. (1995). Early loss of neurons and axon terminals in scrapie-affected mice revealed by morphometry and immunocytochemistry. *Molecular & Chemical Neuropathology*. **24**, pp. 245-249.

Friede, R.L. & DeJong, R.N. (1968). Neuronal enzymatic failure in Creutzfeldt-Jacob disease. *Archives in Neurology*. **10**, pp. 181-195.

Gadian, D.G. (1990). Proton NMR studies of brain metabolism. *Philosophical Transactions of the Royal Society, London, Supplement A*. **333**, pp. 561-570.

Gadian, D.G., Proctor, E., Williams, S.R., Cady, E.B. & Gardiner, R.M. (1986). Neurometabolic effects of an inborn error of amino acid metabolism demonstrated *in vivo* by $^{1}$H NMR . *Magnetic Resonance in Medicine*. **3**, pp. 150-156.

Gajdusek, D.C., Gibbs, C.J., Jr. & Alpers, M. (1966). Experimental transmission of a kuru-like syndrome in chimpanzees. *Nature (London)*. **209**, pp. 794-796.

Gajdusek, D.C. & Zigas, V. (1957). Degenerative disease of the central nervous system in New Guinea: epidemic occurence of "kuru" in the native population. *New England Journal of Medicine*. **257**, pp. 974-978.

Gajdusek, D.C. & Zigas, V. (1959). Clinical, pathological and epidemiological study of an acute progressive degenerating disease of the central nervous system among natives of the Eastern Highlands of New Guinea. *American Journal of Medicine*. **26**, pp. 442-469.

Gerstl, B., Rubinstein, L.J., Eng, L.E. & Tavastsjerna, M. (1966). A neurochemical study of a case of Sudanophilic leukodystrophy. *Archives Neurology*. **15**, pp. 603-614.

Ghosh, S. & McLean Grogan, W. (1990). Activation of myelin-associated cholesteryl ester hydrolase in developing rat brain. *Developmental Brain Research*. **54**, pp. 147-149.

Ghosh, S. & McLean Grogan, W. (1991). Decline in cholesteryl ester hydrolase activity of rat brain with progress of experimental allergic encephalomyelitis followed by rebound during recovery. *Brain Research*. **547**, pp. 327-330.

Gibson, P.H. & Liberski, P.P. (1987). An electron and light microscopic study of the numbers of dystrophic neurites and vacuoles in the hippocampus of mice infected intracerebrally with scrapie. *Acta Neuropathologica (Berl.)*. **73**, pp. 379-382.

Gill, S.S., Thomas, D.G.T., van Bruggen, N., Gadian, D.G., Peden, C.J., Bell, J.D., Cox, I.J., Menon, D.K., Iles, R.A., Bryant, D.J. & Coutts, G.A. (1990). Proton magnetic resonance spectroscopy of intracranial tumours: *in vitro* and *in vivo* studies. *Journal of Computer Assisted Tomography*. **14**, pp. 497-504.

Gordon, W.S. (1946). Advances in veterinary medicine. *Veterinary Research*. **58**, pp. 516-520.

Greenfield, J.G. (1976). Malformations of the spinal cord. In *Greenfield's Neuropathology*. Third Edition. Edited by W. Blackwood & J.A.N. Corsellis. Edward Arnold (Publishers) Ltd. pp. 371-372.

Griffith, J.S. (1967). Self-replication and scrapie. *Nature (London)*. **215**, pp. 1043-1044.

Guan, Z.Z., Soderberg, M., Sindelar, P., Prusiner, S.B., Kristensson, K. & Dallner, G. (1996). Lipid composition in scrapie-infected mouse brain - prion infection increases the level of dolichyl-phosphate and ubiquinone. *Journal of Neurochemistry*. **66**, pp. 277-285.

Gunstone, F.D. (1992). High resolution $^{1}H$ and $^{13}C$ NMR. In *Lipid analysis: a practical approach*. Edited by R.J. Hamilton & S. Hamilton. Oxford University Press, Oxford. Chapter 7, pp. 243-262.

Hardy, J. & Allsop, D. (1991). Amyloid deposition as the central event in the aetiology of Alzheimer's disease. *Trends in Pharmacological Sciences*. **12**, pp. 383-388.

Hare, J.F. (1990). Mechanisms of membrane protein turnover. *Biochimica et Biophysica Acta*. **1031**, pp. 71-90.

Heitzman, R.J. & Skipworth, S. (1969). The fatty acid composition of brain and myelin of normal and scrapie-affected mice. *Journal of Neurochemistry*. **16**, pp. 121-122.

Hitchcock, C. & Hammond, E.W. (1980). In *Developments in Food Analysis*. Second Edition. R.D. King (Ed.). Applied Science Publishers, London.

Hope, J. & Baybutt, H. (1991). The key role of the nerve membrane protein PrP in scrapie-like diseases. *Seminars in the Neurosciences*. **3**, pp. 165-171.

Hope, J., Morton, L.D.J., Farquhar, C.F., Multhaup, G., Beyereuther, K. & Kimberlin, R.H. (1986). The major polypeptide of scrapie-associated fibrils (SAF) has the same size, charge distribution and *N*-terminal protein sequence as predicted for the normal brain protein. *EMBO Journal*. **5**, pp. 2591-2597.

Hope, J., Multhaup, G., Reekie, L.J.D., Kimberlin, R.H. & Beyereuther, K. (1988). Molecular pathology of scrapie-associated fibril protein (PrP) in mouse brain affected by the ME7 strain of scrapie. *European Journal of Biochemistry*. **172**, pp. 271-277.

Hope, J., Reekie, L.J.D., Hunter, N., Multhaup, G., Beyereuther, K., White, H., Scott, A.C., Stack, M.J., Dawson, M. & Wells, G.A.H. (1988). Fibrils from brains of cows with new cattle disease contain scrapie-associated protein. *Nature (London)*. **336**, pp. 390-392.

Hourrigan, J.L. (1990a). Experimentally induced bovine spongiform encephalopathy in cattle in Mission, Texas, and the control of scrapie. *Journal of the American Veterinary Medicine Association*. **196**(10), pp. 1678-1679.

Hourrigan, J.L. (1990b). The scrapie control program in the United States. *Journal of the American Veterinary Medicine Association*. **196**(10), p. 1679.

Hugon, J., Vallat, J.M. & Leboutet, M.J. (1987). *Neuroscience Letters*. **81**, pp. 1-8.

Igarashi, M. & Suzuki, K. (1977). Solubilization and characterization of the rat brain cholesterol ester hydrolase located in the myelin sheath. *Journal of Neurochemistry*. **28**, pp. 729-738.

Jeffrey, M. & Wells, G.A.H. (1988). Spongiform encephalopathy in a nyala (*Tragelaphus angasi*). *Veterinary Pathology*. **25**, pp. 398-399.

Johnson, A.C., McNabb, A.R. & Rossiter, R.J. (1949). Lipids in Wallerian degeneration. *Biochemical Journal*. **45**, pp. 500-508.

Johnson, L.F. & Jankowski, W.C. (1972). Carbon-13 NMR spectra. A collection of assigned, coded, and indexed spectra. John Wiley and Sons, New York.

Johnson, R.C. & Shan, S.N. (1978). Cholesterol ester metabolizing enzymes in human brain: properties, subcellular distribution and relative levels in various diseased conditions. *Journal of Neurochemistry*. **31**, pp. 895-902.

Johnson, R.T. & Gibbs, C.J., Jr. (1974). Koch's postulates and slow infections of the nervous system. *Achives in Neurology*. **30**, pp. 36-38.

Kaluzny, M.A., Duncan, L.A., Merritt, M.V. & Epps, D.E. (1985). Rapid separation of lipid classes in high yield and purity using bonded phase columns. *Journal of Lipid Research*. **26**, pp. 135-140.

Kim, Y.S., Carp, R.I., Callahan, S.M., Natelli, M. & Wisniewski, H.M. (1990a). Vacuolization, incubation period and survival time analyses in three mouse genotypes injected stereotactically in three brain regions with the 22L scrapie strain. *Journal of Neuropathology and Experimental Neurology*. **49**(2), pp. 106-113.

Kim, Y.S., Carp, R.I., Callahan, S.M. & Wisniewski, H.M. (1990b). Incubation periods and histopathological changes in mice injected stereotactically in different brain areas with the 87V scrapie strain. *Acta. Neuropathologica*. **80**, pp. 388-392.

Kimberlin, R.H. (1991). In *Diseases of Sheep*. Second Edition. W.B. Martin, & I.D. Aitken (Eds.). Blackwell Scientific Publishers, London. pp. 163-169.

Kimberlin, R.H. & Cunningham, P.G. (1978). Reduction of scrapie incubation time in mice and hamsters by a single injection of methanol extraction residue of BCG. *FEMS Microbiological Letters*. **3**, pp. 169-172.

Kimberlin, R.H. & Millson, G.C. (1967). Some biochemical aspects of mouse scrapie. *Journal of Comparative Pathology*. **77**, pp. 359-366.

Kimberlin, R.H. & Walker, C.A. (1988). Pathogenesis of experimental scrapie. In *Novel infectious agents and the central nervous system*. G. Bock and J. Marsh (Eds.). Ciba Foundation Symposium 135. Chichester, John Wiley. pp. 37-62.

Kirkwood, J.K., Wells, G.A.H., Wilesmith, J.W., et al. (1990). Spongiform encephalopathy in an Arabian oryx (Oryx leucoryx) and a greater kudu (*Tragelaphus strepsiceros*). *Veterinary Record*. **126**, pp. 418-420.

Koller, K.J., Zaczek, R. & Coyle, J.T. (1984). *N*-acetyl-aspartyl-glutamate: regional levels in rat brain and the effects of brain lesions as determined by a new HPLC method. *Journal of Neurochemistry*. **43**(4), pp. 1136-1142.

Koopmans, R.A., Li, D.K.B., Zhu, G., Allen, P.S., Penn, A. & Paty, D.W. (1993). Magnetic resonance spectroscopy of multiple sclerosis: *in vivo* detection of myelin breakdown products. *Lancet*. **341**, pp. 631-632.

Korey, S.R., Katzman, R. & Orloff, J. (1961). A case of Creutzfeldt-Jacob disease. *Journal of Neuropathology and Experimental Neurology*. **20**, pp. 95-104.

Kretzschmar, H.A., Kufer, P., Riethmuller, G., DeArmond, S.J., Prusiner, S.B. & Schiffer, D. (1991). Prion protein mutation at codon 102 in an Italan family with Gerstmann-Sträussler Scheinker sydrome. *Neurology*. **42**, pp. 809-810.

Kristensson, K., Feuerstein, B., Taraboulos, A., Hyun, W.C., Prusiner, S.B. & DeArmond, S.J. (1993). Scrapie prions alter receptor-mediated calcium responses in cultured cells. *Neurology*. **43**, pp. 2335-2341.

Kurihara, T. & Tsukada, Y. (1967). The regional and subcellular distribution of 2',3'-cyclic nucleotide 3'-phosphohydrolase in the central nervous system. *Journal of Neurochemistry*. **14**, pp. 1167-1174.

Lampert, P.W., Gajdusek, D.C. & Gibbs, C.J., Jr. (1972). Subacute spongiform encephalopathies: scrapie, kuru and Creutzfeldt-Jacob disease: a review. *American Journal of Pathology*. **68**, pp. 626-646.

Landowne, D., Potter, L.T. & Terrar, D.A. (1975). Structure-function relationships in excitable membranes. *Annual Reviews in Physiology*. **37**, pp. 485-508.

Larsson, H.B.W., Christiansen, P., Jensen, M., Fredriksen, J., Heltberg, A., Olesen, J. & Henriksen, O. (1991). Localized *in vivo* proton spectroscopy in the brains of patients with multiple sclerosis. *Magnetic Resonance in Medicine*. **22**, pp. 23-31.

Ledeen, R.W. (1984). Lipid-metabolizing enzymes of myelin and their relation to the axon. *Journal of Lipid Research*. **25**, pp. 1548-1554.

Ledeen, R.W., Yu, R.K. & Eng, L.F. (1973). Gangliosides of human myelin: sialosylgalactosyl-ceramide (G7) as a major component. *Journal of Neurochemistry*. **21**, pp. 829-839.

Macala, L.J., Yu, R.K. & Ando, S. (1983). Analysis of brain lipids by high performance thin layer chromatography and densitometry. *Journal of Lipid Research*. **24**, pp. 1243-1250.

Mackenzie, A. (1983). Immunohistochemical demonstration of glial fibrillary acidic protein in scrapie. *Journal of Comparative Pathology*. **93**, pp. 251-259.

Mackenzie, A. & Wilson, A.M. (1966). Accumulations of fat in the brains of mice affected with scrapie. *Research in Veterinary Science*. **7**(1), pp. 45-54.

Maggio, B., Cumar, F.A. & Maccioni, H.J. (1972). Lipid content in brain and spinal cord during experimental allergic encephalomyelitis in rats. *Journal of Neurochemistry*. **19**, pp. 1031-1037.

Mahley, R. W. (1988). Apolipoprotein E: cholesterol transport protein with expanding role in cell biology. *Science*. **240**, pp. 622-630.

Manuelidis, E.E., Kim, J.H., Mericangas, J.R. & Manuelidis, L. (1985). Transmission of Creutzfeldt-Jacob disease from human blood. *Lancet*. **2**, pp. 896-897.

Marsh, R.F. (1981). Effect of vaccinia-activated macrophages on scrapie infection in hamsters. In *Hamster immune response in infectious and oncologic diseases.* J.W. Streilen, D.A. Hart, J. Stein Streilen, W.R. Duncan and R.E. Billingham (Eds.). New York, Plenum Press. pp. 359-363.

Masters, C.L. & Beyereuther, K. (1988). Neuropathology of unconventional virus infections: molecular pathology of spongiform change and amyloid plaque deposition. In *Novel infectious agents and the central nervous system.* G. Bock and J. Marsh (Eds.). Ciba Foundation Symposium 135. Chichester, John Wiley. pp. 24-36.

Masullo, C., Macchi, G., Xi, Y.G. & Pocchiari, M. (1992). Failure to ameliorate Creutzfeldt-Jacob disease with amphotericin B therapy. *The Journal of Infectious Diseases.* **165**, pp. 784-785.

May, G.L., Wright, L.C., Holmes, K.T., Williams, P.G., Smith, I.C.P., Wright, P.E., Fox, R.M. & Mountford, C.E. (1986). Assignment of methylene proton resonances in NMR spectra of embryonic and transformed cells to plasma membrane triglyceride. *Journal of Biological Chemistry.* **261**(7), pp. 3048-3053.

McKenzie, D., Kaczkowski, J., Marsh, R. & Aiken, J. (1994). Amphotericin B delays both scrapie agent replication and PrP-res accumulation early in infection. *Journal of Virology.* **68**(11), pp. 7534-7536.

Menon, D.K., Baudouin, C.J., Tomlinson, D. & Hoyle, C. (1990a). Proton MR spectroscopy and imaging of the brain in AIDs: evidence of neuronal loss in regions that appear normal with imaging. *Journal of Computer Assisted Tomography.* **14**, pp. 882-885.

Menon, D.K., Sargentoni, J., Peden, C.J., Bell, J.D., Cox, I.J. & Coutts, G.A., Baudouin, C. & Newman, C.G.H. (1990b). Proton MR spectroscopy in herpes simplex encephalitis: assessment of neuronal loss. *Journal of Computer Assisted Tomography.* **14**, pp. 449-452.

Merz, P.A., Somerville, R.A., Wisniewski, H.M. & Igbal, K. (1981). Abnormal fibrils in scrapie-infected brain. *Acta Neuropathologica.* **54**, pp. 63-74.

Merz, P.A., Somerville, R.A., Wisniewski, H.M., Manuelidis, L. & Manuelidis, E. (1983). Scrapie-associated fibrils in Creutzfeldt-Jacob disease. *Nature (London).* **306**, pp. 474-476.

Meyer, R.K., McKinley, M.P., Bowman, K.A., Braunfield, M.B., Barry, R.A. & Prusiner, S.B. (1986). Separation and properties of cellular and scrapie prion proteins. *Proceedings of the National Academy of Sciences, USA.* **83**, pp. 2310-2314.

Mezei, C. (1970). Cholesterol esters and hydrolytic cholesterol esterase during Wallerian degeneration. *Journal of Neurochemistry.* **17**, pp. 1163-1170.

Morgan, K.L. (1988). Bovine spongiform encephalopathy: time to take scrapie seriously. *Veterinary Record.* **122**, pp. 445-446.

Morgan, K.T., Frith, C.H., Swenberg, J.A., McGrath, J.J., Zulch, K.J. & Crowder, D.M. (1984). A morphological classification of brain tumours found in several strains of mice. *Journal of the National Cancer Institute.* **72**, p. 151.

Mountford, C.E., Wright, L.C., Holmes, K.T., Mackinnon, W.B., Gregory, P. & Fox, R.M. (1984). High resolution proton nuclear magnetic resonance spectroscopy analysis of metastaic cancer cells. *Science.* **226**, pp. 1415-1418.

Müller, W.E.G., Ushijima, H., Schröder, H.C., Forrest, J.M.S., Schatton, W.F.H., Rytik, P.G. & Heffner-Lauc, M. (1993). Cytoprotective effect of NMDA receptor antagonists on prion protein (prion$^{sc}$)-induced toxicity in rat cortical cell cultures. *European Journal of Pharmacology.* **246**, pp. 261-268.

Neises, B. & Steglich, W. (1978). Simple method for the esterification of carboxylic acids. *Angew. Chem. Int. Ed. Engl.* **17**(7), pp. 522-523.

Norton, W.T., Poduslo, S.E. & Suzuki, K. (1966). Subacute sclerosing leukoencephalitis. II. Chemical studies including abnormal myelin and abnormal ganglioside pattern. *Journal of Neuropathology and Experimental Neurology.* **25**, pp. 582-597.

Oesch, B., Westaway, D., Walchli, M., McKinley, M.P., Kent, S.B.H., Aebersold, R., Barry, R.A., Tempst, P., Teplow, D.B., Hood, C.E., Prusiner, S.B. & Weissmann, C. (1985). A cellular gene encodes scrapie PrP 27-30 protein. *Cell.* **40**, pp. 735-746.

Olney, J.W. (1990). Excitotoxic amino acids and neuropsychiatric disorders. *Annual Reviews in Pharmacological Toxicology.* **30**, pp. 47-71.

Palmer, M.S., Dryden, A.J., Hughes, J.T. & Collinge, J. (1991). Homozygous prion protein genotype predisposes to sporadic Creutzfeldt-Jacob disease. *Nature (London).* **352**, pp. 340-342.

Pan, K.-M., Baldwin, M., Nguyen, J., Gasset, M., Serban, A., Groth, D., Mehlhorn, J., Huang, Z., Fletterick, R.J., Cohen, F.E. & Prusiner, S.B. (1993). Conversion of α-helices into β-sheets features in the formation of the scrapie prion proteins. *Proceedings of the National Academy of Sciences, USA.* **90**, pp. 10962-10966.

Parry, H.B. (1983). Recorded occurrences of scrapie from 1750. In *Scrapie disease in sheep.* D.R. Oppenheimer (Ed.). Academic, London. pp. 31-59.

Patterson, W.J. & Dealler, S. (1995). Bovine spongiform encephalopathy and the public-health. *Journal of Public Health Medicine.* **17**(3), pp. 261-268.

Pattison, I.H., Gordon, W.S. & Millson, G.C. (1959). Experimental production of scrapie in goats. *Journal of Comparative Pathology and Therapy.* **69**, pp. 300-312.

Pocchiari, M., Schmittinger, S. & Masullo, C. (1987). Amphotericin B delays the incubation period of scrapie in intracerebrally inoculated hamsters. *Journal of General Virology*. **68**, pp. 219-223.

Prusiner, S.B. (1991). Molecular biology of prion diseases. *Science*. **252**, pp. 1515-1522.

Prusiner, S.B., Gartin, D.E., Bariner, J.R. & Cochran, S.P. (1979). On the partial purification and apparent hydrophobicity of the scrapie agent. In *Slow transmissible diseases of the nervous system*. S.B. Prusiner & W.J. Hadlow (Eds.). New York, Academic Press. pp. 425-461.

Prusiner, S.B., McKinley, M.P., Bowman, K.A., Bolton, D.C., Bendheim, P.E., Groth, D.F. & Glenner, G.G. (1983). Scrapie prions aggregate to form amyloid-like birefringent rods. *Cell*. **35**, pp. 349-358.

Prusiner, S.B., Scott, M., Foster, D., Pan, K.-M., Groth, D., Mirenda, C., Torchia, M., Yang, S.-L., Serban, D., Carlson, G.A. (1990). Transgenetic studies implicate interactions between homologous PrP isoforms in scrapie prion replication. *Cell*. **63**, pp. 673-686.

Race, R.E., Fadness, L.H. & Chesebro, B. (1987). Characterization of scrapie infection in mouse neuroblastoma cells. *Jounal of General Virology*. **68**, pp. 1391-1399.

Ramsey, R.B. (1973). new concepts in brain cholesterol metabolism. *Biochemical Society Transactions*. **1**, pp. 341-348.

Rang, H.P. & Dale, M.M. (Eds.). (1991). In *Pharmacology*. Second Edition. Church Livingstone, London. pp. 593-598

Report of the Working Party on Bovine Spongiform Encephalopathy. (1989). London. Department of Health.

Robakis, N.K., Devine-Gage, E.A., Jenkins, E.C., Kascsak, R.J., Brown, W.T., Krawczun, M.S. & Silverman, W.P. (1986). Localization of a human gene homologous to the PrP gene on the *p* arm of chromosome 20 and detection of PrP-related antigens in normal human brain. *Biochemical and Biophysical Research Communications*. **140**, pp. 758-765.

Robinson, N. (1969). Creutzfeldt-Jacob disease: a histochemical study. *Brain*. **92**, pp. 581-588.

Rollins, K., Scrivens, J.H., Jennings, R.C.K., Morden, W.E., Welby, J.K. & Bateman, R.H. (1990). The use of tandem mass spectrometry as a problem-solving tool in the industrial environment. *Rapid Communications in Mass Spectrometry*. **4** (10), p. 454-460.

Rothberg, K.G., Ying, Y.S., Kamen, B.A. & Anderson, R.G. (1990). Cholesterol controls the clustering of the glycophospholipid-anchored membrane receptor for 5-methyltetrahydrofolate. *Journal of Cell Biology*. **111**, pp. 2931-2938.

Safar, J., Ceroni, M., Gajdusek, D.C. & Gibbs, C.J., Jr. (1991). Differences in the membrane interaction of scrapie amyloid precursor proteins in normal and scrapie- or Creutzfeldt-Jacob disease-infected brains. *The Journal of Infectious Diseases*. **163**, pp. 488-494.

Safar, J., Ceroni, M., Piccardo, P., Liberski, P.P., Miyazaki, M., Gajdusek, D.C. & Gibbs, C.J., Jr. (1990). Subcellular distribution and physicochemical properties of scrapie-associated precursor protein and relationship with scrapie agent. *Neurology*. **40**, pp. 503-508.

Safar, J., Roller, P.P., Gajdusek, D.C. & Gibbs, C.J., Jr. (1993). Conformational transitions, dissociation, and unfolding of scrapie amyloid (prion) protein. *Journal of Biological Chemistry*. **268**, pp. 20276-20284.

Scott, J.R. & Fraser, H. (1984). Degenerative hippocampal pathology in mice infected with scrapie. *Acta Neuropathologica*. **65**, pp. 62-68.

Scott, M.D., Groth, D., Foster, D., Torchia, M., Yang, S.-L., DeArmond, S.J. & Prusiner, S.B. (1993). Propagation of prions with artificial properties in transgenic mice expressing chimeric PrP genes. *Cell*. **73**, pp. 979-988.

Scott, P.R. & Henshaw, C.J. (1994). Diagnosis of scrapie: increasing the accuracy of the provisional *ante-mortem* examination. *State Veterinary Journal*. **4**(2), pp. 4-6.

Selvaggini, C., Degioia, L., Cantu, L., Ghibaudi, E., Diomede, L., Passerini, F., Forloni, G., Bugiani, O., Tagliavini, F. & Salmona, M. (1993). Molecular characteristics of a protease-resistant, amyloidogenic and neurotoxic peptide homologous to residues 106-126 of the prion protein. *Biochemical and Biophysical Research Communication*. **194**, pp. 1380-1386.

Shan, S.N. & Johnson, R.C. (1980). Activity levels of cholesterol ester metabolizing enzymes in brain in multiple sclerosis: correlation with cholesterol ester concentrations. *Experimental Neurology*. **68**, pp. 601-604.

Shand, J.H. & West, D.W. (1992). Characterization of a cytosolic protein in rat liver inhibiting neutral cholesteryl ester hydrolase. *Lipids*. **27**(6), pp. 406-412.

Sidle, K.C.L. (1992). Development of immunodiagnostic techniques in human spongiform encephalopathies. *AFRC Biology of Spongiform Encephalopathies Programme Meeting*. University of Reading, April 1992.

Simons, K. & van Meer, G. (1988). Lipid sorting in epithelial cells. Biochemistry. 27, pp. 6197-6202.

Small, R.K., Bates, T.E., Urenjak, J., Bell, J.D., Williams, S.C.R., Riley, K., Watkins, B. & Gadian, D.G. (1990). *N*-Acetylaspartate: a neuronal marker that can predict abnormal brain development. *Society of Magnetic Resonance in Medicine*. New York meeting. Book of abstracts, p. 72.

Smith, P.K., Krohn, R.I., Hermanson, G.T., Mallia, A.K., Gartner, F.H., Provenzano, M.D., Fujimoto, E.K., Goeke, N.M., Olson, B.J. & Klenk, D.C. (1985). Measurement of protein using bicinchoninic acid. *Analytical Biochemistry*. **150**, pp. 76-85.

Somerville, R.A., Ritchie, L.A. & Gibson, P.H. (1989). Structural and biochemical evidence that scrapie-associated fibrils assemble *in vivo*. *Journal of General Virology*. **70**, pp. 25-35.

Sparkes, R.S., Simon, M., Cohn, V.H., Fournier, R.E., Lem, J., Klisak, I., Heinzmann, C., Blatt, C., Lucero, M. & Mohandas, T. (1986). Assignment of the human and mouse prion protein genes to homologous chromosomes. *Proceedings of the National Academy of Sciences, USA*. **83**, pp. 7358-7362.

Stah, S.N. & Johnson, R.C. (1980). Activity levels of cholesterol ester metabolizing enzymes in brain in multiple sclerosis: correlation with cholestrol ester concentrations. *Experimental Neurology*. **68**, pp. 601-604.

Stahl, N., Baldwin, M.A., Hecker, R., Pan, K.-M., Burlingame, A.L. & Prusiner, S.B. (1992). Glycosylinositol phospholipid anchors of the scrapie and cellular prion proteins contain sialic acid. *Biochemistry*. **31**, pp. 5043-5053.

Stahl, N., Baldwin, M.A., Teplow, D.B., Hood, L., Gibson, B.W., Burlingame, A.L. & Prusiner, S.B. (1993). Structural analysis of the scrapie prion protein using mass spectrometry and amino acid sequencing. *Biochemistry*. **32**, pp. 1991-2002.

Stahl, N., Borchelt, D.R., Hsiao, K. & Prusiner, S.B. (1987). Scrapie prion protein contains a phosphatidylinositol glycolipid. *Cell*. **51**, pp. 229-240.

Stahl, N., Borchelt, D.R. & Prusiner, S.B. (1990). Differential release of cellular and scrapie prion proteins from cellular membranes by phosphatidylinositol-specific phospholipase C. *Biochemistry*. **29**, pp. 5405-5412.

Stahl, N. & Prusiner, S.B. (1991). Prions and prion proteins. *FASEB Journal*. **5**, pp. 2799-2807.

Stamp, J.T. (1962). Scrapie: a transmissible disease of sheep. *Veterinary Record*. **74**, pp. 357-362.

Steinbeck, J. (1995). In *East of Eden*. Minerva, London. Chapter 13. p. 147.

Suzuki, K., Suzuki, K. & Kamoshita, S. (1969). *Journal of Neuropathology and Experimental Neurology*. **28**, pp. 25-73.

Sweasey, D. & Patterson, D.S.P. (1974). Fatty acid composition of cholesterol esters in congenital disorders of lambs and piglets. *Biochemical Society Transactions*. 544th Meeting, London. **2**, pp. 290- 292.

Tamai, Y., Kojima, H. & Ikuta, F. & Kumanishi, T. (1978). Alterations in the composition of brain lipids in patients with Creutzfeldt-Jacob disease. *Journal of Neurological Sciences*. **35**, pp. 59-76.

Taraboulos, A., Scott, M., Semenov, A., Avraham, D., Laszlo, L. & Prusiner, S.B. (1995). Cholesterol depletion and modification of COOH-terminal targeting sequence of the prion protein inhibit formation of the scrapie isoform. *Journal of Cell Biology*. **129**(1), pp. 121-132.

Taylor, D.M. (1989). Bovine spongiform encephalopathy and human health. *Veterinary Record*. **125**, pp. 413-415.

Taylor, D.M. (1991). Inactivation of the unconventional agents of scrapie, bovine spongiform encephalopathy and Creutzfeldt-Jacob disease. *Journal of Hospital Infection*. **18** (Supplement A), pp. 141-146.

Taylor, D.M. (1993). Bovine spongiform encephalopathy and its association with the feeding of ruminant-derived protein. In *Transmissible Spongiform Encephalopathies - Impact on Animal and Human Health*. F. Brown (Ed.). Dev. Biol. Stand. Basel, Karger. Volume 80, pp. 215-224.

Telling, G.C., Scott, M., Hsiao, K.K., Foster, D., Yang, S.L., Torchia, M., Sidle, K.C.L., Collinge, J., DeArmond, S.J. & Prusiner, S.B. (1994). Transmission of Creutzfeldt-Jacob disease from humans to transgenic mice expressing chimeric human-mouse prion protein. *Proceedings of the National Academy of Sciences, USA*. **91**, pp. 9936-9940.

Uchino, A., Yoshinaga, M., Shiokawa, O. Kata, H. & Ohno, M. (1991). Serial MR imaging in Creutzfeldt-Jacob disease. *Neuroradiology*. **33**, pp. 364-367.

van der Knapp, M.S., van der Grond, J., Luyten, P.R., den Hollander, J.A., Nauta, J.J.P. & Valk, J. (1992). $^{1}H$ and $^{31}P$ magnetic resonance spectroscopy of the brain in degenerative cerebral disorders. *Annals of Neurology*. **31**(2), pp. 202-211.

Watkin, J.F. & Evans, R.H. (1981). Excitatory amino acid transmitters. *Annual Reviews in Pharmacological Toxicology*. **21**, pp. 165-204.

Watt, N.J. (1996). Storage diseases and myelin disorders. In *Neurology - B.V.M.&S. - Integrated Course III*. pp. 9-11.

Wells, G.A.H. & McGill, I.S. (1992). Recently described scrapie-like encephalopathies of animals: case definitions. *Research in Veterinary Science*. **53**, pp. 1-10.

Wells, G.A.H., Scott, A.C., Johnson, C.T., Gunning, R.F., Hancock, R.D., Jeffrey, M., Dawson, M. & Bradley, R. (1987). A novel progressive spongiform encephalopathy in cattle. *Veterinary Record*. **121**, pp. 419-420.

West, D.W. & Shand, J.H. (1991). Cholesterol ester hydrolase activity in mammary tissue of the lactating rat. *Lipids*. **26**(1), pp. 31-36.

Westaway, D. & Prusiner, S.B. (1986). Conservation of the cellular gene encoding the scrapie prion protein. *Nucleic Acids Research*. **14**, pp. 2035-2044.

Wilesmith, J.W. (1990). Epidemiology and current status of bovine spongiform encephalopathy in the United Kingdom. *Journal of the American Veterinary Medicine Association*. **196**(10), p. 1674.

Will, R.G., Ironside, J.W., Zeidier, M., Cousens, S.N., Estibeiro, K., Alperovitch, A., Poser, S., Pocchiari, M., Hofman, A. & Smith, P.G. (1996). A new variant of Creutzfeldt-Jacob disease in the U.K. *Lancet*. **347**, pp. 921-925.

Will, R.G. & Matthews, W.B. (1982). Evidence for case-to-case transmission of Creutzfeldt-Jacob disease. *Journal of Neurology, Neurosurgery and Psychiatry*. **45**, pp. 235-238.

Xi, Y.G., Ingrosso, L., Ladogana, A., Masullo, C. & Pocchiari, M. (1992). Amphotericin B treatment dissociates *in vivo* replication of the scrapie agent from PrP accumulation. *Nature (London)*. **356**, pp. 598-601.

Yu, R.K., Ledeen, R.W., Gajdusek, D.C. & Gibbs, C.J., Jr. (1974). Ganglioside changes in slow virus diseases: analyses of chimpanzee brains infected with kuru and Creutzfeldt-Jacob disease. *Brain Research*. **70**, pp. 103-112.

Yu, R.K. & Manuelidis, E. (1978). Ganglioside alterations in guinea pig brain at end stages of experimental Creutzfeldt-Jacob disease. *Journal of Neurological Sciences*. **35**, pp. 15-23.

Zajicek, J.P., Wing, M., Scolding, N.J. & Compston, D.A.S. (1992). Interactions between oligodendrocytes and microglia. *Brain*. **115**, pp. 1611-1631.